



**TRANSITION METAL CHELATES WITH SCHIFF BASES  
DERIVED FROM  
SALICYLALDEHYDE AND DIAMINO ETHANE**

**ALVIN PAUL SUMMERTON, B.SC.**

**UNIVERSITY OF ADELAIDE,  
DEPARTMENT OF PHYSICAL AND INORGANIC CHEMISTRY**



**November 1978**

*Awarded April 1979  
Ph.D*

## CONTENTS

Page

SUMMARY

STATEMENT

ACKNOWLEDGEMENTS

ABBREVIATIONS

CHAPTER 1: Introduction 1

### PART I

CHAPTER 2: Preparation and characterization of salen complexes of iron(III) 6

CHAPTER 3: Solution studies 30

CHAPTER 4: Moessbauer spectra 57

### PART II

CHAPTER 5: Preparation, characterization and solid state properties 84

CHAPTER 6: Solution studies 115

CHAPTER 7: Crystal structure of  $\text{Fe}(\text{saen})_2\text{Cl}\cdot\text{H}_2\text{O}$  143

APPENDIX I: Computer Programs

APPENDIX II: Structure Factor Tables

APPENDIX III: Publication

BIBLIOGRAPHY

## SUMMARY

The following study of transition metal complexes with Schiff base ligands comprises two related studies.

### PART I

#### Complexes of the quadridentate ligand, salen.

A number of complexes of general formula  $\text{Fe(III)salenX}$ , where  $X = \text{Cl, Br, I, NO}_3, \text{N}_3, \text{NCS}$  and  $\text{C}_6\text{H}_5\text{COO}$ , have been prepared. Of these species, two ( $X = \text{NO}_3$  and  $\text{N}_3$ ) have not been previously reported and only one ( $X = \text{Cl}$ ) has been intensively studied. In addition, two novel octahedral complex salts  $\text{K[Fesalen(CN)}_2]$  and  $\text{Fe(saen)}_2\text{Cl}\cdot\text{H}_2\text{O}$ , which involve a low spin central metal ion, have been obtained. The salt  $\text{Fe(saen)}_2\text{Cl}\cdot\text{H}_2\text{O}$  has several unusual properties which have been examined in Part II of this thesis.

This investigation of the salen complexes has involved:

- (1) confirmation of structure by microanalysis, i.r. spectra and magnetism;
- (2) a study of the u.v.-visible solution spectra;
- (3) determination of the Moessbauer spectral parameters.

The solution spectra indicated that the species were involved in dissociative equilibria which were utilized to estimate the relative stability of the covalent bond between the metal and the anionic ligand occupying the fifth coordination position. In contrast to previous studies, where a correlation between magnetic properties and the Moessbauer data was indicated, the results of this work suggested that the magnitude of the quadrupole splitting may be related to the nature of the Fe-X bond.

## PART II

### Complexes of the tridentate ligand, saen.

Cationic salts of general formula  $M(\text{III})(\text{saen})_2X \cdot n\text{H}_2\text{O}$ , where  $X = \text{Cl}, \text{Br}, \text{I}, \text{NO}_3, \text{NCS}, \text{ClO}_4, \text{BF}_4$  and  $\text{PF}_6$ ,  $n = 0$  or  $1$ , have been prepared and confirmed by microanalysis for  $M = \text{Cr}, \text{Fe}$  and  $\text{Co}$ . The properties of these salts have been studied in the solid state utilizing a variety of techniques including i.r. spectra, X-ray powder diffraction, magnetic susceptibility and dehydration in vacuo. The characteristic i.r. spectra obtained allowed classification of the salts into one of three general spectral types. This classification was found to be dependent on the nature of both the metal and anion in addition to the presence or absence of water of hydration.

The chloride salts of all three complex metal cations were found to be isostructural monohydrates of particular interest. The water molecule appeared to be unusual in that it:

- (1) produced two sharp absorptions in the O-H stretching region of the i.r. spectrum;
- (2) stabilized the low spin state of  $\text{Fe}(\text{III})$  in  $\text{Fe}(\text{saen})_2\text{Cl} \cdot \text{H}_2\text{O}$ .

The solution properties of the salts were studied via n.m.r. and u.v.-visible spectra, conductance and magnetic susceptibility measurements. In contrast to the results obtained in water and alcohol, association of the chloride salts was observed in the aprotic solvent DMSO, with the evidence supporting the conclusion that the water molecule also remained bound.

In order to rationalize the behaviour of the water mole-

cule, the molecular structure of  $\text{Fe}(\text{saen})_2\text{Cl}\cdot\text{H}_2\text{O}$  was determined by the single crystal X-ray diffraction technique. The water molecule was found to be strongly bound into the crystal lattice via unusual, specific hydrogen bonding interactions. These specific interactions involve one cation ammine hydrogen atom with the water oxygen and one water hydrogen atom with the anion. The mode of bonding of the water molecule has enabled the above-mentioned unusual features to be explained.

## STATEMENT

This thesis contains no material which has been accepted for the award of any other degree or diploma in any University, and to the best of my knowledge and belief, contains no material previously published or written by another person, except where due reference is made in the text of the thesis.

A. P. SUMMERTON

### ACKNOWLEDGEMENTS

My sincerest thanks are extended to all who have been involved with my research project - friends, colleagues and students at both the S.A. Institute of Technology and the University of Adelaide. I am grateful to Prof. R.V. Culver of S.A.I.T. and Prof. D.O. Jordan of the University for making available to me the facilities to undertake this work; to Dr. Mike Snow and Mr. John Westphalen for assistance with the crystal structure, and to Mrs. Trish McMurtrie for the typing of this thesis. The expertise, interest and friendship of Mr. Keith Johnson of S.A.I.T. has been appreciated immensely. The guidance, patience, consideration and advice I have received from my supervisor, Dr. Alex Diamantis, over a number of years, has proved of inestimable value in completing this research.

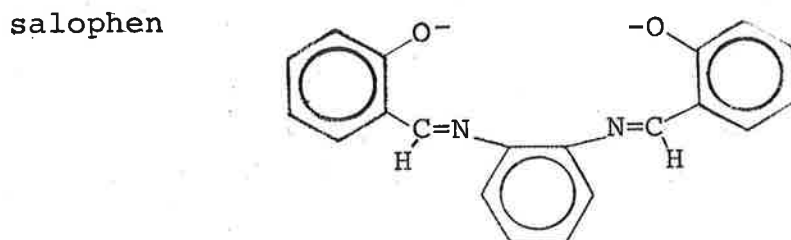
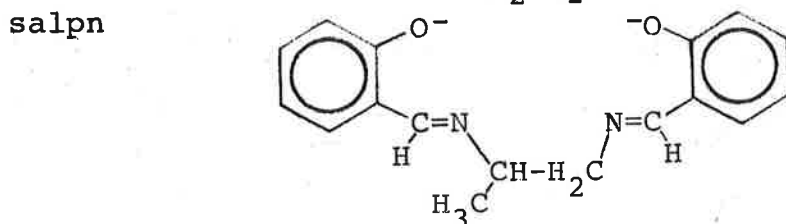
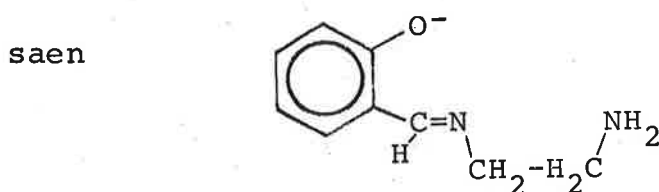
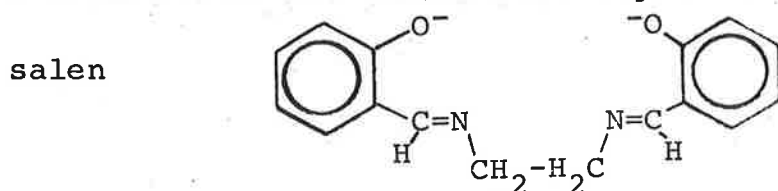
Finally, I am indebted to my parents, my wife Kathryn and daughters, Lynda and Kerry, to whom I wish to dedicate this work.

## ABBREVIATIONS

The following abbreviations have been used in the text of this thesis:

acac	Acetylacetonate
C <sub>6</sub> H <sub>5</sub> COO	Benzoato
DMF	Dimethylformamide
DMSO	Dimethylsulphoxide
EtOH	Ethanol
en	1,2 diaminoethane (ethylenediamine)
MeOH	Methanol
ophen	2 aminoaniline (o-phenylenediamine)
pn	1,2 diaminopropane (propylenediamine)
sal	salicylaldehydato

Structures of the Schiff base ligands involved in this study:





CHAPTER 11.1 INTRODUCTION

From an historical viewpoint, Chemistry received recognition as a scientific discipline in its own right as recently as 1789, with the establishment of the first Chair in Chemistry<sup>(1)</sup>. Prior to this, it was merely considered to be a branch of Medical Science. The profound influence of the 'biological bias' in scientific thought is readily reflected in the controversy surrounding the 'vital force' theory, which many scientists regard as having significantly retarded the advancement of organic chemistry during the early nineteenth century<sup>(2)</sup>. An indication of the animosity generated by this controversy is provided by Berzelius, who, on being informed of Wohler's urea synthesis, is reported to have stated that 'whosoever started on the path of immortal fame with urine was bound to end in it'<sup>(3)</sup>.

Chemistry has rapidly developed during the ensuing period, with the inevitable accumulation of a vast mass of knowledge. It is hardly surprising that sub-division into major areas, such as Analytical, Inorganic, Physical, Organic and Biochemistry, has occurred in an effort to quantify this knowledge. Such areas have become effectively isolated disciplines today, and increasing specialization in narrower and narrower fields appears the norm for postgraduate research.

It is interesting to note an apparent reversal in this trend where emphasis is placed on the interaction between supposedly isolated disciplines. As a particular example, the

rapidly developing field of Bio-inorganic Chemistry overlaps significantly into areas traditionally associated with Biochemistry and Biology<sup>(4)</sup>. In this field, the especial expertise of the coordination chemist is applied to specific problems, of major importance to the 'life sciences', such as the chemistry of the important naturally occurring metalloproteins<sup>(4)</sup>. A particularly useful approach utilizes 'model compounds', whereby, through the invention, synthesis and detailed study of suitable simple systems, some insight into the workings of the natural system may be achieved<sup>(4)</sup>.

A large number of the model systems involve the complexes of a 'family' of ligands collectively referred to as 'Schiff bases'. Such ligands contain the azomethine group ( $-RC=N-$ ), and one class of such compounds which has been intensively studied involves the N,N'-ethylene bis (salicylideneimine) dianion, traditionally abbreviated as salen. Cobalt complexes of this ligand provide a typical illustration of the application of such compounds as biological models. Co(II)salen (a) is able to absorb oxygen reversibly<sup>(5)</sup>, and (b) may be reduced to  $(Co(I)salen)^-$ <sup>(6)</sup>, which reacts with alkyl halides to form complexes formulated as RCo(III)salen. The alkyl group, R, is directly bonded to the cobalt through the carbon atom<sup>(7)</sup>. Similar reactions have been observed with a naturally occurring system involving a coenzyme of vitamin B<sub>12</sub><sup>(8)</sup>.

Although Schiff base complexes have proved of significance in the understanding of biological systems, the chemistry of such compounds is of considerable interest in its own right

and has occupied a central role in the development of modern coordination chemistry<sup>(9)</sup>. Of all the complexes studied, those with salicylaldehyde ligands, and in particular salen, have received the most attention<sup>(9)</sup>. In fact a recent review, devoted solely to the compounds of salen, cites 155 major references covering a six year period<sup>(10)</sup>. No doubt this is due, in part, to the fact that salen complexes have been obtained with many metals, including the majority of the transition elements. However, a significant factor must be the diversity in the chemical behaviour of these compounds, as illustrated in the review article by Hobday and Smith<sup>(10)</sup>.

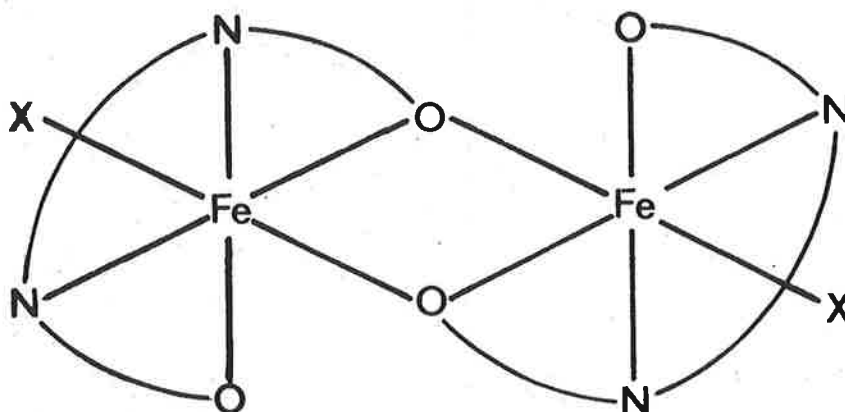
## 1.2 RESEARCH PROGRAM - Aim and Rationale

The primary aim of this research study is the determination of the Moessbauer parameters for a series of iron(III) complexes and the elucidation of the correlation, if any, between these and other information which may be related to the bonding of ligands.

A convenient system, for such a study, would be a series of iron(III) complexes in which the ligand occupying one coordination site may be varied whilst the remaining positions have the same coordination environment. The series selected is that of general formula Fe(III)salenX, where X is the unidentate ligand varied.

Salen is a quadridentate ligand, and the iron(III)salenX complexes would be expected to be square pyramidal. The structure determination of the chloro-complex showed it to be a dimer with asymmetric bridging between the monomers via

intermolecular interactions involving the central ion and an adjacent phenolic oxygen. This results in essentially octahedral coordination as shown in the following diagram<sup>(10,11)</sup>:



At the time this study was commenced (1970), only a few members of the series had been reported ( $X = \text{Cl}$ <sup>(12)</sup>,  $\text{Br}$ <sup>(13)</sup> and  $\text{C}_6\text{H}_5\text{COO}$ <sup>(14)</sup>)<sup>†</sup>. Furthermore, there was substantial disagreement in the Moessbauer data available. The published values for the chloro complex covered a range of 0.57 to 0.71 mm/sec. for the centre shift and 0.71 to 1.45 mm/sec. for the quadrupole splitting<sup>(15,16,17)</sup>.

In broad outline, then, the proposed research program involves the preparation and characterization of the series  $\text{Fe(III)salenX}$ , determination of the Moessbauer parameters and any other data which may be relevant to the bonding of X. This study is presented in Part I (Chapters 2, 3 and 4) of this thesis.

In Part II (Chapters 5, 6 and 7), the properties of complexes of the tridentate ligand, saen, are investigated. The interest in this ligand arose as a consequence of the

---

<sup>†</sup> During the course of this study the complexes with  $X = \text{I}$ <sup>(173)</sup> and  $\text{NCS}$ <sup>(174)</sup> have been reported.

observation of several unusual aspects in the properties of the low spin hydrate, of formula  $\text{Fe(III)(saen)}_2\text{Cl}\cdot\text{H}_2\text{O}$ . In particular, the interest centred on the water molecule which appeared to be responsible for unusual features in the i.r. spectra as well as the stabilization of the low spin state.

P A R T I

Complexes of the quadridentate ligand, salen.

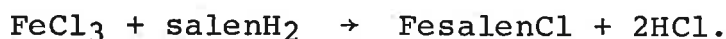
## CHAPTER 2

Preparation and characterization of salen complexes of iron(III).

### 2.1 PREPARATION

#### (i) Application of published methods

The complex  $\text{FesalenCl}$  may be synthesized by the direct reaction of anhydrous ferric chloride,  $\text{FeCl}_3$ , with the Schiff base,  $\text{salenH}_2$ , in the stoichiometric ratio 1:1, utilizing an organic solvent such as acetone or ethanol<sup>(13)</sup>. This reaction may be described by the equation:



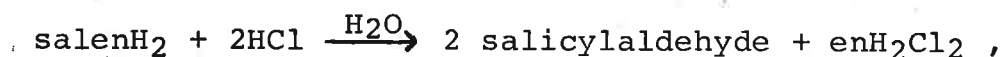
This procedure gives high yields of quite pure product provided small quantities are involved (<0.01 mole).

In this study, larger quantities (c.a. 0.1 mole, 36 grams) were required as a starting material. Attempts to apply this direct reaction on such a scale resulted in low yields (<30%) of impure solid contaminated with free salicylaldehyde. Purification of the impure product by solvent extraction with acetone gave, in addition to crystalline  $\text{FesalenCl}$ , white, acetone insoluble crystals. The latter compound was identified as the hydrochloride salt of 1,2 di-aminoethane, en, and is denoted hereafter as  $\text{enH}_2\text{Cl}_2$ . This information suggested that hydrolysis of  $\text{salenH}_2$  had occurred.

A spectral investigation of the hydrolysis of  $\text{salenH}_2$  (discussed in detail in Chapter 3, section 3.3 (b)) shows that irreversible hydrolysis of  $\text{salenH}_2$  occurs rapidly in acidic solutions. Clearly, then, the problem as outlined

above, is a result of the difficulty in eliminating HCl when large scale preparations are involved. A synthetic procedure of general application to salicylaldehyde complexes recommends reaction of the metal ion and Schiff base in the presence of added base<sup>(9)</sup>. Attempted syntheses utilizing sodium hydroxide, ethoxide, carbonate and acetate, all resulted in the formation, in near quantitative yield, of the well known oxo species, (Fesalen)<sub>2</sub>O. The spectral data in 3.3(b) confirm that in the presence of a strong base, such as sodium hydroxide, the dianion, salen<sup>2-</sup>, is probably present in solution. It would appear that rapid hydrolysis of any FesalenX, formed in solution, to (Fesalen)<sub>2</sub>O is caused by the excess of added alkali.

However, the spectrum of salenH<sub>2</sub> is not affected by the presence of a hundredfold molar excess of en. In fact the only noticeable effect of en is an increase in the solubility of salenH<sub>2</sub>. As the hydrolysis of salenH<sub>2</sub> in acid solution may be represented as:

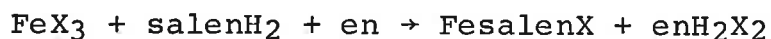


addition of a moderate excess of en to the reaction mixture could be expected to react with the free acid in preference to the hydrolysis.

Syntheses attempted utilizing the Fe(III) salt, salenH<sub>2</sub> and en in the mole ratio 1:1:1.2 proved successful.

(ii) Reaction schemes for the synthesis of FesalenX

Scheme A - modified direct reaction.

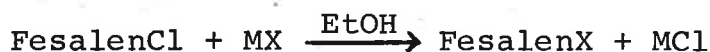


where X = Cl, Br, NO<sub>3</sub> or C<sub>6</sub>H<sub>5</sub>COO.



With this modified procedure, the reaction proceeded smoothly giving high yields of product utilizing either anhydrous or hydrated Fe(III) salts (e.g.  $\text{FeCl}_3 \cdot 6\text{H}_2\text{O}$ ,  $\text{FeBr}_3 \cdot 6\text{H}_2\text{O}$  and  $\text{Fe}(\text{NO}_3)_3 \cdot 9\text{H}_2\text{O}$ ).

Scheme B - metathesis



where X = N<sub>3</sub> and I (M = K or Na), NCS and Br (M = K, Na or NH<sub>4</sub>).

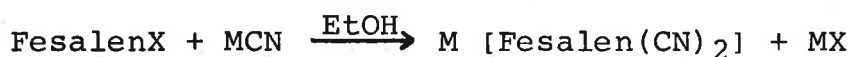
Any salt MX can be used provided  $K_{sp}\text{MX} > K_{sp}\text{MCl}$  in ethanol, which was the solvent utilized. Alternatively, FesalenNO<sub>3</sub> can replace FesalenCl, and acetone may be used as solvent. Attempts to prepare FesalenX with X = CH<sub>3</sub>COO, NO<sub>2</sub>, OH or OEt (M = Na) resulted in the formation of (Fesalen)<sub>2</sub>O.

Purification of the products, FesalenX, by solvent extraction is discussed in the experimental section of this Chapter.

(iii) Novel Compounds

(a) Dicyano complex

Metathetical reactions using cyanide salts resulted in the formation of the green anionic species  $[\text{Fesalen}(\text{CN})_2]^-$ .



where X = any of the ligands Cl, Br, I, NCS, NO<sub>3</sub>, N<sub>3</sub> or C<sub>6</sub>H<sub>5</sub>COO and M = NH<sub>4</sub> or K.

Alternatively, the oxo compound may be used:



(b) Product of reaction with 1,2 diaminoethane

Reaction of  $\text{Fe}(\text{salen})\text{Cl}$  with en yielded a deep blue crystalline solid with a formula corresponding to  $[\text{Fe}(\text{III})\text{salen.en}]\text{Cl}\cdot\text{H}_2\text{O}$ . It was suspected that this species was a mixed bidentate-quadridentate chelate similar to the well studied complex,  $\text{Co}(\text{salen})\text{acac}$ , but in fact proved to be the bistridentate complex  $\text{Fe}(\text{III})(\text{saen})_2\text{Cl}\cdot\text{H}_2\text{O}$ . A more detailed discussion of the properties of complexes with the ligand saen is presented in Part III, however, some information relevant to the  $\text{Fe}(\text{III})$ chloro complex is discussed in this part of the thesis.

2.2 CHARACTERIZATION OF COMPLEXES

(i) Analyses

The data obtained for the elements carbon, hydrogen, nitrogen and iron are presented in Table 2.1.

The analytical data confirm the compounds as formulated.

(ii) Solid state studies

Further characterization of these compounds was effected by measurement of the following solid state parameters:

- (a) Magnetic moments;
- (b) U.V.-visible spectra;
- (c) Infra-red spectra;
- (d) Moessbauer spectra.

The Moessbauer spectra and data are discussed separately in Chapter 4.

TABLE 2.1  
Analytical Data

Compound		Formula	Calculated				Found			
			C	H	N	Fe	C	H	N	Fe
(a)	FesalenX	$C_{16}H_{14}N_2O_2FeX$								
	X = Cl	$C_{16}H_{14}N_2O_2FeCl$	53.7	4.0	7.8	15.6	53.5	4.0	7.9	15.5
	Br	$C_{16}H_{14}N_2O_2FeBr$	47.8	3.5	7.0	13.9	47.9	3.6	7.1	13.6
	I	$C_{16}H_{14}N_2O_2FeI$	42.8	3.1	6.2	12.4	42.9	3.2	6.2	12.4
	NO <sub>3</sub>	$C_{16}H_{14}N_3O_5Fe$	50.0	3.7	10.9	14.5	50.0	3.7	10.9	14.4
	NCS	$C_{17}H_{14}N_3O_2FeS$	53.7	3.7	11.1	14.7	53.7	3.7	11.1	14.6
	N <sub>3</sub>	$C_{16}H_{14}N_5O_2Fe$	52.8	3.9	19.2	15.2	52.7	4.0	19.0	15.2
	C <sub>6</sub> H <sub>5</sub> COO	$C_{23}H_{19}N_2O_4Fe$	62.3	4.3	6.3	12.6	61.9	4.3	6.3	12.7
(b)	(Fesalen) <sub>2</sub> O	$C_{32}H_{28}N_4O_5Fe$	58.2	4.3	8.5	16.9	58.2	4.3	8.4	17.0
(c)	M[Fesalen(CN) <sub>2</sub> ]									
	M = NH <sub>4</sub>	$C_{18}H_{22}N_6O_2Fe$	55.1	4.6	17.9	14.2	54.4	4.5	17.6	14.0
	M = K	$C_{18}H_{14}N_4O_2FeK$	52.3	3.4	13.6	13.5	52.1	3.6	13.4	13.6
(d)	Fe(saen) <sub>2</sub> Cl·H <sub>2</sub> O	$C_{18}H_{24}N_4O_2FeCl$	49.6	5.6	12.9	12.8	49.3	5.6	12.8	12.8

(a) Magnetic moments

The Fe(III) ion has five 3d electrons and the electronic ground state may have five, three or one unpaired electron(s). As the  $t_{2g}^4 e_g^1$  configuration only occurs in a tetragonally distorted field, the possible electronic configurations in an essentially octahedral ligand field are  $t_{2g}^3 e_g^2$  with a total spin,  $S$ , of  $\frac{5}{2}$ , or  $t_{2g}^5$ ,  $S = \frac{1}{2}$  (18). Measurement of magnetic susceptibilities, preferably over a range of temperatures, readily allows the determination of  $S$  in the ground state (18).

As no contribution from the orbital angular momentum is expected for a high spin ( $S = \frac{5}{2}$ ) system the experimental values of the magnetic moment,  $\mu_{eff}$ , should be close to the spin only value of 5.92 B.M. Significant deviations of  $\mu_{eff}$  from this value have been observed and are usually ascribed to dimer formation, as established for  $(FealenCl)_2$  by an X-ray structure determination (19). In such cases the observed range for  $\mu_{eff}$  is 5.0 to 5.4 B.M. (13).

The low spin ( $S = \frac{1}{2}$ ) case is expected to result in values of  $\mu_{eff}$  of the order of 2 B.M., which show considerable temperature dependence.

In this study, magnetic susceptibilities have been determined at room temperature only and as such must be considered of limited value as the sole means of evaluating the ground state configurations. However, as additional information, in the form of Moessbauer data, is available, the variable temperature magnetic studies were not considered essential in this study.

The magnetic susceptibilities and moments are tabulated in Table 2.2.

On the basis of the observed magnetic moments, three categories of iron(III) Schiff base complexes have been proposed<sup>(10,11)</sup>:

- (1) Spin free, paramagnetic systems with  $\mu_{\text{eff}}$  near 5.92 B.M., e.g. the monomer,  $\text{Fe}(\text{salen})\text{Cl}$ .
- (2) Weakly coupled antiferromagnetic systems with  $\mu_{\text{eff}} \approx 5.2$  B.M., e.g. the dimer,  $(\text{Fe}(\text{salen})\text{Cl})_2$ .
- (3) Medium coupled antiferromagnetic systems with  $\mu_{\text{eff}} \approx 2$  B.M., e.g.  $(\text{Fe}(\text{salen}))_2\text{O}$ .

Thus the majority of complexes studied for this work appear to be dimeric ( $X = \text{Cl}, \text{Br}, \text{I}, \text{NCS}$  and  $\text{N}_3$ ) and two monomeric ( $X = \text{C}_6\text{H}_5\text{COO}$  and  $\text{NO}_3$ ).

The two compounds with  $\mu_{\text{eff}}$  near 2 B.M. require further consideration. The above proposal suggests that these compounds are similar to  $(\text{Fe}(\text{salen}))_2\text{O}$ , i.e. dimers with antiferromagnetic exchange occurring between two high spin ( $S = \frac{5}{2}$ ) iron(III) centres resulting in a pseudo low spin value for  $\mu_{\text{eff}}$ . In fact, these compounds are both believed to be low spin ( $S = \frac{1}{2}$ ), although the single temperature magnetic measurements in no way provides conclusive evidence.

A more pertinent argument is provided by the coordination environment of iron(III) in these complexes. In  $\text{Fe}(\text{saen})_2\text{Cl} \cdot \text{H}_2\text{O}$ , the iron(III) is involved in an octahedrally coordinated cation,  $\text{Fe}(\text{saen})_2^+$ <sup>(20)</sup>. The interatomic distances in this

TABLE 2.2

Compound	Colour of finely divided solid	Molar Susceptibility $\bar{\chi}_M$ (corrected) (b)	T°K	$\mu_{eff}$ (a)	$\mu_{eff}$ (published)
FesalenCl	violet-brown	152 458	293.2	5.33	5.34 <sup>(13)</sup>
Br	black	154 594	295.2	5.39	5.40 <sup>(13)</sup>
I	black	145 517	293.1	5.21	
NO <sub>3</sub>	violet	183 134	293.6	5.85	
NCS	chocolate brown	150 343	295.5	5.31	
N <sub>3</sub>	red brown	151 034	294.1	5.33	
C <sub>6</sub> H <sub>5</sub> COO	deep red	188 009	293.9	5.93	5.88 <sup>(14)</sup>
K[Fesalen(CN) <sub>2</sub> ]	bright green	23 739	293.1	2.10	
Fe(saen) <sub>2</sub> Cl.H <sub>2</sub> O	blue	23 606	296.6	2.11	

(a) estimated error  $\pm$  .03 B.M.

(b) S.I. units, i.e.  $\times 10^{-12} \text{m}^3 \text{mol}^{-1}$

cation are consistent with a low spin Fe(III) complex, as discussed later in this thesis. The formulation of the anionic species  $[\text{Fesalen}(\text{CN})_2]^-$  is indicative of octahedral coordination also, and it would appear that the possibility of anti-ferromagnetic coupling is precluded in such complexes. Additional evidence provided by Moessbauer spectral data, as discussed in Chapter 4, strongly support the proposition that both complexes are indeed low spin.

(b) U.v.-visible spectra - reflectance and mull

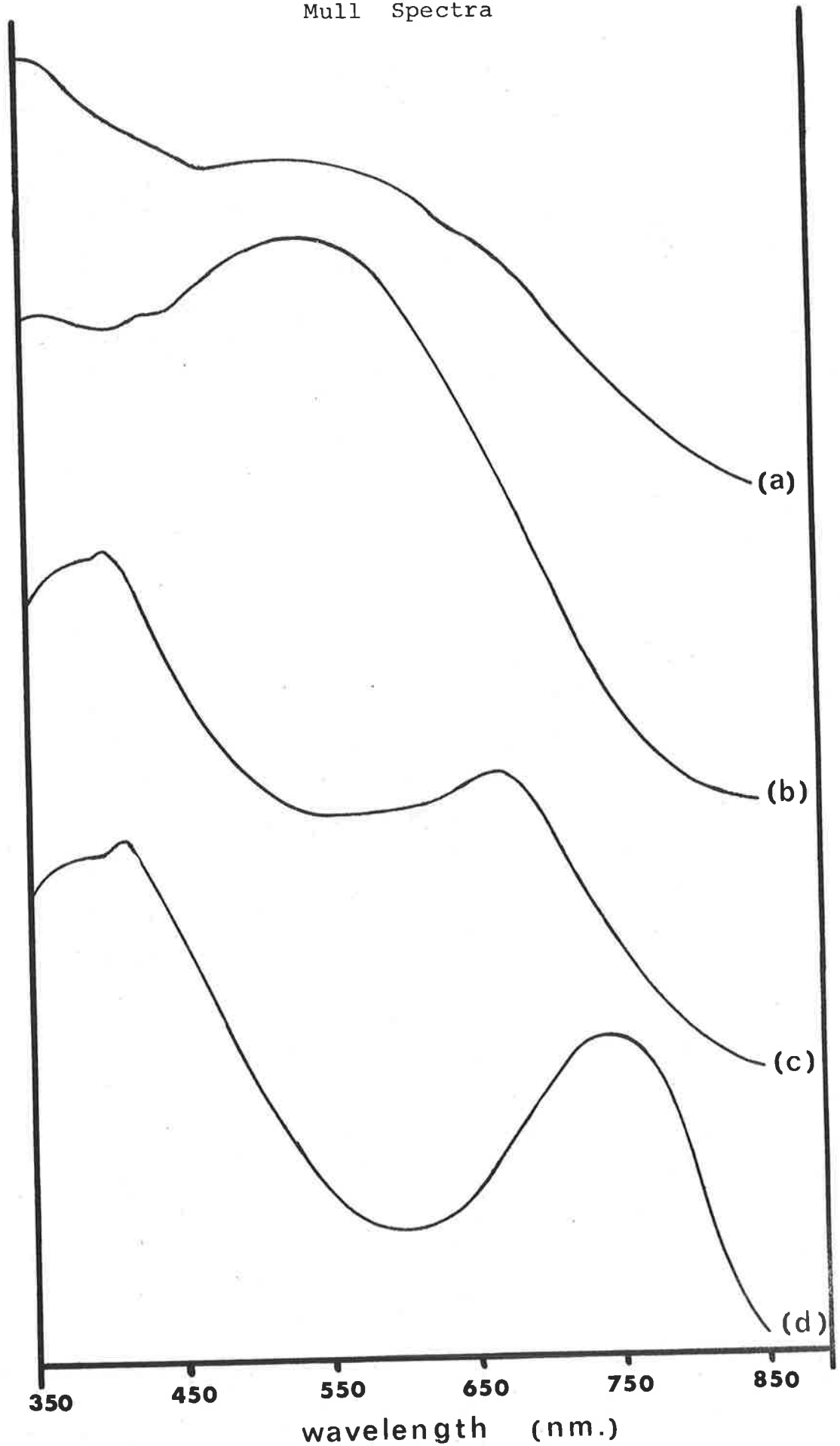
For a  $d^5$  ion in a cubic field, such as a high spin, octahedrally coordinated iron(III) species, the electronic ground state is designated as  ${}^6A$ . As no other spin-sextuplet energy levels occur in this system, all 'd-d' transitions are spin forbidden and would be expected to result in very low intensity transitions in the visible region<sup>(18)</sup>. In addition such transitions may well be obscured by intense metal-ligand charge transfer absorptions, which are known to occur at relatively low energies<sup>(18,21)</sup>.

All of the compounds studied in this work are intensely coloured, suggesting that such charge transfer absorptions probably occur. In particular, the crystalline samples of the FesalenX series are extremely dark, almost black, needles. When finely divided, the solids have a characteristic hue as described in Table 2.2.

The solid state spectra (reflectance and mull) of the complexes show a broad absorption in the visible and near ultraviolet. A representative selection of the mull spectra

Figure 2.1  
Mull Spectra

Absorbance



- (a)  $\text{FesalenCl}$  (b)  $\text{FesalenC}_6\text{H}_5\text{COO}$  (c)  $\text{Fe(saen)}_2\text{Cl}\cdot\text{H}_2\text{O}$   
(d)  $\text{K[Fesalen(CN)}_2]$



are reproduced in Figure 2.1. The major contribution to the spectra of the FesalenX type of compound (spectra (a) and (b)) must be the metal ligand charge transfer absorption(s). However, in two cases (X = NO<sub>3</sub> and C<sub>6</sub>H<sub>5</sub>COO) the presence of 'weak humps' in the broad envelope may indicate the presence of 'd-d' type transitions. It is felt that, in general, no meaningful information may be obtained from these spectra.

The two remaining spectra do have features which may prove of interest. The complexes involved are the low spin octahedral species discussed above. In  $S = \frac{1}{2}$  systems spin-allowed d-d transitions from the  ${}^2T_2$  ground state are well known<sup>(18)</sup>. The prominent bands centred at 640 nm (Fe(saen)<sub>2</sub>Cl·H<sub>2</sub>O - spectrum (c)) and 750 nm (K[Fesalen(CN)<sub>2</sub>] - spectrum (d)) may be assigned to such transitions, with the relatively high intensity being rationalized in terms of the effect of 'mixing' of charge transfer with the 'd-d' absorptions<sup>(18)</sup>.

(c) Infra-red spectra

The infra-red spectra of all compounds have been obtained over the range 4,000 - 400 cm<sup>-1</sup>. Many similar features have been observed, including:

- (1) all have a multiplet near 750 cm<sup>-1</sup>,
- (2) all salen complexes have two prominent bands of similar intensity between 400 and 500 cm<sup>-1</sup>,
- (3) all salen complexes have no prominent bands of significance above 2,200 cm<sup>-1</sup> other than a similar series of very weak C-H stretch vibrations between 2,800 and 3,100 cm<sup>-1</sup>.

In the region from 1,800 to 400 cm<sup>-1</sup> each spectrum is

Figure 2.2  
Infra-red Spectra

- (a) SalenH<sub>2</sub>
- (b) Fe(salen)<sub>2</sub>O
- (c) FesalenCl
- (d) FesalenI
- (e) FesalenNO<sub>3</sub>
- (f) FesalenNCS
- (g) FesalenN<sub>3</sub>
- (h) K[Fesalen(CN)<sub>2</sub>]
- (i) Fe(saen)<sub>2</sub>Cl.H<sub>2</sub>O

Figure 2.2 (a) - (c)

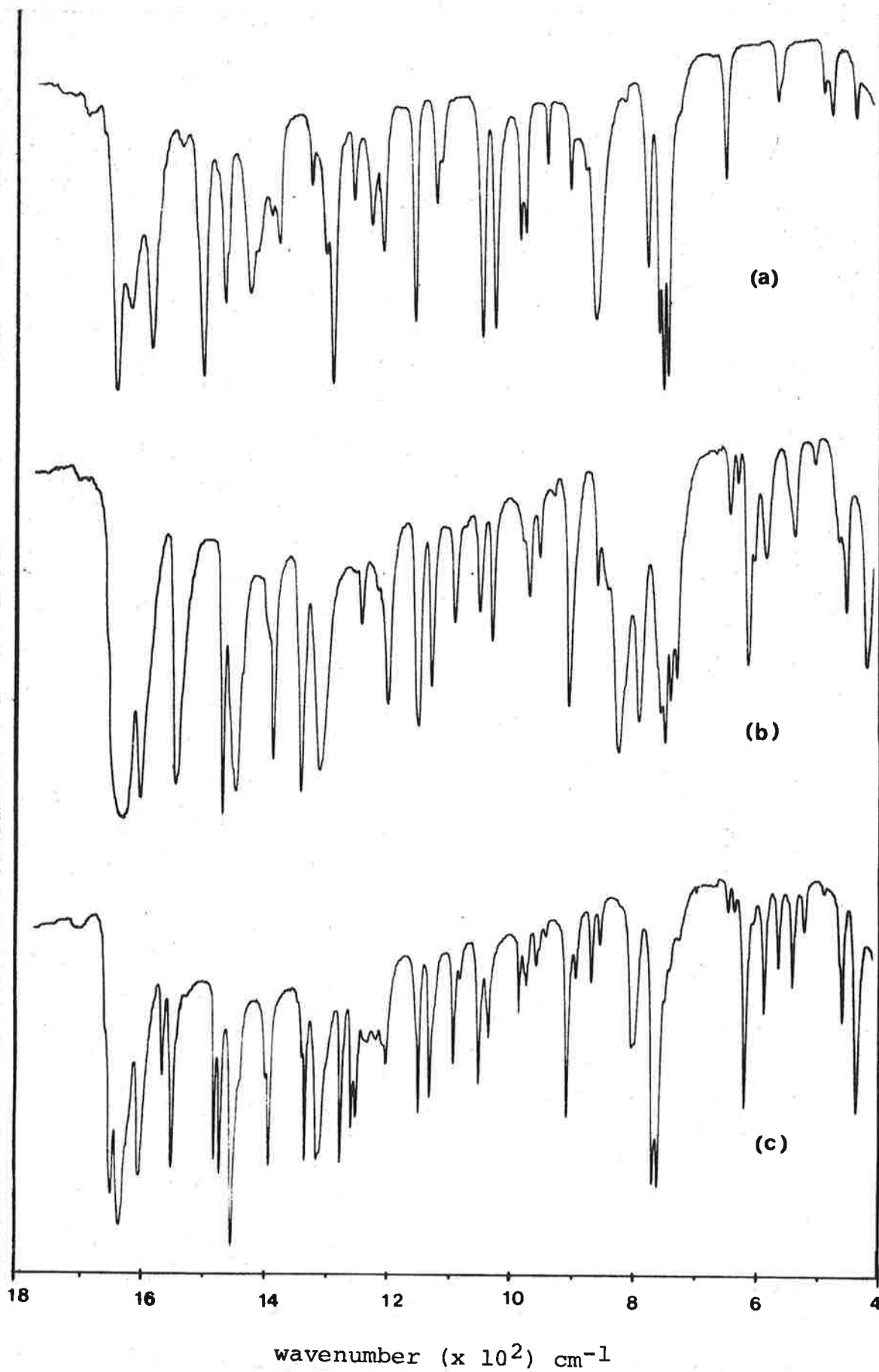


Figure 2.2 (d) - (f)

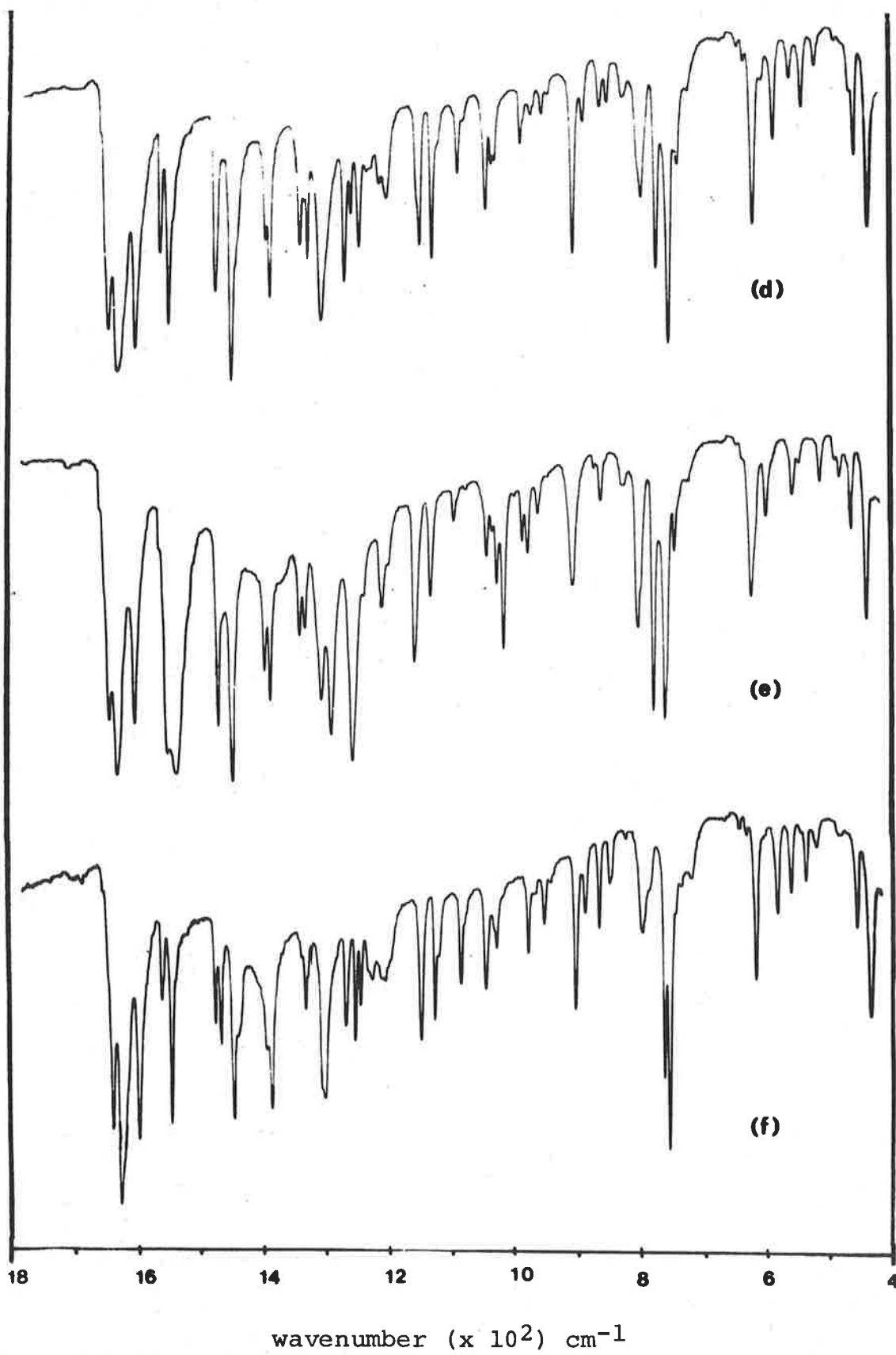
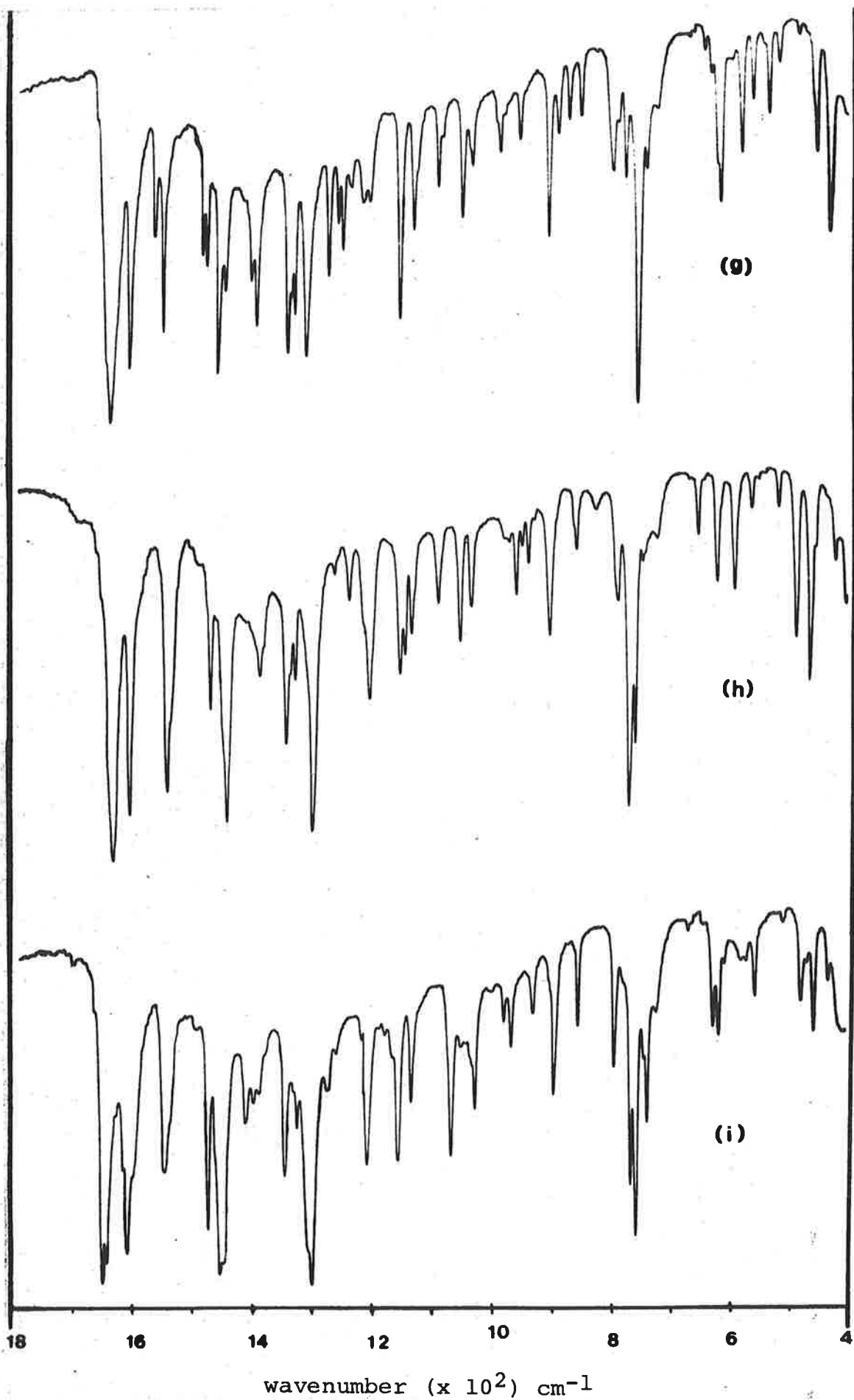


Figure 2.2 (g) - (i)



unique and may thus be considered as characteristic of the individual complex. A representative selection of these spectra have been reproduced in Figure 2.2.

Comparison of the spectrum of the free ligand salenH<sub>2</sub>, (a), with those of the salen complexes, (b) - (h), clearly show that many of the salen ligand vibrational bands are affected markedly on chelation. There appears to be little value in attempting to assign all spectral bands to specific vibrational transitions as the similarities in the spectra are vastly outnumbered by the differences. These spectra have been used as a means of identifying qualitatively species isolated from various reactions.

However, several spectra do contain prominent bands, frequently outside the range 1,800 - 400 cm<sup>-1</sup>, which may be used to confirm that coordination has occurred between the ligand X and the metal. Relevant data are reproduced in Table 2.3, and all band positions are consistent with those expected for coordinated X.

As a further example, in a more detailed examination of the spectrum of the complex FeSalenNCS below 900 cm<sup>-1</sup>, several additional bands, not present in the similar spectrum of FeSalenCl, can be observed. These are:

- (a) at 848 cm<sup>-1</sup>, as a shoulder on the band at 852 cm<sup>-1</sup>;
- (b) a weak doublet, at 485 and 478 cm<sup>-1</sup>.

For the system M-NCS, bands are found between 870-820 cm<sup>-1</sup> ( $\nu_{C-S}$ ) and 485-475 cm<sup>-1</sup> ( $\delta_{NCS}$ ), whereas for M-SCN the corres-

TABLE 2.3

X	$\nu$ $\text{cm}^{-1}$	relative intensity (a)	$\nu_{\frac{1}{2}}$ ( $\text{cm}^{-1}$ ) (b)	Reference
$\text{N}_3$	2055	0.91	45	(22) p.176
NCS (c)	2055	1.02	50	(22) p.173-174
$\text{NO}_3$	1535	1.34	$\approx$ 30	(22) p.161
$\text{C}_6\text{H}_5\text{COO}$	688	0.76	7	(d)
	719	0.98	11	
	1420	1.06	$\approx$ 50	
	1500	0.87	$\approx$ 10	
	1515	0.91	$\approx$ 30	
CN (2 off)	2115	0.62	10	(22) p.166
	2135	0.27	10	

Notes:

(a) Relative Intensity =  $\frac{\text{observed intensity of peak}}{\text{intensity of major peak in } 750 \text{ cm}^{-1} \text{ multiplet}}$

(b)  $\nu_{\frac{1}{2}}$  = peak width at half-height.

Where approximate values of  $\nu_{\frac{1}{2}}$  are given, the value has been estimated from overlapping bands.

(c) Absorption for thiocyanate in range expected for coordination via the nitrogen atom.

(d) Assignment of bands based on comparison with the i.r. spectra of  $\text{C}_6\text{H}_5\text{COO}^-\text{Na}^+$  and  $\text{Fe}(\text{C}_6\text{H}_5\text{COO})_3$ .

ponding transitions are  $760-700 \text{ cm}^{-1}$  ( $\nu_{\text{C-S}}$ ) and  $470-430 \text{ cm}^{-1}$  ( $\delta_{\text{NCS}}$ ) (23). This evidence confirms the proposition that the thiocyanate group is coordinated to the metal via the nitrogen atom.

### 2.3 STRUCTURE OF COMPLEXES IN THE SOLID STATE

The characterization outlined above, confirms that the compounds are as formulated in Table 2.1. Two aspects of the structure of these complexes requiring further clarification are:

- (i) What is the arrangement of the cyanide ligands in the anion  $[\text{Fesalen}(\text{CN})_2]^-$  - cis or trans?
- (ii) Are the species of the series  $\text{FesalenX}$  penta-coordinate monomers or pseudo-octahedral dimers?

#### (i) The Anion, $[\text{Fesalen}(\text{CN})_2]^-$

The assignment of the configuration, cis or trans, of dicyano complexes may be decided on the basis of the number of bands observed in  $\text{C}\equiv\text{N}$  stretch region of the i.r. spectrum. On theoretical grounds, the trans configuration spectrum is expected to have a single band, as is the case in known trans-dicyano complexes (24). On the other hand, two closely spaced bands are indicative of the cis configuration as has also been observed (25).

The Chromium and cobalt analogues of the iron(III) salt have been prepared (26,27) and the trans configuration has been assigned, apparently arbitrarily, to the complex  $\text{K}[\text{Cosalen}(\text{CN})_2]$  (28). A sample of this compound has been prepared, and the



i.r. spectrum examined. The spectra of both the Fe(III) and Co(III) salen dicyano salts are very similar in the 'characteristic' 1,800 - 400  $\text{cm}^{-1}$  region and the  $\text{C}\equiv\text{N}$  stretch region.

The assignment of a trans configuration to these dicyano species could perhaps be justified on the basis that salen acts as a planar, quadridentate ligand. However this justification is clearly in error as at least two species, namely Co(III) salen.acac<sup>(29)</sup> and dioxo Mo(VI)salen<sup>(30)</sup>, have been shown to have a non planar salen moiety. In such non planar systems, the n.m.r. signal assigned to protons in the azomethine group consists of two resonances<sup>(31)</sup>. No splitting could be observed in the n.m.r. spectrum of  $\text{K}[\text{Cosalen}(\text{CN})_2]$ , which indicates that the salen moiety is not coordinated in the same way as in Cosalen.acac.

In addition, a partially characterized complex formulated as  $\text{K}[\text{Fesalophen}(\text{CN})_2]$  has been prepared, and the i.r. spectrum of this compound also has two sharp bands in the  $\text{C}\equiv\text{N}$  stretch region at 2120 and 2140  $\text{cm}^{-1}$ . The ligand salophen is completely conjugated and is known to exhibit planar coordination only<sup>(31)</sup>. This dicyano complex must have a trans configuration.

Laser Raman spectra of the three dicyano species have been attempted, but, due to decomposition of the Fe(III) complexes, meaningful data have only been obtained for  $\text{K}[\text{Cosalen}(\text{CN})_2]$  with sharp absorptions at 2126 and 2150  $\text{cm}^{-1}$ , which is the same as in the i.r. spectrum. The theoretical considerations leading to the prediction of two bands in the i.r. spectrum of a cis dicyano system, require that the bands

should be found at energies some  $100\text{ cm}^{-1}$  higher than in the i.r. spectra. Clearly then these two bands do not occur simply as a result of a cis configuration.

The Fe(III) anions readily undergo decomposition in aqueous solutions, whereas the Co(III) species may be re-crystallized from water. Consequently, a series of salts of the Co(III)salen(CN)<sub>2</sub> anion have been prepared with a number of different cations. The band positions and relative intensities appear anion dependent. The data are tabulated in Table 2.4.

No pattern can be elucidated from this data in terms of cation charge or size, although it would appear reasonable to suggest that packing in the crystal lattice would be influenced by such variables. Therefore it is proposed that the two bands observed in the C≡N stretch region arise because of 'solid state' or 'lattice' effects.

Such behaviour is not uncommon in polynuclear cyano complexes. The spectra of hexacyano species would be expected to have one band only in the C≡N stretch region<sup>(22)</sup>. However, in the complexes  $\text{K}_3[\text{Co}(\text{CN})_6]$ ,  $\text{K}_3[\text{Fe}(\text{CN})_6]$  and  $\text{K}_4[\text{Fe}(\text{CN})_6]$ , three, one and seven bands are observed respectively<sup>(22)</sup>. This is attributed to a 'lattice' effect<sup>(22)</sup>.

The dicyano compounds would appear to have a trans arrangement of the cyanide ligands and a square planar Schiff base moiety. The presence of two bands from the C≡N stretching vibrations is best rationalized as a solid state (or lattice)

TABLE 2.4

Data for salts with the Co(III)salen(CN)<sub>2</sub> anion

Cation	C≡N stretching frequencies (cm <sup>-1</sup> )	Intensity * ratio
K <sup>+</sup>	2130 (ν <sub>1/2</sub> =10), 2155 (ν <sub>1/2</sub> =10)	1:2
Ag <sup>+</sup>	2125 (sh), 2175 (ν <sub>1/2</sub> =20)	1:0.06
Co(saen) <sub>2</sub> <sup>+</sup>	2140 (ν <sub>1/2</sub> =20), 2200 (ν <sub>1/2</sub> =30)	1:0.13
Cosalen <sup>+</sup>	2145 (ν <sub>1/2</sub> =20), 2200 (ν <sub>1/2</sub> =30)	1:0.14
Et <sub>4</sub> N <sup>+</sup>	2140 (ν <sub>1/2</sub> =20), 2200 (ν <sub>1/2</sub> =30)	1:0.23
Ca <sup>2+</sup>	2140 (ν <sub>1/2</sub> =20), 2200 (ν <sub>1/2</sub> =30)	1:0.13
Cu <sup>2+</sup>	2140 (ν <sub>1/2</sub> =20), 2195 (ν <sub>1/2</sub> =30)	1:0.11
Zn <sup>2+</sup>	2145 (ν <sub>1/2</sub> =20), 2180 (sh), 2200 (ν <sub>1/2</sub> =40)	1:0.08
Fe <sup>3+</sup>	2140 (ν <sub>1/2</sub> =20), 2195 (ν <sub>1/2</sub> =30)	1:0.13

\* intensity ratio =  $\frac{\text{Intensity of higher energy absorption}}{\text{Intensity of low energy absorption}}$

effect, indicating the two cyano ligands are not in equivalent environments in the crystal lattice.

(ii) FesalenX series

Previous studies of the chloro complex have established that either dimeric,  $(\text{FesalenCl})_2$ , or monomeric,  $\text{FesalenCl}$ , species may be obtained on recrystallization, depending on the solvent selected<sup>(32)</sup>. The bromo complex apparently behaves in the same way, with the monomeric species having one or more solvent molecules incorporated in the crystal lattice<sup>(16)</sup>. The analytical data presented in Table 2.1 confirm that in the series of FesalenX prepared in this study, no solvent molecules are present. It would appear that solvent incorporation is affected markedly by the rate at which the crystalline species are formed, with the solvent adducts occurring only when the procedure is very slow. Thus the rapid recrystallization, by solvent extraction, used in preparing this series of complexes, would suggest that dimeric species only would be expected.

The assignment of the structure, based on the magnetic moment of the complex, as discussed in section 2.2(ii), indicated that the dimeric structure appeared probable for  $X = \text{Cl}$ ,  $\text{Br}$ ,  $\text{I}$ ,  $\text{NCS}$  and  $\text{N}_3$ , and the monomeric for  $X = \text{NO}_3$  and  $\text{C}_6\text{H}_5\text{COO}$ . An additional criterion has been proposed on the basis of i.r. spectra with supporting evidence from Moessbauer spectra<sup>(16)</sup>. In several cases the magnetic and spectral criteria resulted in differing conclusions, suggesting 'that at least for complexes having magnetic susceptibilities near the spin-only value, the agreement between the magnetic susceptibilities and the suggested dimeric model, is probably fortuitous'<sup>(16)</sup>.

The fundamental premise involves the assignment of an intense band in the i.r. spectra, near  $850\text{ cm}^{-1}$ , to an Fe-O-Fe vibration. The complex  $(\text{Fesalen})_2\text{O}$  has an Fe-O-Fe linkage, and an intense band, near  $825\text{ cm}^{-1}$ , which has been assigned to the assymmetric Fe-O-Fe stretching vibration<sup>(33,34)</sup>. The presence of such a band in the spectra of FesalenX complexes, would then be indicative of a dimeric structure<sup>(16)</sup>.

In order to test this proposition, the i.r. spectra of a number of compounds have been examined in some detail in the region of  $850\text{ cm}^{-1}$ . The positions and relative intensities of the spectral bands are tabulated in Table 2.5.

The M(II)salen complexes, prepared by previously described procedures (where  $M = \text{Co}^{(5)}$ , Cu and Ni<sup>(35)</sup>) are known to have dimeric structures<sup>(10)</sup>. These complexes do have relatively intense bands near  $850\text{ cm}^{-1}$ , however so do all of the other species including the free ligand, salenH<sub>2</sub>.

In the case of the known monomer,  $\text{Fe}(\text{saen})_2\text{Cl}\cdot\text{H}_2\text{O}$ <sup>(20)</sup>, it is not possible for there to be an Fe-O-Fe interaction of the type proposed for  $(\text{FesalenCl})_2$ <sup>(11)</sup>. Furthermore, the Ni(II) complex, denoted in Table 2.5 as Nisalen, is known from the X-ray structural determination to have 'a dimeric structure formed by direct metal-metal interactions'<sup>(10)</sup>.

Consequently, it is suggested that the assignment of a dimeric or monomeric structure solely on the basis of i.r. assignments, is, to say the least, somewhat dubious. Due to the similarity of the spectra, it would appear more reasonable

TABLE 2.5

I.R. SPECTRAL BANDS NEAR 850  $\text{cm}^{-1}$ 

						Structure(2)	
Salen H <sub>2</sub>	902(.25)	878(.20) 862(.67) <sup>(1)</sup>		778(.54)		760(.75) 752(1.0) 745(.96)	
Cu Salen	911(.70)		860(.54) 852(.56)	793(.29)		763(.66) 758(.84) 752(.95) 745(.83) 735(1.0)	D
Co Salen	908(.44)		855(.35) 849(.23)	797(.10)		762(.48) 756(.71) 751(.87) 746(.65) 734(1.0)	D
Ni Salen	905(.70)		855(.40) 848(.44) 832(.17)	800(.25)		750(.85) 740(.96) 733(1.0) 727(.92)	D
(Fe Salen) <sub>2</sub> O	906(.80)		860(.42) 826(.81) <sup>(3)</sup>	792(.98)		759(.93) 751(1.0) 742(.83) 732(.77)	
Fe Salen Cl	906(.58)		891(.18) 866(.20) 855(.11)	801(.43) 795(.41)		767(.96) 758(1.0) 745(.38) 738(.31)	D
Fe Salen Br	905(.60)		889(.27) 862(.22) 851(.22)	798(.57)		776(.84) 755(1.0) 739(.46)	AD
Fe Salen I	905(.59)		888(.22) 862(.19) 850(.17) 827(.15)	797(.47)		772(.77) 753(1.0) 739(.49)	U
Fe Salen NO <sub>3</sub>	905(.41)		872(.06) 862(.16) 827(.09)	802(.60)		778(.97) 760(1.0) 745(.46)	U
Fe Salen C <sub>6</sub> H <sub>5</sub> COO	904(.62)		863(.70) 850(.38) 820(.05)	801(.50) 796(.51)		756(1.0) 740(.39) 734(.40) 719(.98) <sup>(4)</sup>	U
Fe Salen N <sub>3</sub>	905(.49)		888(.21) 870(.19) 850(.19)	798(.41) 789(.27)		776(.46) 755(1.0) 740(.44)	U
Fe Salen NCS	906(.54)		890(.24) 869(.30) 852(.17)	800(.37)		766(.83) 758(1.0) 739(.20)	U
K[Fe Salen(CN) <sub>2</sub> ]	902(.49)		858(.23) 826(.06)	789(.45)		770(1.0) 760(.87) 747(.28)	M
Fe(Salen) <sub>2</sub> Cl.H <sub>2</sub> O	897(.56)		857(.38)	796(.56) 782(.23)		769(.88) 759(1.0) 747(.47) 740(.72)	M

## NOTES:

(1) relative intensities shown in parentheses.

$$\text{relative intensity} = \frac{\text{measured band intensity}}{\text{intensity of prominent band in } \sim 750 \text{ cm}^{-1} \text{ multiplet}}$$

(2) Abbreviations for structure: D = dimeric, AD = assumed dimeric, U = unknown, M = monomeric.

(3) Fe-O-Fe band in (Fe Salen)<sub>2</sub> O.(4) C<sub>6</sub>H<sub>5</sub>COO ligand band.

to assign bands in the 820-890  $\text{cm}^{-1}$  region to salen ligand vibrations, together with the bands at  $904 \pm 7$ ,  $795 \pm 8$   $\text{cm}^{-1}$  and the multiplet near  $750$   $\text{cm}^{-1}$ . Whilst the hypothesis that an Fe-O-Fe linkage may be associated with an i.r. band is valid, the corollary may not necessarily be so.

It appears improbable that a definite assignment of either a dimeric or monomeric structural arrangement to each of the members of the series  $\text{FeSalenX}$  can be decided on the basis of relatively simple data. The only positive method would be to determine the structure of each complex by X-ray diffraction techniques. Such studies would require considerable expenditure of time and effort and may, in fact, be unnecessary, at least for the purposes of this study. There is evidence to suggest that the Moessbauer spectra of monomeric and dimeric species may not be significantly different. This suggestion is explored in detail in Chapter 4.

## 2.4 EXPERIMENTAL

### (i) Starting materials

The purity of the chemicals used did not appear to be critical to the success of the preparative methods. In general, A.R. grade chemicals were used as starting materials and solvents.

### (ii) Preparations

#### (a) SalenH<sub>2</sub>

The condensation reaction between salicylaldehyde and

1,2 diaminoethane, en, is known to occur readily in near quantitative yield<sup>(5)</sup>. A typical example of the ligand preparation follows: A solution of 122.1g of salicylaldehyde (1 mole) in 300 cm<sup>3</sup> of ethanol in a 1 litre beaker, was stirred vigorously and warmed to 60°C. 30g en (0.5 mole) in 300 cm<sup>3</sup> of ethanol was slowly added, and a yellow crystalline solid formed rapidly. The reaction mixture was then gently boiled for 15-20 minutes, allowed to cool overnight and the solid, collected by vacuum filtration, dried for 24 hours at 70°C.

Yield 126g (94%) M.pt. 126°C.

Analysis for C<sub>16</sub>H<sub>16</sub>N<sub>2</sub>O<sub>2</sub>, in quadruplicate:

Calc. C 71.62, H 6.01, N 10.44%

Found C 71.61, H 6.02, N 10.44%

Samples of salenH<sub>2</sub> have been used successfully as a secondary standard in C, H and N determinations.

(b) FesalenX complexes

Scheme A - direct reaction

General method - FeX<sub>3</sub>, salenH<sub>2</sub> and en in mole ratio 1:1:1.2. Finely divided salenH<sub>2</sub> was suspended in a vigorously stirred ethanol-en solution. A solution of the appropriate Fe(III) salt in ethanol was then slowly added to the suspension. Stirring was continued for 30 minutes, and the deeply coloured reaction mixture allowed to stand for a further 30 minutes before vacuum filtration. Any solid product collected was retained, the filtrate evaporated to dryness by rotary evaporation and the solid product collected.



For X = Cl, Br and C<sub>6</sub>H<sub>5</sub>COO, the solid product obtained from the first filtration contained almost all the crude FesalenX, whereas the nitrate was found in the rotary evaporation residue only.

In all cases, the crude product was separated from the enH<sub>2</sub>X<sub>2</sub>, also formed, by extraction in a Soxhlet extraction system with either acetone or chloroform as solvent. The crystalline products, obtained on cooling the resultant solutions, were air dried for 24 hours and analyzed. The samples were found to be essentially pure, and solvent free, after one such extraction, as confirmed by the analyses in Table 2.1.

Example: FesalenNO<sub>3</sub> ( $\frac{1}{10}$  molar scale)

FeNO<sub>3</sub>.9H<sub>2</sub>O, 40g; salenH<sub>2</sub>, 26.8g; en 7g;

ethanol 300 + 300 cm<sup>3</sup>.

Yield of crystalline product 28.3g (74.2%).

All samples were contaminated to some extent with the hydrolytic product, (Fesalen)<sub>2</sub>O. Provided the preparation was completed to the solid crude product stage within 2 to 3 hours, hydrolysis was minimized. As (Fesalen)<sub>2</sub>O is only very slightly soluble in acetone and chloroform, the traces of this complex remained in the extraction thimble with the enH<sub>2</sub>X<sub>2</sub>, and contamination of the purified FesalenX could not be detected.

#### Scheme B - metathesis

General method - FesalenCl or FesalenNO<sub>3</sub> + excess MX.

A suspension of the Fe(III)salen complex in acetone or

ethanol, containing at least a fivefold molar excess of the appropriate MX, was stirred for 24 hours. The solid product was collected, washed with cold water (to remove  $MCl/MNO_3$ ), dried, and then purified by solvent extraction, as above.

Example: FesalenI.

2.0g Fesalen $NO_3$  + 10g NaI in 50 cm<sup>3</sup> of acetone were stirred for 24 hours at room temperature. The black solid formed was collected, washed with 2 x 10 cm<sup>3</sup> portions of cold demineralized water, then 2 x 10 cm<sup>3</sup> portions of diethyl ether and air dried for 3 hours. On recrystallization by solvent extraction with chloroform, 1.1g (47%) of FesalenI were obtained.

(c) Ferric benzoate -  $Fe(C_6H_5COO)_3$

On mixing cold aqueous solutions of  $NH_4C_6H_5COO$  and  $FeCl_3 \cdot 6H_2O$ , an orange-brown precipitate of  $Fe(C_6H_5COO)_3$  formed. The solid was collected by filtration, dried overnight at 70°C, and used without purification. This benzoate salt is insoluble in cold water, but appreciably soluble in hot alcohol<sup>(36)</sup>.

(d) As indicated earlier, aqueous solutions of FesalenX species slowly undergo hydrolysis to  $(Fesalen)_2O$ . The hydrolysis occurs rapidly in the presence of alkali and appears to be quantitative when  $pH \geq 10$ .

Residual solutions from the preparation of FesalenX species were diluted with 1:2 ethanol-water, treated with conc.  $NH_4OH$  solution (5 cm<sup>3</sup>/100 cm<sup>3</sup> of solution) and allowed to stand for 2-3 hours. The red, crude solid  $(Fesalen)_2O$  was

collected, air dried and recrystallized by prolonged solvent extraction with acetone. Approximately 24 hours of extraction were required per gram of crystalline  $(\text{Fesalen})_2\text{O}$ .

With very strong alkali, e.g. NaOH,  $\text{pH} \geq 13$ , breakdown of the complex to solid  $\text{Fe}_2\text{O}_3$  was observed.

(e)  $\text{Fe}(\text{saen})_2\text{Cl}\cdot\text{H}_2\text{O}$

Preparative methods for this complex are discussed in detail in Chapter 5. The sample studied in this section was prepared as follows:

8.9g  $\text{FesalenCl}$  ( $\frac{1}{40}$  mole) + 2g en ( $\frac{1}{30}$  mole) in  $100 \text{ cm}^3$  of ethanol, were refluxed, with stirring for 2 hours. The violet solution was filtered hot and the filtrate allowed to cool overnight. The deep blue crystalline solid was collected, washed with  $2 \times 10 \text{ cm}^3$  portions of diethyl ether and air dried for 24 hours.

Yield: 8.3g (76%).

(f) Dicyano complexes

(1)  $\text{M}[\text{Fesalen}(\text{CN})_2]$

The method employed was essentially that of the metathetical reaction scheme outlined above, with a major modification in the treatment of the reaction product.  $\text{M}[\text{Fesalen}(\text{CN})_2]$  salts are insoluble in the majority of solvents (with the exception of DMSO) and all recrystallization attempts have proved unsuccessful. In fact the only solid product isolated from such attempts was  $(\text{Fesalen})_2\text{O}$ .

The crude product obtained from the metathetical reaction was thoroughly washed with cold water, removing all traces of MCN and MX, then ethanol and the product dried overnight at 70°C. The dried green solid was analyzed directly (Yield 100%).

The  $\text{NH}_4\text{CN}$  reagent was prepared as an alcoholic solution, by stirring an equimolar suspension of KCN and  $\text{NH}_4\text{Cl}$  in ethanol for 24 hours. After allowing the suspension to settle, the supernatant liquid was used directly as the medium for the metathesis.

Alcohol solubility data<sup>(36)</sup>  $\text{NH}_4\text{Cl}$ , 0.6g/100  $\text{cm}^3$ ;  $\text{NH}_4\text{CN}$ , v. soluble; KCN, 0.88g/100  $\text{cm}^3$ ; KCl, slightly soluble.

(2)  $\text{K}[\text{Fesalophen}(\text{CN})_2]$

The procedure as for  $\text{K}[\text{Fesalen}(\text{CN})_2]$  was used, with FesalophenCl as starting material. FesalophenCl was prepared as previously described<sup>(13)</sup>.

(3)  $\text{K}[\text{Cosalen}(\text{CN})_2]^-$

The deep orange crystals were prepared by a previously described method<sup>(28)</sup>.

(4) Salts of  $[\text{Cosalen}(\text{CN})_2]^-$

Hot, aqueous solutions containing a molar excess of the cations  $\text{Ag}^+$ ,  $\text{Co}(\text{saen})_2^+$ ,  $\text{Cosalen}^+$ ,  $\text{Et}_4\text{N}^+$ ,  $\text{Ca}^{2+}$ ,  $\text{Cu}^{2+}$ ,  $\text{Zn}^{2+}$  and  $\text{Fe}^{3+}$  were added to separate hot solutions of  $\text{K}[\text{Cosalen}(\text{CN})_2]$ . On cooling, precipitates of varying hue formed, were collected,

washed with alcohol and air dried. No further purification was attempted.

(iii) Magnetic susceptibilities

The magnetic susceptibility of each complex was determined by the Guoy method, using a Sauter model 414 balance, and an Alpha Scientific model 7600 electromagnet with current regulated power supply producing a field strength of c.a. 0.8T ( $1T = 10^4$  gauss).

From the data obtained, the molar susceptibility,  $\chi_M$ , and the Bohr magneton number,  $\mu_{eff}$ , have been estimated using the method of calculation outlined by Marr and Rockett<sup>(37)</sup>. Diamagnetic corrections (S.I. units) were obtained from this reference.

(iv) Infra-red spectra

The i.r. spectra, as nujol and hexachlorobutadiene mulls, were obtained on a Pye-Unicam model SP1100 spectrophotometer.

The spectra reproduced in this thesis were obtained by photographing directly recorded spectra, covering the appropriate region.

(v) Ultra-violet visible spectra

Reflectance spectra were obtained on a Pye-Unicam model SP500 manual model, fitted with a reflectance attachment.

The nujol mull spectra were obtained on a Pye-Unicam

SP1700 recording spectrophotometer, fitted with a variable path length cell (R11C BM-3). The mull was introduced into the cell, and the windows adjusted to produce a uniform translucent layer c.a. 0.01 to 0.05 mm thick.

(vi) Analyses

(a) C, H and N

Elemental carbon, hydrogen and nitrogen determinations were performed on a Perkin-Elmer model 240, elemental analyser, at S.A.I.T. by the author. The instrument was calibrated with the C, H, N, microanalytical standard, acetanilide, and a secondary standard, salenH<sub>2</sub>. The minimum number of analyses per sample was three.

(b) Metal analyses

Two techniques were used for iron analyses:

(1) Gravimetric

Approximately 100 mg samples, weighed accurately, were ignited in an electric furnace (500°C) for c.a. 2 hours until the residues (Fe<sub>2</sub>O<sub>3</sub>) were at constant weight.

Alternatively, the weight of the residue from micro-analysis may be used. This method is not reliable, as samples frequently 'sputter' on combustion. About 60% of the metal analyses by this method agreed with the controlled ashing procedure.

(2) Atomic Absorption Spectroscopy (A.A.S.)

An acidified, aqueous solution of the complex (c.a. 40 mg/100 cm<sup>3</sup>) can be analysed for Fe directly by A.A.S. without interference from the ligand. The instrument utilized in this study was a Varian-Techtron model AA4, set for the analytical Fe line at 371.99 nm.

(c) Chloride analyses

The complexes  $\text{FesalenCl}$  and  $\text{Fe}(\text{saen})_2\text{Cl}\cdot\text{H}_2\text{O}$  were both analyzed for  $\text{Cl}^-$  by potentiometric titrations against standard  $\text{AgNO}_3$  solution. Approximately 200 mg (accurately weighed) of complex were wetted with alcohol (c.a. 5 cm<sup>3</sup>) and dissolved in 100 cm<sup>3</sup> of dilute  $\text{HNO}_3$  (5 cm<sup>3</sup> 1M  $\text{HNO}_3$ /100 cm<sup>3</sup>). In both cases the solutions remained highly coloured.

$\text{Cl}^-$  in  $\text{Fe}(\text{saen})_2\text{Cl}\cdot\text{H}_2\text{O}$  was then determined by direct titration against 0.02M  $\text{AgNO}_3$ . The endpoint was obtained potentiometrically, via a silver wire placed in the test solution with a calomel reference electrode electrically connected via an ammonium nitrate salt bridge.

Calc.	8.14
Found	8.15

Attempts to determine  $\text{Cl}^-$  in  $\text{FesalenCl}$  by direct titration were unsuccessful - no clear endpoint could be obtained. However, successful analyses were obtained using the back titration technique. An approx. 2 molar excess of  $\text{AgNO}_3$  was added and the excess  $\text{Ag}^+$  determined by titration against standard (0.02M)  $\text{NaCl}$ .

These observations are consistent with the suggestion

that the chloride anion remains bonded, at least to some extent, to the iron in  $\text{FeSalenCl}$ , even in dilute aqueous solution.

Calc. 9.9%

Found 9.8%



CHAPTER 3

## Solution Studies

3.1 INTRODUCTION

The solid state data, presented and discussed in Chapter 2, has provided sufficient information to formulate the complexes but may not be correlated directly with parameters associated with the nature of the Fe-X bond. Frequently, investigations of the properties of a compound in solution will provide relevant data - for example, dissociation constants.

Such studies have proved pertinent in the case of Fesalen Cl. It has been shown that this complex, which is of limited solubility in methanol and water, is monomeric in chloroform solution and non-conducting in nitromethane<sup>(19)</sup>. These observations confirm the presence of an Fe-Cl covalent bond in the complex<sup>(19)</sup>. Further, solvated monomeric species may be obtained on recrystallization from 'coordinating' solvents such as chloroform, nitromethane, methanol, pyridine and methyl cyanide<sup>(32)</sup>.

The analysis for chloride (experimental section, Chapter 2) suggests that at least partial dissociation of the Fe-Cl bond does occur in aqueous solution. Consequently it was anticipated that determination of solution properties, in particular conductances and u.v.-visible spectra, may well prove useful in estimating the 'strength' of the respective Fe-X bonds in the series of complexes.

### 3.2 CONDUCTANCE

The interpretation of conductance data, in terms of the possible structures of coordination compounds, has been used extensively for over 80 years. Data obtained in aqueous solution allowed Werner and co-workers to elucidate the structures of numerous ammine complexes<sup>(38)</sup>. In recent years, conductance measurements in organic solvent have found widespread application as a means of ascertaining the magnitude of the ionic charge on complex species<sup>(38)</sup>.

Conductance measurements in methanol, in the concentration range 3 to 70 x 10<sup>-5</sup>M, have been obtained for all FesalenX and other compounds of interest. Due to the low solubility of several of the FesalenX species, the molar conductances,  $\Lambda_M$ , have been interpolated to 5 x 10<sup>-4</sup>M rather than the conventional concentration of 10<sup>-3</sup>M. The data obtained are tabulated in Table 3.1, together with some single measurements in DMF.

For 1:1 electrolytes, the suggested range of values of  $\Lambda_M$  (at 10<sup>-3</sup>M) are 80-115 for methanol, 65-90 for DMF<sup>(38)</sup>. At face value, the results obtained suggest that all species investigated are essentially 1:1 electrolytes in these solvents, however, closer examination reveals the situation to be more complex. Specifically:

- (1) The value of  $\Lambda_M$  for the known 1:1 electrolyte Et<sub>4</sub>N<sup>+</sup>Cl<sup>-</sup> occurs near the lower limit of the suggested range whereas those for the FesalenX species, with the exception of X = C<sub>6</sub>H<sub>5</sub>COO, are found to be closer to the upper limit.

TABLE 3.1

Molar conductivity,  $\Lambda_M$  ( $\text{Scm}^2\text{mol}^{-1}$ ), at 25°C

Species	Methanol		DMF	
	M	$\Lambda_M$	M	$\Lambda_M$
FesalenX	$5 \times 10^{-4}$			
X = Cl		91.2	$9.5 \times 10^{-4}$	74.0
Br		99.5		
I		112.1		
NO <sub>3</sub>		92.6	$1.26 \times 10^{-3}$	77.7
NCS		88.7	$9.0 \times 10^{-4}$	65.5
N <sub>3</sub>		80.4		
C <sub>6</sub> H <sub>5</sub> COO		59.6		
Fe (saen) <sub>2</sub> Cl.H <sub>2</sub> O		78.1		
Et <sub>4</sub> N <sup>+</sup> Cl <sup>-</sup>		77.5	$1.37 \times 10^{-3}$	73.8

- (2) The limiting equivalent conductances,  $\Lambda^{\circ}$ , for the anions  $\text{Cl}^{-}$ ,  $\text{Br}^{-}$ ,  $\text{I}^{-}$  and  $\text{NO}_3^{-}$  ( $\text{H}_2\text{O}$  at  $25^{\circ}\text{C}$ ) are 75.5, 77.4, 75.9, 70.6  $\text{Scm}^2\text{mol}^{-1}$  respectively<sup>(39)</sup>. The values in methanol are expected to be approximately 0.7 times these aqueous values, and show a similar trend<sup>(40)</sup>. The observed spread in the values obtained is much greater than that anticipated for completely ionized species.
- (3)  $\text{Fe}(\text{saen})_2\text{Cl}\cdot\text{H}_2\text{O}$  has a similar value of  $\Lambda_{\text{M}}$  to that of  $\text{Et}_4\text{N}^{+}\text{Cl}^{-}$ , and is known to be ionic. (The crystal structure<sup>(20)</sup> and chemical studies of  $\text{Fe}(\text{saen})_2\text{Cl}\cdot\text{H}_2\text{O}$  are discussed in Part II of this thesis.) The difference between the mode of bonding the anion, X, in the  $\text{Fe}(\text{saen})_2$  and  $\text{Fesalen}$  species, is illustrated by the procedures used for halide analysis (experimental, Chapter 2). In the case of  $\text{Fe}(\text{saen})_2\text{Cl}\cdot\text{H}_2\text{O}$ , the  $\text{Cl}^{-}$  may be determined by direct argentometric titration in alcoholic solution, whereas for  $\text{FesalenX}$  (X = Cl, Br, I and NCS) the back titration technique must be employed, even in aqueous solution. Hydrolysis of  $\text{FesalenX}$  species, and the consequent cleavage of the Fe-X bond, occurs slowly and does not go to completion. Clearly, then, the bonding in  $\text{FesalenX}$  involves a covalent Fe-X bond and complete dissociation in solution does not occur.

These results and observations suggest that the species  $\text{FesalenX}$ , in all probability, are involved in rather complex solution equilibria in which solvolysis may be of significance. Such equilibria would be difficult to resolve by conductance studies alone.

### 3.3 U.V.-VISIBLE SPECTRA

In the visible and ultra-violet region, the absorption spectrum of a complex originates, in general, from three types of electronic transition, viz. excitation of the metal ion, excitation within the ligand and charge transfer excitation. As outlined in Section 2.2(ii)(b), metal excitation is not expected to be of significance for Fe(III) high spin complexes.

The conjugated system of ligands such as salen, would be expected to involve transitions such as  $\eta \rightarrow \sigma^*$ ,  $\eta \rightarrow \pi^*$  and  $\pi \rightarrow \pi^*$  in the spectral region above 200 nm. Complexation would be expected to result in changes in the energy and intensity of the ligand absorptions, although these changes would be expected to be small. The spectrum resulting from ligand transitions would be similar to that of the protonated ligand, salenH<sub>2</sub><sup>(41)</sup>.

Charge transfer transitions may well be of significance as the intense colour of many complexes, particularly those of Fe(III), is frequently associated with such transitions<sup>(41)</sup>. During the preparation of the series of complexes, FesalenX, intensely coloured solutions have been observed, varying somewhat in hue depending both on X and the solvent utilized. Solvent and anion (X) dependent spectra have indeed been obtained.

In order to rationalize such spectra, it is necessary as a first step to resolve which absorption bands may be considered as arising from the ligand transitions, as distinct from those also involving the coordinated metal.

(a) Spectra of the ligand

A number of workers have undertaken spectral studies of salenH<sub>2</sub> utilizing a variety of solvents<sup>(42,43,44,45)</sup>. As substantial improvements in spectrometer technology have occurred during the last 20 years, a check of this earlier data was considered worthwhile. The results obtained in this work are compared in Table 3.2 with the earlier data, using methanol as the solvent in all cases.

Four absorption bands have been observed between 200 and 410 nm and in this study have been labelled as  $\lambda_1$  to  $\lambda_4$ , in increasing order of energy, i.e. decreasing wavelength. As a measure of the intensity of each band, the logarithm of the respective molar extinction coefficients,  $\log \epsilon$ , is included (where available) after each absorption maximum.

The assignment of bands  $\lambda_2$ ,  $\lambda_3$  and  $\lambda_4$  to  $\pi \rightarrow \pi^*$  type transitions is consistent with the partial assignments given in references 37 and 38. In particular,  $\lambda_2$  is consistent with the  $\pi \rightarrow \pi^*$  transition of the imine (-HC=N-) chromophore<sup>(43,45,46,47)</sup>. The bands  $\lambda_3$  and  $\lambda_4$  may be assigned to  $\pi \rightarrow \pi^*$  transitions associated with the substituted aromatic ring<sup>(46,47)</sup>.

The band near 405 nm has been the subject of some controversy. It has been suggested that this band is an  $n \rightarrow \pi^*$  transition, influenced by the 'hydrogen bonding between the nitrogen atom and the phenolic oxygen in the ortho position'<sup>(42)</sup>. In the solid state spectrum (as a nujol mull) intense bands occur at 210, 256 and 325 nm only, i.e.  $\lambda_1$  is absent. The intensity and position of band  $\lambda_1$  is very solvent dependent

TABLE 3.2

Methanol solution spectra of salenH<sub>2</sub>

Source	$\lambda_1$	$\lambda_2$	$\lambda_3$	$\lambda_4$	Concentration
This study	405 (3.23)	317 (3.93)	255 (4.36)	215 (4.61)	3-80x10 <sup>-5</sup> M
Ref. 45	406 (3.20)	320 (3.85)	262 (4.33)	≈220 (4.65)	8-75x10 <sup>-5</sup> M
Ref. 44	408 (3.21)	320	≈265		not stated
Ref. 42	403 (3.10)	318 (3.85)			not stated

and is only observed in solution spectra where the solvent molecule is a weak Lewis base<sup>(43)</sup>. It would appear that the  $\lambda_1$  band is consistent with an  $\eta \rightarrow \pi^*$  transition and it has been assigned as such in this study, as has the corresponding transition (405 nm) in the closely related ligand salpnH<sub>2</sub><sup>(42)</sup>.

(b) Related studies

The spectral investigations were extended with the view to:

- (i) investigating the conditions for acid hydrolysis of salenH<sub>2</sub> as mentioned in Section 2.1;
- (ii) determining whether or not the free tridentate ligand saenH exists in solution.

Representative spectral data for salenH<sub>2</sub> in the presence of a 100-fold molar excess of acid (HCl), alkali (NaOH) and en are tabulated in Table 3.3. The data for a similar study with salicylaldehyde are also included in Table 3.3. However, as salicylaldehyde contains one chromophore per molecule whereas salenH<sub>2</sub> has two, the values of  $\epsilon$  for the salicylaldehyde study have been multiplied by 2 to allow direct comparison of the log  $\epsilon$  values.

The positions and intensity of the absorption bands suggest:

- (1) the absorbing species present in solutions (a), (b) and (c) is the same - probably salenH<sub>2</sub>;
- (2) salenH<sub>2</sub> is probably hydrolyzed in acidic solution to salicylaldehyde (and enH<sub>2</sub><sup>2+</sup>);
- (3) salenH<sub>2</sub> is distinct from salicylaldehyde in alkaline solutions.



TABLE 3.3

Spectral data for salenH<sub>2</sub> and salicylaldehyde study

Solution	$\lambda_1$	$\lambda_2$	$\lambda_3$	$\lambda_4$ *
(a) salenH <sub>2</sub> (3-80x10 <sup>-5</sup> M)	405 (3.23)	317 (3.93)	255 (4.36)	215 (4.61)
(b) salenH <sub>2</sub> (6-40x10 <sup>-5</sup> M) with excess en	404 (3.20)	315 (3.91)	254 (4.30)	215 (4.68)
(c) salicylaldehyde (3-40x10 <sup>-5</sup> M) with excess en	405 (3.23)	314 (3.94)	254 (4.37)	213 (4.57)
(d) salicylaldehyde (3-10x10 <sup>-5</sup> M)		325 (3.94)	254 (4.37)	214 (4.57)
(e) salicylaldehyde (5-50x10 <sup>-5</sup> M) with excess H <sup>+</sup>		325 (3.93)	256 (4.38)	213 (4.57)
(f) salenH <sub>2</sub> (5-60x10 <sup>-5</sup> M) with excess H <sup>+</sup>		325 (3.90)	257 (4.36)	213 (4.56)
(g) salenH <sub>2</sub> (2-30x10 <sup>-5</sup> M) with excess OH <sup>-</sup>		380 (4.03)	265 (4.10)	215 (4.74)
(h) salicylaldehyde with excess OH <sup>-</sup>		379 (4.22)	264 (4.26)	225 (4.66)

\* The values of log  $\epsilon$  for  $\lambda_4$  are uncertain due to the solvent absorption band observed below 220 nm.

On increasing gradually the amount of  $\text{OH}^-$ , the band near 380 nm can be shown to originate from the band near 315 nm for  $\text{salenH}_2$  and that near 325 nm for salicylaldehyde. In both cases, the band near 265 nm arises from that near 255 nm in the neutral solutions. These spectral changes may be reversed by neutralization of the excess alkali.

The changes noted in the spectrum of  $\text{salenH}_2$  as the amount of acid is gradually increased, suggest that the hydrolysis to salicylaldehyde and  $\text{enH}_2^{2+}$  is the only observable reaction taking place. The reaction cannot be reversed by neutralization. It would appear that rapid, irreversible hydrolysis of  $\text{salenH}_2$  occurs in alcoholic solutions when the pH is below 5 and small amounts of water are present.

There is no evidence to suggest that the free ligand  $\text{saenH}$  exists in solution. All attempts to obtain the free ligand have been unsuccessful, with  $\text{salenH}_2$  being the only product isolated. It would appear that the ligand exists only when coordinated to a metal. As explored further in Part II, the conversion of salen complexes to saen complexes, and vice versa, occurs readily with the most stable reaction product being formed.

(c) Spectra of Schiff base complexes

Although formally the dianion,  $\text{salen}^{2-}$  (spectrum (g)) is the species coordinated to the metal, the band positions and intensities would be expected, as stated earlier, to be similar to those of  $\text{salenH}_2$ <sup>(41)</sup>. Thus bands could be anticipated near 215, 260, 320 and 400 nm with extinction coefficients

of the order of  $10^4$ . The  $\lambda_1$  band, which has been assigned to an  $\eta \rightarrow \pi^*$  transition modified by hydrogen bonding, would not be observed for two reasons:

- (1) the phenolic hydrogen atom responsible for the interaction is no longer present in the anionic species; and
- (2) the non-bonded electrons on the imine nitrogen are coordinated to the central metal ion.

Thus, while  $\eta \rightarrow \pi^*$  transitions may be observed, they must certainly occur at a much higher energy (lower  $\lambda$ ) than 400 nm.

The spectrum of Zn(II)salen, where the only transitions occurring would be essentially those of the ligand, has been studied and bands were found near 350 nm ( $\lambda_2$ ), 260 nm ( $\lambda_3$ )<sup>(45)</sup>. The spectrum of the similar complex, Zn(II)salpn, was found to be almost identical with the  $\lambda_2$  band at 348 nm and no evidence of an  $\eta \rightarrow \pi^*$  transition<sup>(48)</sup>.

Spectral analysis of the methanol solution circular dichroism spectra of Ni(II)salpn, a  $d^8$  square planar complex, has been recently performed<sup>(48,49)</sup>. Three categories of transition have been suggested:

- (1) Ligand transitions, with  $\epsilon > 10^4$ , below 350 nm.
- (2) Solvent dependent charge transfer transitions, of the  $d \rightarrow \pi^*$  type, with  $\epsilon \approx 7 \times 10^3$  near 400 nm.
- (3) Magnetic dipole allowed 'd-d' transitions ( $\epsilon \approx 200$ ) above 500 nm.

As previously outlined in Section 2.2(ii)(b), for a high spin  $d^5$  system the 'd-d' transitions, which are both

Laporte and spin forbidden, would be expected to be of very low intensity ( $\epsilon < 1$ ) if observed at all<sup>(18)</sup>. However, a large number of Fe(III) complexes are known to be intensely coloured, as are the complexes in this study, with the colour being ascribed to charge transfer transitions. It has been shown that Fe(III) complexes with dipyridyl, dimethyl glyoximate and other conjugated ligands show Ligand  $\rightarrow$  Metal charge transfer ( $\pi \rightarrow d$  type) bands<sup>(50)</sup>. It appears reasonable to suggest that such transitions may well be responsible for the intense colour of the FesalenX complexes.

Recently the methanol solution spectra of several iron(III) chelates, including FesalenCl, have been studied<sup>(51)</sup>. Intense bands near 500 and 400 nm ( $\epsilon > 10^3$ ) have been assigned to 'd-d' absorptions, with the intensity rationalized in terms of 'borrowing from low-lying charge transfer bands in the imine ligand'<sup>(51)</sup>. Further, it was suggested that the u.v. spectra may provide structural information for Schiff base complexes of iron(III) in that:

- (1) pentacoordinate complexes show two bands in the visible region;
- (2) hexacoordinate complexes show four bands, two between 400 nm and 500 nm with  $\epsilon > 10^3$  and two weaker bands at longer wavelengths<sup>(51)</sup>.

This proposition is not in agreement with observations made in this study.

- (i) Methanol spectra of Fe(saen)<sub>2</sub><sup>+</sup> (Fig. 3.1(a))

The methanol spectra of this cation have been obtained,

utilizing the complex  $\text{Fe}(\text{saen})_2\text{Cl}\cdot\text{H}_2\text{O}$ <sup>(20)</sup>. The cation has octahedral coordination and, as discussed in Part II, has the high spin  $d^5$  configuration in solution. The chromophoric group, viz. an imine conjugated to an aromatic ring with a phenolic oxygen in the ortho position, is considered sufficiently similar to salen to allow comparisons to be made. The spectra obtained, which obeyed Beer's Law over the concentration range  $4$  to  $80 \times 10^{-5}\text{M}$ , are characterized by the following absorption maxima:

$500 \text{ nm}$  ( $\log \epsilon = 3.44$ ),  $332$  ( $3.87$ ),  $262$  ( $4.32$ ) and  $230$  ( $4.64$ ) - a shoulder was observed at  $292 \text{ nm}$  ( $\log \epsilon = 3.83$ ).

The position and intensity of the bands at  $332$ ,  $262$  and  $230 \text{ nm}$  compare favourably with those obtained for the  $\lambda_2$ ,  $\lambda_3$  and  $\lambda_4$  bands with  $\text{salenH}_2$ , reinforcing the suggestion that these bands are essentially ligand transitions.

A single band only can be observed between  $400$  and  $850 \text{ nm}$ , suggesting that the  $d-d$  assignment as outlined above may be in error.

(ii) Methanol spectra of  $\text{Fe}(\text{saen})\text{X}$

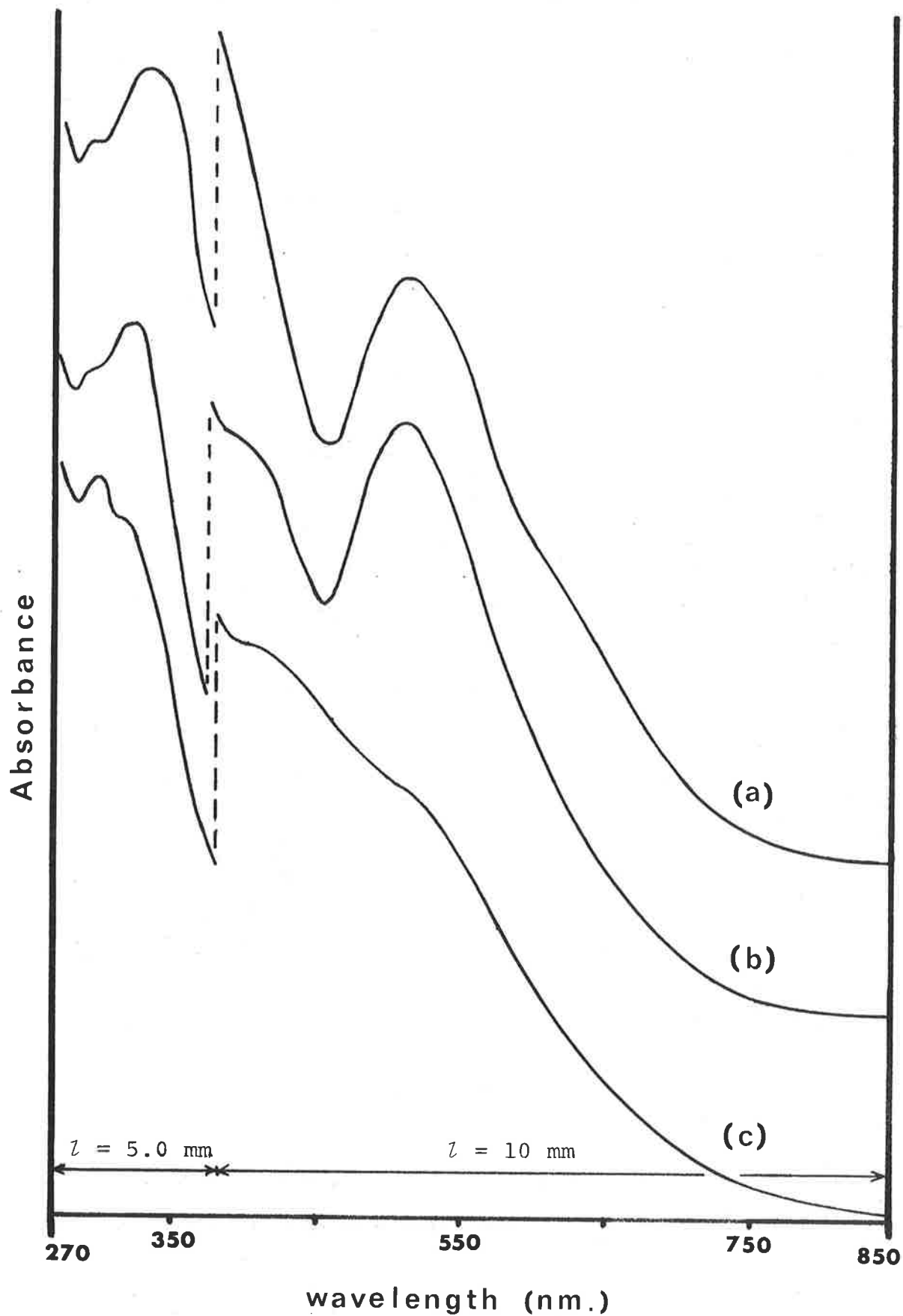
On examination, the spectra obtained appear to fall into two broad types:

Type I -  $\text{X} = \text{Cl}, \text{Br}, \text{I}, \text{NO}_3$  and  $\text{NCS}$  (Fig. 3.1(b))

The spectra are characterized by distinct bands at  $505 \text{ nm}$  and near  $325$ ,  $260$  and  $230 \text{ nm}$ , with prominent shoulders at  $390 \text{ nm}$  and near  $300 \text{ nm}$ . Substantial deviations from Beer's Law were observed on dilution (over the concentration range  $2 - 40 \times 10^{-5}\text{M}$ ).

Figure 3.1

Methanol solution spectra



(a)  $\text{Fe(saen)}_2\text{Cl}\cdot\text{H}_2\text{O}$     (b)  $\text{FealenNO}_3$     (c)  $\text{FealenC}_6\text{H}_5\text{COO}$

Type II - X = N<sub>3</sub>, C<sub>6</sub>H<sub>5</sub>COO (Fig. 3.1(c))

These spectra are characterized by distinct bands near 320, 260 and 230 nm with prominent shoulders at 390 nm and near 500 and 300 nm. The deviations from Beer's Law were not as great as for Type I.

As deviations from Beer's Law have been observed, it must be considered that all absorptions cannot be attributed to a single species. Clearly, this is not consistent with the assignment of the bands at 505 and 390 nm to d-d type transitions nor, for that matter, to charge transfer transitions in the solvated FesalenX species.

However, as indicated earlier, partial dissociation of the FesalenX species occurs in solution, and the spectra of FesalenX and Fesalen<sup>+</sup> would be expected to be different. In particular, a Ligand → Metal charge transfer band would occur at a lower energy (longer wavelength) in the cationic species than in the neutral molecule<sup>(50)</sup>. Consequently, it is proposed that the band near 500 nm is characteristic of a charge transfer transition in the Fesalen<sup>+</sup> species whilst a band near 400 nm corresponds to the equivalent transition in the associated species, FesalenX. The position and intensity of these bands would be expected to show considerable solvent dependence<sup>(50)</sup>.

The above observations and discussion suggest that the equilibrium reaction



may be readily confirmed by spectral studies, in which the solvent or anion are varied.

(1) Solvent

Such spectral studies were performed with chloroform, methanol and aqueous solutions. The results indicate that:

- (a) the position of the bands attributed to charge transfer absorptions are sensitive to the electron donating ability of the solvent. As expected, the charge transfer absorptions occur at longer wavelengths (lower energy) with the weakly coordinating solvent, chloroform<sup>(50)</sup>.
- (b) the assignment of the bands near 500 and 400 nm is consistent with the cationic and associated species respectively. In the presence of a substantial (2 - 10 fold) molar excess of the anion  $X^-$  ( $X = Cl$  and  $NCS$ ), the band at 505 nm (MeOH solution) decreased in intensity, whilst that at 390 nm increased, with an increase in the concentration of  $X^-$ .
- (c) the extent of the equilibrium reaction is solvent dependent, with the dissociation being more complete in aqueous solution. All spectra in aqueous solution are of Type I, irrespective of  $X$ , whereas in chloroform solution the majority are of Type II. Such solution spectra may be used to assess the extent of the dissociation.

The equilibrium reaction, as proposed above, is described by the equation

$$K = \frac{[Fesalen^+][X^-]}{[FesalenX]}$$

where  $K$  is the equilibrium or dissociation constant.

Assuming that the intensity of the band at 505 nm is related to  $[Fesalen^+]$  and that at 390 nm is related to  $[FesalenX]$



then, as a first approximation,

$$K \propto \frac{(\epsilon_{505})^2}{\epsilon_{390}} \quad \text{for methanol solutions.}$$

Thus the ratio  $(\epsilon_{505})^2/\epsilon_{390}$  would be expected to reflect any anion dependent trend in the event of dissociation for the FesalenX species in solution.

TABLE 3.4

Dissociation of FesalenX in methanol solution  
(c.a.  $4 \times 10^{-4}M$ )

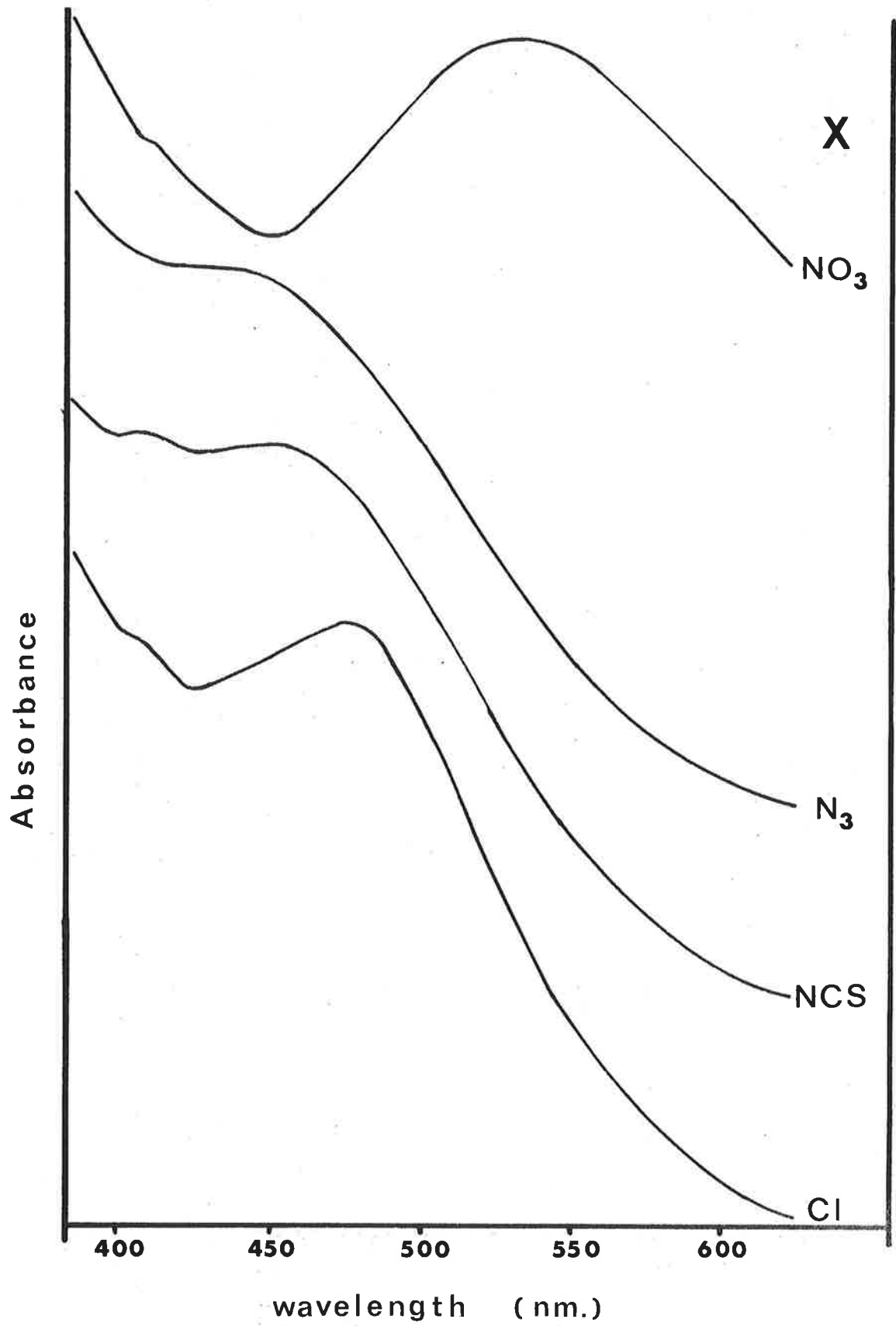
X	Cl	Br	I	NO <sub>3</sub>	NCS	N <sub>3</sub>	C <sub>6</sub> H <sub>5</sub> COO
$\epsilon_{505}:\epsilon_{390}$	0.985	0.998	1.012	0.996	0.983	0.464	0.385
$(\epsilon_{505})^2:\epsilon_{390}$ ( $\times 10^{-3}$ )	0.970	0.996	1.024	0.992	0.966	0.215	0.148

The ratios in Table 3.4 which are related only approximately to the absolute value of K, suggest that in methanol the complexes of Type I dissociate to a much greater extent than those of Type II. Clearly FesalenN<sub>3</sub> dissociates more readily than FesalenC<sub>6</sub>H<sub>5</sub>COO, but the relative values for Type I (i.e. X = Cl, Br, I, NO<sub>3</sub> and NCS) do not positively establish whether the apparent order is real or not. In order to differentiate between those species with close ratios, the chloroform spectra have been examined.

(iii) Studies in chloroform

The spectra in chloroform for Type I (X = NO<sub>3</sub>, Cl, NCS), with a representative of Type II for comparison (X = N<sub>3</sub>), are reproduced between 390 and 700 nm. All spectra were found to

Figure 3.2



Chloroform solution spectra of FesalenX

be similar in the region 250 to 400 nm, with absorption maxima at 270 and 330 nm.

Above 400 nm significant features may be readily observed. All spectra have a shoulder near 420 nm, and it appears reasonable to suggest that this band corresponds to that at 390 nm in the methanol spectra.

With respect to the prominent band found near 500 nm in methanol solution, no single equivalent band can be found in the chloroform spectra. Anion dependent maxima were observed, however, at 448 nm (X = NCS), 480 nm (X = Cl) and 532 nm (X = NO<sub>3</sub>). No equivalent peak was found for X = N<sub>3</sub>.

By assuming that a band near 430 nm correlates with the FesalenX transition, and that at 532 nm with Fesalen<sup>+</sup>, an interpretation, equivalent to that for the methanol spectra, may be proposed.

(1) The observation of bands at 448 and 480 for X = NCS and Cl respectively, may be rationalized in terms of the additivity of overlapping absorption bands, i.e. the absorbance at any particular energy (or wavelength) is the sum of the contributions from a number of transitions which have a finite absorbance at that energy<sup>(52)</sup>. By assuming that these bands have a Gaussian distribution of the absorbance with energy, it has proved possible to calculate spectra similar to those in Fig. 3.2 utilizing four absorbance bands at 532, 435, 330 and 270 nm respectively. The procedure employed is discussed in the experimental section of this Chapter (3.5(iv)). However, the assumptions made in these calculations are equivalent to

proposing that the degree of dissociation for the FesalenX species are respectively 70% (X = NO<sub>3</sub>), 54% (X = Cl), 50% (X = NCS) and 20% (X = N<sub>3</sub>).

(2) The ratios of  $(\epsilon_{532})^2/\epsilon_{430}$ , as estimated from the spectra, are respectively 1.28 (X = NO<sub>3</sub>), 0.494 (X = Cl), 0.407 (X = NCS), 0.216 (X = N<sub>3</sub>). These ratios clearly illustrate the trend suggested above.

(3) The conductance of each of the chloroform solutions has been measured. The results obtained are tabulated below:

X	N <sub>3</sub>	NCS	Cl	NO <sub>3</sub>
$\Lambda_M$ (Scm <sup>2</sup> mol <sup>-1</sup> )	non-conducting	≈0.1	≈0.1	≈0.2

These values of  $\Lambda_M$  are extremely low, but are comparable with the limited data available, e.g. for the 1:1 electrolyte Et<sub>4</sub>N<sup>+</sup>Cl<sup>-</sup> in chloroform at a similar concentration,  $\Lambda_M \approx 0.4$  Scm<sup>2</sup>mol<sup>-1</sup> (40). These results indicate that the assumptions made above, in order to rationalize the spectra, are probably valid.

(d) Deviations from Beer's Law on dilution

The above discussion supports the proposition that solution equilibria may be utilized to rationalize the u.v.-visible solution spectra of the FesalenX series.

It would be expected that, for a simple equilibrium reaction, such as that proposed, viz.



the 'degree of dissociation' would increase on dilution. The

concentration of Fesalen<sup>+</sup>, relative to that of FesalenX, would be expected to be increasingly larger the more dilute the solution. For the methanol solution spectra, the band at 505 nm should become increasingly more intense, relative to that at 390 nm, and should be reflected in an increasing ratio  $\epsilon_{505}/\epsilon_{390}$  on dilution.

In Fig. 3.3, the spectra of FesalenCl in methanol, between 370 and 625 nm, have been reproduced. Data relevant to this study follow in Table 3.5.

TABLE 3.5

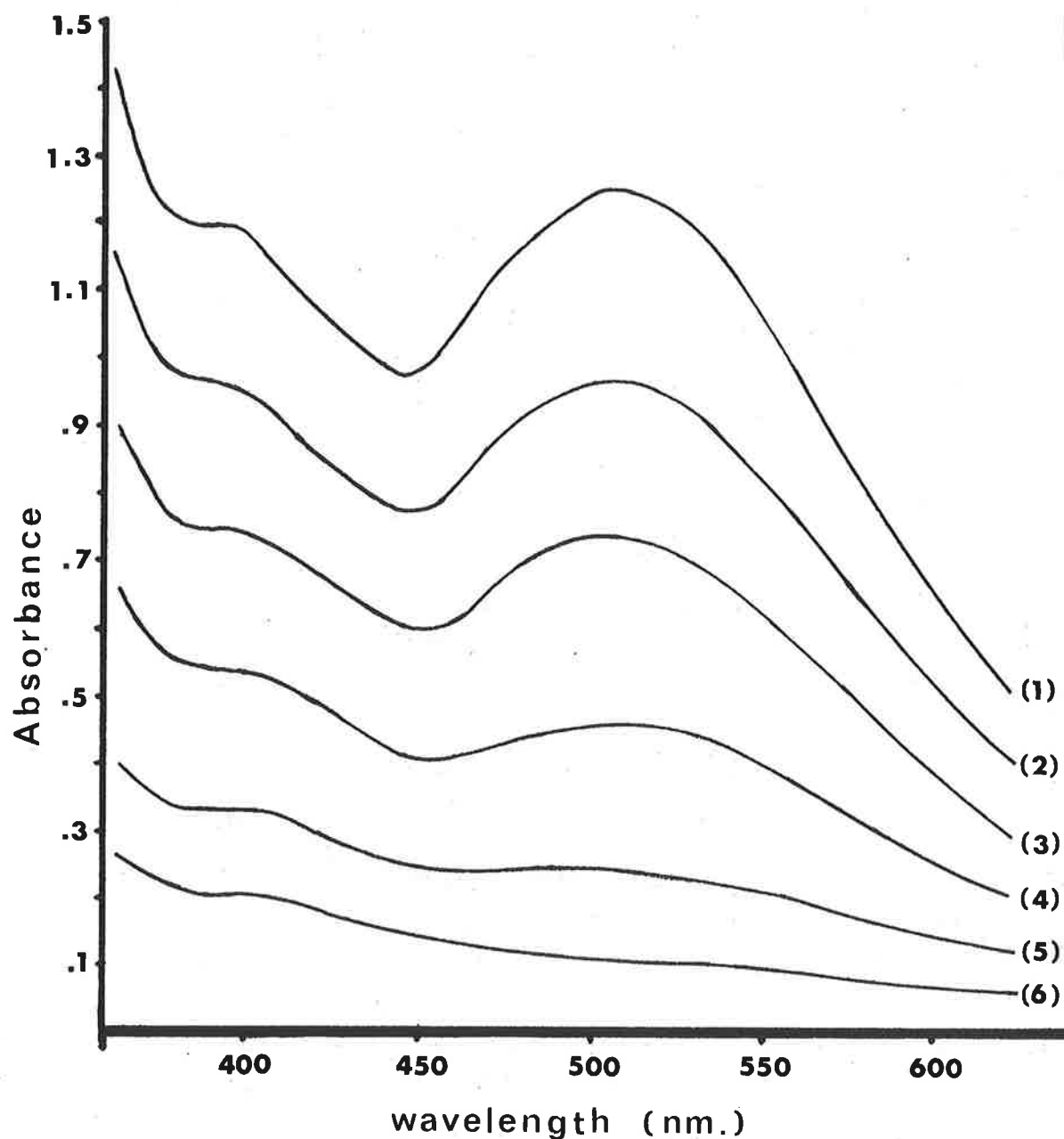
Variation, on dilution, of FesalenCl methanol solution spectra

Spectrum	Concentration	$\epsilon_{505}$	$\epsilon_{390}$	$\epsilon_{505}/\epsilon_{390}$
(1)	$3.5 \times 10^{-4}M$	$3.21 \times 10^3$	$3.05 \times 10^3$	1.05
(2)	2.8	2.98	3.00	0.99
(3)	2.1	3.00	3.10	0.97
(4)	1.4	2.56	3.14	0.82
(5)	0.7	2.26	3.57	0.63
(6)	0.35	1.57	4.00	0.39

Clearly the ratio  $\epsilon_{505}/\epsilon_{390}$  follows a trend in direct opposition to that predicted. This apparent anomaly could be rationalized in a number of ways.

- (1) The criteria proposed above for the identification of the species are incorrect.
- (2) The intensity of the 390 nm band is accentuated by overlap of lower wavelength bands.

Figure 3.3



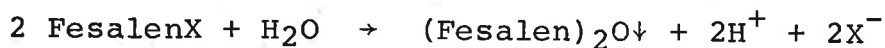
Variation of FesalenCl methanol solution spectra on dilution:

Spectrum	1	2	3	4	5	6
Concentration ( $\times 10^{-4}M$ )	3.5	2.8	2.1	1.4	0.7	0.35

- (3) The equilibrium is more complex than that proposed.

Suggestion (3) is considered the major reason for the apparent anomaly, and an indication of the complexity of the solution equilibria may be provided in the following observations. In Table 3.4, the ratio  $\epsilon_{505}:\epsilon_{390}$  obtained for a c.a.  $4 \times 10^{-4}$ M methanol solution of FesalenCl is stated as 0.985. From Table 3.5, the ratio for a  $3.5 \times 10^{-4}$ M solution is 3.21/3.05, i.e. 1.05. On examination of the relevant spectral records, the only apparent experimental variation was in the supplier of the methanol. That the spectra appear sensitive to small changes in the concentration or nature of solvent impurities is in itself anomalous. The major impurity present in spectral grade methanol would be water, probably absorbed from the atmosphere, due to the known hygroscopic behaviour of methanol<sup>(53)</sup>.

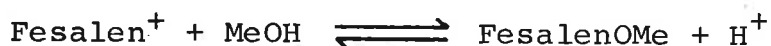
Earlier in this work, it has been stated (Section 3.3 (c)(ii)) that spectral studies indicate the dissociation is more complete in aqueous solution. For such studies, the solvent utilized was 1:1 methanol-water, whereas in spectral grade methanol, the maximum water content is of the order of 0.05%<sup>(54)</sup>. However, even with a water content of 0.05%, the molar concentration of water in the solvent is 0.028M, i.e. approximately 100 times the concentration of any of the species involved in the dissociation reaction. Traces of water could be significant, if a reaction occurs in solution in which water may be involved. It is known that in aqueous solution, FesalenX may be hydrolyzed to the binuclear oxo bridged species, according to the equation<sup>(33)</sup>:



Presumably this occurs via an intermediate species, FesalenOH.

Sealed methanol solutions, prepared for this study over two years ago, do not appear to have undergone any spectrally observable deterioration and no precipitate of  $(\text{Fesalen})_2\text{O}$  can be observed. However, with a 1:1 methanol-water mixture as solvent,  $(\text{Fesalen})_2\text{O}$  can be observed after 24 hours. Clearly then, the water present in the solvent is not the only species responsible for the spectral anomalies observed, but serves to 'magnify' the solution equilibria occurring.

Consequently it is proposed that a further equilibrium occurs in solution, in which the solvent methanol is involved. The solvolytic equilibrium proceeds according to the equation



Solvolysis has been confirmed experimentally as follows:

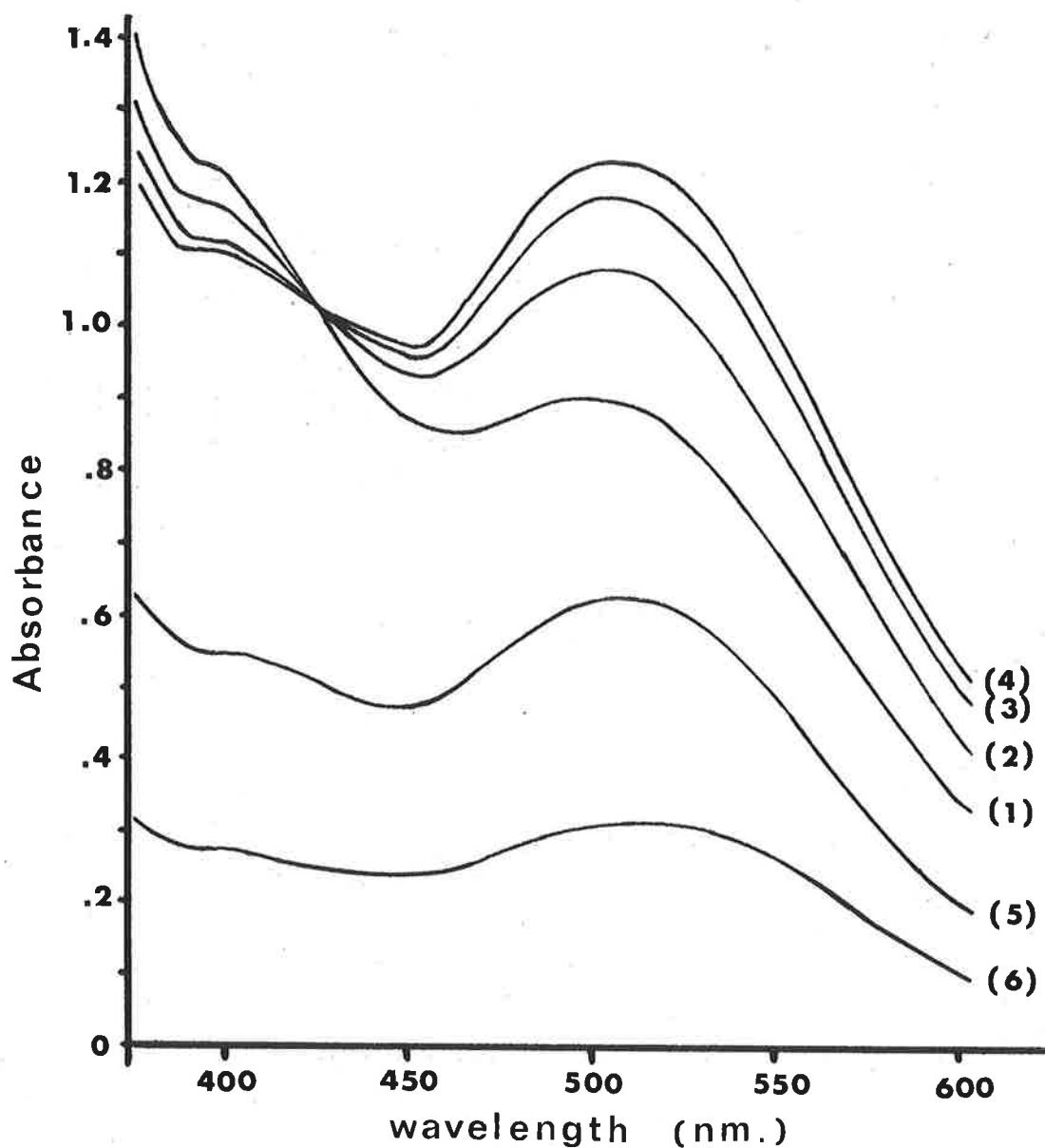
(1) In the presence of increasing amounts of acid,  $\text{HClO}_4$ , maintaining  $[\text{FesalenX}]$  constant throughout, the intensity of the peak at 505 nm increases to a maximum, whereas that of the 390 nm peak decreases. This behaviour is illustrated in Fig. 3.4, for  $\text{X} = \text{C}_6\text{H}_5\text{COO}$ . Similar results were obtained for  $\text{X} = \text{Cl}$ ,  $\text{NCS}$  and  $\text{N}_3$ .

(2) In the presence of a 3-fold molar excess of  $\text{H}^+$ , the spectra followed the trend on dilution as expected from the simple equilibrium proposal.

This proposed two-step solution equilibrium accounts for the anomalous features of the spectral study. Clearly the



Figure 3.4



Spectra of FealenC<sub>6</sub>H<sub>5</sub>COO in aqueous methanol, in the presence of added HClO<sub>4</sub>

Spectrum	1	2	3	4	5	6
[Fe complex] x 10 <sup>-4</sup> M	1.72	1.72	1.72	1.72	0.86	0.43
[HClO <sub>4</sub> ] x 10 <sup>-4</sup> M	0	0.45	0.90	3.62	5.43	7.24

deviations from Beer's Law observed, are entirely consistent with the proposed assignment of the spectral bands. The band at 505 nm, in methanol, may be attributed to the ion, Fesalen<sup>+</sup>, whilst that at 390 nm corresponds to the equivalent transition in the associated species FesalenX and FesalenOMe.

Additional confirmation of these equilibria has been obtained by measuring the response of a glass electrode immersed in the methanol solutions. It has been assumed that such measurements indicate the 'pH' of these solutions.

TABLE 3.6

Solute	Concentration	pH
-	pure MeOH	8.30
FesalenCl	$7.00 \times 10^{-4} \text{M}$	6.20
FesalenBr	$4.36 \times 10^{-4} \text{M}$	6.10
FesalenI	$4.72 \times 10^{-4} \text{M}$	6.05
FesalenNO <sub>3</sub>	$3.91 \times 10^{-4} \text{M}$	6.15
FesalenNCS	$6.45 \times 10^{-4} \text{M}$	6.30
FesalenN <sub>3</sub>	$3.54 \times 10^{-4} \text{M}$	7.20
FesalenC <sub>6</sub> H <sub>5</sub> COO	$3.43 \times 10^{-4} \text{M}$	7.25
(Fesaen) <sub>2</sub> Cl.H <sub>2</sub> O	$4.64 \times 10^{-4} \text{M}$	8.30

Although the measured pH must be considered of limited theoretical value, it does confirm that hydrogen ions have been released through a solvolytic reaction. Further, as the solvolysis occurs in methanol solution, the equilibrium constant of the solvolysis,  $K_{\text{sol}}$ , is given by the relation

$$K_{sol} = \frac{[FesalenOMe][H^+]}{[Fesalen^+]} = \frac{[H^+]^2}{[Fesalen^+]}$$

i.e.  $p\text{Fesalen}^+ = pK_{sol} - 2pH$

Now, as  $K_{sol}$  must be the same for all FesalenX, the solution pH is dependent on  $[Fesalen^+]$  as the only variable. Clearly, then, the lower the pH of the solution, the greater the concentration of  $Fesalen^+$ . Thus the pH values may be used to indicate the extent of dissociation of the FesalenX species in solution.

Similar effects have been observed in EtOH and H<sub>2</sub>O, and it is probable that such equilibria would occur in any amphiprotic solvent. The equilibria may be summarized in a general form, as



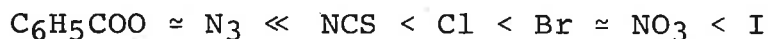
Investigations in both basic and acidic amphiprotic solvents may well allow a more positive differentiation of the extent of the various equilibria. Such an investigation has not been undertaken in this study because the information required, viz. the apparent ease of dissociation of the Fe-X bond, may be obtained from the data available.

### 3.4 DISCUSSION

The data presented above in Sections 3.3(c) and (d), in particular that in Tables 3.4 and 3.6, when considered in toto, support the conclusion that the extent to which dissociation occurs varies according to the nature of X, i.e. may well

reflect the strength of the Fe-X bond.

The apparent ease of dissociation of the species  $\text{FealenX}$  to  $\text{Fealen}^+$  and  $\text{X}^-$  follows the order:

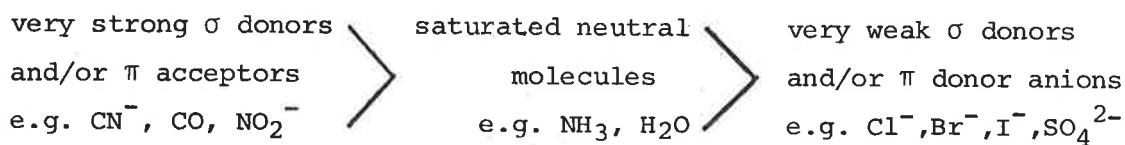


Presumably this is the reverse order of the strength of the Fe-X bond.

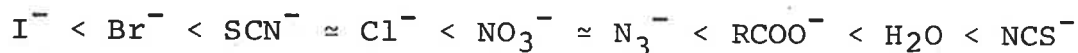
In an attempt to rationalize the apparent sequence of bond strengths, correlations have been sought with a number of known effects, in particular those obtained from spectroscopic investigations. Two well established examples, which are ligand dependent and of possible relevance, are the spectrochemical and nephelauxetic series. In both cases, the position of each ligand in the series has been determined from spectral measurements of the observed 'd-d' transitions<sup>(55,56)</sup>.

(a) Spectrochemical series

The energy of separation,  $\Delta$ , between the ground and first excited state, may be obtained from the spectra of a series of transition metal compounds. It has been observed that for many transition metal cations, an approximately constant (neutral molecule and anion) ligand series occurs. This ligand series cannot be rationalized simply in terms of obvious properties such as the anion acid dissociation constants,  $K_a$ , or the electrostatic field strength,  $10Dq$ , operating on the central metal d electrons. The generally accepted rationalization, based on the molecular orbital model, is that the values of  $\Delta$ , as observed, follow the order<sup>(56)</sup>:

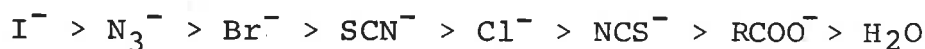


Although there is disagreement in some of the published data, the generally occupied positions of the ligands relevant to this study (arranged in order of increasing  $\Delta$ ) are<sup>(55,56,57,58,59,60)</sup>:



(b) Nephelauxetic series

The interelectron repulsion, frequently expressed as the Racah parameter,  $B(\text{cm}^{-1})$ , may also be obtained from spectroscopic measurements. The value of  $B$ , which is extremely sensitive to changes in the electronic environment of the metal 'atom', increases with both  $Z$ , the atomic number, and the oxidation state<sup>(56)</sup>. From the decrease in the value of  $B$  for complex species, when compared to the gaseous metal ion, a ligand series may be built up<sup>(56)</sup>. This series, termed the nephelauxetic series, reflects the polarizability of the ligand. The covalent character of the metal-ligand bond may well be related to this polarizability<sup>(56,60)</sup>. The generally accepted positions of the relevant ligands in this case are<sup>(56,58,59,60)</sup>



The observed sequence of apparent strengths for the Fe-X bond, in the FesalenX series, cannot be rationalized in terms of either of these effects.

(c) Anion-acid dissociation constants

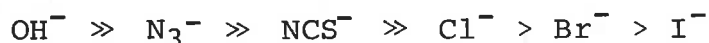
In the case of the Fe(III)-X bond, a more accurate re-

flection of the coordinating 'ability' of the anionic ligand,  $X^-$ , may well be provided by this experimentally determinable property. The covalent Fe-X bond would be expected to be predominantly of ' $\sigma$  character' and consequently the stability of this bond may well correlate with the stability of the H-X bond.

The Hard-Soft Acid Base (HSAB) theory proposed by Pearson, 'has proved useful in accounting for and predicting the stability of coordination compounds' <sup>(61)</sup>. According to this theory, the ions  $H^+$  and  $Fe^{3+}$  are both classified as hard acids <sup>(62)</sup> and would thus be expected to show similar trends. Whilst it is not clear what influence, if any, the presence of the coordinated anion ligand  $salen^{2-}$  may have on the hardness of the central metal ion, it appears unlikely that the  $Fe^{3+}salen^+$  ion would be considered soft. In general, those species classified as 'soft' acids appear to be complexes in which significant  $\pi$  bonding occurs between the metal and ligand <sup>(61)</sup>. Such bonding is unlikely to be of significance in the Fe(III) case.

However, as data is available for both 'hard' and 'soft' acid equilibria with many of the ligands of interest to this study, both cases are tabulated in Table 3.5. The cations selected are  $H^+$  as the hard acid and methyl mercury,  $MeHg^+$ , as the soft acid.

In both cases, it can be seen that the stability of the M-X bonds (where M = Hg or H) follow the order:



The position in this series, of the anions  $C_6H_5COO^-$  and  $NO_3^-$  is not definite. However, it appears reasonable to suggest that

TABLE 3.5

Basicity of ligand X towards hard ( $H^+$ ) and soft ( $MeHg^+$ )  
acidic cations

Anion, $X^-$	$pK_{[H^+]}$ (61,63)	$pK_{[MeHg^+]}$ (62)
$Cl^-$	- 5.26	- 12.25
$Br^-$	- 7.26	- 15.62
$I^-$	- 7.76	- 18.10
$NO_3^-$	0.37	
$NCS^-$	2.70	- 6.7
$N_3^-$	6.46	- 1.3
$C_6H_5COO$	5.94	
$OH^-$	15.74	6.3

Notes:

1. Equilibria



$$K_1 = \frac{[MeHgX][H_3O^+]}{[MeHg^+.H_2O][HX]}, \quad K_2 = \frac{[X^-][H_3O^+]}{[H_2O][HX]}$$

and  $pK = -\log K$ .

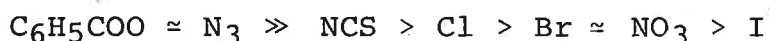
2. Thiocyanate ligand coordination, through S in  $MeHgX^{(62)}$   
and through N in  $HX^{(23)}$ .

$C_6H_5COO^-$  would be near the  $N_3^-$  ion, simply on the basis of their relative  $pK_{[H^+]}$  values.

The case of  $NO_3^-$  is not as clear cut, as much contradictory evidence as to the coordinating ability of this ion has been presented.

- (1) From the acid dissociation data, the order suggested is  $NO_3^- > Cl^- > Br^- > I^-$ .
- (2) Substitution reactions involving the replacement of  $H_2O$  in  $[Co(III)(en)_2(NO_2)H_2O]^{2+}$  by  $X^-$ , suggest that the Co-X bond strength follows the sequence<sup>(64)</sup>:  
 $SCN^- > Cl^- \approx Br^- \approx NO_3^-$ .
- (3) For  $[Co(III)(NH_3)_5 X]$  species, the Co-X bond strength order is<sup>(64)</sup>:  
 $NCS^- > Cl^- > I^- > Br^- > NO_3^-$ .

Thus it would appear reasonable to suggest that the order of bond strengths suggested for the Fe-X bonds in the FesalenX series, viz.



is consistent with that expected from the anion acid dissociation constant data.

### 3.5 EXPERIMENTAL

- (i) All solvents utilized for the conductance and spectral measurements were of spectral grade.
- (ii) Conductance measurements

Conductance measurements were made on a Phillips Model



PR9500 Conductivity meter, utilizing a conductance cell fitted with a B24 cone. Approximately 20 cm<sup>3</sup> of test solution was placed in a 100 cm<sup>3</sup> test tube, with B24 socket, and the conductance cell inserted. The tube and contents were then thermostatted at 25°C for 15 minutes before measurement.

Solutions were prepared using A grade volumetric flasks. The conductance cell was calibrated against aqueous solutions of A.R. KCl - cell constant,  $L/A$ , 0.843 cm<sup>-1</sup>. The conductances have been corrected for the solvent conductance and  $\Lambda_M$  calculated using the formula

$$\Lambda_M = C \cdot \frac{L}{A} \cdot \frac{10^3}{M}$$

where C = conductance or resistance (ohm)<sup>-1</sup>

M = molar concentration.

### (iii) Ultraviolet visible spectra

Solution spectra were obtained on a Perkin-Elmer Model 402 recording u.v.-visible spectrophotometer, calibrated as per the manufacturer's recommendations, with a reproducibility in absorbance readings of ± .5% and an accuracy of ± 1%. Absorbance values were estimated to three significant figures and obtained directly from the recorded spectra. Values of the molar extinction coefficient,  $\epsilon$ , were calculated from the formula

$$\epsilon = \frac{10A}{CL}$$

where A = Absorbance; C = molar concentration;

and L = path length in mm.

The values of  $\epsilon$  have been expressed to three significant figures throughout this work. Clearly the uncertainty lies in the third figure.

For all studies for which results appear in the same Table, the same sample of solvent has been utilized. All solutions were prepared and stored in tightly stoppered volumetric flasks.

(iv) Calculated spectra

Each spectral band may be described by the Gaussian distribution function<sup>(65)</sup>:

$$A = \epsilon 2^{-\left(\nu - \nu_n / \delta_n\right)^2}$$

where  $A$  = Absorbance;  $\epsilon$  = extinction coefficient;

$\nu$  = frequency ( $\text{cm}^{-1}$ );  $\nu_n$  = frequency at maximum absorbance of  $n^{\text{th}}$  band;  $\delta_n$  = halfwidth ( $\nu_{\frac{1}{2}}$ ) of  $n^{\text{th}}$  band ( $\text{cm}^{-1}$ ).

The spectrum, as obtained, may be considered as the sum of a number of overlapping bands with the absorbance, at any particular frequency, being described by the relation<sup>(65)</sup>:

$$A_{\text{total}} = \sum_{i=1}^n A_i$$

For this study  $n = 4$ , and the values of the respective parameters  $\nu_n$  and  $\delta_n$ , as obtained from the original spectra, are:

$$\begin{aligned} \nu_1 &= 18,800 \text{ cm}^{-1} \text{ (532 nm)}, & \delta_1 &= 2700 \text{ cm}^{-1} \\ \nu_2 &= 23,000 \text{ cm}^{-1} \text{ (435 nm)}, & \delta_2 &= 2500 \text{ cm}^{-1} \\ \nu_3 &= 30,300 \text{ cm}^{-1} \text{ (330 nm)}, & \delta_3 &= 3400 \text{ cm}^{-1} \\ \nu_4 &= 37,700 \text{ cm}^{-1} \text{ (270 nm)}, & \delta_4 &= 3800 \text{ cm}^{-1} \end{aligned}$$

The values of the extinction coefficient parameters, which are of the order of  $10^3$  to  $10^4$ , selected for the calculation need only be in the same ratio as the experimental values. In this case the values of  $\epsilon_3$  and  $\epsilon_4$  chosen were 60 and 100 respectively and were held constant throughout. The values of  $\epsilon_1$  and  $\epsilon_2$  were varied between 0 and 40, such that  $\epsilon_1 + \epsilon_2 = 40$ .

Close approximations of the observed spectra were obtained over the range of interest, viz.  $18,000 \text{ cm}^{-1}$  (555 nm) to  $25,000 \text{ cm}^{-1}$  (400 nm).

The values of  $\epsilon_1$  and  $\epsilon_2$  utilized, together with the positions of the calculated and experimental maxima, are tabulated below:

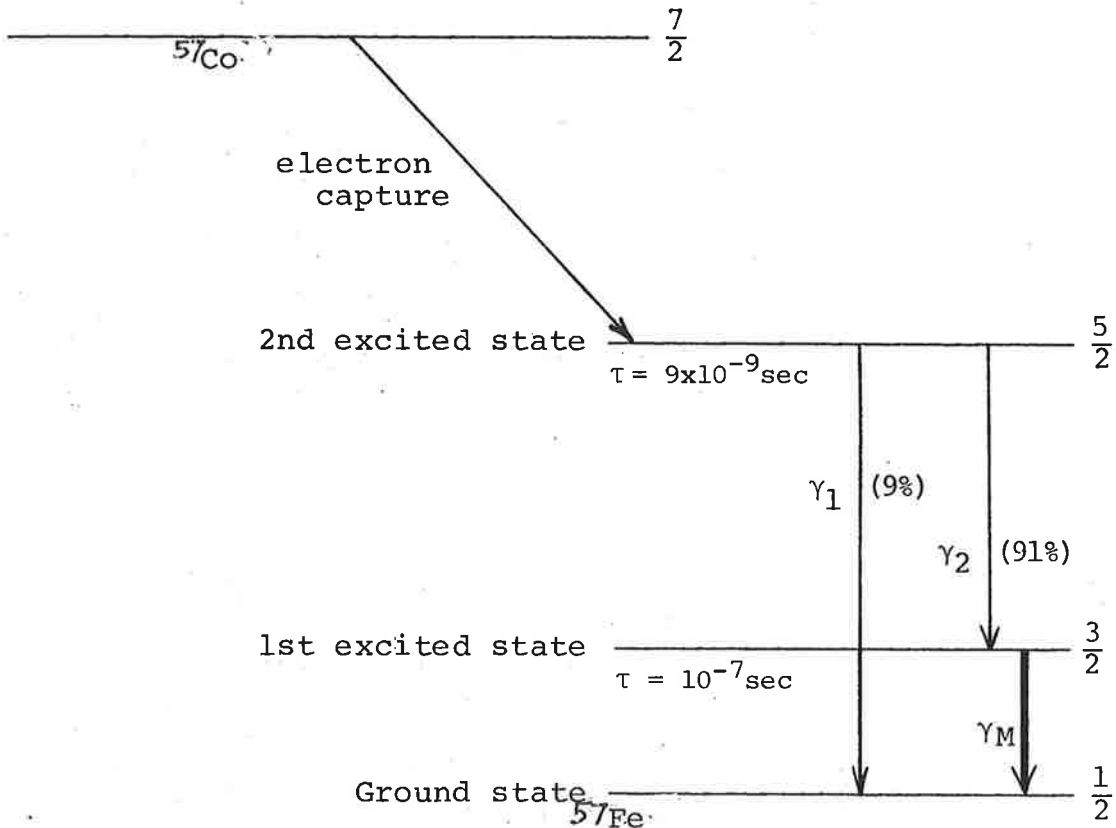
X	Calc. $\nu_1 (\text{cm}^{-1})$	Exp. $\nu_1 (\text{cm}^{-1})$	$\epsilon_1$	$\epsilon_2$
$\text{NO}_3$	19,200	18,800	28	12
Cl	20,800	20,800	21.6	18.4
NCS	22,300	22,300	20	20
$\text{N}_3$	shoulder from 22,400 - 24,300	shoulder from 22,200 - 24,400	8	32

CHAPTER 4Moessbauer Spectra4.1 THE PRINCIPLES OF MOESSBAUER SPECTROSCOPY (15,66,67,68,69)(i) Source of radiation, energy and modulation

Until comparatively recently, the physical behaviour of the atomic nucleus was considered to be independent of chemical bonding. The widespread application of nuclear magnetic resonance spectroscopy to chemical problems highlights the fallacy of this belief. Another resonance phenomenon involving atomic nuclei, the Moessbauer effect, also yields significant information regarding chemical bonding<sup>(68)</sup>.

Moessbauer spectroscopy is similar to other spectroscopic techniques in that a source of electromagnetic radiation, an absorber and a detector measuring the incident radiation intensity are required. Transitions occurring between nuclear energy levels are studied and the photon energies involved are typically in the range 10 to 200 keV<sup>(70)</sup>. The radiation detector is essentially a gamma ray spectrometer<sup>(66)</sup> and the radiation source a radioactive nuclide.

The nucleus involved in this study is that of the isotope of iron of atomic mass 57, denoted as  $^{57}\text{Fe}$  which has a natural abundance of 2.19%<sup>(71)</sup>. The required excited nuclear states of  $^{57}\text{Fe}$  result from the decay of the radionuclide,  $^{57}\text{Co}$ .  $^{57}\text{Co}$  has a half life ( $t_{1/2}$ ) of 270 days<sup>(71)</sup> and decays according to the following scheme<sup>(72)</sup>:



where  $\gamma_1 = 136.47 \text{ keV}$ ,  $\gamma_2 = 122.06 \text{ keV}$ ,

$\gamma_M = 14.41 \text{ keV}$  (Moessbauer transition) <sup>(71)</sup>.

The half integral values listed to the right of each level are the values of the nuclear spin quantum number,  $I$ .

The absolute value of the 14.4 keV Moessbauer transition is known accurately to only three significant figures, as there is considerable disagreement about the fourth in published data <sup>(73)</sup>. However, the transition is extremely well defined as it produces a very sharp line with a natural line width,  $\Gamma_{\text{nat}}$ , of  $4.6 \times 10^{-12} \text{ eV}$  <sup>(74)</sup>. Thus the relative energy of the transition is defined to better than one part in  $10^{12}$ , with an absolute value near 14.4 keV. The radiation may be considered as effectively monochromatic.

For resonant absorption of this monochromatic radiation

to be observed, it is necessary to modulate the radiation source in such a way that a range of energies may be scanned. This may be achieved by utilizing the Doppler effect which allows the source energy to be varied slightly depending on the relative velocity of the source with respect to the stationary absorber. Such a variation is described by the relation:

$$s_{E_{\gamma}} \pm \left(\frac{v}{c}\right) s_{E_{\gamma}} = a_{E_{\gamma}} \quad (69)$$

where  $v$  = velocity of source,  $c$  = velocity of light and  $s_{E_{\gamma}}$  and  $a_{E_{\gamma}}$  are the transition energies for the source and absorber respectively.

Experimentally, the source is oscillated through a range of velocities within the limits +10 mm/sec to -10 mm/sec, covering the region required for resonant absorption with  $^{57}\text{Fe}$  nuclei in the majority of cases. This velocity range corresponds to an energy scan of +4.8 to  $-4.8 \times 10^{-7}$  eV.

Resonant absorption of quanta of the appropriate energy produces absorption minima on a plot of incident radiation intensity against energy, i.e. the Moessbauer spectrum. In common with other types of spectroscopy, there are three main characteristics of interest in the spectra. These are the width, position and multiplet structure for the absorptions.

(ii) Line width

Ideally the line width of the observed absorption is simply twice the natural line width, i.e.  $2\Gamma_{\text{nat}}$  <sup>(75)</sup> where  $\Gamma_{\text{nat}}$  is calculated from the uncertainty principle by

$$\Gamma_{\text{nat}} = h/2\pi\tau$$

and  $\tau$  is the lifetime of the excited state.

In practice the observed line width,  $\Gamma_{\text{obs}}$ , is always larger than  $2\Gamma_{\text{nat}}$ , sometimes by an order of magnitude<sup>(75)</sup>. There are a number of causes, three of which are of importance in the practical requirements of the Moessbauer experiment.

(a) Recoil of emitter/absorber atom

Emission/absorption of the high energy gamma quanta would be expected to be accompanied by significant movement or recoil of the atom concerned. The fraction of the available energy lost to a free recoiling atom is quite small and for <sup>57</sup>Fe is of the order of 0.002 eV<sup>(76)</sup>.

This is significant when compared with  $\Gamma_{\text{nat}}$  ( $4.6 \times 10^{-12}$  eV) and such a variation in  $E_{\gamma}$  would lead to broadening of the sharp transition line to the extent where resonant absorption could not be observed. This problem is prevented by ensuring that both emitter and absorber nuclei are held tightly into a crystal lattice so a large proportion of the transitions are effectively recoil-free<sup>(77)</sup>.

(b) Thermal motion

As discussed above, motion of atomic nuclei leads to line broadening. Consequently it would be expected that vibration of nuclei in the crystal lattice should also contribute somewhat. This is observed and the fraction of transitions which are recoil free shows temperature dependence<sup>(78)</sup>.

For the majority of Moessbauer nuclides, this effect necessitates that both the source and absorber be maintained at low temperatures (78°K or lower). Fortunately, with  $^{57}\text{Fe}$  the recoil-free fraction is significant, and consequently allows spectra to be obtained, over a wide range of temperatures<sup>(78)</sup>. Data can be obtained readily for  $^{57}\text{Fe}$  at room temperature.

(c) Thickness of absorber

The absorber thickness contributes to the line width and the difference between  $\Gamma_{\text{obs}}$  and  $2\Gamma_{\text{nat}}$  shows a direct relationship to this thickness<sup>(68)</sup>. Corrections can be made, if required, but are not of great significance if the absorber is less than 1 mm thick.

(d) Other effects

There are a number of other causes of line broadening which are more difficult to evaluate. Examples include non-homogeneity of the chemical environment of the resonant atoms in the source and/or absorber, and localized magnetic effects which may average out over the sample.

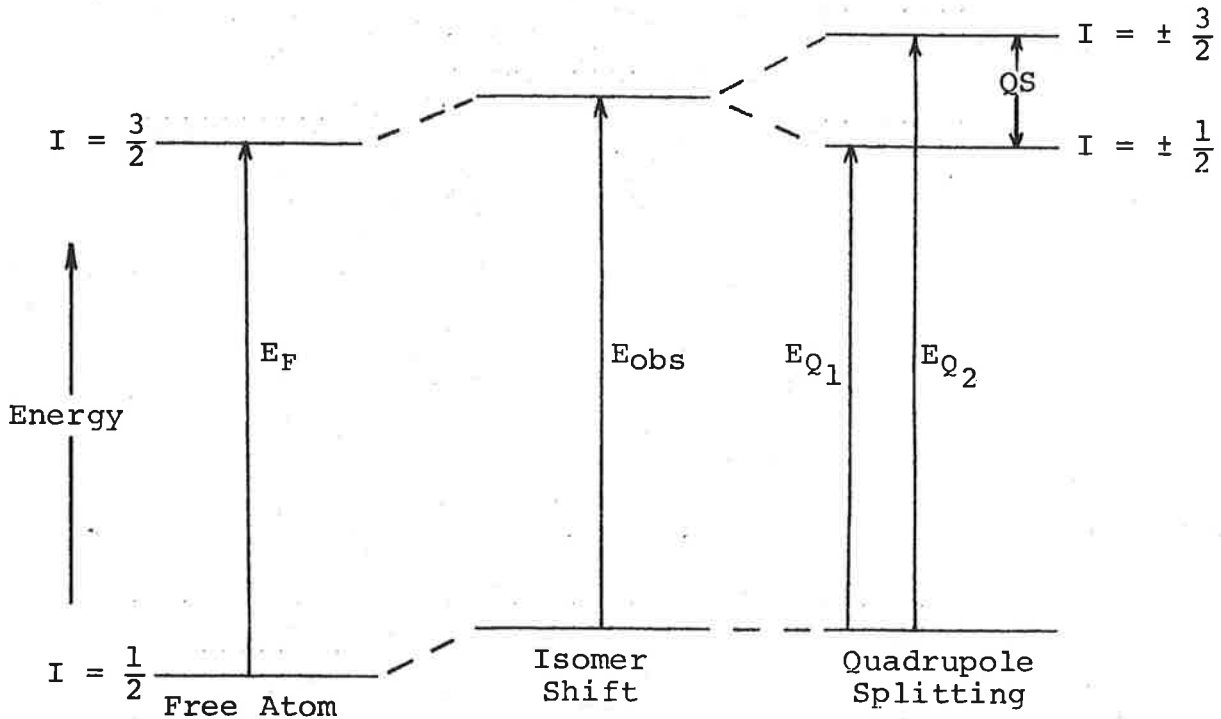
The value of the ratio  $\Gamma_{\text{obs}}/2\Gamma_{\text{nat}}$  provides a measure which allows assessment of the 'quality' of the data obtained from a Moessbauer spectrometer<sup>(79)</sup>.

(iii) Position and multiplet structure

As different compounds have been observed to give characteristic spectra, it may be reasonably concluded that the nuclear energy levels are sensitive to the extra-nuclear en-



vironment. The interactions responsible are those between the nuclear charge distribution and the electrostatic and magnetic fields produced by the electron clouds<sup>(80)</sup>. The effects of such interactions may be summarized diagrammatically as follows (81):



(a) Isomer (or Chemical) shift

The electrostatic interaction between the nucleus and electrons which have a finite probability of being in the region of the nucleus results in a slight shift of both the ground and excited energy levels relative to those of a free atom. Thus the isomer shift may be defined as the difference in energy between that of the observed transition,  $E_{Obs}$ , and that of the free atom,  $E_F$ . The free atom situation is difficult to achieve experimentally and the isomer shift is usually expressed relative to the position of a standard absorber. Two materials are in common use - natural iron and sodium nitroprusside ( $Na_2[Fe(CN)_5NO] \cdot 2H_2O$ ), with the latter being the preferred reference<sup>(82)</sup>.

(b) Quadrupole splitting (QS or  $\Delta E_Q$ )

A further interaction of an electrostatic nature occurs between the nuclear quadrupole moment,  $Q$ , and the electrostatic field gradient, E.F.G., due to the geometry of the electronic charge around the nucleus. The quadrupole splitting is the separation between the two peaks observed in the spectrum, i.e.

$$Q.S. = EQ_2 - EQ_1 \quad (\text{or } \Delta E_Q)$$

The isomer shift, in this case, is obtained from the centroid of the two peaks. An alternative, and possibly preferable, term is the centre shift, C.S.<sup>(83)</sup>. The abbreviations to be used in this work are  $\Delta E_Q$  and C.S.

(c) Magnetic hyperfine splitting

The degeneracy of the nuclear energy states may be lifted in a magnetic field giving rise to  $2I + 1$  levels in each case. The allowed transitions between the ground and excited states produce six line spectra. In general, this requires the application of a substantial external magnetic field and such measurements have not been attempted in this study.

(iv) Relationship of the Moessbauer parameters to the chemical environment

The influence of the chemical bonding of the iron atom is reflected mainly in the magnitude of the isomer/centre shift and the quadrupole splitting parameters.

(a) Centre Shift (C.S.)

This electrostatic interaction may be calculated using a classical, quantum mechanical treatment. Electrons in s orbitals

have a significant 'near-nuclear' population and the magnitude of the shift follows a linear relationship to the s electron density, the shift increasing with a decrease in the density.

P and d electrons, although they have zero density at the nucleus, also influence the shift. Hartree-Fock calculations, for different  $d^n$  configurations, show a marked increase in the nuclear electron density with a decrease in the value of  $n$ <sup>(84)</sup>. This arises indirectly because the orbital of the 3s electrons, which spend a fraction of their time further from the nucleus than the 3d electrons, expands significantly with increasing  $n$ . On this basis the range of shifts for various  $d^n$  configurations should show the trend  $d^6 > d^5 > d^4$ , and the values obtained for the following Fe ions confirm this<sup>(85)</sup>:

$d^6$ ( $\text{Fe}^{2+}$ )	range	1.5 - 1.6 mm/sec
$d^5$ ( $\text{Fe}^{3+}$ )	range	0.7 - 0.8 mm/sec
$d^4$ ( $\text{FeO}_4^{2-}$ )		0.6 mm/sec

In the case of compounds with significant covalent character, the pattern is more complicated, due to modification of s, p and d electron densities by covalent bonding. Shifts vary between 0 and 0.65 mm/sec with little or no dependence on the formal oxidation state (metallic iron falls in this range also)<sup>(86)</sup>. This may be rationalized using the Pauli electro-neutrality principle which suggests that the charge may be 'adjusted' between the central metal atom and ligands such that the effective charge on the metal atom is between -1 and +1<sup>(86)</sup>. This arises from the important bonding interactions for <sup>57</sup>Fe, namely  $\sigma$ -bonding and  $\pi$ -back bonding, which both contribute to a change in the 4s and 3d populations from those in 'free' iron compounds.

Calculations of the shift values for covalently bonded complex molecules are of limited validity but the use of relative shifts to estimate the relative changes in the valence orbital populations finds wide application. An increase in the isomer shift corresponds to an increase in the 3d or a decrease in the 4s electron density<sup>(87)</sup>.

(b) Quadrupole splitting ( $\Delta E_Q$ )

The magnitude of  $\Delta E_Q$  is proportional to the electric field gradient (E.F.G.) which interacts with the quadrupole moment,  $Q$ , of the nucleus. The nine term E.F.G. tensor, with proper selection of the coordinate axes, reduces to three non-zero terms - one component along each of the three axes. As these terms are interdependent, further reduction to two independent parameters can be effected. The two terms are  $q$ , the field gradient component in the Z direction, and  $\eta$ , the assymetry parameter (a combination of the three terms). Thus

$$\Delta E_Q = \frac{1}{2}e^2qQ\left(1 + \frac{\eta^2}{3}\right)^{\frac{1}{2}} \quad (88)$$

where  $e$  is the protonic charge and values of  $\eta$  lie between 0 and 1.

Ideally the required information from Q.S. data is the magnitude of  $q$  and  $\eta$  and the sign of  $q$ . Although  $\Delta E_Q$  may be readily measured, the required data cannot be obtained directly from the powder spectra. Special techniques may be used to determine the sign of  $q$  and to estimate  $\eta$ <sup>(89)</sup>. To a first approximation, the  $\eta$  term may be neglected as values lie between 1 and 1.15.

The E.F.G. term can be conveniently divided into two components with

$$q = (1 - \gamma_{\infty})q_{\text{lat.}} + (1 - R)q_{\text{val.}}$$

where  $q_{\text{lat.}}$  is the contribution from external ligand charges and  $q_{\text{val.}}$  the contribution from valence electrons. ( $R$  and  $\gamma_{\infty}$  are the Sternheimer anti-shielding factors, which allow for the effect of the inner, non-valence electrons on  $q_{\text{lat.}}$  and  $q_{\text{val.}}$ . These magnify the contributions to  $q$  by a factor of about 7.)

These quantities can be evaluated if the crystal structure and valence orbital populations are known. As the latter is not usually the case, such calculations are difficult. However, generalizations may be made<sup>(89)</sup>:

- (1) If the electronic and ligand charges have cubic symmetry,  $q_{\text{lat.}} = q_{\text{val.}} = 0$ .
- (2) If the 3p orbitals are equally populated,  $q_{\text{val.}} = 0$ .
- (3) If the ligand charges are of equal magnitude in an octahedral arrangement,  $q_{\text{lat.}} = 0$ .

The valence electron contribution term can be further subdivided

$$q_{\text{val.}} = q_{\text{c.f.}} + q_{\text{m.o.}}$$

$q_{\text{c.f.}}$  = valence contribution considering a crystal field model with NO overlap of ligand and metal orbitals - a temperature dependent term.

$q_{\text{m.o.}}$  = valence contribution considering metal-ligand covalent bonding only - a temperature independent term.

For octahedral complexes, the dominant term will be<sup>(89)</sup>:  
 $q_{c.f.}$  for Fe(II) high spin ( $t_{2g}^4 e_g^2$ ) and Fe(III) low spin ( $t_{2g}^5$ ).  
 $q_{m.o.}$  for Fe(II) low spin ( $t_{2g}^6$ ) and Fe(III) high spin ( $t_{2g}^3 e_g^2$ ).

In summary, the anticipated results for octahedral iron complexes are<sup>(90)</sup>:

- . asymmetric ground state (Fe(II) high spin, Fe(III) low spin) - large  $\Delta E_Q$ , in the range 1.7 to 3.6 mm/sec.
- . symmetric ground state (Fe(II) low spin, Fe(III) high spin) - small  $\Delta E_Q$ , in the range 0 to 0.7 mm/sec.

These expectations are essentially confirmed by the experimental results, with the major anomalies occurring in the second case. Many complexes, with a symmetric ground state, have substantial Q.S. values but this is generally attributable to significant distortion from octahedral symmetry<sup>(89)</sup>.

(v) The additivity principle and correlations with bonding

As indicated above, prediction of expected Moessbauer parameters by calculation finds somewhat limited application. In the main, these parameters have been rationalized using semi-empirical methods. One of these, the additivity model, has been of particular use in interpreting the spectra of Sn(IV), Fe(II) low spin and Fe(III) compounds<sup>(89)</sup>.

The basic premise of the model is that the parameters may be regarded, at least to a first approximation, as the sum of

independent contributions - one from each of the bonded ligands. Tables of partial quadrupole splittings, p.q.s., have been developed for Fe(II) low spin and Sn(IV) compounds and a table of partial centre shifts, p.c.s., for the Fe(II) low spin case (91).

The possible bonding factors which are expected to influence the value of  $\Delta E_Q$  are inequalities in  $\sigma$  or  $\pi$  bonding ( $q_{m.o.}$ ) and ligand charges ( $q_{lat.}$ ). For Fe(II) low spin,  $q_{val.}$  is expected to be the dominant contributor to the E.F.G. with  $\sigma$  bonding inequalities of more importance than  $\pi$  bonding, although  $\pi$  acceptor ability may be significant<sup>(92)</sup>.

The centre shift for Fe(II) low spin, reflects both the  $\sigma$  and  $\pi$  bonding abilities of ligands, with a decrease in C.S. correlating with an increase in  $\sigma$  donating ability and/or  $\pi$  acceptor ability<sup>(92)</sup>. Using the partial field strengths of a series of ligands (calculated from the optical spectra of Co(III) complexes) a correlation between the p.c.s. value and the ranking of the ligand on the spectrochemical series has been observed<sup>(92)</sup>.

The additivity principle, which has proved of value in the rationalization of some Moessbauer data, is expected to find application in the Fe(III) high spin case<sup>(89)</sup>. Although a large amount of data for this system appears in the literature, there appears to have been no systematic attempt to evaluate such correlations.

In broad outline then, the object of this section of the research program is to determine the Moessbauer parameters for

the series of high spin complexes of general formula Fe(III) salenX. This data will then be compared with that obtained in the preceding chapters with the prime objective being the elucidation of any correlation between the Moessbauer parameters and information related to the bonding of the ligand X. As indicated above, the Fe(III) high spin system would be expected to show similarities to the Fe(II) low spin system and thus correlations could well involve spectrochemical or nephelauxetic effects.

#### 4.2 REVIEW OF PUBLISHED DATA - Correlation with Structure

For a systematic study as proposed, the preferred environment for the Fe(III) atom would involve octahedral coordination where the ligand atoms in five of the positions remain constant and the coordinating group in the remaining position may be varied systematically. The 'family' of compounds of formula FeSalenX would be suitable if all complexes were dimeric and thus effectively six coordinate. A similar theoretical consideration to that discussed for octahedral coordination has been applied to pentacoordinate monomeric complexes<sup>(16)</sup>. Thus it is considered that the exact structure of the complexes in the solid state is not vital for a comparative study, if either the structure can be assumed to be the same for all X or the Moessbauer data obtained for known monomeric/dimeric species do not differ significantly.

The data available for FeSalenX (X = Cl or Br) and solvated adducts are tabulated in Table 4.1.



TABLE 4.1

Room temperature Moessbauer parameters of Fe(III) high spin complexes with salen

Compound	Structure	C.S.	$\Delta E_Q$	Reference	
(FesalenCl) <sub>2</sub>	dimer	.65 ± .01	1.45 ± .01	(16)	
		.62 ± .02	1.38 ± .02	(17)	
		.66	1.40	(13)	
FesalenCl.2MeNO <sub>2</sub>	monomer	.58 ± .01	1.30 ± .01	(16)	
		XMeNO <sub>2</sub>	.61	1.34	
		2CHCl <sub>3</sub>	.63 ± .01	1.40 ± .01	(16)
		2MeOH	.64 ± .01	1.45 ± .01	(16)
(FesalenBr) <sub>2</sub>	dimer (assumed)	.67 ± .01	1.63 ± .01	(16)	
FesalenBr.2CHCl <sub>3</sub>	monomer (assumed)	.65 ± .01	1.65 ± .01	(16)	
		2MeOH	.67 ± .02	1.63 ± .01	(16)
			.67 ± .01	0.87 ± .01	(16)
		2MeNO <sub>2</sub>	.62 ± .01	1.61 ± .01	(16)
		MeNO <sub>2</sub>	.67 ± .01	1.13 ± .01	(16)

The variation in the parameters obtained for  $(\text{FesalenCl})_2$  is consistent with the limitations expected for the Moessbauer technique and these results agree well with each other<sup>(69)</sup>. All samples were prepared in the same way, viz. recrystallization from acetone, and it would be reasonable to expect that the average of these values represents an accurate estimate of the parameters. Normal statistical practice would require a minimum of three standard deviations for a 90% confidence interval<sup>(93)</sup> and as such, the expected Moessbauer parameters for  $(\text{FesalenCl})_2$  are C.S. =  $0.64 \pm .03$  mm/sec,  $\Delta E_Q = 1.41 \pm .06$  mm/sec. Applying similar statistical criteria, it would appear that there is not a significant difference between

- (a) (for X = Cl), the dimer and  $\text{CHCl}_3$  and MeOH adducts;
- and (b) (for X = Br), the dimer,  $\text{CHCl}_3$  and one of each of the MeOH and  $\text{MeNO}_2$  adducts.

Furthermore, there is considerable uncertainty as to the structure (i.e. monomer or dimer) of several of these complexes. The assignment of structure, based on i.r. spectral criteria, has been criticized in Chapter 2, and the Moessbauer data obtained<sup>(16)</sup> would appear to contradict several of the structural assignments based on magnetic data<sup>(11)</sup>. Only two structures may be regarded as definite, viz.  $(\text{FesalenCl})_2$  and the nitromethane adduct, because the crystal and molecular structures have been determined by X-ray diffraction techniques<sup>(19,94)</sup>. Consequently, it is suggested that structural assignments based on criteria other than X-ray studies should be considered as suspect in the case of 'FesalenX' type complexes.

The determination of the crystal structure of each 'FesalenX' complex was considered to be outside the scope of this study. In order to rationalize the Moessbauer parameters obtained, it has been assumed that the environment of the metal atom in all FesalenX species is similar, with the major difference arising from the Fe-X bond. This assumption would be considered valid if either

- (a) all species have a similar solid state structure, viz. that of the dimer (FesalenCl)<sub>2</sub>;
- or (b) association in the solid state does not influence the magnitude of the Moessbauer parameters markedly.

It appears that (b) may well be a reasonable proposition. The Moessbauer data for the known monomeric species, FesalenCl. 2MeNO<sub>2</sub>, do not differ greatly from the data obtained for the dimer. Furthermore, the majority of the solvated species, particularly those with weakly coordinating solvents, have similar Moessbauer parameters to those of the non-solvated dimers<sup>(16)</sup>. It would appear that structural assignments based on data, other than a crystal structure, must be regarded as doubtful. All species obtained in this work have been shown to be non-solvated (Chapter 2) and there is no evidence to suggest any pronounced structural dissimilarities.

#### 4.3 MOESSBAUER PARAMETERS

A summary of the relevant data obtained from the Moessbauer spectra is presented in Table 4.2.

The data obtained in this study are in reasonable agreement with the previously published values (X = Cl and Br) in

TABLE 4.2

Room Temperature <sup>(a)</sup> Moessbauer Parameters <sup>(b)</sup>

Compound	C.S.	$\Delta EQ$	$v_{1/2}^{(c)}$	% Absorption <sup>(d)</sup>
(i) Reference standards				
Sodium nitroprusside	0.00 $\pm$ 0.01	1.73	0.45	8.1
Stainless steel(enriched)	-0.16 $\pm$ 0.02	-	0.43	21
(ii) FesalenX				
X = Cl	0.65 $\pm$ 0.03	1.35 $\pm$ 0.06	0.53	1.7
Br	0.78 $\pm$ 0.03	1.64 $\pm$ 0.05	0.48	1.6
I	0.77 $\pm$ 0.03	1.78 $\pm$ 0.05	0.49	1.1
NO <sub>3</sub>	0.78 $\pm$ 0.03	1.62 $\pm$ 0.05	0.51	2.1
NCS	0.67 $\pm$ 0.03	1.26 $\pm$ 0.05	0.52	2.6
N <sub>3</sub>	0.77 $\pm$ 0.04	1.08 $\pm$ 0.07	0.57	1.0
C <sub>6</sub> H <sub>5</sub> COO	0.68 $\pm$ 0.04	0.81 $\pm$ 0.08	0.60	1.1
(iii) Novel Compounds				
K[Fesalen(CN) <sub>2</sub> ]	0.31 $\pm$ 0.02	2.15 $\pm$ 0.04	0.36	2.0
[Fe(saen) <sub>2</sub> ]Cl.H <sub>2</sub> O	0.42 $\pm$ 0.02	2.75 $\pm$ 0.04	0.43	4.0
[Fe(saen) <sub>2</sub> ]I	0.59 $\pm$ 0.04	0.35 $\pm$ 0.08	0.62	0.8

Notes:

- (a) Room temperature 294 $\pm$ 1.5°K.
- (b) Units mm/sec, with centroid of sodium nitroprusside spectrum as reference (zero velocity) point.
- (c)  $v_{1/2}$  = peak width at half height - average value of two peaks (where applicable).
- (d) %Absorption values average of two peaks (where applicable).

Table 4.1, with the exception of the C.S. value for the bromo complex. However the values for both the chloro and bromo complexes agree more favourably with those summarized in a recent review article (69).

#### 4.4 DISCUSSION

##### (i) Spin state

The relevance of the Moessbauer parameters has been discussed earlier in this Chapter. One application, of significance to this study, is the determination of the spin state of Fe(III) in the complexes.

A summary of relevant observations follows:

##### Magnitude of $\Delta E_Q$ (15,33,69)

(1) Fe(III) low spin,  $S = \frac{1}{2}$  (assymmetric ground state)

$\Delta E_Q$  large,  $> 2$  mm/sec.

(2) Fe(III) high spin,  $S = \frac{5}{2}$  (symmetric ground state)

(a) octahedral symmetry

$\Delta E_Q$  small,  $< 0.7$  mm/sec

(b) distorted octahedral symmetry

$0.7 < \Delta E_Q < 2$  mm/sec

##### Centre Shift (C.S.) (15,33,69)

The range of C.S. values is not clearcut for the Fe(III) low spin state, with values being found in the range 0 to 0.6 mm/sec. However in the majority of cases, the C.S. range is 0 to 0.45 mm/sec.

For the Fe(III) high spin state, the C.S. values are significantly higher than in the low spin case and are found to lie between 0.55 and 0.85 mm/sec.

(a) Octahedral complexes

In the case of those complexes which can be considered as having essentially octahedral symmetry, the Moessbauer data unambiguously confirm the spin state of Fe(III), as illustrated by:

Compound	$\mu_{\text{eff}}$ (B.M.)	C.S.	$\Delta E_Q$	Spin state
Fe(saen) <sub>2</sub> I	6.06	0.59	0.35	S = 5/2
K[Fe(salen)(CN) <sub>2</sub> ]	2.10	0.31	2.15	S = 1/2
Fe(saen) <sub>2</sub> Cl.H <sub>2</sub> O	2.11	0.42	2.75	S = 1/2
(Fesalen) <sub>2</sub> O(33)	1.87	0.58	0.92	S = 5/2

Clearly the Moessbauer data discount the possibility that the low value of the magnetic moment observed with K[Fe(salen)(CN)<sub>2</sub>] and Fe(saen)<sub>2</sub>Cl.H<sub>2</sub>O arises from antiferromagnetic coupling of two Fe(III) S =  $\frac{5}{2}$  states, similar to that established for (Fesalen)<sub>2</sub>O. The two compounds must then be considered as having the Fe(III) in the 'true' low spin (S =  $\frac{1}{2}$ ) state.

(b) Distorted octahedral complexes

The data for the series of compounds of formula FesalenX, clearly indicate that all involve Fe(III) in the S =  $\frac{5}{2}$  state.

(ii) Distortion from octahedral symmetry

The magnitude of the  $\Delta E_Q$  values for the FesalenX series, suggest significant distortion from octahedral symmetry.

Calligaris and co-workers have related this distortion from octahedral symmetry to deviations from planarity in the coordinated tetradentate ligand, salen<sup>(95)</sup>. Such deviations have been attributed to interactions between this ligand and the apical ligand, X. This argument has been supported by the observation that the 'more bulky' the ligand X, 'the larger the distortions in the tetradentate ligand'<sup>(95)</sup>. It would appear that this argument is not correct because the benzoate ligand, C<sub>6</sub>H<sub>5</sub>COO, must be considered as the 'bulkiest' of those studied yet it produces by far the lowest  $\Delta E_Q$  value. Further, it is difficult to rationalize the polyatomic ligands NCS and N<sub>3</sub> which would appear larger than Cl<sup>(96)</sup>. In both cases the  $\Delta E_Q$  value is lower than that of the chloro complex.

Clearly the cause of the distortion from octahedral symmetry is not related simply to the size of the ligand X. Whether the magnitude of  $\Delta E_Q$  correlates precisely with the distortion of the planar salen moiety cannot be positively decided without structural evidence for all of the complexes. It would appear, however, that this must be considered a possibility.

### (iii) Correlation of $\Delta E_Q$ values

The order of magnitude of  $\Delta E_Q$  observed in this study is: I > Br  $\approx$  NO<sub>3</sub> > Cl > NCS > N<sub>3</sub> > C<sub>6</sub>H<sub>5</sub>COO. This order correlates with that observed for the apparent extent of dissociation, in solution, of the Fe-X bond in FesalenX, as discussed in Chapter 3. This would suggest that the magnitude of  $\Delta E_Q$  may well be related to the nature of the Fe-X bond. The relationship would be such that the stronger the Fe-X bond (i.e. the greater the covalent character) the smaller the value of  $\Delta E_Q$  observed.

As discussed above, the lifting of the degeneracy of the

nuclear energy levels, which results in quadrupole splitting, occurs as a result of the interaction between the nuclear quadrupole moment and the electric field gradient, E.F.G. The E.F.G. arises from two fundamental sources<sup>(89)</sup>:

- (1) the charges on the coordination sphere ions or ligands;
- (2) the electrons in the incompletely filled shells of the atom itself.

The coordination sphere charges contribute providing the symmetry is lower than cubic.

In the case of the FesalenX series, where the electronic arrangement has been established as the same, the variations in  $\Delta E_Q$  must arise from variations in the effective charge on the distant atoms of the ligands. It would appear reasonable to propose that the bonding between the salen ligand and the metal is substantially covalent whereas the Fe-X bond is much more polar in nature. This is consistent with the observations of Chapter 3. As a consequence the E.F.G. must be substantially asymmetric, with a major component directed along the Fe-X bond. The larger the magnitude of the effective charge on X, the greater the E.F.G. and thus  $\Delta E_Q$ .

The order of magnitude of  $\Delta E_Q$  for the various X is consistent with the order observed for the polarity of the Fe-X bonds. In this respect the observations for the Fe(III) high spin system parallel those outlined above (4.1(iv) and (v)) for the Fe(II) low spin system.

(iv) Correlation of C.S. values

The values of C.S. for the FesalenX series fall within



the range 0.65 to 0.78 mm/sec. While this range supports the assignment of the  $S = \frac{5}{2}$  spin state for Fe(III), it would appear too narrow to allow the elucidation of any anion dependent trend in these centre shifts. At first glance it would appear that the C.S. values fall into two distinct groups, viz.  $0.67 \pm .02$  mm/sec (X = Cl, NCS and C<sub>6</sub>H<sub>5</sub>COO) and  $0.77 \pm .01$  mm/sec (X = Br, I, NO<sub>3</sub> and N<sub>3</sub>). No correlation can be found with any parameter which could be associated with the Fe-X bond, including all those discussed in the preceding Chapters.

Furthermore, the C.S. values should be considered in the light of reservations as to their respective absolute values. The error estimates in Table 4.2 indicate the reproducibility (or precision) of this parameter and do not truly reflect its accuracy. The uncertainty arises as a consequence of the experimental procedure whereby individual spectra were obtained for each unknown compound and reference sample. It is worth noting that the uncertainty only applies to parameters, such as the centre shift, which have been obtained from different spectra. The procedure utilized is discussed in more detail in the experimental section of this Chapter.

It is felt therefore that the data obtained do not conclusively confirm whether or not there is a significant difference between any of the C.S. values. Indeed it is possible that the C.S. value may well be independent of the nature of the Fe-X bond in such a series of Fe(III) high spin complexes. This is contrary to the expectation, based on analogy with the Fe(II) low spin case, of a correlation with the spectrochemical series. Clearly data of a higher accuracy are required to resolve this situation. The application of an

internal standard technique similar to that employed in N.M.R. spectroscopy, with the increased availability of computing facilities, may well now be a feasible method of achieving this aim. In addition, studies at lower temperatures (e.g. c.a. 100°K), where the recoil fraction is known to be higher than at room temperature, may well facilitate such studies.

#### 4.5 : EXPERIMENTAL

##### (1) Summary

The Moessbauer spectrometer, constructed at S.A.I.T., was operated in the constant acceleration mode to produce spectra covering a velocity range of c.a. +5 to -5 mm/sec. All data were obtained in the form of typewritten digital output which was handplotted to give the individual spectra. The position of absorption minima was estimated with the aid of computer curve fitting programs. Details of the construction, calibration and experimental procedure are discussed in the following sections.

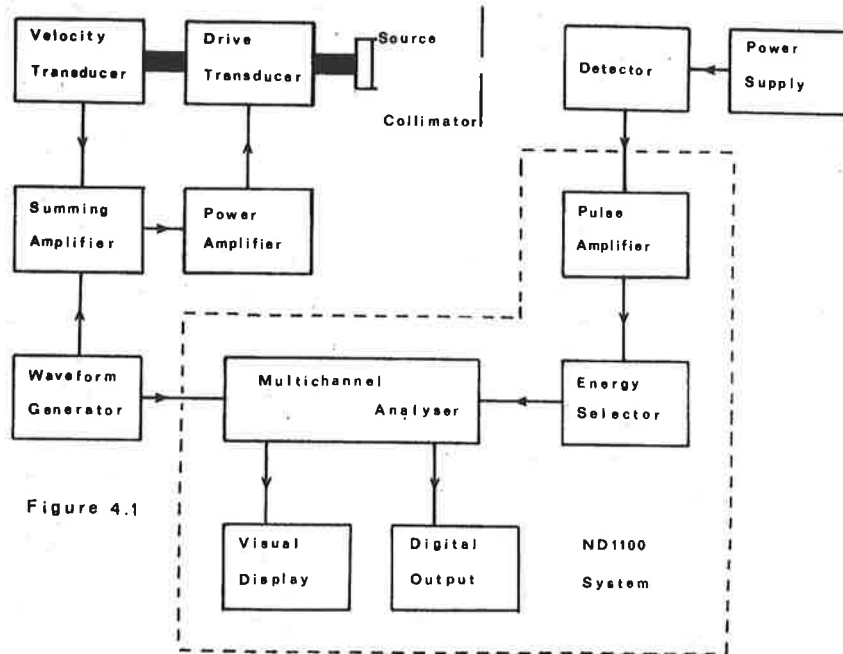
##### (2) Moessbauer spectrometer

The following block diagram (Fig. 4.1) summarizes the components of the spectrometer.

The spectrometer was based on the modular Nuclear Data series 1100 Analyzer system, consisting of the following modules:

- (a) 512 channel memory, data handling and analog to digital converter which comprise the basic multichannel analyzer (MCA).

- (b) ND520 PAD, preamplifier, amplifier and discriminator.
- (c) ND522 SCA, single channel analyzer (energy selector).
- (d) Fairchild Model 701 Oscilloscope (visual display).
- (e) ND316 Autofinger drive for IBM model 721 Selectric Typewriter (digital output).
- (f) Stabilized power supply incorporated in mounting rack.



The components constructed at S.A.I.T. are discussed in detail below:

(i) Detector

A sealed, gas-filled, proportional counter was used to detect the 14.4 keV Moessbauer transition. This type of detector has been shown to provide optimum resolution for low energy ( $< 30$  keV)  $\gamma$  radiation<sup>(97)</sup>, and the principles of counter design and construction have been described by Culhane<sup>(98)</sup>.

The counter gas chamber, constructed from 10 mm Al plate, was rectangular in shape (150 x 150 x 230 mm, volume c.a. 5.1 litres) and also acted as the electrical cathode. A tungsten

wire (0.05 mm diameter), acting as the anode, was operated at a potential of c.a. 1500V provided by a Phillips PW4022 stabilized power supply. The radiation entered the detector chamber via an Al foil window 0.05 mm thick and 60 mm in diameter. The counter gas utilized was a 90% Argon - 10% Methane (P10) mixture at approximately atmospheric pressure. Replacement of the counter gas may be effected, as required, via needle valves and the sealed system was shown to have a useable lifetime of c.a. 28 days.

The counter was purged and refilled before each unknown sample was studied.

(ii) Electromechanical system

The drive unit consisted of two mechanically coupled transducers, viz.

- Drive transducer - magnet and coil assembly of a Wharfedale 250 mm high compliance low frequency loud speaker;
- Velocity transducer - Sanborn Model 6LV2.

The configuration of the drive unit was essentially as previously described by Cohen et al<sup>(99)</sup> and Zane<sup>(100)</sup>. The unit was enclosed in an Al housing incorporating the Pb collimator, radiation source and appropriate Pb shielding.

(iii) Wave form generator and summing amplifier

The ultrastable triangular wave generator developed by Cohen<sup>(101)</sup> was modified to make use of current electronic technology, with the recommended operational amplifiers being replaced by Fairchild  $\mu$ A739C integrated circuits. These I.C.'s

required few additional stabilizing components and the circuit was essentially as published<sup>(101)</sup>. The synchronizing signal was obtained from the triangular generator as a positive pulse to suit the Nuclear Data M.C.A.

The linearity of the final velocity wave form was optimized by the 'shape compensation' technique of Zane<sup>(100)</sup>. This involves 'mixing' a parabolic wave form, obtained by integrating the reference triangular wave form, with the original signal. The optimization procedure was followed visually on an oscilloscope connected to the independent auxiliary output of the 6LV2 transducer.

The summing amplifier was of a simple variable gain design based on the  $\mu$ A739C I.C., with the 'mixed' signal introduced into the non-inverting input and negative feedback from the velocity transducer coupled to the inverting input.

(iv) Power amplifier

The drive transducer was driven by a power amplifier based on the General Electric PA246 I.C. Direct coupling was employed throughout to minimize phase changes in this final stage. The amplifier power supply was derived from the positive and negative rails of the stabilized mounting rack supply utilizing the symmetric voltage technique such that D.C. component in the output voltage wave form was less than 1 mV.

(v) Reference materials for calibration

Iron foil, 0.125 mm thick, of natural isotopic composition.

Stainless steel foil, 0.25 mm thick.

The above calibration foils were provided with the Moessbauer source.

Sodium Nitroprusside - Fluka, purum grade.

(vi) Moessbauer source

$^{57}\text{Co}$  in Pd matrix, obtained from the Amersham Radio-chemical Centre, England. The activity of the source was initially 10.8 mCi, with a natural line width,  $\Gamma$ , of 0.097 mm/sec.

(vii) Absorbers

The metal foils were fastened directly in position with adhesive tape. Polycrystalline samples were placed in a 12 mm diameter hole in a 25 mm square, 0.6 mm thick Al plate and held in place with adhesive tape. The sample was then attached to the lead collimator between the source and proportional counter window.

(3) Experimental Procedure

(i) Initial optimization

The constant acceleration mode of operation requires that the source velocity changes linearly with time, i.e. the output from the velocity transducer produces a triangular wave form. For this reason the 6LV2 transducer output wave form was observed via the independent auxilliary output, i.e. the output not involved in the feedback loop.

The drive transducer was optimized at a frequency of 9.5 hz to produce a symmetric triangular wave approximately 140 mV peak to peak on the C.R.O. screen. This corresponds to a velocity range of c.a. +6 to -6 mm/sec as the 6LV2 transducer calibration was quoted as 12 mV/mm.sec<sup>-1</sup>.

An appropriate energy window (14.4 ± 2 keV) was then selected utilizing the M.C.A. in the pulse height analysis mode. The spectrum of the natural iron foil was then obtained and the positions of the six absorption minima determined and checked against the published values to ensure linear operation. Minor adjustments were made as required.

The velocity range was then decreased slightly to 120 mV peak to peak (or +5 to -5 mm/sec) such that the inner four lines of the natural iron spectrum only were resolved. These absorptions were found between channels 80 and 430 and the positions utilized as a final check of the linearity of the system.

#### (ii) Calibration

Spectra of the three calibrants were obtained with c.a.  $2 \times 10^5$  counts/channel being accumulated in each case. The positions of the absorption minima were then determined and the calibration constant (velocity increment/channel) calculated from the literature values. The data have been listed in Table 4.3.

#### (iii) Spectra of unknown compounds

The spectra of the samples described in Chapter 2 were obtained in a similar manner, with c.a.  $5 \times 10^5$  counts/channel

TABLE 4.3

Line (a)	Velocity mm/sec (b)	Channel Number
Iron (2)	3.340	105 ± 1
Iron (3)	1.096	216 ± 1
Nitroprusside (1)	0.865	226.5 ± 0.5
Iron (centroid)	0.258	257.5 ± 1
Stainless steel	0.161	262 ± 1.5 <sup>(c)</sup>
Nitroprusside (centroid)	0.000	269.25 ± 0.5
Iron (4)	-0.580	298 ± 1
Nitroprusside (2)	-0.865	312 ± 0.5
Iron (5)	-2.820	409 ± 1

Calibration constant 1 channel =  $0.0203 \pm .0001$  mm/sec.

Notes:

- (a) Spectral lines have been numbered in accordance with the accepted criteria for the natural iron spectrum, viz. the first line (iron(1)) is that found at the most positive velocity.
- (b) All velocities have been expressed relative to the centroid of the nitroprusside spectrum which has been assigned an arbitrary value of zero. The velocity data has been taken from references (102), (97) and (69).
- (c) The stainless steel data represent the average of 12 separate calibration checks taken throughout this study. The estimated error of ± 1.5 channels covers the total spread of values.



being accumulated for each.

(iv) Treatment of data and errors

The data accumulated in the 512 channel memory consisted of six digit numbers which may be addressed in sequence and displayed on the C.R.O. or typed onto a sheet of paper.

From this raw data, the position of the absorption minima is required with some accuracy. This is usually achieved by computerized curve fitting techniques, for which purpose programs specific to the nature of the individual spectrometer are generally developed. Due to the lack of computing experience on the part of the author the procedure adopted involved a compromise to allow the use of an existing 'library' program.

The raw data was first hand-plotted in graphical form (count against channel number) and the approximate positions of the minima visually estimated. The position of each minimum was then accurately determined by fitting the experimental points 20 channels each side of the estimated position to a Lorentzian line shape function. The minimum value of this function was expressed to the nearest 0.1 of a channel. The standard deviation of the experimental data in the linear portion of the spectrum was then estimated and on the basis of this information, the position of each minimum has been rounded to the nearest 0.5 channel. The errors have been calculated as three standard deviations and accordingly expressed as for the minima, covering the range 0.001 to 0.003 mm/sec. A summary of the data obtained appear in Tables 4.3 and 4.4.

TABLE 4.4

Sample	C.S.	Positions of minima	
		Line (1)	Line (2)
(a) FesalenX			
X = Cl	237.3	204±1	270.5±1
Br	230.5	190±1	271±1
I	231.3	187.5±1	275±1
NO <sub>3</sub>	230.5	190.5±1	270.5±1
NCS	236	205±1	269±1
N <sub>3</sub>	231	205±2	257.5±2
C <sub>6</sub> H <sub>5</sub> COO	236	216±2	256±2
(b) K[Fesalen(CN) <sub>2</sub> ]			
Fe(saen) <sub>2</sub> Cl.H <sub>2</sub> O	248.8	181±.5	316.5±.5
Fe(saen) <sub>2</sub> I	240.3	233.5±2	249±2

$$\text{C.S.} = \frac{1}{2}[\text{Line (1)} + \text{Line (2)}]$$

## P A R T I I

Transition metal complexes with the tridentate ligand, saen, are discussed in the following Chapters.

CHAPTER 5

Preparation, characterization and solid state properties.

5.1 INTRODUCTION(a) Rationale

This study was undertaken in order to rationalize several unusual aspects of the chemical behaviour of the complex  $\text{Fe}(\text{saen})_2\text{Cl}\cdot\text{H}_2\text{O}$ . Some of the properties of interest, observed when studying this compound in the solid state, appeared to be directly attributable to the presence of a water molecule.

The following comparison of properties of  $\text{Fe}(\text{saen})_2\text{Cl}\cdot\text{H}_2\text{O}$  and  $\text{Fe}(\text{saen})_2\text{I}$ , provides an illustration of the features of the behaviour of the 'hydrated' species which were considered anomalous.

- (1) The i.r. spectra of each complex differ substantially both in the O-H stretching and the fingerprint regions.
- (2) The chloride salt has a low spin magnetic moment<sup>†</sup>, with  $\mu_{\text{eff}} = 2.11$  B.M. at room temperature<sup>(20)</sup>, whereas the iodide is high spin, with  $\mu_{\text{eff}} = 6.06$  B.M.<sup>(17)</sup>.

---

<sup>†</sup>The room temperature value of  $\mu_{\text{eff}}$ , which will be discussed later in this section, does not necessarily indicate the  $S = \frac{1}{2}$  spin state for the Fe(III). The additional supporting evidence is discussed in the following Chapters.

Recently, a variable temperature study of this complex has been undertaken by Dr. K. Murray (Monash University, Victoria). The data obtained confirm the low spin state, with  $\mu_{\text{eff}}$  values in the range 1.99 - 1.80 B.M. over the temperature range 313 - 90.5°K. In addition, the  $\mu_{\text{eff}}$  values are field independent and exhibit Curie - Weiss behaviour ( $\theta = 180\text{K}$ ).

Dr. K. Murray - private communication, May 1978.

- (3) In solution, the magnetic moment of the chloride salt,  $\mu_{\text{eff}} = 5.96$  B.M., is close to that expected for Fe(III) high spin compounds<sup>(18)</sup>.
- (4) The i.r. and u.v.-visible spectra, in methanol solution, of the iodide and chloride salts are indistinguishable.
- (5) Interconversion of one species to the other by metathetical reactions occurs readily.
- (6) The chloride salt may be reversibly dehydrated under vigorous conditions (e.g. heating the solid in a vacuum for several hours). The dehydrated complex is high spin, with  $\mu_{\text{eff}} > 5.8$  B.M., and has an i.r. spectrum identical to that of the iodo compound.

These observations support the conclusion, alluded to in Part I of this thesis, that in solution both salts generate the  $\text{Fe}(\text{saen})_2^+$  cation. Iron(III) complex ions are known to be labile<sup>(103)</sup>, and this may be readily seen in Fe(III) Schiff base systems. For example, the solution reaction between  $\text{Fe}(\text{salen})\text{X}$  and  $\text{en}$  to give  $\text{Fe}(\text{saen})_2^+$  occurs rapidly, as also does the hydrolysis of  $\text{Fe}(\text{saen})^+$  to  $(\text{Fe}(\text{salen}))_2\text{O}$ . Consequently the solution properties outlined above could be rationalized in terms of such lability. However the solid state properties suggest that the low spin complex  $\text{Fe}(\text{saen})_2\text{Cl}\cdot\text{H}_2\text{O}$  is not a simple hydrated species. Indeed the evidence strongly supports the proposition that the two complexes are not related at all. In particular the four major observations, felt to be anomalous, with respect to the chloro complex, are:

- (1) the presence of two sharp absorptions in the O-H stretching region of the i.r. spectrum;
- (2) the substantial differences in the fingerprint region;

- (3) the extreme conditions required for dehydration;
- (4) the apparent stabilization of the low spin state by the water molecule.

These four areas of concern, which could not be resolved by chemical methods, have in fact been rationalized by the structural determination discussed later in this thesis<sup>(20)</sup>.

In an attempt to solve the problem by chemical means, a series of complexes of general formula  $M(\text{III})(\text{saen})_2X \cdot n\text{H}_2\text{O}$  have been prepared and studied utilizing a variety of techniques. The preparation, characterization and chemical properties of these complexes are discussed in the following sections.

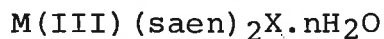
(b) Previously published work

O'Connor and West have described the preparation of several complexes of formula  $\text{Cr}(\text{III})(\text{saen})_2X$ , where  $X = \text{Br}$ ,  $\text{I}$  and  $\text{ClO}_4$ , from tris(salicylaldehydato) chromium (III),  $\text{Cr}(\text{sal})_3$ <sup>(104)</sup>. The crystal structure determination of the iodo complex has confirmed the proposed octahedral coordination by the two tridentate ligands in the meridional configuration<sup>(105)</sup>. The Fe(III) analogue,  $\text{Fe}(\text{saen})_2\text{I}$ , has also been described<sup>(17)</sup>.

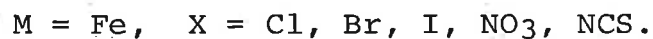
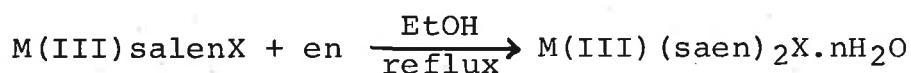
A Cobalt(III) complex, proposed as a mixed bidentate-quadridentate complex  $[\text{Co}(\text{III})\text{salen.en}]\text{ClO}_4$ , has been reported by Dey and De<sup>(106)</sup>. In this study the complex has been shown to be  $\text{Co}(\text{saen})_2\text{ClO}_4$ . The meridional configuration of  $\text{Co}(\text{saen})_2^+$  has been confirmed recently by Benson et al<sup>(107,108)</sup>.

It has been suggested that heterochelates of Mn(III) formulated as  $[\text{Mn(III)salen.en}]X$ , exist. Dey and Ray suggested that these compounds, in common with those now established as involving the cation  $\text{Co(saen)}_2^+$ , had structures similar to the mixed bidentate-quadridentate chelate,  $\text{Cosalen.acac}^{(109)}$ . The spectra and chemical properties of these Mn(III) complexes do not support the existence of either a mixed bidentate-quadridentate or a bistridentate configuration.

## 5.2

(i) Preparation of complexes of general formula,

The preparative methods employed involved refluxing an ethanolic solution of a suitable transition metal complex in the presence of a slight molar excess of en. The aromatic moiety was present as either free or coordinated salen or as coordinated salicylaldehyde. The source of the anion was either the transition metal complex or an appropriate salt which was subsequently added to the reaction mixture. For convenience the methods have been divided into five categories:

(a)  $\text{M(III)salenX}$  as reactant(b)  $\text{M(III) (sal)}_3$  as reactant

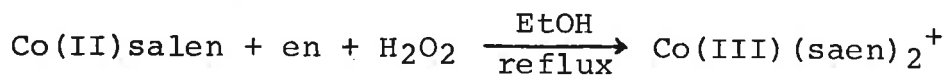
On addition of an aqueous solution containing the appropriate anion, the crystalline product  $M(\text{III})(\text{saen})_2X.n\text{H}_2\text{O}$  was obtained.

$M = \text{Cr}, X = \text{Cl}, \text{Br}, \text{I}, \text{NCS}, \text{ClO}_4.$

$M = \text{Fe}, X = \text{Cl}, \text{OH}, \text{Br}, \text{I}, \text{NCS}, \text{NO}_3 \text{ and } \text{ClO}_4.$

(c)  $\text{Co}(\text{II})\text{salen}$  as reactant

The  $\text{Co}(\text{II})$  complex was oxidized to  $\text{Co}(\text{III})$  by atmospheric oxidation or aqueous hydrogen peroxide.

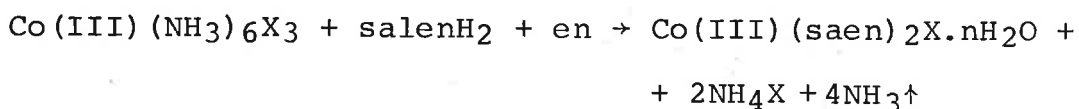


The crystalline salts  $\text{Co}(\text{III})(\text{saen})_2X.n\text{H}_2\text{O}$  were obtained on addition of an aqueous solution containing the appropriate anion.

$X = \text{Cl}, \text{Br}, \text{I}, \text{NO}_3, \text{NCS}, \text{ClO}_4, \text{BF}_4 \text{ and } \text{PF}_6.$

(d)  $\text{Co}(\text{III})$  ammine complexes as reactants

Aqueous solutions of the  $\text{Co}(\text{III})$  complexes were slowly added to a refluxing ethanol solution of  $\text{salenH}_2$  and  $\text{en}$ . The reflux was continued until the evolution of  $\text{NH}_3$  ceased and the crystalline product obtained on cooling the reaction mixture.

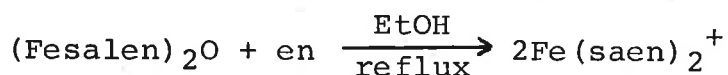


$X = \text{Cl}, \text{Br}, \text{I}, \text{NO}_3.$

Similar results were obtained with other  $\text{Co}(\text{III})$  ammine complexes, e.g.  $[\text{Co}(\text{III})(\text{NH}_3)_5\text{H}_2\text{O}]\text{Cl}_3.$



(e) (Fesalen)<sub>2</sub>O as reactant



Addition of the appropriate anion resulted in crystallization of the required salt as before.

X = Cl, OH, Br, I, NCS, NO<sub>3</sub> and ClO<sub>4</sub>.

Purification of the reaction products was effected by solvent extraction with chloroform or a 1:1 (v/v) ethanol-diisopropyl ether mixture. In many cases such purification was found to be unnecessary as the majority of reaction products, particularly those from methods (a), (c) and (e), analyzed correctly without further purification. In one case, when M = Co, X = PF<sub>6</sub>, analyses on recrystallized products showed a poor correlation with calculated values, probably due to thermal instability.

(ii) Attempted preparations

(a) Manganese(III)

The preparation, outlined in Ref.(109), was essentially similar to method (c) above, using Mn(II)salen as starting material. Following the procedure as reported, solid reaction products were obtained, however, the i.r. spectra and analyses did not correlate with those reported<sup>(109)</sup>. Purification of the reaction product by recrystallization from chloroform gave well formed, golden brown crystals which had a different i.r. spectrum from that of the reaction product. Analysis of these recrystallized compounds suggested they were Mn(III)salenX (X = Cl, Br and ClO<sub>4</sub>). The i.r. spectrum of the chloro complex

correlated precisely with the spectrum published by Boucher<sup>(110)</sup>.

After a prolonged reflux (48 hours) of Mn(III)salenCl with en in EtOH, Mn(III)salenCl was the only observable product. Clearly Mn(III)salenX cannot react to give Mn(III)(saen)<sub>2</sub>X. In addition, on drying the complex formulated as Mnsalen.en.Cl at 100°C for 12 hours, the dried solid had an identical i.r. spectrum to that of Mn(III)salenCl.

It is suggested therefore that the Mnsalen.en.X species are not bidentate-quadridentate chelates but are simply Mn(III)salenX complexes with en of crystallization.

(b) M(II)(saen)<sub>2</sub> species

Attempts to prepare these neutral bivalent transition metal complexes (M = Co, Cu and Ni) from M(II)salen, resulted in no apparent reaction. The starting materials were recovered unchanged after prolonged reflux. For Cu(II) and Ni(II), the reflux was carried out with no special precautions whereas for Co(II) the procedure required an inert (N<sub>2</sub>) atmosphere.

5.3 CHARACTERIZATION OF COMPLEXES

(i) Analyses of compounds of general formula,  
M(III)(saen)<sub>2</sub>X.nH<sub>2</sub>O viz. M.C<sub>18</sub>H<sub>22</sub>N<sub>4</sub>O<sub>2</sub>.X.nH<sub>2</sub>O

(a) Fe(saen)<sub>2</sub>Cl.H<sub>2</sub>O

For this complex, analyses were used as a 'quality control' check for the 'purity' of numerous preparations. To date, 18 consistent analyses have been obtained and

statistical calculations confirm that the mean values can be expressed to a higher degree of precision than usually accepted. For this reason the analysis for this compound is presented to 2 decimal places throughout.

Analysis for  $C_{18}H_{24}N_4O_3FeCl$

Calculated	C	49.62	H	5.55	N	12.86	Fe	12.82	Cl	8.14
Found	C	49.58	H	5.52	N	12.87	Fe	12.79	Cl	8.15

All other analyses are expressed to one decimal place and have been performed at least in triplicate.

(b)  $M(III)(saen)_2Cl \cdot H_2O$

M = Cr

Calculated	C	50.1	H	5.6	N	13.0	Cr	12.0	Cl	8.2
Found	C	49.9	H	5.6	N	13.0	Cr	12.2	Cl	8.1

M = Co

Calculated	C	49.3	H	5.5	N	12.8	Co	13.4	Cl	8.1
Found	C	49.5	H	5.5	N	12.6	Co	13.4	Cl	8.2

(c)  $M(III)(saen)_2X \cdot nH_2O$

In all other cases, analyses for carbon, hydrogen and nitrogen only have been obtained. Estimates for metal content from the combustion residues have been included in the following table, where applicable. In some cases, particularly when  $X = ClO_4$ , explosive combustion occurred and no metal estimates have been attempted.

The data are tabulated in Table 5.1.

TABLE 5.1

Analyses for  $M(\text{III})(\text{saen})_2X.n\text{H}_2\text{O}$  (a)

M	X	n	Calculated				Found			
			C	H	N	M	C	H	N	M
Fe	OH	1	51.8	6.0	13.4	13.4	51.1	5.8	13.2	13.3
Fe	Br	0	46.8	4.8	12.1	12.1	47.0	4.9	12.1	12.2
Fe	NO <sub>3</sub>	0	48.7	5.0	15.8	12.6	48.9	5.1	16.0	12.4
Fe	NCS	0	51.8	5.0	15.9	12.7	51.5	5.1	15.6	12.9
Fe	ClO <sub>4</sub>	0	44.9	4.6	11.6	11.6	44.7	4.6	11.8	-
Cr	NCS	0	52.3	5.1	16.1	11.9	51.9	5.2	16.0	11.8
Co	Br	1	44.7	5.0	11.6	12.2	44.7	4.9	11.5	12.1
Co	I	1	40.8	4.6	10.6	11.1	40.8	4.4	10.6	10.9
Co	NO <sub>3</sub>	1	46.5	5.2	15.1	12.7	46.5	5.2	15.0	13.0
Co	NCS	0	51.5	5.0	15.8	13.3	51.1	5.0	15.8	13.0
Co	ClO <sub>4</sub>	1	43.0	4.8	11.1	11.7	42.8	4.7	11.2	-
(b) Co	ClO <sub>4</sub>	0	44.6	4.6	11.6	12.2	44.6	4.6	11.7	-
(b) Co	BF <sub>4</sub>	0	45.8	4.7	11.9	12.5	45.6	4.7	12.0	-
(c) Co	PF <sub>6</sub>	0	40.8	4.2	10.6	11.1	41.3	4.3	10.7	10.7

Notes:

- (a) Analyses for compounds previously described, viz.  $M = \text{Cr}$ ,  $X = \text{Br}$ ,  $\text{I}$ ,  $\text{ClO}_4$  and  $M = \text{Fe}$ ,  $X = \text{I}$  have not been included.
- (b) Compounds recrystallized from  $\text{CHCl}_3$ .
- (c) Analyses for  $\text{Co}(\text{saen})_2\text{PF}_6$ , in particular recrystallized samples, were erratic, with carbon analyses being  $\approx 2\%$  high. The data presented here was obtained with a sample obtained from a  $\text{CHCl}_3$  solution which had not been heated.

(ii) Infra red spectra(a) Classification of spectra

The i.r. spectra of all complexes have been obtained. In contrast to the characteristic spectra of the salen complexes, discussed in Chapter 2, the spectra of the  $M(\text{III})(\text{saen})_2X.n\text{H}_2\text{O}$  complexes appeared to fall into three distinctive groups. Each spectrum has been classified into one of these groups, utilizing as criteria for classification the number and position of absorptions between  $4000$  and  $3050 \text{ cm}^{-1}$ .

For each spectral type, the characteristic absorptions are:

Type A ( $n = 1$ )

Four bands near  $3620$  ( $\nu_{\frac{1}{2}} \approx 20$ ),  $3400$  ( $\nu_{\frac{1}{2}} \approx 40$ ),  $3200$  ( $\nu_{\frac{1}{2}} \approx 40$ ) and  $3100 \text{ cm}^{-1}$  ( $\nu_{\frac{1}{2}} \approx 40 \text{ cm}^{-1}$ ).

Type B ( $n = 0$ )

Two bands near  $3230$  ( $\nu_{\frac{1}{2}} \approx 50$ ) and  $3130 \text{ cm}^{-1}$  ( $\nu_{\frac{1}{2}} \approx 30 \text{ cm}^{-1}$ ).

Type C ( $n = 0$  or  $1$ )

Two bands near  $3330$  ( $\nu_{\frac{1}{2}} \approx 30$ ) and  $3280 \text{ cm}^{-1}$  ( $\nu_{\frac{1}{2}} \approx 30 \text{ cm}^{-1}$ ).

When  $n = 1$ , a weak, broad absorption ( $\nu_{\frac{1}{2}} \approx 200 \text{ cm}^{-1}$ ) is observed near  $3500 \text{ cm}^{-1}$ .

In Fig. 5.1 examples of each spectral type in the region  $4000 - 3050 \text{ cm}^{-1}$  have been reproduced.

The classification of the complexes of formula  $M(\text{III})(\text{saen})_2X.n\text{H}_2\text{O}$  according to spectral type is presented below in Table 5.2.

Figure 5.1  
I.r. spectra, O—H and N—H  
stretching region.

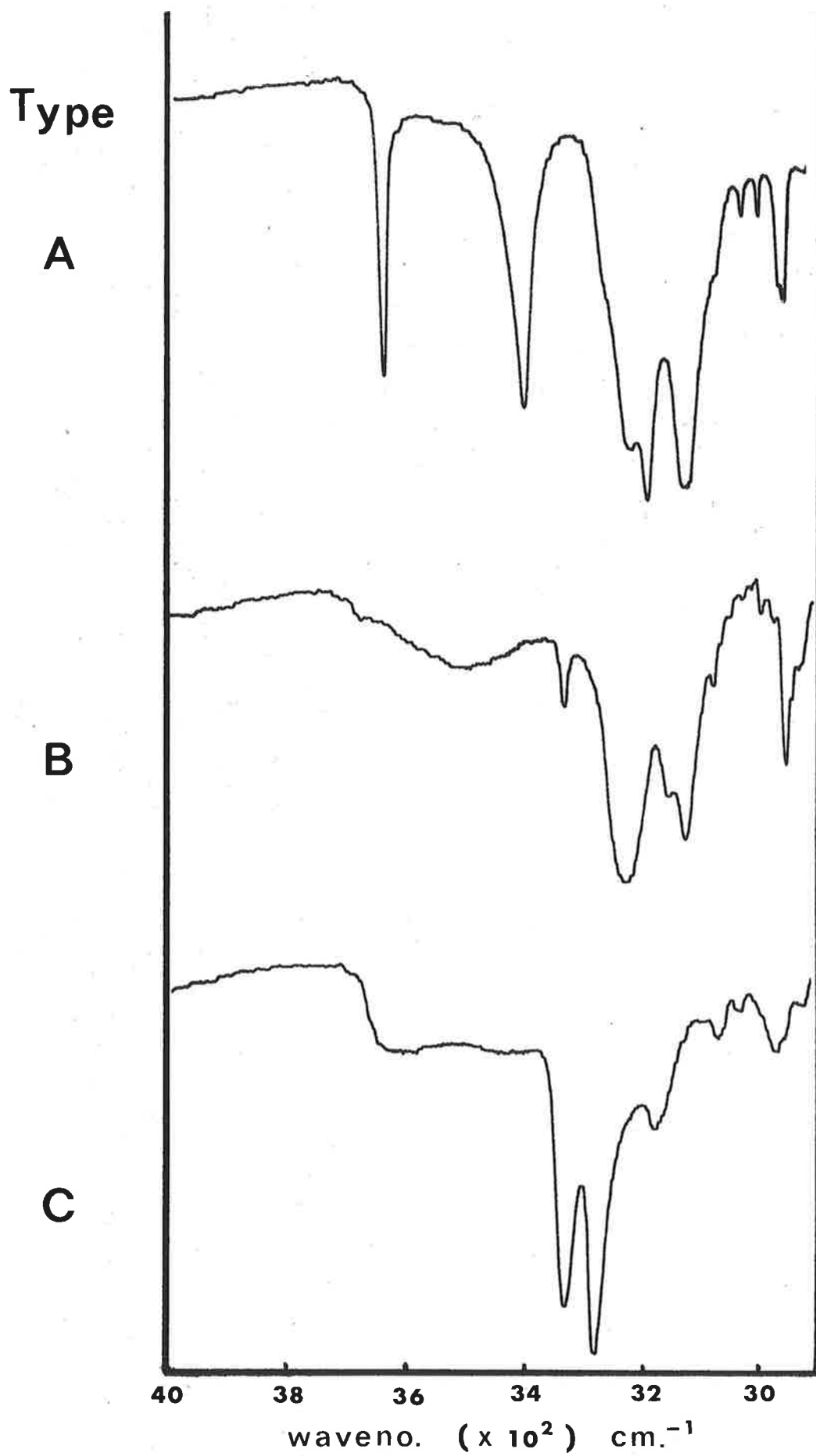


TABLE 5.2

Spectral Classification of  $M(\text{III})(\text{saen})_2X \cdot n\text{H}_2\text{O}$ 

Spectral Type	M = Cr	M = Fe	M = Co
A	X = Cl, Br	X = Cl, OH	X = Cl, Br, I, NO <sub>3</sub>
B	X = I, NO <sub>3</sub> , NCS	X = Br, I, NO <sub>3</sub> , NCS	X = NCS
C	X = ClO <sub>4</sub>	X = ClO <sub>4</sub>	X = ClO <sub>4</sub> , BF <sub>4</sub> , PF <sub>6</sub>

The 'spectral type' is dependent on the nature of both the metal and anion. However, for the three metals studied, when X = Cl, the spectrum is Type A, when X = NCS it is Type B and when X = ClO<sub>4</sub>, Type C.

Discounting absorptions due to the anion (viz. X = NO<sub>3</sub>, NCS, ClO<sub>4</sub>, PF<sub>6</sub> and BF<sub>4</sub>) within each type the spectra are essentially similar in the region 1800 - 400 cm<sup>-1</sup>, but different from the other types. The spectra of the chloride salts, as reproduced in Fig. 5.2, illustrate the similarity of the Type A spectra.

As typical examples of the three spectral types, spectra of the Co(III) complexes have been reproduced in Fig. 5.3. For Type A, X = Br and for Type B, X = NCS. The Type C spectrum, as shown, has been obtained by combining the individual spectra for X = ClO<sub>4</sub>, BF<sub>4</sub> and PF<sub>6</sub>, omitting the broad anion absorptions found in the range 1150 - 1050 cm<sup>-1</sup> when X = ClO<sub>4</sub>, 1050 - 950 cm<sup>-1</sup> when X = BF<sub>4</sub> and 900 - 800 cm<sup>-1</sup> when X = PF<sub>6</sub>.

Figure 5.2  
I.r. spectra of the isostructural chloride salts

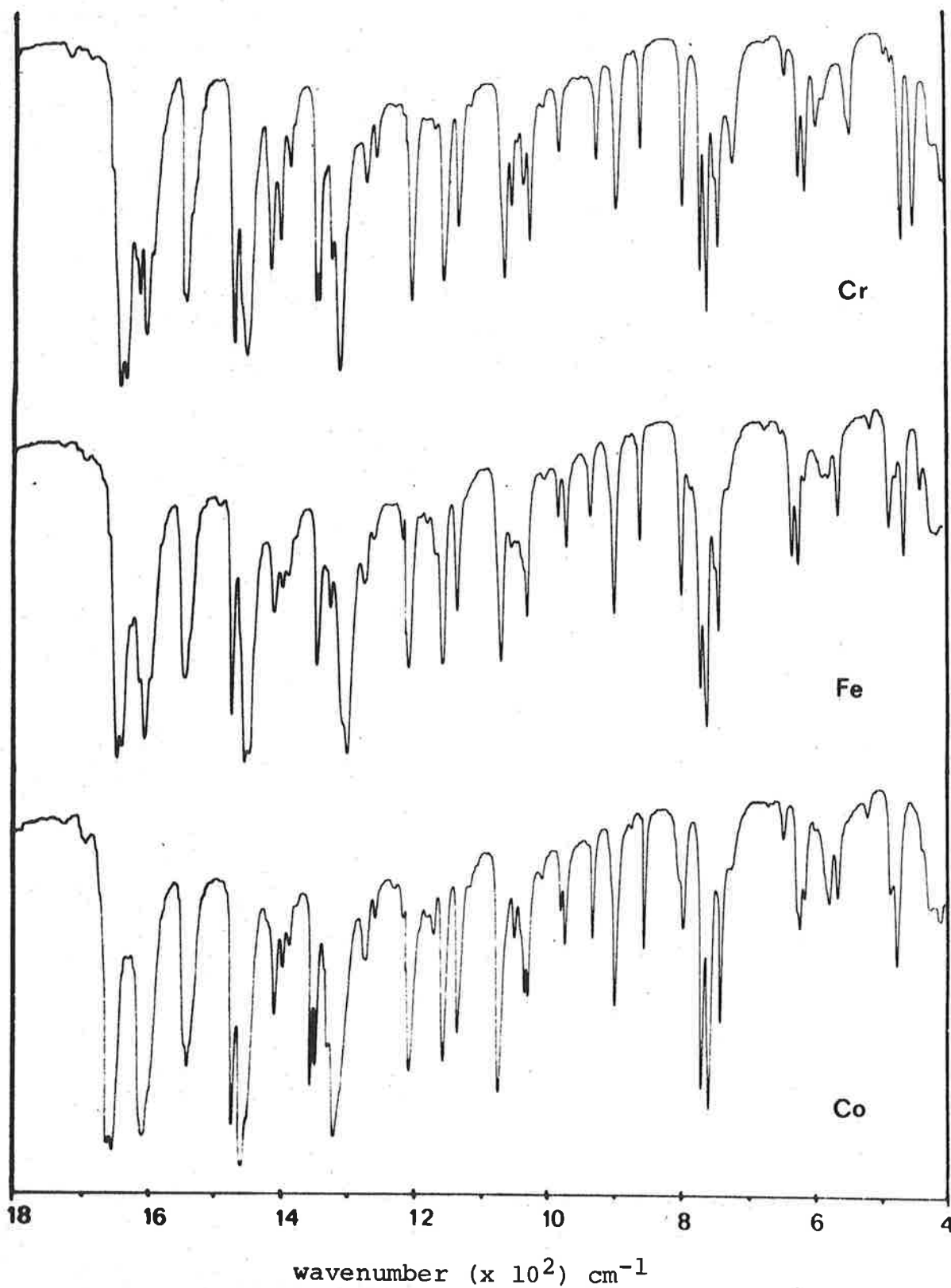
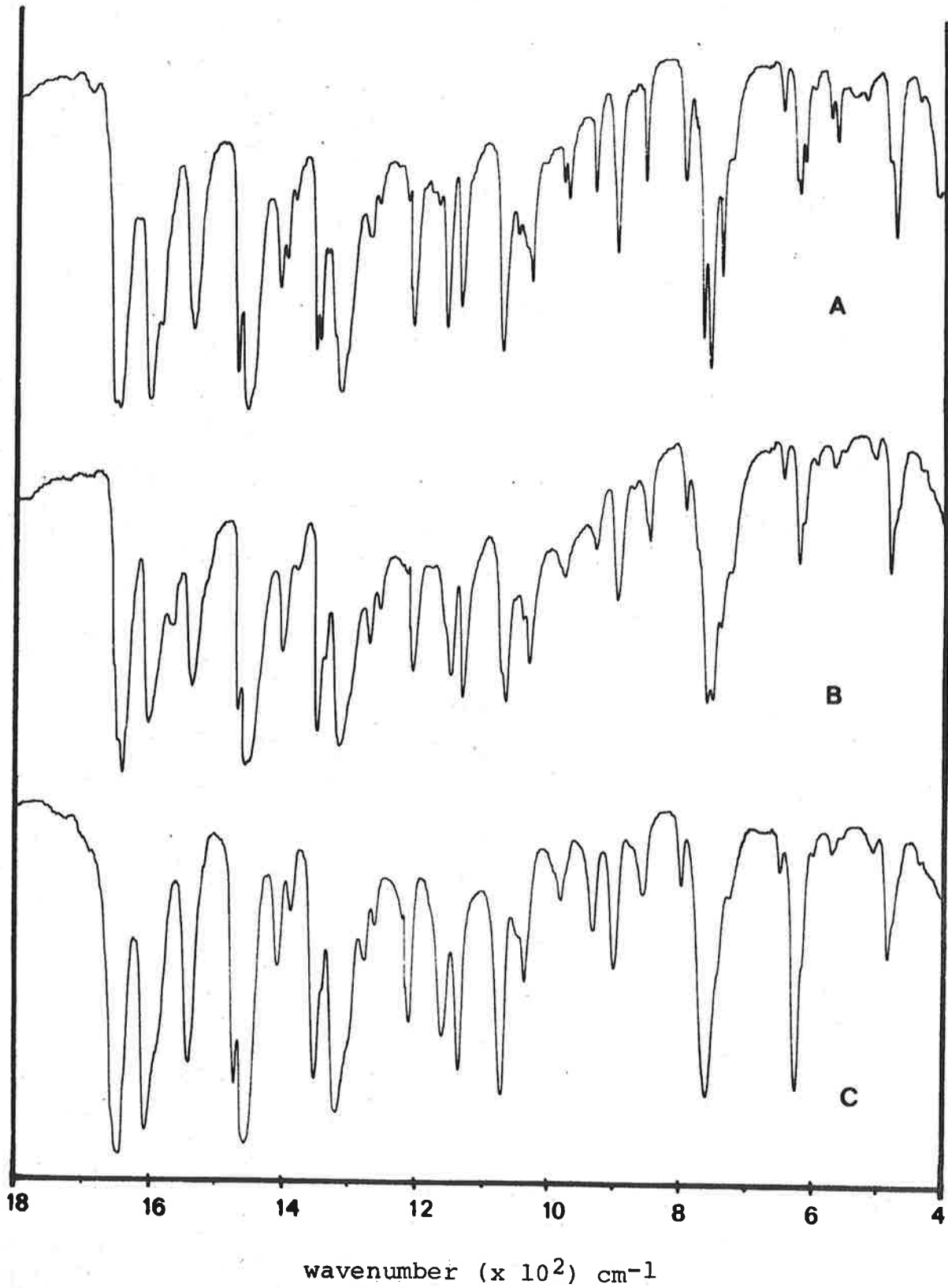




Figure 5.3

Representative examples of the three spectral types



(b) Bands between 3000 and 4000  $\text{cm}^{-1}$

The classification of the  $\text{M(III)(saen)}_2\text{X}\cdot\text{nH}_2\text{O}$  spectra into three distinctive types, strongly suggests that the solid state environment of the cationic species, within each class, is similar.

As a focal point for comparison of these spectra, the Type B case has been selected because the structure of the complex  $\text{Cr(saen)}_2\text{I}$  has been determined<sup>(105)</sup>. Hydrogen bonding occurs between the anion and cation such that all four hydrogen atoms on the  $-\text{NH}_2$  groups interact with adjacent iodide anions. The positions of the N-H stretching absorptions between 3050 and 3350  $\text{cm}^{-1}$  for the  $\text{Cr(III)saen}$  complexes with  $\text{X} = \text{Br}, \text{I}$  and  $\text{ClO}_4$  have been discussed in terms of a simple anion dependent hydrogen bonding model by O'Connor and West<sup>(104)</sup>.

It would appear from the current study that this rationalization is inadequate in that for the Type A and B spectra, where hydrogen bonding would be expected to result in significant 'shifts', the observed positions of the two N-H stretching absorptions are essentially independent of the nature of either the metal or the anion.

(1) Type B and C spectra

For convenience in the following discussion, the spectra have been subdivided into two groups. In the spectral region above 3000  $\text{cm}^{-1}$ , the spectra of both Type B and C complexes exhibit two well-defined absorptions which have been assigned as N-H stretching transitions. The relevant data have been listed in Table 5.3.

As indicated in Part I of this thesis, there is no evidence supporting the existence of the free ligand, saenH. All attempts to prepare it have proved unsuccessful. As a consequence, 1,2 diaminoethane(en) has been selected as a reference to allow rationalization of changes in  $\nu_{\text{N-H}}$  on coordination. In common with saen complexes, two absorptions occur in the N-H stretching region in the en spectra. In  $\text{CCl}_4$  solution, the  $\nu_{\text{N-H}}$  positions are at 3390 and 3310  $\text{cm}^{-1}$  and are shifted to 3370 and 3300  $\text{cm}^{-1}$  respectively in the liquid film spectrum. Presumably the shift is caused by inter-molecular hydrogen bonding in the liquid phase.

A further decrease in the frequency of these absorptions would be observed on coordination (111).

TABLE 5.3

M(III)(saen)<sub>2</sub>X complexes: N-H stretching frequencies ( $\text{cm}^{-1}$ )

	M	X	Band positions	
Type B	Cr	I	3205	3110
	Cr	NO <sub>3</sub>	3220	3130
	Cr	NCS	3205	3115
	Fe	Br	3215	3115
	Fe	I	3215	3115
	Fe	NO <sub>3</sub>	3225	3135
	Fe	NCS	3215	3115
	Co	NCS	3205	3115
Type C	Cr	ClO <sub>4</sub>	3295	3250
	Fe	ClO <sub>4</sub>	3295	3255
	Co	ClO <sub>4</sub>	3305	3255
	Co	BF <sub>4</sub>	3315	3265
	Co	PF <sub>6</sub>	3340	3290

In all cases, the values of  $\nu_{\text{N-H}}$  obtained indicate that coordination has occurred between the metal ion and the  $-\text{NH}_2$

group. However, the magnitude of the 'shift' for the Type C complexes is substantially less than for Type B. The anions in the Type C complexes are considered unlikely to be involved in strong hydrogen bonding interactions and the higher values for  $\nu_{\text{N-H}}$ , relative to those for Type B, indicate such interactions are minimal.

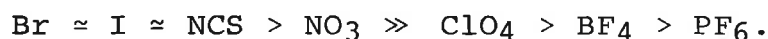
The anions of the Type B complexes are known to frequently be involved in substantial hydrogen bonding interactions which may be reflected in a significant shift of the  $\nu_{\text{N-H}}$  absorptions to lower frequencies. Indeed for the series of complexes of formula  $[\text{Co(III)(NH}_3)_6]\text{X}_3$ , the position(s) of  $\nu_{\text{N-H}}$  show extreme sensitivity to the nature of X, as shown in the following data<sup>(112)</sup>:

X	ClO <sub>4</sub>	NO <sub>3</sub>	I	Br	Cl
$\nu_{\text{N-H}}$	3320, 3240	3290, 3200	3150	3120	3070

These values probably reflect the relative 'strength' of the H-X 'bond'.

In contrast to the above, the  $\nu_{\text{N-H}}$  values obtained for the Type B complexes appear remarkably insensitive to the nature of X. In view of the known structure, this appears somewhat unusual in that it suggests that all of the H-X 'bonds' are of similar 'strength'.

Further, it would appear that the  $\nu_{\text{N-H}}$  values which do seem to follow a trend of the type expected, are observed when X = ClO<sub>4</sub>, BF<sub>4</sub>, PF<sub>6</sub> and NO<sub>3</sub>. Thus the apparent 'hydrogen bonding ability' of the anions indicated follows the order:



The reason for this observation is not clear, but it is possible that the apparent 'levelling' of the hydrogen bonding interactions may well result from the packing of the cations and anions in the crystal lattice. The structural information available is considered in Chapter 7.

(2) Type A spectra

In addition to two N-H stretching bands between 3100 and 3250  $\text{cm}^{-1}$ , two additional bands are found at higher frequencies. The data for the four band positions are tabulated in Table 5.4.

TABLE 5.4

Type A, M(III)(saen)<sub>2</sub>X.H<sub>2</sub>O complexes: Absorptions in N-H and O-H stretching regions

M	X	Additional bands		$\nu_{\text{N-H}}$	( $\text{cm}^{-1}$ )
Cr	Cl	3615	3355	3175	3105
Cr	Br	3610	3390	3180	3110
Fe	Cl	3620	3365	3165	3105
Fe	OH	3605	3370	3160	3115
Co	Cl	3605	3370	3165	3105
Co	Br	3600	3405	3165	3105
Co	I	3600	3420	3165	3105
Co	NO <sub>3</sub>	3605	3425	3245	3145

The positions of  $\nu_{\text{N-H}}$  follow a similar pattern to that discussed above for the Type B complexes, i.e. the  $\nu_{\text{N-H}}$  values appear insensitive to the nature of either M or X, implying that the H-X bonds are also of similar strength in this case.

Of interest, however, is the further observation that  $\nu_{\text{N-H}}$  values for  $X = \text{NO}_3$  are apparently independent of the spectral type with band positions of  $3235 \pm 10$  and  $3135 \pm 10 \text{ cm}^{-1}$ . On the basis of this observation it may be expected that all nitrate salts have similar solid state structures. The i.r. spectra between  $1800$  and  $400 \text{ cm}^{-1}$  suggest that this is not so, as the Type A spectrum differs in many respects from those of Type B.

With respect to the Type A spectra, the major problem of interest is the rationalization of the two additional sharp bands above  $3350 \text{ cm}^{-1}$ . All Type A complexes are monohydrates and it appears reasonable to assume that the two bands are associated with the presence of a 'water molecule'.

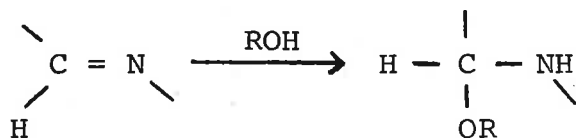
Water may be incorporated into the crystalline salt in the form of molecules trapped in the lattice (lattice water) or coordinated to the metal ion(s) (coordinated water)<sup>(113)</sup>. In general, a broad absorption, observed in the i.r. spectrum between  $3550$  and  $3200$  is considered typical of either case<sup>(113)</sup>. Lattice water in particular may usually be removed under relatively mild conditions, e.g. heating for a few hours at  $110^\circ\text{C}$  (atmospheric pressure).

The Type C complex,  $\text{Co}(\text{saen})_2\text{ClO}_4$ , has been obtained as a monohydrate from aqueous ethanol and as the anhydrous salt by drying at  $110^\circ\text{C}$  for 3 hours or by recrystallization from chloroform. The presence of the water molecule in the hydrate has been demonstrated by a weak, broad i.r. band ( $3500$  to  $3300 \text{ cm}^{-1}$ ) with the remainder of the i.r. spectra of both species being indistinguishable.

As discussed later in this Chapter, the water molecule in the hydrated chlorides with  $M = Fe$  and  $Cr$ , may be removed under vigorous conditions whereas for  $M = Co$  dehydration could not be confirmed. The water molecule is tightly held and it appears unlikely that it is simply lattice water. It is highly improbable that the water molecule could be coordinated to the metal ion as this would require a seven coordinate metal ion. Furthermore, on recrystallization from 'coordinating' solvents such as DMSO and alcohol, the monohydrated species only are obtained, thus negating the possibility of a labile coordination site such as would be expected with a  $M-OH_2$  bond.

However, the observation that monohydrate species were invariably recovered suggested that the water molecule was involved in a very strong, specific interaction in these  $M(III)(saen)_2X.H_2O$  complexes.

Recently, a similar effect was observed in a series of copper complexes with the ligand  $N,N'$ -bis(2-pyridylmethylene)-ethane-1,2diamine (abbreviated as bpe). The  $Cu(II)bpe$  complexes were formulated as monohydrates or alcoholates and gave rise to i.r. spectra with sharp bands near  $3400$  and  $3250\text{ cm}^{-1}$ . In these complexes, addition of  $ROH$  ( $R = H, Me, Et$ ) across one of the azomethine groups has occurred<sup>(114)</sup>, i.e.



A similar reaction was considered to be feasible in the Type A complexes. An i.r. band near  $3600\text{ cm}^{-1}$  would be consistent with a 'free' (i.e. nonhydrogen bonded) O-H stretching

vibration and a band near  $3400\text{ cm}^{-1}$  would correlate with a 'free' N-H stretching vibration<sup>(115)</sup>.

Attempts to verify this proposition profoundly influenced the direction of the ensuing research program. Much of the chemical evidence obtained may be rationalized in terms of this model, however, the problem could not be conclusively resolved by chemical studies alone. Consequently, the crystal structure determination of the complex  $\text{Fe}(\text{saen})_2\text{Cl}\cdot\text{H}_2\text{O}$ , as presented in Chapter 7, was undertaken.

This structure determination has unambiguously established that this Type A complex is, in fact, a true hydrate. Briefly, the water molecule is bound into the crystal lattice such that only one hydrogen atom is involved in a hydrogen bonding interaction with the anion<sup>(20)</sup>. The i.r. bands may be rationalized in terms of a hydrogen bonded O-H stretch near  $3400\text{ cm}^{-1}$  and a 'free' O-H stretch near  $3600\text{ cm}^{-1}$ <sup>(116)</sup>.

The position of the hydrogen bonded O-H stretch reflects an anion dependent trend with the order of  $\nu_{\text{O-H}}$  (bonded) being  $\text{NO}_3 > \text{I} > \text{Br} > \text{Cl}$ . This correlates with the expected order predicted from studies such as that with the Co(III) hexammine complexes<sup>(112)</sup>.

#### 5.4 FURTHER SOLID STATE STUDIES

In addition to the analytical and i.r. spectral data discussed above, investigations of further properties of these saen complexes, in the solid state, were undertaken and information of particular interest obtained from:





- (i) magnetic moments
- (ii) X-ray powder diffraction photographs
- (iii) dehydration of the Type A monohydrates.

(i) Magnetic moments

(a) General comments

The data obtained in the majority of cases, was quite predictable, as summarized below<sup>(117)</sup>:

- (1) when  $M = Cr$ ,  $\mu_{eff}$  values were in the range 3.7 - 3.9 B.M.
- (2) all Co(III) complexes were diamagnetic
- (3) the Type B and C complexes of Fe(III) were found to be high spin, with  $\mu_{eff}$  near the spin only value of 5.92 B.M.

The only unusual behaviour was observed with the low spin complex,  $Fe(saen)_2Cl.H_2O$ .

(b) Magnetic susceptibility of  $Fe(III)(saen)_2Cl.H_2O$

As previously reported in Chapter 2,  $\mu_{eff}$  for this complex, as determined initially, was 2.11 B.M. As a consequence of the more detailed study undertaken for Part II of this thesis, the magnetic susceptibility of a number of samples of this complex have been measured. Considerable variation in the value of  $\mu_{eff}$  was observed, and it has been established that this variation can be related to the 'history of the sample'. By studying the susceptibility of 'analytically pure' samples, the following generalizations may be made:

- (1) samples obtained from the initial reaction mixture have

$$\mu_{\text{eff}} = 1.93 \pm .01 \text{ B.M.}$$

- (2) on exposure to the atmosphere,  $\mu_{\text{eff}}$  gradually increases with time to c.a. 2.3 B.M. (after six months).
- (3) samples purified by recrystallization from chloroform or an ethanol-diisopropyl ether mixture, have  $\mu_{\text{eff}} = 2.11 \pm .01 \text{ B.M.}$

These observations may be explained by considering the effect on the apparent value of  $\mu_{\text{eff}}$  of 'contamination' with small quantities of a high spin complex. As can be seen from the data in Table 5.5, 5% contamination will increase  $\mu_{\text{eff}}$  from 1.93 to 2.31 B.M.

TABLE 5.5

Effect of a high spin contaminant on  $\mu_{\text{eff}}$  of a low spin complex

x	0	1	2	3	4	5	6	7	8	9	10	20
$\mu_{\text{eff}}$	1.93	2.01	2.09	2.16	2.24	2.31	2.37	2.44	2.50	2.57	2.63	3.18

where x = % of high spin contaminant

In aqueous solution,  $\mu_{\text{eff}}$  of  $\text{Fe}(\text{saen})_2\text{Cl}\cdot\text{H}_2\text{O}$  is 5.96 B.M. Consequently it appears reasonable to propose that the 'high spin contaminant' is, in fact, the high spin form of the complex which, as shown later (Section 5.4 (iii)), is simply the anhydrous complex.

It is worth noting that with as much as 10% 'contamination' with this high spin form no significant difference in the i.r. spectrum or the analysis could be detected. For example, consider the following analytical data:

Calc. (0% high spin) C 49.62 H 5.55 N 12.86 Fe 12.82

Calc. (10% high spin)	C 49.84	H 5.53	N 12.91	Fe 12.88
Found	C 49.58	H 5.52	N 12.87	Fe 12.79

Clearly, the value of the magnetic susceptibility is a far more sensitive means of assessing the 'purity' of samples of  $\text{Fe}(\text{saen})_2\text{Cl}\cdot\text{H}_2\text{O}$  than the other readily available techniques.

(ii) X-ray powder diffraction

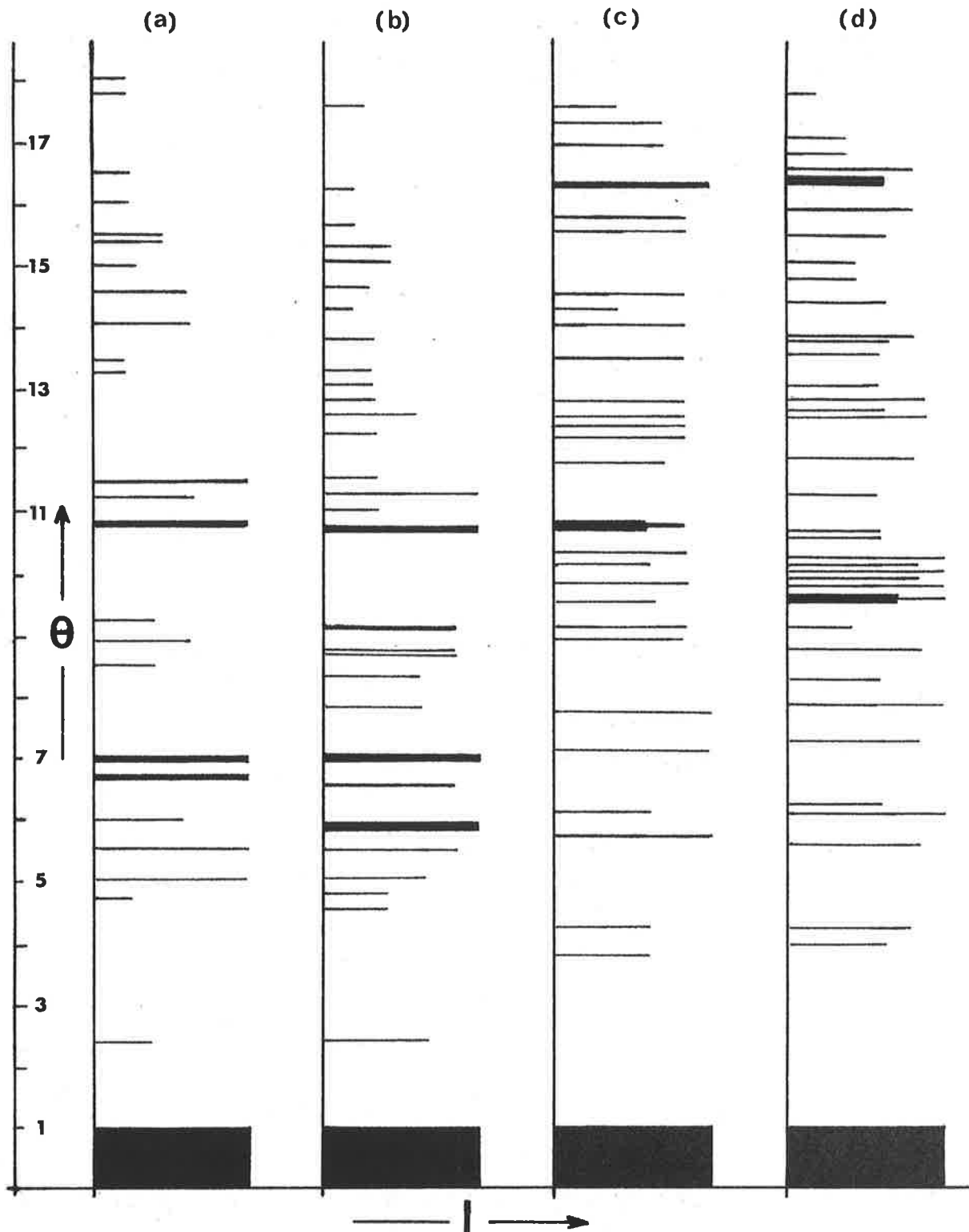
The powder photographs of a number of the species of formula  $\text{M}(\text{III})(\text{saen})_2\text{X}\cdot\text{nH}_2\text{O}$  have been obtained.

The experimental procedure allowed simultaneous determination of four separate samples, thus facilitating direct visual comparison of the diffraction patterns. From these patterns, reproduced diagrammatically in Fig. 5.4, the following conclusions have been made:

- (1) When  $\text{X} = \text{Cl}$ , the solids are isostructural, ( $\text{M} = \text{Cr}, \text{Fe}$  and  $\text{Co}$ ).
- (2) When  $\text{X} = \text{Br}$ ,  $\text{M} = \text{Co}$  and  $\text{Cr}$ , the solids are probably isostructural and similar to the chloride salts.
- (3) When  $\text{X} = \text{I}$ ,  $\text{M} = \text{Cr}$  and  $\text{Fe}$ , the solids are not isostructural, nor are they similar to the chloride salts.

On this basis it would appear that the crystal structures of all three chloride salts are identical, and are similar to the Type A bromides, as previously suggested by the i.r. spectra. In the case of the iodide salts, the solid state arrangement is not the same even though the Type B i.r. spectra are similar.

Figure 5.4  
 Diagrammatic representation of powder  
 diffraction photographs



- (a) M = Fe, Cr or Co; X = Cl
- (b) M = Cr or Co; X = Br
- (c) M = Fe; X = I
- (d) M = Cr; X = I

(iii) Dehydration of Type A complexes

Attempts have been made to dehydrate the isostructural chlorides, estimating the extent of the dehydration (if any) by following changes in the weight and i.r. spectra of samples. In the case of the Fe(III) complex, changes in the magnetic susceptibility have also been utilized.

(a) Fe(saen)<sub>2</sub>Cl.H<sub>2</sub>O

Quantitative dehydration was achieved by heating the sample in a vacuum pistol for four hours at 110°C.

- (1) The observed weight change was 4.28%, compared with the value as calculated for a monohydrate of 4.13%. Water was rapidly absorbed from the atmosphere (50% within 15 mins., 75% within 30 mins. with quantitative absorption after 3 hours). In addition, quantitative absorption of water occurred with a dehydrated sample stored overnight over phosphorus pentoxide in a dessicator.
- (2) The i.r. spectrum of the dehydrated species was characterized by the absence of the  $\nu_{\text{O-H}}$  bands and a general similarity to the Type B spectrum. After 30 mins. exposure to the atmosphere, the spectrum of the partially rehydrated species was essentially that of the original Type A complex.
- (3) A sample of the monohydrate was dissolved in D<sub>2</sub>O, filtered and 'freeze dried' overnight. The i.r. spectrum of the resultant violet solid was indistinguishable from that of the Type B complex Fe(saen)<sub>2</sub>I. After a few minutes, it was noted that the mull, a deep violet colour

initially, was slowly changing to a bright blue colour. This colour change was accompanied by changes in the i.r. spectrum, and after a few hours the spectrum obtained was of Type A. Presumably, this was a result of water adsorption from the mulling agent (nujol).

In addition, a weak doublet was found in these spectra between 2300 and 2400  $\text{cm}^{-1}$ . Bands in this region would be assigned to O-D and N-D stretching vibrations<sup>(118)</sup>.

- (4) A sample of the dehydrated complex was exposed to  $\text{D}_2\text{O}$  saturated  $\text{N}_2$  gas. The i.r. spectrum was essentially similar to the Type A spectrum with four prominent new bands at 2305, 2385, 2490 and 2650  $\text{cm}^{-1}$  respectively. The general 'shape' of this series of bands was essentially similar to the O-H and N-H stretching absorptions between 3100 and 3620  $\text{cm}^{-1}$ . On exposure to the atmosphere, the bands at 2490 and 2650  $\text{cm}^{-1}$  rapidly 'disappeared' (over a period of 10 minutes) with a corresponding increase in intensity for the bands at 3365 and 3620  $\text{cm}^{-1}$ .

Clearly, then, deuterium exchange had occurred with both the ammine and water hydrogen atoms and the bands may be assigned as:

2650 $\text{cm}^{-1}$	'free' O-D stretch
2490 $\text{cm}^{-1}$	'hydrogen bonded' O-D stretch
2385, 2325 $\text{cm}^{-1}$	N-D stretch (doublet)

The 'water' molecule appears to be labile with respect to isotopic exchange, whereas the ammine groups appear relatively inert.

(5) A sample of the monohydrate was placed in a Guoy tube and dehydrated in the vacuum pistol at 110°C. At approximately 24 hour intervals, the tube and contents were sealed under an atmosphere of dry N<sub>2</sub> and the magnetic susceptibility determined. Over a period of 7 days, the value of  $\mu_{\text{eff}}$  increased from 1.93 B.M. to c.a. 5.8 B.M. with a corresponding weight loss of 4%.

(b) Cr(saen)<sub>2</sub>Cl.H<sub>2</sub>O and Co(saen)<sub>2</sub>Cl.H<sub>2</sub>O

Dehydration of the Cr(III) complex, under the same conditions as for Fe(III), required 8 hours for quantitative removal of H<sub>2</sub>O. The weight and i.r. spectral changes were as described for the Fe(III) case.

In contrast, after 24 hours at 110°C in vacuo, no weight loss could be detected in the Co(III) case. However, evidence for the removal of H<sub>2</sub>O was obtained indirectly. After heating the complex for 8 hours at 110°C in the vacuum pistol, D<sub>2</sub>O saturated N<sub>2</sub> was introduced and the complex allowed to stand in this atmosphere overnight. The changes in the i.r. spectra were similar to those noted above, with the exception that the N-D bands were much weaker than in the case of Fe(III). Exchange with atmospheric moisture also appeared to occur more slowly than with the Fe(III) complex as the O-D bands were still prominent after one hour exposure to the atmosphere. In addition, it would appear that heating in vacuo is a necessary prerequisite to deuterium exchange as exposure of the Co(III) monohydrate to the D<sub>2</sub>O saturated atmosphere overnight did not result in the presence of detectable O-D peaks in the i.r. spectrum.

However, with all three complexes, deuterium exchange occurs readily in solution, as discussed in the next Chapter.

## 5.5 CONCLUSIONS

The complexes of formula  $M(\text{III})(\text{saen})_2\text{Cl}\cdot\text{H}_2\text{O}$ , and presumably other Type A hydrates, all have a water molecule strongly bound, via hydrogen bonding interactions in the crystal structure. In contrast, to the 'normal' behaviour of water in hydrated complexes, the water molecule in these complexes appears to be unusual in that -

- (a) it gives rise to two sharp i.r. absorptions, assigned as  $\nu_{\text{O-H}}$  'free' and  $\nu_{\text{O-H}}$  'bonded'.
- (b) the 'strength' of the bonding interactions is high and appears to be comparable with covalently bonded -OH groups.
- (c) in the case of the Fe(III) complex, it apparently stabilizes the low spin Fe(III) state and is responsible for the difference in colour observed, in the solid state, with the hydrated and dehydrated samples of the Type A Fe(III) salt.

It would be expected that the behaviour of the complex salts of Types A, B and C should be essentially similar in solution and thus present fewer problems in the interpretation of the data obtained. The solution properties of the series of complexes are discussed in the following Chapter.

## 5.6 EXPERIMENTAL

- (i) Starting materials



In general, AR grade chemicals were used as starting materials and solvents.

(a) M(II)salen species

- (1) The preparation of Co(II)salen was essentially as described by Bailes and Calvin<sup>(5)</sup>.

Salicylaldehyde, 12.2g (0.1 mol) was dissolved in 150 cm<sup>3</sup> of EtOH and heated under reflux. 3.0g of en (0.05 mol) in 50 cm<sup>3</sup> of EtOH were added slowly. A solution of 12.5g of Cobalt acetate tetrahydrate (0.05 mol) in 60 cm<sup>3</sup> of H<sub>2</sub>O was warmed to 60°C, filtered, and then slowly added to the vigorously stirred refluxing solution of salenH<sub>2</sub>. The reaction mixture was refluxed for a further hour then allowed to cool slowly. The red crystalline solid product was filtered, washed and dried. Yield 13.2g; 80%.

- (2) The equivalent Mn(II) complex was prepared by a similar procedure utilizing Manganese acetate tetrahydrate. The yellow solid product was obtained in approximately 50% yield, and was observed to be air sensitive in solution as reported previously<sup>(10)</sup>.

(b) M(III)salenX species

- (1) M = Fe(III). The complexes of formula FesalenX have been described together with (Fesalen)<sub>2</sub>O in Chapter 2 (section 2.4) of this work.

- (2)  $M = \text{Co(III)}, \text{Co(III)salenX} \cdot 2\text{H}_2\text{O}$  where  $X = \text{Cl}, \text{Br}, \text{I}$ .

The filtrate from the preparation of  $\text{Co(II)salen}$  as described above was rendered slightly acidic to pH test paper (pH c.a. 4-6) with the appropriate dilute acid, HX. On standing overnight, dark green-brown crystals of  $\text{CosalenX} \cdot 2\text{H}_2\text{O}$  formed, were filtered off and dried.

- (3)  $M = \text{Cr(III)}, X = \text{Cl}$ .

$\text{CrsalenCl} \cdot 2\text{H}_2\text{O}$  was prepared as described by Coggin et al<sup>(120)</sup>.

An aqueous solution of  $\text{CrCl}_3 \cdot 6\text{H}_2\text{O}$  was reduced with zinc amalgam under an atmosphere of  $\text{N}_2$ . The aqueous solution of  $\text{Cr(II)}$  was then added to a stirred, hot alcohol solution containing the stoichiometric quantity of  $\text{salenH}_2$ . The reaction mixture was stirred vigorously for a further hour, then allowed to cool whereupon the brown solid product formed. The crude product was purified by recrystallization from water.

- (4)  $M = \text{Cr(III)}, X = \text{Br and I}$ .

These salts were prepared by metathesis by adding a 10-fold molar excess of the appropriate sodium salt to a hot aqueous solution of the chloride salt. On cooling crystals of the appropriate salt of  $[\text{Crsalen}(\text{H}_2\text{O})_2]^+$  were obtained.

- (c) Co(III) hexammine salts,  $\text{Co}(\text{NH}_3)_6\text{X}_3$  where X = Cl, Br, I and  $\text{NO}_3$

The complexes were prepared as described in Inorganic Syntheses (121).

- (d)  $\text{M}(\text{III})(\text{sal})_3$

The Cr(III) complex was prepared as described by O'Connor and West (104), and the Fe(III) complex as described by van den Bergen et al (122).

- (ii)  $\text{M}(\text{III})(\text{saen})_2\text{X}\cdot n\text{H}_2\text{O}$  complexes

The preparative methods as outlined in Section 5.2 were found to be essentially similar with respect to procedure and yields. Consequently typical examples are considered in the following more detailed discussion.

- (a)  $\text{M}(\text{III})\text{salenX}$  as reactant

The preparation of  $\text{Fe}(\text{saen})_2\text{Cl}\cdot\text{H}_2\text{O}$  as described in Chapter 2 (section 2.4(ii)(e)) may be regarded as typical.

The yield of product obtained was improved significantly by concentrating the filtered reaction mixture (utilizing a rotary evaporator) to about half the initial volume.

Yields of products were within the range of 60-80% for M = Fe and Co, and 40-50% for M = Cr.

(b) M(III)(sal)<sub>3</sub> as reactant

Preparation of Cr(saen)<sub>2</sub>NCS.

A solution of Cr(sal)<sub>3</sub>, 4.2g (.01 mol), and en, 1.5g (.025 mol), in 100 cm<sup>3</sup> of EtOH, was refluxed for one hour. A solution of NH<sub>4</sub>CNS, 1.5g (.02 mol), in c.a. 20 cm<sup>3</sup> of H<sub>2</sub>O was then added and the reflux continued for a further hour. The hot reaction mixture was then filtered, allowed to cool and concentrated by slow evaporation for c.a. 2 days. A yield of 2.49g (59%) of red crystalline product was obtained.

(c) Co(II)salen as reactant

The following preparations of Co(saen)<sub>2</sub>X.H<sub>2</sub>O illustrate the advantage of oxidizing the Co(II)salen with H<sub>2</sub>O<sub>2</sub> rather than air.

(1) Co(II)salen, 10.8g (.033 mol), and en, 4.0g (.067 mol), in 200 cm<sup>3</sup> of EtOH were heated under reflux until no more red solid Co(II)salen could be observed (c.a. 20 hours) and a yellow-brown solution only was present. 2.7g of solid NH<sub>4</sub>Cl (.05 mol) was then added and reflux continued until the evolution of NH<sub>3</sub>, as detected by damp indicator paper, had ceased (c.a. 24 hours). On cooling the reaction mixture, 9.9g (67%) of crystalline Co(saen)<sub>2</sub>Cl.H<sub>2</sub>O was obtained.

(2) Co(II)salen, 5.4g, and en, 2.0g, in 100 cm<sup>3</sup> EtOH were heated under reflux with stirring. A solution of 2 cm<sup>3</sup> of 100 vol. H<sub>2</sub>O<sub>2</sub> in c.a. 10 cm<sup>3</sup> of H<sub>2</sub>O was added dropwise over a period of 10 minutes. At this stage a yellow brown solution only could be observed and a solution of 2 cm<sup>3</sup> of conc. HBr in 5 cm<sup>3</sup> of H<sub>2</sub>O was added. The reflux was continued for 30

minutes and the hot reaction mixture filtered. On cooling 5.8g (72%) of olive brown crystalline  $\text{Co}(\text{saen})_2\text{Br}\cdot\text{H}_2\text{O}$  was obtained.

(d) Co(III) ammine complexes as reactants

To a refluxing solution of  $\text{salenH}_2$ , 6.7g (.025 mol), and en, 3.0g (.05 mol), in 200  $\text{cm}^3$  of EtOH, an aqueous solution (50  $\text{cm}^3$ ) containing  $\text{Co}(\text{NH}_3)_6\text{Cl}_3$ , 6.7g (.025 mol), was slowly added over a period of c.a. 30 minutes. The reaction mixture was refluxed until evolution of  $\text{NH}_3$  had ceased (c.a. 2 hours), filtered hot and the filtrate allowed to stand overnight. Well formed crystals of  $\text{Co}(\text{saen})_2\text{Cl}\cdot\text{H}_2\text{O}$  were obtained. Yield 9.2g; 84%.

(e) (Fesalen) $_2$ O as reactant

(Fesalen) $_2$ O, 6.6g (.01 mol), and en, 2.4g (.04 mol), in 100  $\text{cm}^3$  of EtOH were heated under reflux for one hour. An aqueous solution of  $\text{NH}_4\text{ClO}_4$  was prepared by rendering a solution of 2  $\text{cm}^3$  of 80%  $\text{HClO}_4$  in 10  $\text{cm}^3$  of  $\text{H}_2\text{O}$  slightly alkaline with conc.  $\text{NH}_4\text{OH}$  (added dropwise). The solution of  $\text{NH}_4\text{ClO}_4$  was then added slowly to the refluxing reaction mixture and the reflux continued for 2 hours. The resulting violet solution was filtered hot and allowed to stand overnight. Well formed violet-black crystals of  $\text{Fe}(\text{saen})_2\text{ClO}_4$  were obtained. Yield 4.8g; 50%.

(iii) The analytical data, i.r. spectra and magnetic susceptibilities were obtained as previously described in section 2.4.

The solution susceptibility of  $\text{Fe}(\text{saen})_2\text{Cl}\cdot\text{H}_2\text{O}$  was estimated using the Evan's n.m.r. technique<sup>(119)</sup>, and is described in more detail in Chapter 6.

(iv) X-ray powder diffraction photographs

The 'powder photographs' were obtained on Kodak X-ray film strips mounted in a Nonius Guinier-De Wolff camera and required c.a. 30 minutes exposure to filtered  $\text{Cu K}\alpha$  radiation. Finely powdered samples of the complexes were mounted on the sample holder with adhesive tape.

(v) Dehydration experiments

(a) Vacuum pistol

The system was based on a Gallenkamp heated vacuum dessicator fitted with ground glass adaptors to allow introduction of dry or  $\text{D}_2\text{O}$  saturated  $\text{N}_2$  as required. A 'Quickfit' test tube was used as a reaction vessel and all operations subsequent to the experiment were performed in an atmosphere of dry  $\text{N}_2$ . For example, the test tube was sealed with a tight fitting ground glass stopper inside the pistol under a positive flow of the gas.

(b) I.r. spectra

All mulls were prepared in a portable glove box under dry  $\text{N}_2$ .

(c) 'Freeze drying' experiment

The  $\text{D}_2\text{O}$  solution of  $\text{Fe}(\text{saen})_2\text{Cl}\cdot\text{H}_2\text{O}$  was placed in a small

(20 cm<sup>3</sup>) 'Quickfit' test tube and attached to a vacuum line. The solution was frozen with liquid nitrogen then exposed to a vacuum for c.a. 12 hours. The mull for the i.r. spectral work was then prepared as in (b) above.

## CHAPTER 6

Solution studies of the series of complexes of general formula  $M(\text{III}) (\text{saen})_2X \cdot n\text{H}_2\text{O}$ .

### 6.1 INTRODUCTION

It is apparent that much of the anomalous behaviour of the salts, as discussed in Chapter 5, may be rationalized in terms of the strong hydrogen bonding interactions observed in the solid state. The occurrence of hydrogen bonds is not unexpected in view of the presence of a primary amine functional group in the ligand. However, it does seem reasonable to expect that the solution properties of the salts would be simpler to interpret because of dissociation into the cation,  $M(\text{III}) (\text{saen})_2^+$ , and the anion,  $X^-$ . Ready dissociation in solution has already been encountered with the anion analyses of the salts (Chapters 3 and 5). The solution properties, then, would be expected to be characteristic of the cationic species in particular, with the anion behaving as an almost independent entity.

### 6.2 GENERAL SOLUTION PROPERTIES

In general, the solution properties studied have, with one important exception, confirmed the above expectation. In the solvents dimethyl sulphoxide, DMSO, and its deuterated analogue, DMSO-d<sub>6</sub>, the results obtained require considerable discussion. This is done later in this Chapter, following a general discussion of the properties in solvents such as water, methanol, ethanol and chloroform.



(i) I.r. spectra

The chloroform solution spectra of a number of complexes of Types A, B and C were found to be virtually indistinguishable. No doubt this may be attributed, in part, to the rather limited solubility of the compounds in chloroform and solvent absorptions in the fingerprint region.

However, in the region of the spectrum above  $3000\text{ cm}^{-1}$ , where solvent absorptions are negligible, all spectra obtained showed distinctive  $\nu_{\text{N-H}}$  bands. In Chapter 5 the considerable sensitivity of these absorptions to hydrogen bonding effects has been discussed. The band positions in the solution spectra were remarkably similar to those of the Type C solid state spectra, viz. near  $3250$  and  $3300\text{ cm}^{-1}$ . No metal or anion dependent effects were observed. These observations support the proposition that the spectra obtained relate to an isolated solvated cation.

In addition, the monohydrate complexes had a relatively sharp band near  $3600\text{ cm}^{-1}$  ( $\nu_{\frac{1}{2}} \approx 40\text{ cm}^{-1}$ ), presumably due to a free water molecule<sup>(118)</sup>.

(ii) Conductances

Utilizing methanol as solvent, the values of  $\Lambda_M$  obtained for all complexes, at concentrations of  $10^{-3}\text{M}$ , were found to be within the range  $75 - 115\text{ Scm}^2\text{mol}^{-1}$ , as expected for 1:1 electrolytes<sup>(38)</sup>. In contrast to the Fe(III)salenX series discussed in Chapter 3, no evidence of partial association was observed, e.g.

- (a) the 'pH' of all solutions was 8.32, i.e. identical to the 'pH' value for pure methanol;
- (b) plots of  $\Lambda_M$  against  $C^{1/2}$ , over the concentration range  $5 \times 10^{-3}$  to  $10^{-5} M$ , were linear in agreement with ideal 1:1 electrolyte behaviour.

(iii) U.V.-visible spectra

The spectra of all complexes in methanol also proved relatively simple to interpret. In all cases, prominent ligand absorptions were observed below 400 nm, and for the Cr(III) species weak bands, previously ascribed to 'd-d' type transitions, were found near 500 nm<sup>(104,108)</sup>. The corresponding 'd-d' transitions were found near 500 and 600 nm for the Co(III) salts<sup>(108)</sup>.

The Fe(III) complexes gave rise to spectra indistinguishable from that of  $Fe(saen)_2Cl \cdot H_2O$ , as described in Chapter 3.

(iv) Magnetic susceptibility of Fe(III) complexes

The magnetic susceptibility of solutions of  $Fe(saen)_2Cl \cdot H_2O$  have been measured, employing the n.m.r. technique described by Evans<sup>(119)</sup>. In aqueous solution,  $\mu_{eff}$  has been determined as 5.96 B.M. and similar values have been estimated for solutions in chloroform and methanol. The Type B complexes (X = Br and I) also have solution magnetic moments near the spin only value of 5.92 B.M.

(v) Proton n.m.r. spectra of Co(III) complexes

Attempts were made to obtain proton n.m.r. spectra of all

the different salts of  $\text{Co(III)(saen)}_2^+$ . These attempts were unsuccessful in deuterio-chloroform,  $\text{CDCl}_3$ , due to the low solubility of the compounds. In addition, suitable spectra could not be obtained in deuterio-methanol,  $\text{CD}_3\text{OD}$ , and deuterium oxide,  $\text{D}_2\text{O}$ , because of rapid proton exchange between the relatively labile ammine protons and the solvents.

However, the spectra of all three types of salt in the solvents deuterio-ethanol,  $\text{C}_2\text{D}_5\text{OD}$ , and trifluoroacetic acid,  $\text{CF}_3\text{COOH}$ , were similar and thus consistent with the proposition of the existence of the simple cation,  $\text{Co(saen)}_2^+$ , in solution. The positions and assignments of the spectral bands are discussed in the following section.

The spectra of the  $\text{Co(III)}$  salts in  $\text{DMSO-d}_6$  initially presented considerable difficulty in their interpretation but have been rationalized by considering the probability of appreciable association in solution. A more detailed discussion of the results obtained from the n.m.r., conductance, u.v.-visible and magnetic susceptibility studies is presented in the following section, with particular emphasis on the case of  $\text{DMSO}$  as solvent.

### 6.3 PROTON N.M.R. SPECTRA

#### (i) Ligand spectra

Due to the non-availability of the free ligand,  $\text{saenH}$ , the spectra of  $\text{salenH}_2$  and free and coordinated  $\text{en}$  have been utilized as a basis for the assignment of the observed band positions in the spectra of salts of the cation  $\text{Co(saen)}_2^+$ .

(a) SalenH<sub>2</sub>

Disregarding absorptions obviously attributable to the solvent utilized, all solution spectra of salenH<sub>2</sub> consisted of four distinct groups of bands. The band positions and integrated intensities allowed ready interpretation because the salenH<sub>2</sub> molecule has only four major environments for the sixteen hydrogen atoms, viz. phenolic O-H(2), Aromatic C-H(8), imine CH=N(2) and methylene =N-CH<sub>2</sub>(4).

The positions and assignments of the resonances for the salenH<sub>2</sub> spectra are tabulated below in Table 6.1.

(b) Resonances for the -CH<sub>2</sub>-NH<sub>2</sub> moiety from free and coordinated en

The resonances and assignments for en in a number of solvents and for Co(en)<sub>3</sub>I<sub>3</sub>H<sub>2</sub>O in DMSO-d<sub>6</sub> are tabulated below in Table 6.2.

The resonance at  $\delta = 2.65 \pm .02$  ppm may be considered to be characteristic of the methylene protons in the -CH<sub>2</sub>-NH<sub>2</sub> group and could reasonably be anticipated for the saen spectra. However, the position of resonances for -NH<sub>2</sub> protons would be expected to be uncertain. In part, this may be attributed to the effects of metal-nitrogen coordination which would, in general, result in a downfield shift of the resonance<sup>(123)</sup>. A more important variable effect would result from solvent interactions with the -NH<sub>2</sub> protons which have been well documented in the literature<sup>(124)</sup>.

TABLE 6.1

Assignment of salenH<sub>2</sub> spectra

Solvent	-CH=N (2)	Aromatic (8)	=N-CH <sub>2</sub> (4)
CDCl <sub>3</sub>	8.26 (1.98)	7.4-6.6 (8.00)	3.82 (3.98)
DMSO-d <sub>6</sub>	8.48 (2.11)	8.1-7.1 (8.00)	3.92 (4.10)

Notes:

- (1) Integrated areas have been included in parentheses following the resonance position ( $\delta$  in ppm from TMS).
- (2) The broad multiplet near 7 ppm, typical in 'shape' and position to that frequently attributed to aromatic protons<sup>(123)</sup>, has been assigned as an aromatic multiplet of integrated area 8.00.
- (3) The phenolic O-H resonances were found downfield near  $\delta = 13$  (CDCl<sub>3</sub>) and  $\delta = 14$  (DMSO-d<sub>6</sub>).

TABLE 6.2

## Assignment of free and coordinated en spectra

Solvent	-CH <sub>2</sub> -	-NH <sub>2</sub>
CCl <sub>4</sub>	2.65	1.00
CDCl <sub>3</sub>	2.66	1.27
DMSO-d <sub>6</sub>	2.65	1.70
neat liquid	2.63	1.55
Co(en) <sub>3</sub> I <sub>3</sub> .H <sub>2</sub> O in DMSO-d <sub>6</sub>	2.66 (12.00)	4.74 (11.78)

Notes:

- (1) -NH<sub>2</sub> resonances in free en assigned on the basis of the observed solvent dependence of the resonance position<sup>(124)</sup>.
- (2) The spectrum of the Co(III) salt included an additional band at  $\delta = 3.37$  (2.32) attributed to H<sub>2</sub>O<sup>(125)</sup>.
- (3) The coordinated -NH<sub>2</sub> resonance at  $\delta = 4.74$  was confirmed by deuterium exchange with D<sub>2</sub>O<sup>(126)</sup>.

(c) Free water

The position of the resonance associated with the water molecule in the Type A hydrated salts would also be expected to show substantial solvent dependence. The variation in the position of the H<sub>2</sub>O resonance has been examined for all solvents of interest over a range of concentration. The data are tabulated below in Table 6.3.

(ii) Spectra of salts of Co(saen)<sub>2</sub><sup>+</sup> in C<sub>2</sub>D<sub>5</sub>OD and CF<sub>3</sub>COOH

The positions and intensities of the proton resonances of two of the members of the series Co(saen)<sub>2</sub>X.nH<sub>2</sub>O viz. X = Cl and ClO<sub>4</sub> have been tabulated below in Table 6.4. In Part (a) of this table definite band assignments, based on the resonances in the ligands discussed above, have been included. The positions and intensities of the other resonances only have been presented.

The intense band at 5.15 in the C<sub>2</sub>D<sub>5</sub>OD spectra is mainly due to H<sub>2</sub>O in the solvent (integrated intensity 9.2 in solvent spectrum). The increased intensity in the spectra of the complexes may be attributed to absorption of atmospheric moisture<sup>(127)</sup> plus the water of hydration in the case of the chloride salt.

The overlapping bands, resulting in the broad absorption, must be attributable to the remaining unassigned ligand protons, and it appears reasonable to suggest that the signals for the four =N-CH<sub>2</sub> protons and the four -NH<sub>2</sub> protons are involved.

TABLE 6.3

Position of H<sub>2</sub>O n.m.r. resonances in the concentration range 0-10% H<sub>2</sub>O (v/v)

Solvent	C <sub>2</sub> D <sub>5</sub> OD	D <sub>2</sub> O	DMSO-d <sub>6</sub>	CF <sub>3</sub> COOH
Range ( $\delta$ )	5.2-4.7	4.67	3.21-3.43	11.5-9.3

Notes:

- (1) The range shown is in order of increasing concentration.
- (2) Only one resonance signal was observed in the case of CF<sub>3</sub>COOH, due to rapid exchange between the -COOH and H<sub>2</sub>O protons. Spectra of the Co(III) salts in CF<sub>3</sub>COOH will not show H<sub>2</sub>O resonances below  $\delta = 10$  ppm.

TABLE 6.4

Proton n.m.r. spectra of the salts of the cation Co(saen)<sub>2</sub><sup>+</sup>

(a) Complex	Solvent	-CH=N	Aromatic	-CH <sub>2</sub> -NH <sub>2</sub>
Co(saen) <sub>2</sub> Cl.H <sub>2</sub> O	CF <sub>3</sub> COOH	8.54 (2.02)	6.8-7.7(8.00)	2.85(4.01)
	C <sub>2</sub> D <sub>5</sub> OD	8.38 (2.10)	6.2-7.4(8.00)	2.60(4.10)
Co(saen) <sub>2</sub> ClO <sub>4</sub>	CF <sub>3</sub> COOH	8.48 (2.05)	6.9-7.7(8.00)	2.85(4.05)
	C <sub>2</sub> D <sub>5</sub> OD	8.40 (2.12)	6.3-7.4(8.00)	2.62(4.15)

(b) Additional bands for both complexes:

(1) CF<sub>3</sub>COOH - broad absorption 3.2-4.8(8.1) consisting of overlapping bands, with the major component centred at  $\delta = 4.45$  having c.a. 2/3 total integrated area.

(2) C<sub>2</sub>D<sub>5</sub>OD (a) broad absorption 3.9-4.6(7.5) consisting of overlapping bands, with the major component centred at  $\delta = 4.8$  having c.a. 2/3 total integrated area

(b) intense sharp band at  $\delta = 5.15$  - integrated intensity anion dependent with area 11.6 when X = ClO<sub>4</sub> and 13.4 when X = Cl.

Ammine protons often give rise to broad absorptions<sup>(128, 129)</sup>, which may be rationalized in two ways:

- (1) moderately slow chemical exchange of protons. The exchange rate,  $R$ , is defined as  $\frac{1}{2\tau}$ , where  $2\tau$  is the lifetime of the proton in a given environment. If  $\tau$  is comparable with the uncertainty in the time of measurement  $\Delta t$ , it can be shown, via the Heissenberg uncertainty principle, that the uncertainty in the energy of the resonance is reflected in an increased linewidth with  $\nu_{\frac{1}{2}} \approx \frac{1}{\tau}$  (128). This chemical exchange may involve replacement of an ammine proton with one from another complex molecule or a solvent molecule or impurity (such as H<sub>2</sub>O).
- (2) broadening due to quadrupole effects. If a pair of coupled nuclei undergo moderately rapid relaxations of nuclear spin state due to quadrupole effects, the multiplet of one of the nuclei may be broadened by a large amount<sup>(128)</sup>. The nucleus N<sup>14</sup> relaxes moderately rapidly and produces inherently broad proton resonance signals via coupled nuclei. For example, the n.m.r. spectrum of formamide consists of 3 broad proton resonances and may be sharpened considerably by N<sup>14</sup> decoupling such that the anticipated multiplet structure can be observed<sup>(130)</sup>.

Thus the broad absorptions in the range 3.2-4.8 ppm (CF<sub>3</sub>COOH) and 3.9-4.6 ppm (C<sub>2</sub>D<sub>5</sub>OD) may be attributed, in part, to the -NH<sub>2</sub> protons. The prominent sharper band near 4.45 (CF<sub>3</sub>COOH) or 4.18 (C<sub>2</sub>D<sub>5</sub>OD) is considered consistent with the -C=N-CH<sub>2</sub> resonance. The observed integrated areas may be rationalized in terms of the overlapping of the resonances.



The resonance signals observed for the methylene protons of both types  $=N-\underline{CH}_2$  and  $-\underline{CH}_2-NH_2$  are somewhat broader than in the 'free' ligand cases. This was also observed with the spectra of the  $Co(en)_3^{3+}$  salt investigated earlier (6(i)(c)) and such broadening may be rationalized by quadrupole coupling effects involving the  $Co^{59}$  nucleus (100% natural abundance). Such coupling would also increase the 'width' of the  $-NH_2$  resonances (129).

(iii) Spectra of Co(III)saen complexes in DMSO-d6

In contrast to the spectra in  $CF_3COOH$  and  $C_2D_5OD$ , the proton n.m.r. spectra of the series of complexes of formula  $Co(saen)_2X.nH_2O$  utilizing DMSO-d6 as solvent are not anion independent. Representative spectra have been reproduced in Fig. 6.1.

Spectrum (a)  $n = 1, X = I, NO_3, ClO_4$

Spectrum (b)  $n = 1, X = Cl$ . Similar when  $X = Br$ .

Spectrum (c)  $n = 0, X = NCS, ClO_4, BF_4, PF_6$ .

The positions of the resonance signals are tabulated below in Table 6.5, with the unambiguous assignments in part (a). The positions and intensities of the other resonances, listed in part (b), are discussed in the subsequent text.

The weak resonance near 3.2 ppm in the spectra of the anhydrous species may be reasonably assigned to traces of  $H_2O$  in the solvent, as the spectral grade solvent has a weak peak at  $\delta = 3.21$  ppm. Consequently the peak near 4.06 ppm must be assigned to the 4  $NH_2$  protons plus the 4  $=N-\underline{CH}_2$  protons which

Figure 6.1

$H^1$  n.m.r. spectra of  $Co(saen)_2X.nH_2O$

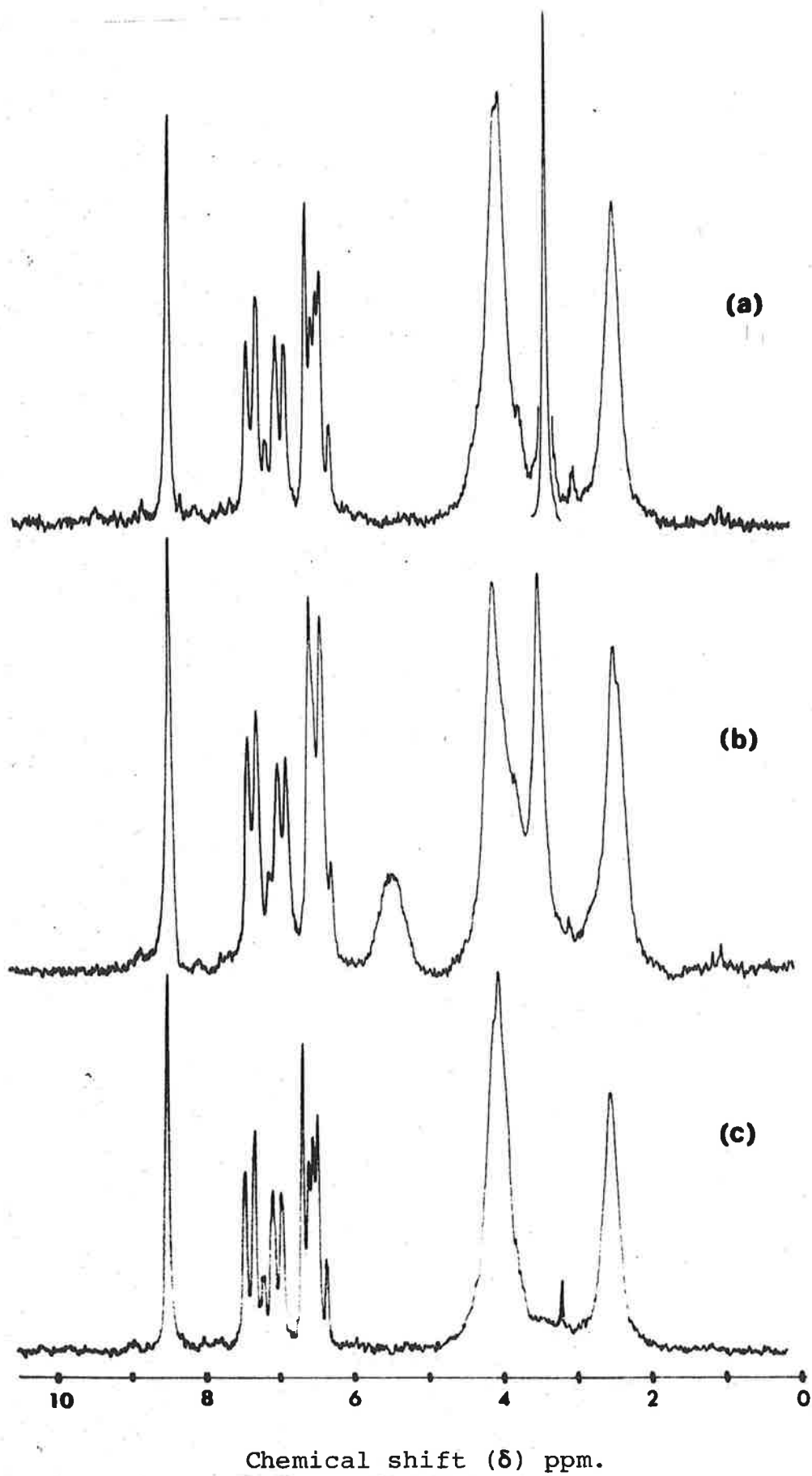


TABLE 6.5

Proton n.m.r. spectra of Co(III) (saen)<sub>2</sub>X.nH<sub>2</sub>O in DMSO-d<sub>6</sub>

(a) Unambiguous assignments for all spectra

<u>-CH=N</u>	Aromatic multiplet	- <u>CH<sub>2</sub></u> -NH <sub>2</sub>
8.46±.02 (2.0±.1)	6.2-7.5±.5 (8.00)	2.46±.02 (4.0±.1)

(b) X	Resonance 1	2	3
I, NO <sub>3</sub> , ClO <sub>4</sub>		4.09±.02 (8.0±.1)	3.36±.04 (2.0±.1)
Cl	5.45 (1.98)	4.10	3.55
Br	4.35 (1.9)	4.08 (6.1)	3.45 (2.05)
NCS, PF <sub>6</sub> , BF <sub>4</sub>		4.06±.02 (8.1±.1)	3.20±.02 (0.2)

Notes:

(1) When X = ClO<sub>4</sub>, n = 1, i.e. Type C hydrate investigated.

(2) When X = Cl, the total area for resonances 2 and 3 = 8.03.

appear to exhibit 'accidental coincidence' i.e. both resonances occur at almost the same frequency and cannot be resolved<sup>(126)</sup>.

It is worth noting that the position of resonance 2 in the DMSO solution spectra is similar to that of the major component of the broad absorption observed in the CF<sub>3</sub>COOH and C<sub>2</sub>D<sub>5</sub>OD solution spectra. The absorptions due to the =N-CH<sub>2</sub> protons in these solvents are shifted slightly downfield and the -NH<sub>2</sub> signals are somewhat broader in comparison to the DMSO-d<sub>6</sub> spectra. Both observations may be rationalized in terms of the hydroxylic nature of the solvents CF<sub>3</sub>COOH and C<sub>2</sub>D<sub>5</sub>OD, with the proton deshielding resulting from hydrogen bonding and the broadening of the -NH<sub>2</sub> signal being attributed to proton exchange with the solvent<sup>(128,129)</sup>.

The DMSO-d<sub>6</sub> spectra of the monohydrated species, with X = I, NO<sub>3</sub> and ClO<sub>4</sub>, may be interpreted in a similar manner. Resonance 2 corresponds to the -NH<sub>2</sub> and =N-CH<sub>2</sub> protons and resonance 3 to the water molecule.

However the interpretation of the spectra for X = Cl and Br is complicated somewhat by the presence of the additional band, resonance 1. Clearly, resonance 2 involves the four =N-CH<sub>2</sub> protons, but the integrated area (c.a. 6) suggests that only two of the -NH<sub>2</sub> protons resonate at this energy. The broad absorption downfield, with an integrated area, c.a. 2, is consistent with the two remaining -NH<sub>2</sub> protons. Resonance 3 is assigned to the H<sub>2</sub>O molecule.

From the above considerations, the spectral data for most of the complexes are consistent with the existence of the cation,  $\text{Co}(\text{saen})_2^+$ , in DMSO-d6 solution. However, the spectra obtained with  $X = \text{Cl}$  and  $\text{Br}$  suggest that in these two cases at least, the situation is more complicated. Bearing in mind the strong hydrogen bonding interactions, observed in the solid state, it would seem to be valid to propose that the cation and anion may remain associated in solution. Such association would involve the maintenance of hydrogen bonds between the anion and ammine hydrogens on solution in DMSO. In contrast to the solid state case, the solvent molecules would be competing with the anion for the available hydrogen bonding sites. Consequently it is not surprising that the only cases where the cation-anion interaction appears to be significant is with those anions known to be able to form strong hydrogen bonds, viz.  $X = \text{Cl}$  and  $\text{Br}$ . Furthermore, the magnitude of the separation between the two sets of  $-\text{NH}_2$  resonances, viz.  $\text{Cl} > \text{Br}$ , is consistent with this suggestion.

(iv) Confirmation of ion pairing in solution

A simple test to confirm the above proposition would be to investigate the effect of excess anion on the position of the  $-\text{NH}_2$  resonance. In a molecule containing exchangeable protons, the observed n.m.r. signal may be the average of the signals for different environments<sup>(128)</sup>. For a solution equilibrium such as  $\text{Co}(\text{saen})_2\text{X} \rightleftharpoons \text{Co}(\text{saen})_2^+ + \text{X}^-$ , the  $-\text{NH}_2$  protons in the ion pair and cation would be expected to have different environments. The position of the signal resulting from averaging the two signals, would be dependent on the population of each site<sup>(128)</sup>. Consequently the position of

the  $\text{-NH}_2$  resonance should be influenced by the concentration of the anion present, and the peak should move in the direction of the resonance position for the associated species, if such an effect occurs in this case.

A saturated solution of dried LiBr in DMSO-d6 was added to a solution of  $\text{Co}(\text{saen})_2\text{Br}\cdot\text{H}_2\text{O}$ , and the spectra obtained. The position of the broad  $\text{-NH}_2$  resonance at 4.35 ppm moved downfield as the  $\text{Br}^-$  concentration was increased, to a maximum observed value of 5.1 ppm in the presence of a threefold molar excess of  $\text{Br}^-$ . This observation strongly supports the proposed ion pair association in DMSO.

Similar splitting of  $\text{-NH}_2$  resonances has recently been observed with salts of  $\text{Co}(\text{medien})_2^{3+}$  in DMSO-d6. The anion dependence of the magnitude of the splitting has been rationalized in terms of hydrogen-bonded ion pair association<sup>(129)</sup>.

(v) Resonances attributed to water

As can be seen from Table 6.5(b) and Fig. 6.1, the position and linewidth of the  $\text{H}_2\text{O}$  resonance for the chloride salt is substantially different from that of the other monohydrates. In fact the  $\nu_{\frac{1}{2}}$  values for the  $\text{H}_2\text{O}$  resonances are respectively 4 ( $X = \text{Cl}$ ) and 2.5 ( $X = \text{Br}$ ) times that of the resonance for the perchlorate salt. In addition the band position is somewhat downfield, suggesting that the electron density experienced by both  $\text{H}_2\text{O}$  protons is less than that of the free water molecule in DMSO. It would appear that the water molecule may also be involved in the ion pair association via hydrogen bonding.

In order to ascertain the validity of this suggestion, the proton n.m.r. spectra of  $\text{Co}(\text{saen})_2\text{Cl}\cdot\text{H}_2\text{O}$  solutions have been obtained under a variety of conditions.

(a) Removal or addition of  $\text{H}_2\text{O}$

A solution of  $\text{Co}(\text{saen})_2\text{Cl}\cdot\text{H}_2\text{O}$  in  $\text{DMSO-d}_6$  was progressively dried over molecular sieves and spectra obtained at regular intervals over a period of 48 hours. The total area between  $\delta = 3.0$  and  $4.7$  ppm relative to the aromatic multiplet ( $8.00$  assumed) was utilized to estimate the relative number of  $\text{H}_2\text{O}$  molecules/cation. Additional spectra of the chloride salt were obtained in the presence of a twofold and threefold molar excess of added water. For purposes of comparison, a similar study of the perchlorate salt was performed. A representative selection of relevant data have been tabulated in Table 6.6 and selected spectra, as indicated, have been reproduced in Fig. 6.2

TABLE 6.6

$\text{H}_2\text{O}$  proton resonances in  $\text{Co}(\text{saen})_2\text{X}$  spectra

Spectrum	X	$\delta_{\text{H}_2\text{O}}$	Shape	Total area(1)	Relative mols $\text{H}_2\text{O}$
(a)	Cl	3.55	broad	8.03	1.0
(b)	Cl	3.65	broad	7.61	0.8
(c)	Cl	3.77	broad	7.28	0.6
(d)	Cl	$\approx 3.85$	shoulder <sup>(2)</sup>	6.96	0.5
	Cl	3.38	sharp	9.08	2.0
(e)	Cl	3.36	sharp	10.06	3.0
	$\text{ClO}_4$	3.36	sharp	10.12	1.0
(f)	$\text{ClO}_4$	3.36	sharp	9.05	0.5

Notes:

- (1) Total area = integrated area between  $\delta = 3.0$  and  $4.7$  for  
 X = Cl, area:  $4 =\text{N-CH}_2 + 2 \text{NH}_2 + 2\text{H}_2\text{O}$  protons for

Figure 6.2  
H<sub>2</sub>O proton resonances

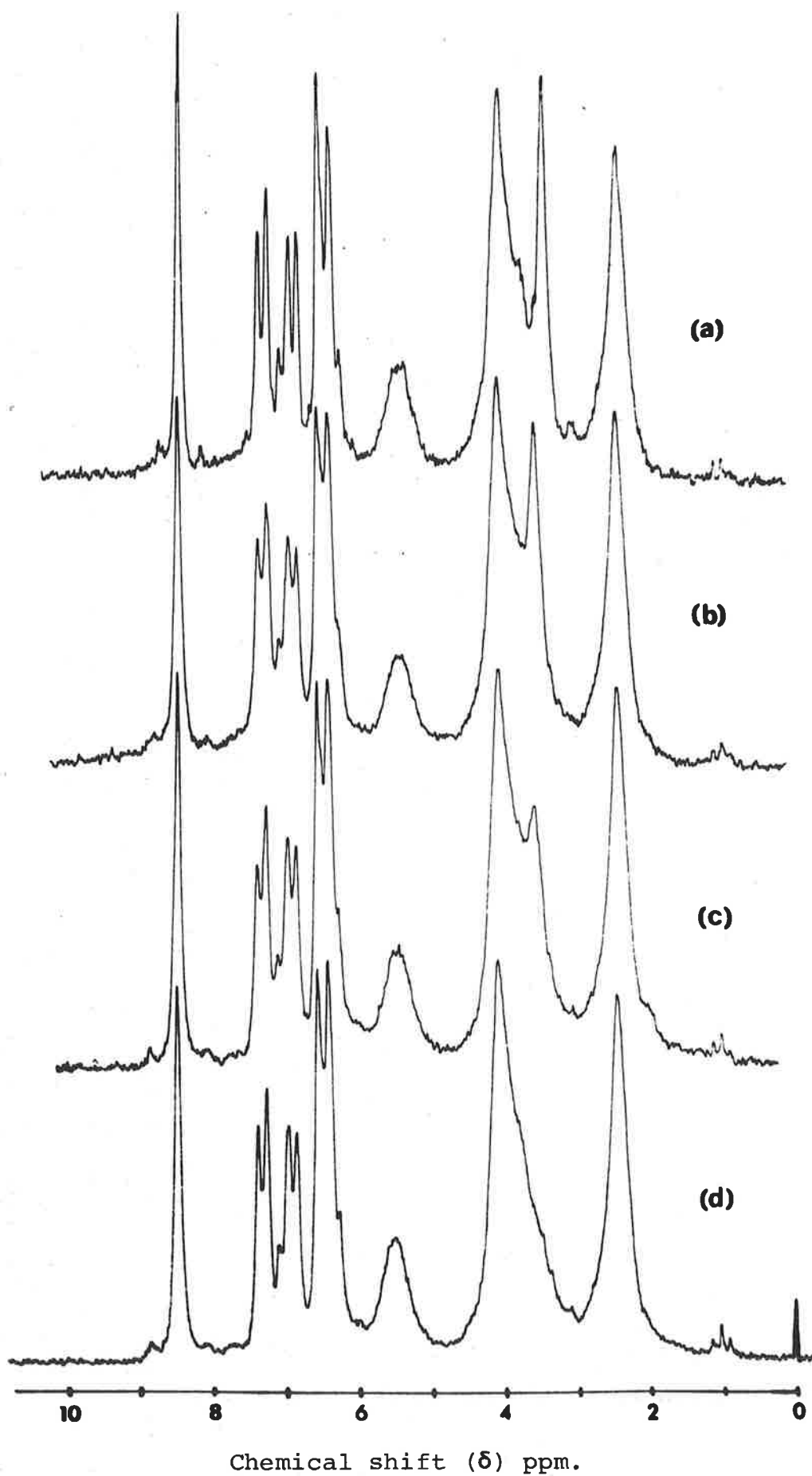
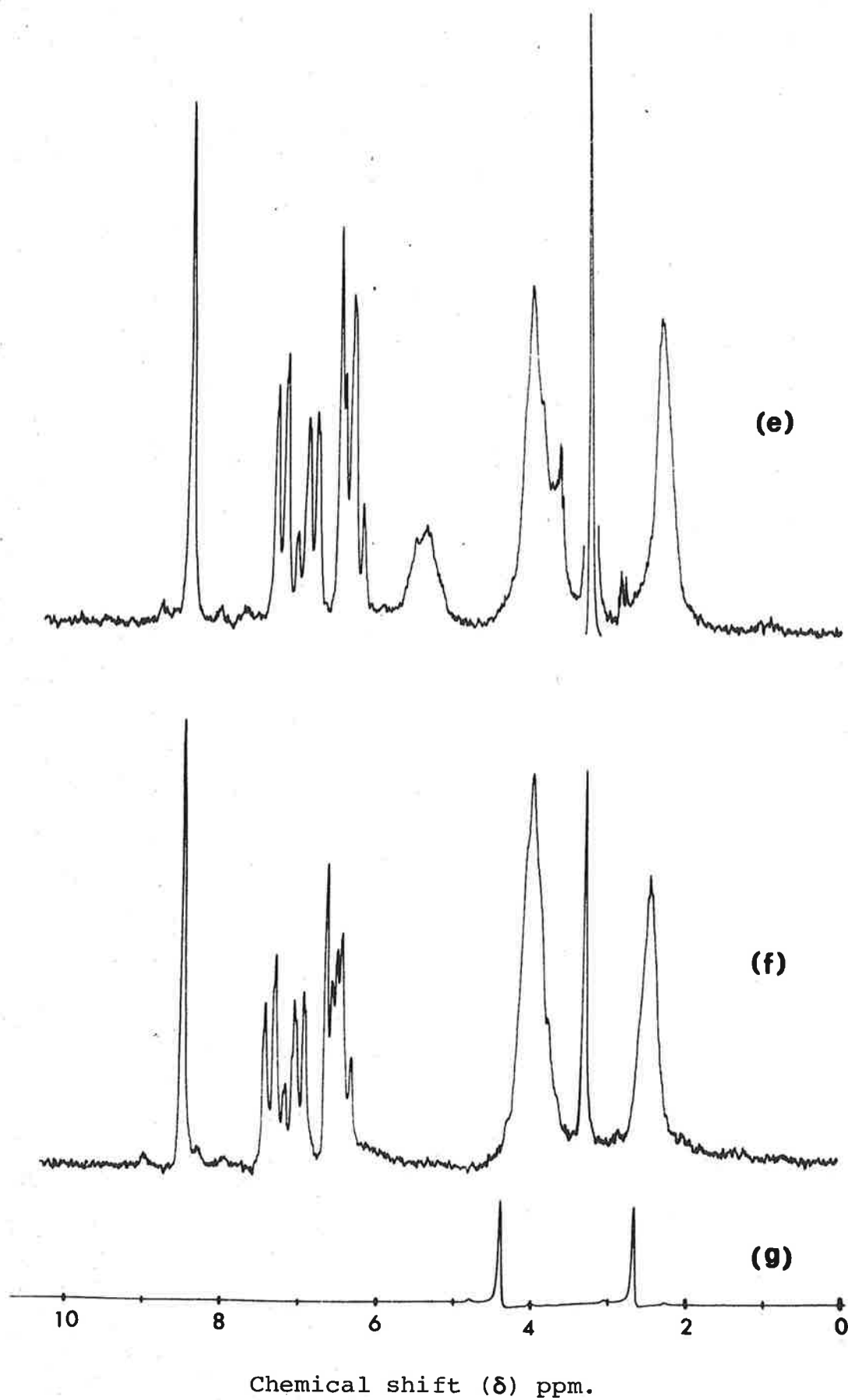




Figure 6.2 (cont.)



X = ClO<sub>4</sub>, area: 4 =N-CH<sub>2</sub> + 4NH<sub>2</sub> + 2H<sub>2</sub>O protons.

- (2)  $\delta_{\text{H}_2\text{O}}$  assumed - shoulder on the broad band centred at 4.1 ppm.

(b) Determination of  $\delta_{\text{H}_2\text{O}}$  in the solvent only

Before attempting to interpret the above behaviour it was considered to be essential that the spectra of H<sub>2</sub>O in DMSO-d<sub>6</sub> be investigated over a wide range of concentrations. A series of spectra were obtained by adding increasing volumes of a 3:1 molar mixture of H<sub>2</sub>O and DMSO-h<sub>6</sub> to 1.00 cm<sup>3</sup> of the DMSO-d<sub>6</sub>. The DMSO-h<sub>6</sub> was used to provide a secondary reference signal (viz.  $\delta_{\text{CH}_3}$ ) in case the TMS reference signal became too weak due to the limited solubility of TMS in aqueous solutions. Over the concentration range studied, this precaution proved unnecessary and  $\delta_{\text{CH}_3}$  was found to vary slightly from  $\delta = 2.44$  ppm for the pure solvent to 2.62 ppm for the neat 3:1 mixture.

The position of  $\delta_{\text{H}_2\text{O}}$  and the approximate concentration of H<sub>2</sub>O have been tabulated in Table 6.7. Spectrum (g) of Fig. 6.2 illustrates the typically sharp resonance signals observed throughout the study.

The position of the H<sub>2</sub>O resonance,  $\delta_{\text{H}_2\text{O}}$ , exhibits an essentially linear dependence on the concentration of water, [H<sub>2</sub>O], up to about 4M. The concentration of all Co(III) complexes investigated was of the order of 10% w/v (i.e. c.a. 0.2M). Thus the concentration of H<sub>2</sub>O in all of the spectral studies must be less than 1M. Consequently  $\delta_{\text{H}_2\text{O}}$  should lie between 3.21 and 3.30 ppm if the H<sub>2</sub>O molecule in solution is

TABLE 6.7

Water resonances in DMSO solution

Volume added	$\delta_{\text{H}_2\text{O}}$	[H <sub>2</sub> O]
0 cm <sup>3</sup>	3.21	0
0.005	3.22	0.12
0.010	3.23	0.24
0.015	3.24	0.35
0.050	3.30	1.1
0.075	3.35	1.7
0.100	3.38	2.4
1.000	4.01	12
3:1 mixture	4.39	24

essentially 'free', and for most of the solutions studied (those without added water),  $\delta_{\text{H}_2\text{O}}$  would be expected to be near 3.23 ppm.

In all cases,  $\delta_{\text{H}_2\text{O}}$  is observed downfield from this value and clearly the presence of the complex must influence the position of the  $\text{H}_2\text{O}$  resonance. It would appear reasonable to propose that this deshielding may result from a hydrogen bonding interaction between the cation, anion and water molecule in DMSO solution.

However, in the chloride salt spectra, the shift in  $\delta_{\text{H}_2\text{O}}$  is much greater than that found with other anions, and it becomes more pronounced when the solution is progressively dehydrated. These observations, coupled with the broadening of the  $\text{H}_2\text{O}$  resonance suggest strongly that a three-way association between the cation, chloride ion and water molecule occurs in DMSO solution.

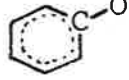
A similar proposition appears to apply for the bromide salt also, but it is unlikely that appreciable association occurs with other anions.

#### 6.4 CARBON $^{13}\text{C}$ n.m.r. SPECTRA

The  $\text{C}^{13}$  n.m.r. spectra of the DMSO solutions have been obtained for  $\text{X} = \text{Cl}$ ,  $\text{NO}_3$  and  $\text{ClO}_4$ . Making allowances for the solvent resonance bands, only 9 separate ligand  $\text{C}^{13}$  resonances of almost equal intensity could be observed. This strongly suggests that the carbon skeletons of the two bistridentate ligands are in equivalent environments. The chemical shift

data, arranged in decreasing order relative to TMS, appear in Table 6.8 below, together with partial assignments.

TABLE 6.8  
 $C^{13}$  chemical shift data, and assignments, for saen complexes

X	Solvent	1	2	3	4	5	6	7	8	9	
NO <sub>3</sub>	DMSO/10% C <sub>6</sub> D <sub>6</sub>	166.5	165.5	135.2	134.5	123.0	119.9	114.4	61.6	43.0	
Cl	DMSO/10% C <sub>6</sub> D <sub>6</sub>	166.1	165.5	135.1	134.1	122.8	119.8	114.0	61.8	39.8	
Cl	DMSO-d <sub>6</sub>	166.2	165.4	135.1	134.1	122.7	119.9	114.2	61.7	39.6	
ClO <sub>4</sub>	DMSO-d <sub>6</sub>	166.5	165.4	135.3	134.5	123.0	119.8	114.6	61.7	42.3	
Assignment - based on references (129, 131,132)		C <sub>1,10</sub> 	C <sub>7,16</sub> C = N	C <sub>2,3,4,5,6</sub> ; C <sub>11,12,13,14,15</sub> Aromatic carbons					C <sub>8,17</sub> =N   C-	C <sub>9, C18</sub> C-NH <sub>2</sub>	

Note: Atomic labelling scheme described in Fig. 7.2 (or Fig. 1, Ref. (20)).

On the basis of this data, it would appear that the environments of the carbon atoms, in all complexes, are essentially the same, with the possible exception of  $\underline{C}$ -NH<sub>2</sub>. However, any conclusions regarding the respective values of the  $\underline{C}$ -NH<sub>2</sub> chemical shifts must be considered as dubious because the DMSO solvent produces an intense resonance centred at 41.4 ppm. Attempts to obtain  $C^{13}$  spectra in other solvent systems have proved unsuccessful due to the limited solubility of the complexes.

#### 6.5 CONDUCTANCE STUDIES OF DMSO SOLUTIONS

The molar conductivity,  $\Lambda_M$ , for a  $10^{-3}M$  solution of a 1:1 electrolyte in DMSO, would be expected to lie within the range 23-42  $Scm^2mol^{-1}$  (38). Furthermore, a plot of  $\Lambda_M$  against  $C^{1/2}$  would be expected to closely approximate a straight line over a considerable concentration range, limited only by the solubility limit and the approach of the experimental values to that of the pure solvent (38). Solutions of saen complexes in methanol exhibited such behaviour (Section 6.2(ii)).

In the previous section, the n.m.r. spectra of the Co(III)(saen)<sub>2</sub> chloride salt strongly supported an ion-pair association in DMSO. An association of this type should be evident in a conductance study over a wide range of solute concentrations, and would be reflected in significant deviations from the behaviour expected for a 1:1 electrolyte.

For this study four complex salts were investigated, viz. Co(saen)<sub>2</sub>ClO<sub>4</sub>.H<sub>2</sub>O, Co(saen)<sub>2</sub>ClO<sub>4</sub>, Co(saen)<sub>2</sub>Cl.H<sub>2</sub>O and Fe(saen)<sub>2</sub>Cl.H<sub>2</sub>O. In all cases, the values of  $\Lambda_M$  at  $10^{-3}M$

were in the range expected for a 1:1 electrolyte, however, at higher concentrations significant deviations were observed for the chloride salts. The data obtained have been tabulated below in Table 6.9, and a plot of  $\Lambda_M$  against  $C^{1/2}$  reproduced in Fig. 6.3.

The conductivity data and graphical plot support an unequivocal associative equilibrium for both chloride salts and essentially complete dissociation for the perchlorates.

It would further appear reasonable to propose that both of the chloride salts are less than 30% dissociated in c.a. 0.2M solution. In the case of the Co(III) salt, the interpretation suggested for the proton n.m.r. spectra is supported by the conductance data because almost 80% of the 'salt' is involved in an ion-pair association at the concentration of the n.m.r. test solutions.

It is worth noting the importance of determining the molar conductance over a range of concentrations. A single concentration conductance measurement (at  $10^{-3}M$ ) could reasonably be interpreted as implying the chloride salts are 1:1 electrolytes in DMSO solution.

## 6.6 U.V.-VISIBLE SPECTRA OF DMSO SOLUTIONS OF THE FE(III) SAEN COMPLEXES

### (i) Fe(saen)<sub>2</sub>Cl.H<sub>2</sub>O

The ion-paired association established in the preceding section for DMSO solutions of the complex Fe(saen)<sub>2</sub>Cl.H<sub>2</sub>O, is known to occur in the solid state. In conjunction with the

TABLE 6.9

Conductivity data at 25°C for saen complexes

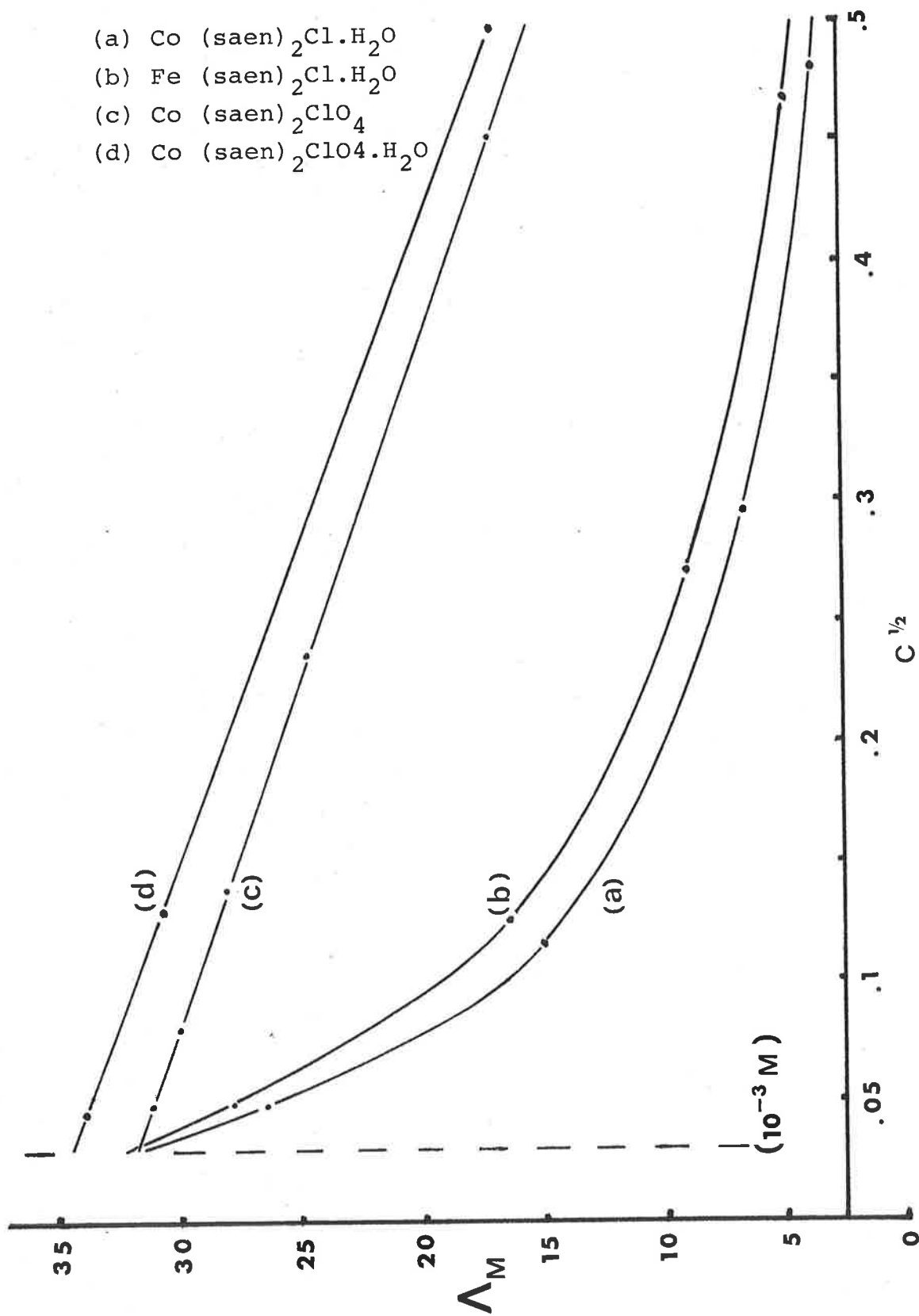
(a) Co(saen) <sub>2</sub> Cl.H <sub>2</sub> O		(b) Fe(saen) <sub>2</sub> Cl.H <sub>2</sub> O		(c) Co(saen) <sub>2</sub> ClO <sub>4</sub>		(d) Co(saen) <sub>2</sub> ClO <sub>4</sub> .H <sub>2</sub> O	
$\Lambda_M$	C	$\Lambda_M$	C	$\Lambda_M$	C	$\Lambda_M$	C
3.73	0.230	4.77	0.218	17.0	0.203	16.8	0.247
6.54	0.0836	8.86	0.0732	24.6	0.0561	30.6	0.0168
15.0	0.0134	16.4	0.0156	28.0	0.0193	33.8	0.00208
26.4	0.00231	27.8	0.00237	30.0	0.00665		
34.6	0.000384	34.4	0.000476	31.2	0.00243		
				33.0	0.00062		
$\Lambda_M$ 31.2 at 10 <sup>-3</sup> M		$\Lambda_M$ 32.2 at 10 <sup>-3</sup> M		$\Lambda_M$ 31.7 at 10 <sup>-3</sup> M		$\Lambda_M$ 34.4 at 10 <sup>-3</sup> M	

Notes:(a) Units -  $\Lambda_M$  Scm<sup>2</sup>mol<sup>-1</sup>, C mol.dm<sup>-3</sup>(b)  $\Lambda_M$  values at C = 10<sup>-3</sup>M obtained by extrapolation from Fig. 6.3.



Figure 6.3

Plot of conductivity data



hydrogen bonded water molecule, these interactions have been shown to stabilize the low spin state for Fe(III). Although no n.m.r. studies were possible with the paramagnetic Fe(saen)<sub>2</sub><sup>+</sup> cation, the conductance studies above suggest that the isostructural Fe(III) and Co(III) chloride salts have similar associative interactions. Thus it would be reasonable to expect that the involvement of the water molecule in the ion-pair interaction may also apply to the Fe(III) chloride salt in DMSO solution. Consequently it was anticipated that evidence for the existence of the low spin Fe(III) species may be obtained from the u.v.-visible spectra of the DMSO solutions. Indeed the concentrated DMSO solution utilized for the conductance study was observed to have a distinct blue hue, in contrast to the deep violet colour of methanol solutions.

The spectra of DMSO solutions of Fe(saen)<sub>2</sub>Cl.H<sub>2</sub>O have been obtained and were observed to be concentration dependent over the range 0.0009 to 0.213M. Representative spectra have been reproduced in Fig. 6.4, the absorbance scale being normalized as outlined in Section 6.8(vi). The spectra may be simply rationalized in terms of two overlapping bands centred near 510 and 600 nm respectively and the concentration dependence is reflected in the variation of the ratio  $\epsilon_{510}:\epsilon_{600}$ , as tabulated below in Table 6.10.

TABLE 6.10

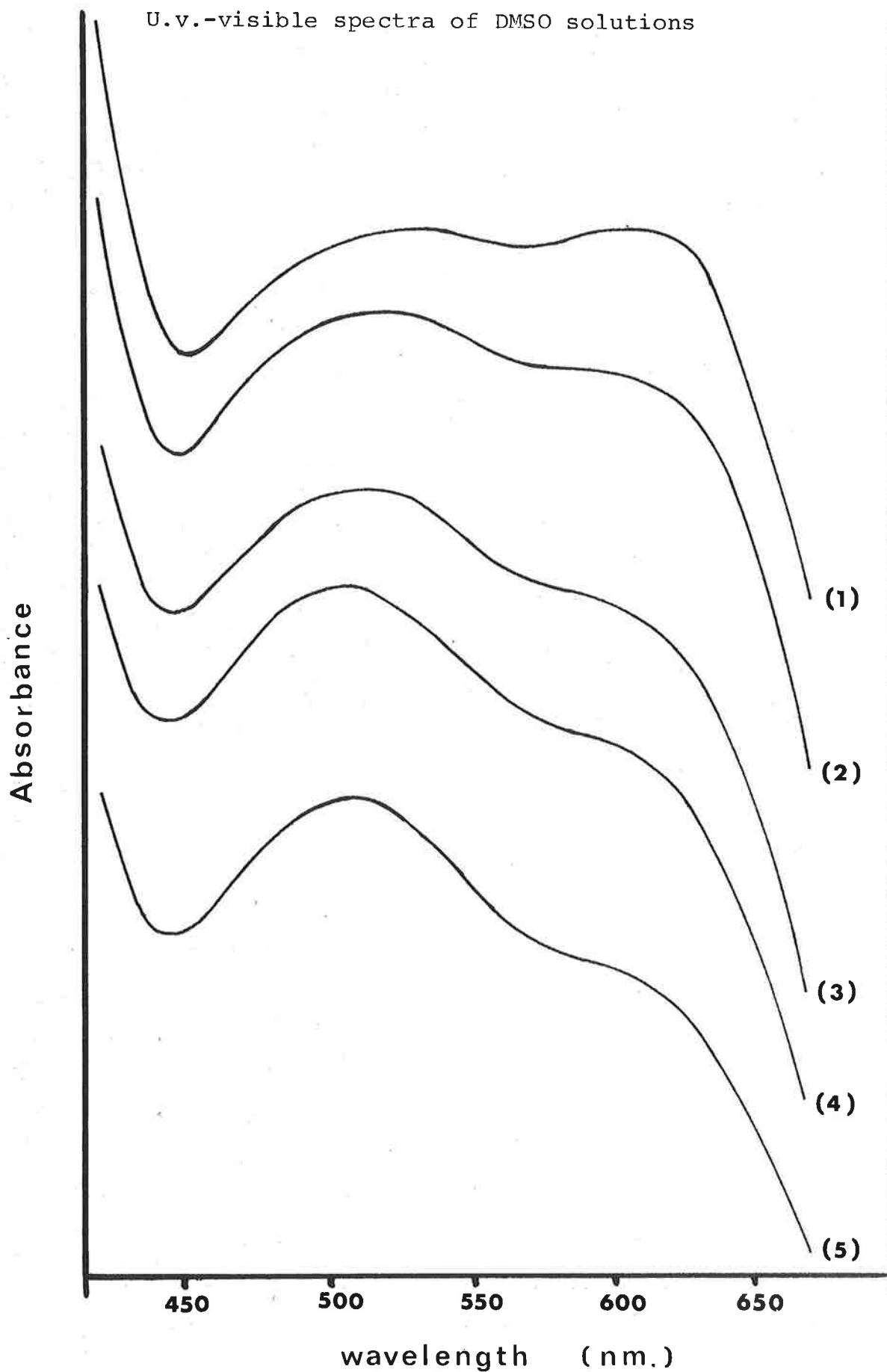
Concentration effect in the u.v.-visible spectra of Fe(saen)<sub>2</sub>Cl.H<sub>2</sub>O in DMSO solution

Concentration	0.213	0.0213	0.0042	0.0009
$\epsilon_{510}:\epsilon_{600}$	0.991	1.08	1.18	1.25

The data are consistent with ion-pair association, where

Figure 6.4

U.v.-visible spectra of DMSO solutions



$\text{Fe}(\text{saen})_2\text{Cl}\cdot\text{H}_2\text{O}$ ; (1) 0.213, (2) 0.0213, (3) 0.0043,  
(4) 0.0009 M.  
 $\text{Fe}(\text{saen})_2\text{NCS}$ ; (5) 0.161 M.

the associated species is characterized by the absorption at 600 nm and the cation by one at 510 nm.

However, the energy difference between the two electronic transitions (c.a.  $3000 \text{ cm}^{-1}$ ) is larger than would be anticipated for equilibria not involving the central metal ion directly. In fact no variation in the electronic spectra of the Cr(III) and Co(III)saen complexes could be observed under similar conditions to those of the Fe(III) case. The origin of the two bands must then be attributable to some 'change' involving the central metal ion, Fe(III), which does not occur with either Cr(III) or Co(III).

In contrast to these other metal complexes,  $\text{Fe}(\text{saen})_2^+$  salts exist in two distinguishable spin states. Indeed the mull spectrum of  $\text{Fe}(\text{saen})_2\text{Cl}\cdot\text{H}_2\text{O}$  is characterized by a band near 640 nm (Chapter 2) whereas the methanol solution spectrum has a prominent band near 510 nm (Chapter 3). Thus the observed results can be rationalized in terms of the associative equilibrium in which the associated species contains Fe(III) in the  $S = \frac{1}{2}$  (low spin state) and the cation contains Fe(III) in the  $S = \frac{5}{2}$  (high spin state).

As a consequence, the average magnetic moment of Fe(III) in the DMSO solutions would be expected to exhibit concentration dependence consistent with the evidence from the conductance and spectral measurements, viz.  $\mu_{\text{eff}}$  should increase on dilution. The variation of  $\mu_{\text{eff}}$  with concentration has been determined utilizing both the Gouy and Evan's n.m.r. techniques. The data obtained have been listed in Table 6.11.

TABLE 6.11

Variation of  $\mu_{\text{eff}}$  with concentration of  $\text{Fe}(\text{saen})_2\text{Cl}\cdot\text{H}_2\text{O}$  in DMSO

Concentration (M)	0.213	0.119	0.0424
$\mu_{\text{eff}}$ (B.M.)	2.58 $\pm$ 0.02	3.24 $\pm$ 0.05	3.8 $\pm$ 0.1

The observed variation of  $\mu_{\text{eff}}$  with concentration appears to validate the proposed equilibrium. The values of  $\mu_{\text{eff}}$  obtained suggest the proportion of the high spin (dissociated) species present in solution increases from c.a. 10% (0.2M) to c.a. 40% (0.04M) which correlates, to a first approximation, with the conductance data.

(ii) Other Fe(III)saen complexes

The DMSO solution spectra of the Type B complexes  $\text{Fe}(\text{saen})_2\text{X}$ , with  $\text{X} = \text{Br}, \text{I}, \text{NCS}$  and  $\text{NO}_3$ , have been obtained. These spectra also show two bands but no variation on dilution could be detected. In all cases, the ratio  $\epsilon_{510}:\epsilon_{600}$  was observed to be 1.25 $\pm$ 0.01 and the spectra were indistinguishable from spectrum (d) of Fig. 6.4. In addition, the values of  $\mu_{\text{eff}}$  for c.a. 0.2M solutions were found to be near 3.9 B.M., suggesting the presence of both low and high spin species in DMSO solutions of these Type B complexes also.

(iii) Discussion

From the magnetic and spectral data considered above it would appear that attributing the behaviour of the monohydrate Type A complexes to association in solution is inadequate. Whilst it is tempting to rationalize the observations in terms of the presence or absence of association, it is clear that

the low spin value for the Type B complexes cannot be accounted for in this way because:-

- (1) the spectral data showed no concentration dependence;
- (2) the n.m.r. spectra of the Co(III) analogues showed no evidence of ion-pair association;
- (3) the Type B complexes have solid state values of  $\mu_{\text{eff}}$  near 5.92 B.M., i.e. an  $S = \frac{5}{2}$  spin state.

Information of particular relevance to this problem has been provided by the solution behaviour of salts of the cationic complex,  $\text{Fe(III)(sal}_2\text{trien)}^+$ . Tweedle and Wilson<sup>(133)</sup> have examined a number of salts of this cation and reported the observation of 'variable temperature magnetic, electronic spectral and  $\text{H}^1$  n.m.r. properties commensurate with a  ${}^2\text{T}$  (low spin)  $\rightleftharpoons$   ${}^6\text{A}$  (high spin) equilibrium for Fe(III) in a tetragonally distorted octahedral field environment'. Relevant observations included<sup>(133)</sup>:

- (1) The equilibrium was solvent dependent and attributed to specific solvent interactions with N-H in the complex. DMSO was one of the ten solvents used and showed the strongest interaction.
- (2) Ion-pair association, although not reported, 'must be considered as potentially important'<sup>(133)</sup>.
- (3) A number of salts of general formula  $\text{Fe(sal}_2\text{trien)X.nH}_2\text{O}$  were reported. The effect of the anion and degree of hydration of the value of  $\mu_{\text{eff}}$  were noted, e.g. when  $\text{X} = \text{PF}_6$  ( $n = 0$ ),  $\mu_{\text{eff}} = 5.81$ ;  $\text{X} = \text{Cl}$  ( $n = 2$ ),  $\mu_{\text{eff}} = 1.94$ ;  $\text{X} = \text{I}$  ( $n = 1$ ),  $\mu_{\text{eff}} = 2.33$  B.M. In the case of the iodide salt, other workers obtained a value  $\mu_{\text{eff}} = 1.81$  when

$n = 1.5$ <sup>(134)</sup>. It was concluded that both 'anion and hydration effects' are likely to be 'operative and non-mutually exclusive' influences on the spin state in such complexes<sup>(133)</sup>.

Such solvent-cation interactions can provide an explanation for the magnetism and electronic spectra of the  $\text{Fe}(\text{saen})_2^+$  salts in DMSO. Thus the Type B salts, which would be expected to be essentially completely ionized in solution, produce the solvated cation,  $\text{Fe}(\text{saen})_2^+\text{-DMSO}$ , only. The solvated cations then consist of an equilibrium mixture of low spin and high spin isomers, estimated from the resultant magnetic moment of 3.9 B.M. to be in the ratio 60:40 respectively.

The situation with the chloride salt is complicated further by the additional associative equilibrium in that the solution contains an associated low spin species plus the solvated cation. From the conductance data for an approximately 0.2M solution of  $\text{Fe}(\text{saen})_2\text{Cl}\cdot\text{H}_2\text{O}$  in DMSO, c.a. 74% association is indicated. For such a solution containing 74% ion-pairs ( $\mu_{\text{eff}} = 1.93$ ) and 26%  $\text{Fe}(\text{saen})_2^+\text{-DMSO}$  ( $\mu_{\text{eff}} = 3.9$ ), the resultant average value of the magnetic moment is calculated as 2.59 B.M. The agreement with the value measured for the 0.218M solution, viz. 2.58 B.M. (Table 6.11) may merely be fortuitous, but obviously lends weight to the above proposition.

## 6.7 CONCLUSION

The spin state behaviour of salts of the  $\text{M}(\text{III})(\text{saen})_2^+$  cations in solution is clearly dependent on ion-pair association and/or cation-solvent interactions. These interactions are of particular importance when DMSO is the solvent utilized and

this observation could be attributed to the following:

- (1) DMSO is well known as a 'strongly coordinating solvent' due primarily to its basicity with respect to hydrogen and metal ions and the ability to form hydrogen bonds with acidic hydrogen atoms. Further, it would appear that DMSO is a Lewis base of comparable strength to H<sub>2</sub>O, and may in fact be stronger<sup>(135)</sup>.
- (2) As a solvent, DMSO is particularly effective in its ability to solvate cations but relatively poor with respect to small anions. For example, the anion Cl<sup>-</sup> is less solvated in DMSO than in methanol, whereas ClO<sub>4</sub><sup>-</sup> is more solvated in DMSO<sup>(135)</sup>. This is generally attributed to the aprotic nature of DMSO and the consequent lack of stabilizing hydrogen bonds with small anions.
- (3) The extent of the ion-pair association is favoured by high concentration of the salt. Consequently, the observation of ion-pairing in DMSO may simply be due to the much greater solubility of the complexes in the solvent. The solubility of Fe(saen)<sub>2</sub>Cl.H<sub>2</sub>O in DMSO is approximately 10 times that in H<sub>2</sub>O and 100 times that in methanol.
- (4) Attempts to obtain the chloride salts containing molecules of solvent of crystallization other than H<sub>2</sub>O were unsuccessful. This indicates that the Lewis base strength of the solvent cannot be the major contributing factor to the occurrence of the solvated cationic salts because, on this basis, DMSO solvates could be anticipated.

Thus the behaviour of the M(III)(saen)<sub>2</sub><sup>+</sup> salts in DMSO may be rationalized in terms of any one or more of the above



observations (1) to (3). In particular, the strong hydrogen bonding interaction between the cation ammine hydrogens and the oxygen of the DMSO may be sufficient to increase the crystal field splitting sufficiently to increase the low spin Fe(III) isomer population significantly. The anion solvation effects and the increased solubility probably both contribute to the ion-pair association observed.

However, the existence of the ion-pair associated low spin species in the case of the  $\text{Fe}(\text{saen})_2\text{Cl}\cdot\text{H}_2\text{O}$  requires further consideration. The n.m.r. spectra of the Co(III) analogue suggested that the  $\text{H}_2\text{O}$  molecule remains associated under conditions where the DMSO solvent could reasonably be expected to displace  $\text{H}_2\text{O}$ . Thus the low spin Fe(III) associated species may in fact be 'molecular aggregates' with the  $\text{H}_2\text{O}$  remaining bound onto the cation. This may result from either the relative size of  $\text{H}_2\text{O}$  compared with DMSO or the aprotic nature of the solvent. Clearly, the role of the water molecule requires further investigation.

## 6.8 EXPERIMENTAL

(i) In general, the solvents utilized were A.R. grade with the exception of the following n.m.r. solvents:  $\text{C}_2\text{D}_5\text{OD}$  and  $\text{CDCl}_3$  Merck-Uvasol (99% min),  $\text{D}_2\text{O}$  Merck-Uvasol (99.75% min),  $\text{CF}_3\text{COOH}$  Koch-Light Puriss and  $\text{DMSO-d}_6$  C.E.A.-France (99.8% min).

(ii) Solution studies in solvents other than DMSO

Conductance, i.r. and u.v.-vis. spectral data were

obtained as described in Chapter 3 (Section 3.5).

(iii) N.M.R. Spectra

(a) H<sup>1</sup> spectra

The p.m.r. spectra were obtained on an Hitachi Perkin Elmer Model R20B operated under the following conditions:

H<sub>0</sub> 1.4087T,  $\nu$  60.0 MHz, TMS internal reference, probe temperature 34°C, sample tube size 3mm.

The spectra reproduced in this work were recorded on blank paper and photographically reduced. In all cases, saturated solutions of solid ligands and complexes were utilized.

(b) C<sup>13</sup> spectra

The broad-band proton decoupled 22.625 MHz carbon-13 n.m.r. spectra in DMSO were obtained on a Bruker HX-90E spectrometer, operating in Fourier transform mode, connected to a Nicolet BNC-12 computer with 8192 data table. The spectrometer was locked to deuterium and a reference signal obtained from c.a. 1% C<sub>6</sub>D<sub>6</sub> (shift of central peak 128.5 ppm from TMS) introduced into the c.a. 1:1 DMSO-d<sub>6</sub> and DMSO-h<sub>6</sub> solvent utilized. Solution concentrations used were c.a. 10% w/v in 10 mm tubes at 28°C.

(iv) Conductance measurements in DMSO

Conductances were measured on a precision conductivity bridge with a cathode ray tube null point indicator. The

instrument was built at the University of Adelaide and allowed measurement of resistances to a precision better than 0.1%.

The DMSO solvent was dried over molecular sieves and all operations performed in an atmosphere of dry N<sub>2</sub>. The conductance cell and A grade volumetric glassware used for solution preparations were dried at 110°C for at least 2 hours and cooled in a dessicator for 30 minutes prior to use.

(v) Magnetic susceptibility of Fe(III) complexes in solution

(a) Gouy method

The magnetic susceptibility of each solution was determined by the Gouy method utilizing the equipment described in Chapter 2. The sample tube was calibrated with a NiCl<sub>2</sub> solution as described by Marr and Rocket<sup>(37)</sup>.

The solutions of the complexes were prepared as described above for the conductance study. The sample tube, and contents, was sealed with a tight-fitting plastic stopper to prevent absorption of moisture by the hygroscopic solvent.

All data were corrected for solvent diamagnetism and corrections for the ligand atoms applied as previously described (Section 2.4(iii)). The error estimates in Table 6.11 were obtained by summing all uncertainties in the measured weights.

(b) Evans n.m.r. technique

The technique, as originally described by Evans<sup>(119)</sup>, involved measurements in aqueous solution, utilizing c.a. 10%

w/v tertiary butanol-water as solvent and reference. The difference between the respective methyl resonances may be related to the solution paramagnetism by the relation with the mass susceptibility of the solute,  $\chi_g$ ;

$$\chi_g = \frac{3 \Delta\nu}{2\pi\nu m} + \chi_o + \chi_o \frac{(d_o - d_s)}{m}$$

where  $\Delta\nu$  = separation between  $\text{CH}_3$  resonances (Hz)

$\nu$  = frequency of spectrometer (60.0 MHz)

$m$  = mass solute/cm<sup>3</sup> solution

$\chi_o$  = mass susceptibility of solvent

$d_o$  and  $d_s$  are the respective densities of the solvent and solution respectively.

The test solution was placed in a standard n.m.r. tube and a capillary containing the solvent only introduced. When the tube was placed in the sample spinner, the capillary assumed a position such that both the sample tube and the capillary were concentric. The frequency difference,  $\Delta\nu$ , between the two sharp resonance lines was estimated with a Takeda-Riden TR3824-X frequency counter and accurately measured from the graphical plots. The values of  $\Delta\nu$  (c.a. 20-50 Hz) were determined in this way with an accuracy of 4 significant figures.

In addition, the sharp resonances observed with methanol ( $\text{CH}_3$ ) and chloroform were found to be suitable for such studies. The methyl proton resonance for the DMSO solutions was observed to be significantly broader than the appropriate resonance for the other solvent systems. Presumably this may be attributed to the cation-solvent interaction as previously

discussed. As a consequence the measured values of  $\Delta v$  could only be considered to, at best, 3 significant figures, although due to the higher concentration of the complexes in DMSO, the values of  $\mu_{\text{eff}}$  were of the same order of precision as the data obtained via the Gouy method.

(vi) U.v.-visible spectra of DMSO solutions

The solutions prepared for the conductance and magnetic susceptibility studies were utilized. Spectra were obtained over the range 400 - 850 nm with a Pye-Unicam SP1700 recording spectrometer fitted with a variable path length cell. The cell path length was adjusted to produce an absorbance at 510 nm of c.a. 1.00 in each case.

As the accuracy of the actual path length was not checked, accurate estimates of molar extinction coefficients have not been presented in this study, although the general order of  $\epsilon_{510}$  and  $\epsilon_{600}$  appears to be  $1-2 \times 10^3$ . It was considered preferable to indicate the extent of the equilibrium via the ratio  $\epsilon_{510}:\epsilon_{600}$  as this quantity is not affected by uncertainty in the cell path length.

CHAPTER 7

The crystal structure of  $\text{Fe(III)(saen)}_2\text{Cl}\cdot\text{H}_2\text{O}$

7.1 INTRODUCTION

The unusual features of the physical and chemical behaviour of the Type A monohydrates of general formula  $\text{M(III)(saen)}_2\text{X}\cdot\text{H}_2\text{O}$  ( $\text{M} = \text{Fe}, \text{Cr}$  and  $\text{Co}$ ) have been documented in the preceding chapters. The chloride salts have been shown to be isostructural, and as such the structure determination of any of these complexes should provide the required information. The  $\text{Fe(III)}$  complex has been selected because of the additional interest in the  $S = \frac{1}{2}$  spin state. Thus the principle aims of this structure determination are threefold, being:

- (1) to verify the suspected bistridentate configuration;
- (2) to obtain structural parameters for the low spin state;  
and
- (3) to ascertain the mode of bonding of the water molecule.

The structure of the  $\text{Fe(III)}$  salt was initially presented at the COMO 7 conference (Melbourne 1977). Subsequently, Benson et al<sup>(108)</sup> published the structure of the Type A complex  $\text{Co(saen)}_2\text{I}\cdot\text{H}_2\text{O}$ , which also showed the meridional bistridentate configuration of essentially planar ligands and the presence of the water molecule as a simple hydrate. No attempt was made to investigate the role of the water in this structure.

A report on the structural determination of  $\text{Fe(III)(saen)}_2\text{-Cl}\cdot\text{H}_2\text{O}$  has recently been published<sup>(20)</sup>, and consequently the presentation in this thesis will differ somewhat in format from that in the publication and the preceding chapters. The

experimental procedure will be discussed concurrently with the results in an endeavour to explain the significance of each. The final structural data will be then considered in relation to the rationalization of the solution equilibria, magnetic and electronic spectra of  $\text{Fe}(\text{saen})_2\text{Cl}\cdot\text{H}_2\text{O}$ .

## 7.2 PRELIMINARY INVESTIGATION

### (i) Crystal selection and mounting

The complex,  $\text{Fe}(\text{saen})_2\text{Cl}\cdot\text{H}_2\text{O}$ , was prepared as described earlier and specimens recrystallized from 1:1 ethanol-diisopropyl ether mixture were examined. The crystals were reasonably large, well formed plates which could not be cleaved easily - samples tended to 'shatter' or cleave micaceously. A large fragment of one plate was found, attached to a thin glass fibre and mounted on a goniometer head following the procedure outlined by Stout and Jensen<sup>(136)</sup>. Careful examination of the mounted crystal suggested that three mutually perpendicular axes could be observed. A sketch of the shape and dimensions of the fragment, with the directions of the apparently orthogonal axes, is presented in Fig. 7.1.

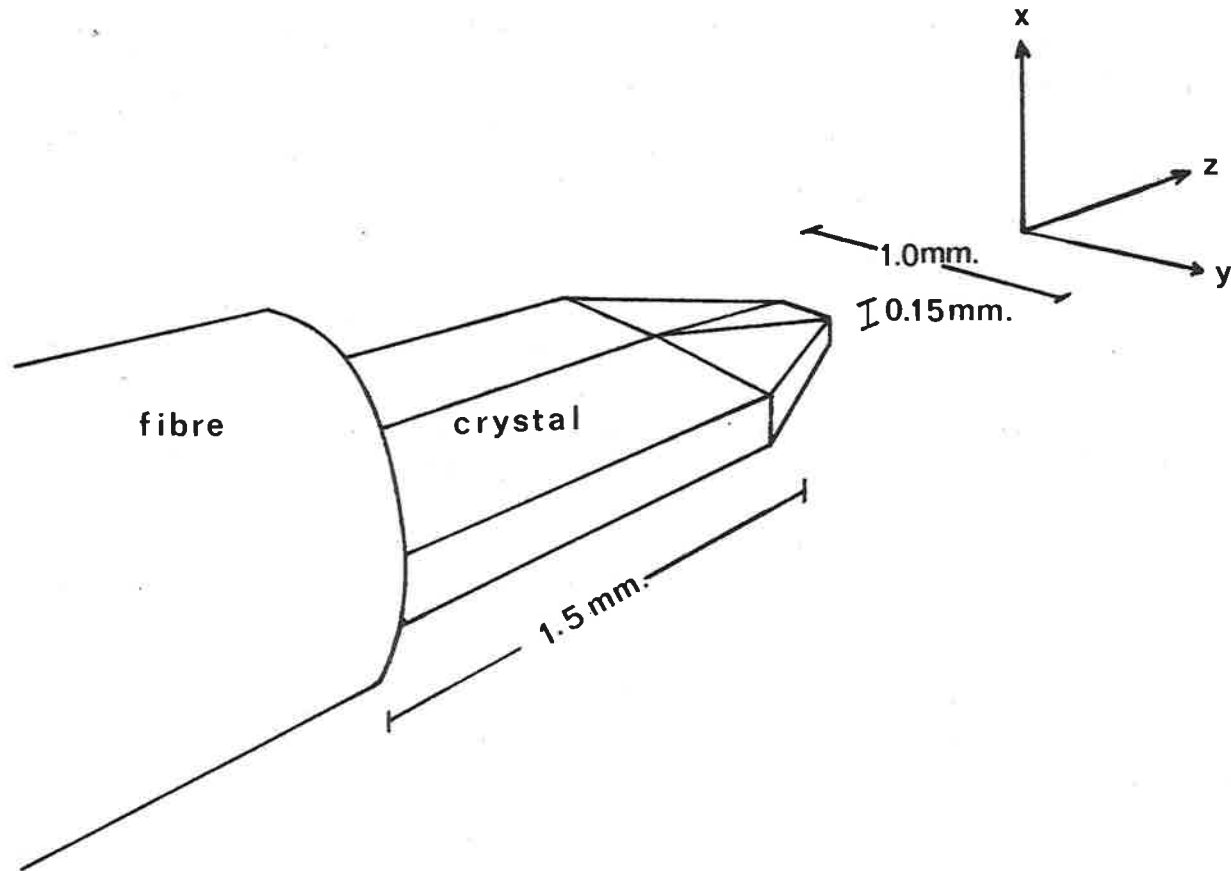
### (ii) Oscillation photographs

#### (a) Outline of technique

In this procedure, the crystal is mounted in the Weissenberg camera, with the rotation axis along an apparent crystal axis. If correctly aligned, when the crystal is rotated while being irradiated, the diffracted X-ray beam will intersect a surrounding cylinder of film such that the resulting photograph

Figure 7.1

Crystal fragment dimensions





will consist of a series of 'spots' (or 'reflections') arranged in parallel rows termed 'layer lines'<sup>(137)</sup>. The rotation technique suffers from the disadvantage that the complete reciprocal lattice is condensed into two dimensions and frequently too many reflections occur<sup>(137)</sup>. In addition, exposure times required are of the order of six hours or more. The oscillation technique involves partial rotation over a much smaller angle ( $\pm 5^\circ$  to  $20^\circ$ ) and thus produces a more readily interpreted photograph with a shorter exposure time.

Rotation and oscillation photographs may be used to<sup>(138)</sup>:

- (1) align the crystal;
- (2) measure the cell 'edge' along the axis of rotation;
- (3) obtain preliminary information about the crystal symmetry.

(b) Alignment

The goniometer head and crystal were mounted in the Weissenberg camera and optically aligned such that the axis of rotation was the apparent crystal axis along the z direction, with the crystal centred in the X-ray beam. The specimen was then irradiated with unfiltered Cu radiation for 1 hour, using an oscillation range of  $\pm 7.5^\circ$ . The crystal was then rotated  $180^\circ$  and irradiated for a further 30 minutes with the same oscillation range. On developing the film it was found that the zero level lines did not correspond. Corrections for the arc settings of  $-0.5^\circ$  and  $+2.8^\circ$  (arcs A and B respectively)<sup>(136)</sup> were calculated utilizing the method described by Stout and Jensen<sup>(138)</sup>. A subsequent double oscillation photograph after application of these corrections showed that the crystal was now aligned.

(c) Axial length (139)

From a single oscillation photograph (range  $\pm 7.5^\circ$ ) with filtered Cu  $K_\alpha$  radiation, the perpendicular distances between the layer lines was measured. The distance between the zero and nth layer,  $\zeta_n$ , may be related to  $\zeta_1$  by the relation  $\zeta_1 = \frac{\zeta_n}{n}$ . An average value for  $\zeta_1$  of 0.1286 reciprocal lattice units (r.l.u.) was obtained. The interplanar spacing,  $d$ , is equal to  $\lambda/\zeta_1$ , where  $\lambda$  is the wavelength of the radiation ( $\lambda = 1.5418 \text{ \AA}$  for Cu  $K_\alpha$ ). In this case a value of 12.0  $\text{\AA}$  was obtained for the unit cell dimension along the axis of rotation (i.e. crystal z axis). Thus the cell dimension,  $c$ , is approximately 12.0  $\text{\AA}$  for Fe(III)(saen) $_2$ Cl.H $_2$ O.

(d) Symmetry (140)

The number of possible symmetries for the intensity-weighted reciprocal lattice is smaller than those for the crystal structure. As a result, oscillation photographs exhibit one of five possible symmetries, viz. 1,  $\bar{1}$ ,  $m_x$ ,  $m_y$  and  $mm$ .

In this study, the oscillation photographs were found to be of  $mm$  symmetry. Thus the reciprocal lattice must have at least one mirror plane perpendicular to the axis of rotation and therefore must belong to the monoclinic class or higher<sup>(140)</sup>. Thus a mirror plane must be directed along the z axis in the crystal.

(iii) Weissenberg photographs - unit cell parameters (141)

The major disadvantage with rotation and oscillation

photographs is that the information contained in an entire reciprocal lattice plane is condensed into a one dimensional layer line. Utilizing the Weissenberg technique, a single reciprocal lattice plane may be mapped onto an entire sheet of film, allowing simplified indexing of the reflections<sup>(142)</sup>.

From the oscillation data, the values of the required parameters - the screen shift,  $s$ , and the inclination angle,  $\mu$ , - were calculated as described by Stout and Jensen<sup>(143)</sup>. The calculated settings were checked with a rotation photograph and corrected when necessary.

Weissenberg photographs were obtained for the levels  $l = 0$  to 4, utilizing Cu  $K\alpha$  filtered radiation, an oscillation of  $\pm 95^\circ$  and c.a. 48 hour exposure time.

From the photographs obtained, an initial examination yielded the following results and conclusions<sup>(141,142)</sup>:

- (1) The axes appeared to be mirror lines dividing the festoons into distorted mirror images. This suggests, when considered in conjunction with the oscillation photographs, that the crystal has  $mmm$  point group symmetry.
- (2) The axes were found to be  $90^\circ$  apart. Following on from (1) above, the crystal symmetry must be orthorhombic or higher.

The zero level Weissenberg photograph may be utilized to provide measurements of the reciprocal lattice parameters  $a^*$  and  $b^*$ , from which the unit cell dimensions,  $a$  and  $b$ , may be

calculated. The reciprocal lattice parameters were obtained utilizing the published chart, PC32<sup>(144)</sup>.

The  $b^*$  axis had a spacing of 0.160 r.l.u., giving  $b = 9.63 \text{ \AA}$ . The zero level spacing for the  $a^*$  axis was 0.097 r.l.u. but the level 2 photograph indicated that the true  $a^*$  spacing was in fact half this value, i.e. on the zero level photograph, only alternate reflections were observed along  $a^*$ . The value of  $a$  then is  $31.8 \text{ \AA}$ .

Thus the crystal symmetry is orthorhombic and approximate unit cell dimensions are  $a = 31.8$ ,  $b = 9.63$ ,  $c = 12.0 \text{ \AA}$ . These cell dimensions probably involve errors of the order of 2-3% due to indeterminate film shrinkage following development<sup>(139)</sup>.

(iv) Space group

Examination of the Weissenberg photographs, as outlined above, indicated that the crystal had mmm point group symmetry. The photographs were then indexed as described by Stout and Jensen<sup>(142)</sup>, and examined for systematic absence of reflections. From these observations, summarized below, the conditions required for reflections of general index ( $hkl$ ) were determined.

(1) Zero level photograph ( $l = 0$ )

$a^*$  axis, alternate reflections absent when  $h$  odd. Therefore for the  $h00$  reflections, the condition required for reflection is that the value of the  $h$  index is even, i.e.  
 $h = 2n$ .

$b^*$  axis - similar to  $a^*$  axis in that reflections absent when  $k$  odd. Thus the condition for reflection of  $0k0$  requires  
 $k = 2n$ .

(2) Level 1 photograph ( $l = 1$ )

$a^*$  axis - all reflections absent.

$b^*$  axis - reflections with  $k$  odd absent. Condition for  $Ok\bar{l}$  reflection then requires  $k = 2n$ .

(3) Level 2 photograph ( $l = 2$ )

$a^*$  axis - reflections present at half spacing of  $a^*$  axis in zero level photograph. This confirms the condition for  $h00$  as  $h = 2n$ .

General  $hk2$  reflections - for  $k = 2n$ , reflections observed at half spacing of the corresponding festoons in the zero level photograph. Thus for  $hk0$  reflections the conditions for reflection require  $h = 2n$ .

(4) Level 3 photograph ( $l = 3$ )

$a^*$  axis - all reflections absent as for level 1. This suggests that for  $h0\bar{l}$  reflections, the conditions for reflection require  $l = 2n$ .

From this data, the following conditions for reflection apply:

$hk\bar{l}$	no general conditions
$h00$	$h = 2n$
$0k0$	$k = 2n$
$h0\bar{l}$	$l = 2n$
$0k\bar{l}$	$k = 2n$
$hk0$	$h = 2n$

From these Weissenberg photographs, no conditions may be deduced for  $00\bar{l}$  reflections as these cannot be observed because of the X-ray beam stop which excludes all reflections with both  $h$  and  $k = 0$ .

However, the conditions for reflection for lattice planes with indices  $h0l$ ,  $0kl$  and  $hk0$  indicate the presence of three orthogonal glide planes as major symmetry elements<sup>(145)</sup>. This determines the Laue group as  $mmm$  which, considered with the above reflection conditions and  $mmm$  point group symmetry, uniquely determines the space group as  $Pbca$ ,  $\left[ D_{2h}^{15} \text{ no. } 61 \right]$ <sup>(146)</sup>.

The next stage of the structural determination required collection of intensity data for each reflection, and for this purpose, a Stoe-Weissenberg automatic diffractometer fitted with a graphite monochromator was utilized.

### 7.3 STRUCTURE DETERMINATION

#### (i) Collection of intensity data

The automatic diffractometer is of the integrating Weissenberg type (i.e. two circle) which allows each reflected 'spot' visible on the Weissenberg photographs to be examined in turn. For each layer, the inclination angle,  $\mu$ , is set and optimized, and each reflection is sequentially examined by rotation about the axes.

These rotations and the required counter position are calculated and set by a dedicated minicomputer. Providing the unit cell parameters introduced into the computer programming are correct, the intensity of each reflection may then be automatically collected and recorded.

#### (a) Check of all parameters

The goniometer head and previously aligned crystal were

mounted in the automatic diffractometer and centred in the X-ray beam. After confirming the alignment of the specimen, the cell parameters obtained earlier were introduced into the Stoe supplied control program. These parameters were checked utilizing  $\omega$  scans of the  $h00$ ,  $0k0$  and  $00l$  reflections. The unit cell data from the photographs were found to be slightly in error. The corrected data with estimated errors in parentheses (3 standard deviations, i.e.  $3\sigma$ ) as calculated from the observed variations, have been tabulated below:

$$a = 32.694 (22), b = 10.083 (7), c = 12.274 (8) \text{ \AA}$$

$$\alpha = \beta = \gamma = 90^\circ.$$

The estimated errors represent an accuracy of 0.07% which agrees well with the previously demonstrated capabilities of the equipment, viz. 0.05%<sup>(148)</sup>.

Utilizing the above data, the unit cell volume,  $U$ , is 4046.2 (82)  $\text{\AA}^3$ . The formula weight of  $\text{Fe}(\text{saen})_2\text{Cl}\cdot\text{H}_2\text{O}$  is 435.72 and the density, as measured by the zero flotation technique<sup>(149)</sup>, is 1.429 (1)  $\text{gm}\cdot\text{cm}^{-3}$ . The number of 'molecules' in the unit cell,  $Z$ , may be calculated as 7.99 (1), i.e.  $Z = 8$ .

(b) Reflection data

Typically, the operating routine for an automatic diffractometer involves the following sequence of operations:

- (1) read setting information;
- (2) move to background;
- (3) count background intensity,  $n_1$ , for time  $t$ ;
- (4) scan through reflection by rotation of a crystal  $\omega$  scan in equal steps such that total counting time is  $2t$  and

the total count is  $n$ ;

(5) count background,  $n_2$ , beyond the reflection for time  $t$ .

The intensity of the reflection,  $I$ , will be given by the relation

$$I = n - (n_1 + n_2)$$

The Stoe control program operates in a similar manner with the additional facility of allowing a preliminary observation of the reflection peak count rate. On the basis of this prescan either an attenuator may be inserted (>4,000 counts per sec.) or the measuring time may be increased in multiples of two up to a factor of 8. This ensures that all reflection data has the same statistical significance.

The basic step counting time for each  $0.01^\circ$  of the scan range is 0.5 sec., with 12.5 sec. for each background count. Reflections with rates less than 8 counts per second are automatically rejected as weak.

For upper level reflections, the scan range,  $\Delta\omega$ , is varied according to the formula:

$$\Delta\omega = A + B \sin \mu / \tan(\psi/2)$$

where  $\mu$  = equi-inclination angle and  $\psi$  = detector angle<sup>(148)</sup>.

The values of  $A$  and  $B$  utilized for this study were 1.0 and 0.6 respectively. The reflection data for each of the levels  $l = 0$  to  $l = 7$  were collected and recorded on paper tape. For each level, an intense reflection was selected as a reference and the intensity data automatically measured after every 30 reflections.



(ii) Treatment of data(a) Structure factor (150)

In order to solve the crystal structure, i.e. locate the positions of atoms in the unit cell, the fundamental information required for each set of planes with Miller index  $(hkl)$  is the structure factor modulus,  $|F_{hkl}|$ . Now if the atomic positions are known, these structure factors may be calculated theoretically. Thus the procedure employed to solve the structure involves calculation of the structure factors for a series of trial structures and comparison with the values of the corresponding observed factors. The trial structures are 'improved' until a close correlation between the calculated and observed factors occurs.

The values of the structure factors may be deduced from the intensity data, utilizing the relationship

$$I_{hkl} = K \cdot L_{hkl} P_{hkl} A_{hkl} |F_{hkl}|^2$$

where  $K$  is a constant for the experiment.

$P_{hkl}$ , the polarization factor, is equal to  $\frac{1 + \cos^2\theta}{2}$  i.e. depends on the angle of diffraction only.

$L_{hkl}$ , the Lorentz factor, is specific for the experiment and depends on the motion of the crystal during the recording.

$A_{hkl}$  represents the physical factors affecting the intensity. One of the more important contributions arises from 'absorption' or attenuation of the X-ray beam by the crystal such that

$$I = I_0 e^{-\phi t}$$

where  $\phi$  is the linear absorption coefficient and  $t$  is the thickness of the crystal.

(b) Data reduction

The paper tape output from the diffractometer consisted of diffractometer count rates for the two backgrounds and the reflection together with the information on the counting times, attenuators and detector and crystal angles. This reflection data was processed on a CDC6400 computer, utilizing the program AUPTP, to give intensities with standard deviations ( $\sigma^2$ ), corrected for Lorentz and polarization effects, normalized on the basis of the standard reflection for each level†. In addition the values of the structure factor and standard deviation ( $\sigma$ ) for each reflection were determined during this processing.

The intensity data, and structure factors, were then corrected for crystal absorption effects utilizing the program ABSCOR. The value of the linear absorption coefficient,  $\phi$ , was calculated from the relation:

$$\phi = \rho_{xt} \sum \phi_i f_i = 8.36 \text{ cm}^{-1}$$

where  $\rho_{xt}$  = density of crystal =  $1.429 \text{ gcm}^{-3}$

$\phi_i$  = absorption coefficient for element  $i$  (151)

$f_i$  = fraction of element  $i$  in compound (from analysis).

†Footnote

A programming error in relation to the first level was recently discovered in that the standard reflection was incorrectly assigned. The value of  $\sigma^2$  for the correct level one standard is approximately one half that of the reflection actually used. The data has been checked and found to have no significant effect on the magnitude of the residual factor,  $R$ , for the structural determination.

Finally, the data for each level were scaled together by the non-iterative least-squares method of Rae<sup>(152)</sup>, utilizing the program AULACT. The processed data was stored on a magnetic tape file for use in the operations following.

A total of 2170 reflections were obtained of which 1587 had intensities greater than three standard deviations in the intensity measured, i.e.  $I > 3\sigma(I)$ . These non-zero reflections were used to solve the structure.

(iii) Determination of trial structure<sup>(153,154)</sup>

(a) Location of Fe atom

In order to determine the crystal structure, it is necessary to propose an initial trial structure so that the calculated structure factors may be compared with the observed factors. As the complex under investigation involves a central metal atom/ion, a large proportion of the scattering of the X-ray beam will be caused by the electrons of this heavy atom. Such heavy atoms may be located from Patterson maps<sup>(153,154)</sup>.

The Patterson function is a Fourier series directly related to the reflection intensities and will produce maxima at the ends of vectors between the atom locations, i.e. for every distinct pair of maxima in the electron density map, there is a maximum in the 'Patterson density'. In general, the most prominent peaks will be those representing the vectors between the atoms with the largest atomic numbers. The intensity of the vector peak may be related to the atomic number,  $Z$ , for the atoms considered, by finding the sum of the  $Z^2$  values for the atoms concerned<sup>(154)</sup>.

Now for Fe-Fe,  $\Sigma Z^2 = 1352$ , Fe-Cl 965, Cl-Cl 578, Fe-O 740, Fe-N 725, Fe-C 712.

Thus, the most prominent peaks in the Patterson map will be those representing the Fe-Fe vectors, with the vectors between other atomic species and Fe being substantially weaker.

The Patterson map was produced utilizing the program FORDAP (Patterson option). From the computer listing of the 100 most intense peak positions, those representing the vectors between the 8 symmetry related Fe atoms in the unit cell were located by applying the principles outlined in Stout and Jensen<sup>(154)</sup> to the particular case of the *Pbca* space group. The coordinates of the Fe atom, in unit cell dimensions, were determined as

$$x/a = 0.153 \quad y/b = 0.035 \quad z/c = 0.015.$$

Attempts were made to locate other atoms from the Patterson map. In retrospect, such attempts were overambitious in view of the complications implied by the relative values of  $\Sigma Z^2$  above. However, several of the suspected vectors for Fe-Cl were assigned, suggesting the coordinates for Cl were near  $x/a = 0.22$ ,  $y/b = 0.10$ ,  $z/c = 0.49$ .

(b) Location of Cl atom

A difference Fourier map, (I), based on the ( $F_{\text{obs}} - F_{\text{calc}}$ ) method of synthesis<sup>(155,156)</sup>, was produced with the program FORDAP (Fourier option). The resulting electron density map was expected to include all significant regions of electron density in the unit cell region selected, other than that

associated with the Fe atom. One of the most intense peaks in the listing ( $\approx 9e\text{\AA}^{-3}$ ) had coordinates  $x/a = 0.221$ ,  $y/b = 0.090$ ,  $z/c = 0.500$  and was assigned to the Cl atom/ion.

(c) Refinement of atomic positions for Fe and Cl (157,158)

The iterative least-squares method of refinement is based on the prediction, from error theory, that if errors in the measured values of  $F_{hkl}$  are random and follow the Gaussian law, the best atomic and thermal parameters will be those which result in a minimum value, for the case of a linear system, in the relation

$$\sum w (|F_{\text{obs}}| - |F_{\text{calc}}|)^2$$

where  $w$  is the 'weight' for a particular observation, and is proportional to the reciprocal of the square of the probable error for that observation.

This relation can be expanded to cover the 'real' or non-linear situation, providing a reasonable set of trial parameters is available, whereupon the function minimized becomes

$$\sum w (|F_{\text{obs}}| - \frac{1}{k}|F_{\text{calc}}|)^2$$

The parameter  $\frac{1}{k}$  is the scale factor required to ensure the values of  $F_{\text{calc}}$  and  $F_{\text{obs}}$  are on the same relative scale.

The full-matrix, least squares program, FUORFLS, requires additional information regarding atomic scattering factors,  $f_0$ , and estimates of the atomic thermal parameters. Scattering factor tables were obtained from previously published data (148, 151,159,160). The atomic positions determined above for Fe and Cl were utilized. The eight scale factors required were

estimated as 0.132. The isotropic temperature factors were assigned values of 2.0 and 3.0 for Fe and Cl respectively and  $w$  was taken as unity.

The probability of the model selected being correct or reasonable may be assessed from changes in the value of the residual index,  $R$ , during the refinement.

$$R = \frac{\sum (|F_{\text{obs}}| - |F_{\text{calc}}|)}{\sum |F_{\text{obs}}|} \quad \frac{\sum |\Delta F|}{\sum |F_{\text{O}}|}$$

The value of  $R$  should decrease, ideally to zero, during the refinement, however, progress of the refinement may be estimated qualitatively, for a centrosymmetric structure, from the following<sup>(161)</sup>:

- (1)  $R = 0.83$  for a random arrangement of atoms
- (2)  $R \approx 0.45$ , model not hopeless but substantial changes required
- (3)  $R \approx 0.35$ , model may be reasonable and will refine
- (4)  $R < 0.25$ , model probably correct

A 'well behaved structure' should refine to  $R < 0.2$  and in most cases to  $R < 0.1$ <sup>(161)</sup>.

The initial value of  $R$  for this study, based on the Fe and Cl parameters, was 0.592. After two cycles of refinement of the scale factors and atomic positions, the  $R$  value was 0.423. The atomic positions were altered slightly but the scale factors increased significantly to between 0.20 and 0.22. Due to the relatively smooth refinement it was felt that the Fe and Cl atoms were placed very near to the correct positions, and the value of  $R$  may probably be attributed to the inadequate model used.

(d) Location of O, N and C atoms

A further difference Fourier map, (II), was obtained at this stage over one-eighth of the unit cell. All atoms except for Fe and Cl were expected to be present in this electron density map. The remaining 25 non-hydrogen atoms were located from the electron density printout as follows:

- (1) The non-symmetry related peaks of the first 40 listed were located.
- (2) A three-dimensional scale 'ball and stick' model was constructed and the potential atomic positions examined visually.
- (3) Obviously spurious peaks were rejected, bearing in mind the possible molecular structures consistent with the chemical data obtained earlier.
- (4) Where necessary, potential 'atoms' were shifted into the model utilizing the symmetry transformations for the *Pbca* space group.

The three oxygen, four nitrogen and eleven of the carbon atoms were found to correspond to the first eighteen peaks in the printout. The remaining seven carbon atoms were found to be interspersed among symmetry related peaks between peaks 20 and 35. Two potential atomic positions only were rejected as spurious, and in all cases the electron density of the peaks selected was  $> 3.5 \text{ e } \text{\AA}^{-3}$ .

(e) Refinement of atomic positions

These additional atomic positions, with arbitrary isotropic temperature factors of 2.30, were introduced into

further cycles of refinement. After six cycles involving the simultaneous refinement of the scale and temperature factors with the atomic positions, all variations in the parameters were less than the respective estimated standard deviations, i.e. the refinement had effectively converged to an overall value of R of 0.153.

At this stage, a further difference Fourier synthesis map, (III), showed that there were no significant peaks in the electron density above  $1.1 \text{ e } \text{\AA}^{-3}$ , thus confirming that all of the major (non-hydrogen) atoms had been located.

(f) Anisotropic thermal motion<sup>(162)</sup>

For the refinement thus far, isotropic temperature factors only have been considered with the scattering factors for each atom being modified by multiplication by the expression:

$$e^{-B(\sin^2\theta)/\lambda^2}$$

where B is the isotropic temperature factor which typically has values between 2 and 5 in organic molecules<sup>(162)</sup>. These values correlate with those obtained in this study. For this type of correction to  $f_0$ , it has been assumed that all atomic vibrations are spherically symmetric, which, although it facilitates the speed of the computations, is obviously an inadequate approximation to the 'real' thermal motion of the atoms in molecules. The more realistic anisotropic model abandons the assumption of spherical symmetry and the single thermal parameter, B, is replaced by six parameters which describe the size and orientation of the vibration ellipsoid.



The control data for the FUORFLS program was modified to allow anisotropic refinement for all atoms. The processing time requirements necessitated that the structural refinement proceeded with alternate cycles of scale factor - atomic position and thermal parameter optimization. During these operations, difficulty was experienced with the anisotropic refinement in that three of the carbon atoms could not be refined. The factors for C10, C15 and C17 continually refined to negative values. Consequently the refinement was modified to allow isotropic refinement of the temperature factors for these atoms, whereupon the refinement proceeded smoothly.

In addition, correction terms,  $\Delta f'$  and  $\Delta f''$ , were included to allow for the effects of anomalous dispersion in the case of the Fe and Cl atoms. The data were obtained from reference (160).

Convergence to an R value of 0.125 was achieved with four cycles of refinement.

(f) Hydrogen atom positions

The positions of the twenty-two ligand hydrogen atoms were calculated with the program PLANEH. These calculated positions were included in the FUORFLS control data, together with arbitrary isotropic temperature factors,  $B$ , selected such that  $B_H = 1 + B_N$  or  $C$ . Refinement of the O, N and C atom parameters only, was continued and convergence to  $R = 0.114$  occurred rapidly (2 cycles). Slight movement of the ligand N and C atoms was observed, which was consistent with contraction of the ligand bonds, due to the inclusion of the hydrogen atoms.

The positions of the ligand hydrogens were then recalculated on the basis of these final atomic positions utilizing the following bond-length criteria:

- (1) aliphatic C-H bond = 1.02 Å.
- (2) N-H bond = 0.91 Å.
- (3) aromatic C-H = 0.92 Å.

A final difference Fourier map (IV) showed no peaks with electron density  $> 0.83 \text{ e } \text{Å}^{-3}$ .

The Fourier maps (III) and (IV) were then examined for significant peaks in the electron density in the region of the water oxygen atom  $O_3$ , i.e. within 1.5 Å. In map III three prominent peaks with density  $> 0.65 \text{ e } \text{Å}^{-3}$  were found to be near atom  $O_3$ . Two of the intense peaks (density  $> 0.65 \text{ e } \text{Å}^{-3}$ ) in map IV corresponded to those in map III. These two peaks have been assigned to the hydrogen atoms of the water molecule.

The final positional and thermal parameters for the major atoms have been tabulated in Table 7.1, with those for the hydrogen atoms in Table 7.2.

The final observed and calculated structure factor tables have been included in the appendices.

(g) Interatomic distances and angles

The interatomic distance, AB, between two atoms A and B, with orthogonal coordinates  $(x_1, y_1, z_1)$  and  $(x_2, y_2, z_2)$  respectively may be calculated from the formula<sup>(163)</sup>:

$$AB = [(x_1 - x_2)^2 + (y_1 - y_2)^2 + (z_1 - z_2)^2]^{1/2}$$

TABLE I. Positional and Thermal Parameters ( $\times 10^4$ ). The form of the anisotropic thermal ellipsoid is  $\text{Exp} [-(\beta_{11}h^2 + \beta_{22}k^2 + \beta_{33}l^2 + 2\beta_{12}hk + 2\beta_{13}hl + 2\beta_{23}kl)]$ 

Atom	x/a	y/b	z/c	$\beta_{11}$	$\beta_{22}$	$\beta_{33}$	$\beta_{12}$	$\beta_{13}$	$\beta_{23}$
Fe	1522 (1)	357 (3)	251 (3)	4.6 (0.3)	55.9 (2.7)	27.9 (3.9)	-0.6 (0.8)	0.5 (0.8)	3.4 (2.6)
Cl	2204 (2)	871 (6)	4890 (7)	7.7 (0.6)	86.5 (6.1)	80.6 (9.8)	3.8 (1.5)	-6.2 (1.7)	-9.6 (6.1)
O(1)	1026 (4)	-428 (14)	-173 (13)	6 (1)	90 (16)	26 (19)	2 (4)	-2 (4)	-11 (14)
O(2)	1264 (4)	1721 (13)	1056 (14)	5 (1)	86 (17)	29 (19)	7 (4)	2 (3)	-11 (13)
O(3)	3473 (6)	1328 (16)	162 (19)	15 (2)	78 (18)	137 (28)	10 (6)	1 (7)	7 (18)
N(1)	1553 (5)	-636 (16)	1592 (16)	4 (2)	68 (19)	38 (24)	2 (5)	0 (5)	0 (15)
N(2)	1518 (5)	1347 (14)	-1119 (16)	7 (2)	45 (17)	29 (23)	-10 (5)	5 (5)	-30 (14)
N(3)	2072 (5)	1064 (18)	713 (20)	5 (2)	67 (19)	55 (26)	-1 (5)	-4 (5)	15 (16)
N(4)	1796(5)	-1058 (17)	-681 (20)	7 (2)	35 (16)	68 (27)	-1 (5)	-4 (5)	16 (16)
C(1)	757 (6)	-972 (20)	518 (22)	7 (3)	67 (24)	36 (35)	11 (6)	6 (6)	16 (21)
C(2)	367 (7)	-1223 (23)	100 (26)	7 (2)	98 (27)	57 (37)	7 (6)	4 (7)	-4 (24)
C(3)	87 (7)	-1852 (30)	822 (30)	7 (3)	167 (40)	51 (43)	-4 (8)	5 (8)	-21 (30)
C(4)	179 (8)	-2265 (28)	1872 (32)	7 (3)	142 (37)	80 (47)	-12 (8)	13 (8)	-12 (29)
C(5)	559 (9)	-2044 (26)	2266 (29)	13 (3)	80 (26)	92 (42)	-6 (7)	2 (9)	-1 (26)
C(6)	866 (6)	-1402 (17)	1582 (22)	8 (2)	29 (19)	43 (33)	-4 (5)	1 (6)	-7 (18)
C(7)	1265 (7)	-1220 (21)	2149 (25)	9 (2)	63 (21)	49 (35)	9 (6)	-3 (7)	13 (20)
C(8)	1959 (8)	-568 (23)	2163 (31)	9 (2)	67 (25)	77 (38)	4 (6)	-1 (7)	2 (23)
C(9)	2134 (7)	793 (25)	1923 (26)	8 (2)	95 (26)	43 (35)	-8 (7)	-9 (7)	-2 (22)
C(10)	1044 (6)	2690 (19)	633 (23)	<sup>a</sup> 2.35 (0.43)					
C(11)	768 (8)	3435 (26)	1313 (24)	11 (3)	99 (26)	24 (33)	8 (7)	3 (7)	3 (23)
C(12)	548 (7)	4459 (21)	911 (26)	11 (3)	57 (23)	40 (34)	13 (7)	9 (7)	-20 (20)
C(13)	580 (7)	4827 (24)	-202 (29)	7 (2)	92 (28)	71 (37)	9 (7)	-13 (7)	-19 (25)
C(14)	816 (7)	4103 (21)	-888 (26)	9 (2)	37 (20)	88 (37)	2 (6)	1 (7)	9 (20)
C(15)	1060 (6)	3056 (20)	-484 (23)	<sup>a</sup> 2.40 (0.42)					
C(16)	1316 (6)	2446 (23)	-1332 (26)	7 (2)	72 (22)	55 (36)	-3 (6)	-2 (7)	5 (20)
C(17)	1768 (8)	757 (24)	-1988 (26)	<sup>a</sup> 3.52 (0.51)					
C(18)	1717 (6)	-734 (23)	-1882 (27)	4 (2)	88 (26)	101 (38)	4 (6)	2 (7)	28 (23)

<sup>a</sup>Isotropic thermal parameter refinement only for C(10), C(15), and C(17).

TABLE III. Interatomic Distances and Angles with Their Standard Deviations.

Distances			
Fe-Cl	4.37 (.01) Å	C(3)-C(4)	1.39 (0.4) Å
Fe-O (3)	4.06 (.02)	C(4)-C(5)	1.35
Fe-O (1)	1.88	C(5)-C(6)	1.46
Fe-O (2)	1.89	C(6)-C(1)	1.42
Fe-N(1)	1.93	C(6)-C(7)	1.49
Fe-N(2)	1.96	C(7)-N(1)	1.31 (.03)
Fe-N(3)	2.02	N(1)-C(8)	1.50
Fe-N(4)	2.04	C(8)-C(9)	1.52 (.04)
O(1)-C(1)	1.34 (.03)	C(9)-N(3)	1.52 (.03)
C(1)-C(2)	1.40 (.04)	O(2)-C(10)	1.32
C(2)-C(3)	1.42	C(10)-C(11)	1.44 (.04)
C(11)-C(12)	1.35 (.04) Å		
C(12)-C(13)	1.42		
C(13)-C(14)	1.36		
C(14)-C(15)	1.41		
C(15)-C(16)	1.42		
C(15)-C(16)	1.47		
C(16)-N(2)	1.32 (.03)		
N(2)-C(17)	1.47		
C(17)-C(18)	1.52 (.04)		
C(18)-N(3)	1.53 (.03)		

Angles			
O(1)-Fe-O(2)	93.7 (2.0)°	C(5)-C(6)-C(1)	119.5 (2.5)°
O(1)-Fe-N(1)	93.6	C(1)-C(6)-C(7)	127.6
O(1)-Fe-N(2)	88.3	C(6)-C(7)-N(1)	116.3 (2.0)
O(1)-Fe-N(3)	175.8	C(7)-N(1)-C(8)	114.5
O(1)-Fe-N(4)	86.0	N(1)-C(8)-C(9)	106.5
O(2)-Fe-N(1)	87.4	C(8)-C(9)-N(3)	107.6
O(2)-Fe-N(2)	94.3	C(9)-N(3)-Fe	109.2
O(2)-Fe-N(3)	89.7	Fe-O(2)-C(10)	125.2
O(2)-Fe-N(4)	177.2	O(2)-C(10)-C(15)	123.5
N(1)-Fe-N(2)	177.3	C(15)-C(10)-C(11)	116.5 (2.5)
N(1)-Fe-N(3)	84.1	C(10)-C(11)-C(12)	121.3
N(1)-Fe-N(4)	95.3	C(11)-C(12)-C(13)	120.7
N(2)-Fe-N(3)	93.9	C(12)-C(13)-C(14)	120.0
N(2)-Fe-N(4)	83.0	C(13)-C(14)-C(15)	120.3
N(3)-Fe-N(4)	90.8	C(14)-C(15)-C(10)	120.9
Fe-O(1)-C(1)	124.3	C(10)-C(15)-C(16)	126.5
O(1)-C(1)-C(6)	123.0	C(15)-C(16)-N(2)	119.8 (2.0)
C(6)-C(1)-C(2)	120.7 (2.5)	C(16)-N(2)-C(17)	118.2
C(1)-C(2)-C(3)	116.0	N(2)-C(17)-C(18)	106.0
C(2)-C(3)-C(4)	124.9	C(17)-C(18)-N(4)	106.0
C(3)-C(4)-C(5)	118.9	C(18)-N(4)-Fe	108.4
C(4)-C(5)-C(6)	119.9	N <sub>3</sub> -Cl-N <sub>4</sub>	52.0

TABLE II. Hydrogen Atoms. Positional ( $\times 10^4$ ) and Isotropic Thermal Parameters.<sup>a</sup>

	x/a	y/b	z/c	B (Å <sup>2</sup> )
C(2) H	295	-994	-600	3.50
C(3) H	175	-1997	574	3.50
C(4) H	15	-2683	2293	3.50
C(5) H	624	-2297	2966	3.50
C(7) H	1306	-1504	2853	3.50
C(8) H(1)	2194	-1288	1876	4.50
C(8) H(2)	1920	-688	2982	4.50
C(9) H(1)	2438	810	2106	4.50
C(9) H(2)	1986	1493	2373	4.50
C(11) H	741	3208	2036	3.50
C(12) H	375	4923	1364	3.50
C(13) H	441	5556	-457	3.50
C(14) H	817	4295	-1621	3.50
C(16) H	1335	2832	-2009	3.50
C(17) H(1)	1669	1070	-2732	4.50
C(17) H(2)	2068	1013	-1891	4.50
C(18) H(1)	1922	-1215	-2366	4.50
C(18) H(2)	1427	-1006	-2095	4.50
N(3) H(1)	2273	654	324	3.50
N(3) H(2)	2083	1953	590	3.50
N(4) H(1)	2070	-1062	-550	3.50
N(4) H(2)	1690	-1868	-518	3.50
O(3) H(1)	3468	145	216	3.50
O(3) H(2)	3318	332	78	3.50

<sup>a</sup> All parameters calculated except the positional parameters for O(3) H(1) and O(3) H(2).

The bond angle,  $\theta$ , between three atoms A, B and C may be calculated from the interatomic distances AB, BC and AC according to the relation<sup>(163)</sup>:

$$\theta = \cos^{-1} \left[ \frac{(AB)^2 + (AC)^2 - (BC)^2}{2(AB)(AC)} \right]$$

The errors involved in these calculations may be estimated in terms of the standard deviations of the atomic positions if these are known.

In Table 7.3 the interatomic distances, angles and estimated standard deviations for the non-hydrogen atoms are tabulated. These values were calculated with the computer program BLANDA.

Table 7.4 contains the interatomic distances and angles for the potential hydrogen bonding interactions. These values were calculated from the above equations. No attempt has been made to estimate errors in this case due to the way in which these atomic positions have been determined.

Finally, the Figures 7.2 and 7.3 present a perspective view of the complex showing the atom labelling scheme and a stereoscopic view of the molecular structure. Both figures were obtained from CALCOMP plots, utilizing the thermal ellipsoid control program ORTEP, followed by photographic reduction.

(h) Magnitude of residual index, R

The final value of R obtained on convergence of the refinement, viz. 0.114, is substantially higher than expected in view of previous structural determinations in the same

Figure 7.2

Perspective view showing the atom labelling scheme

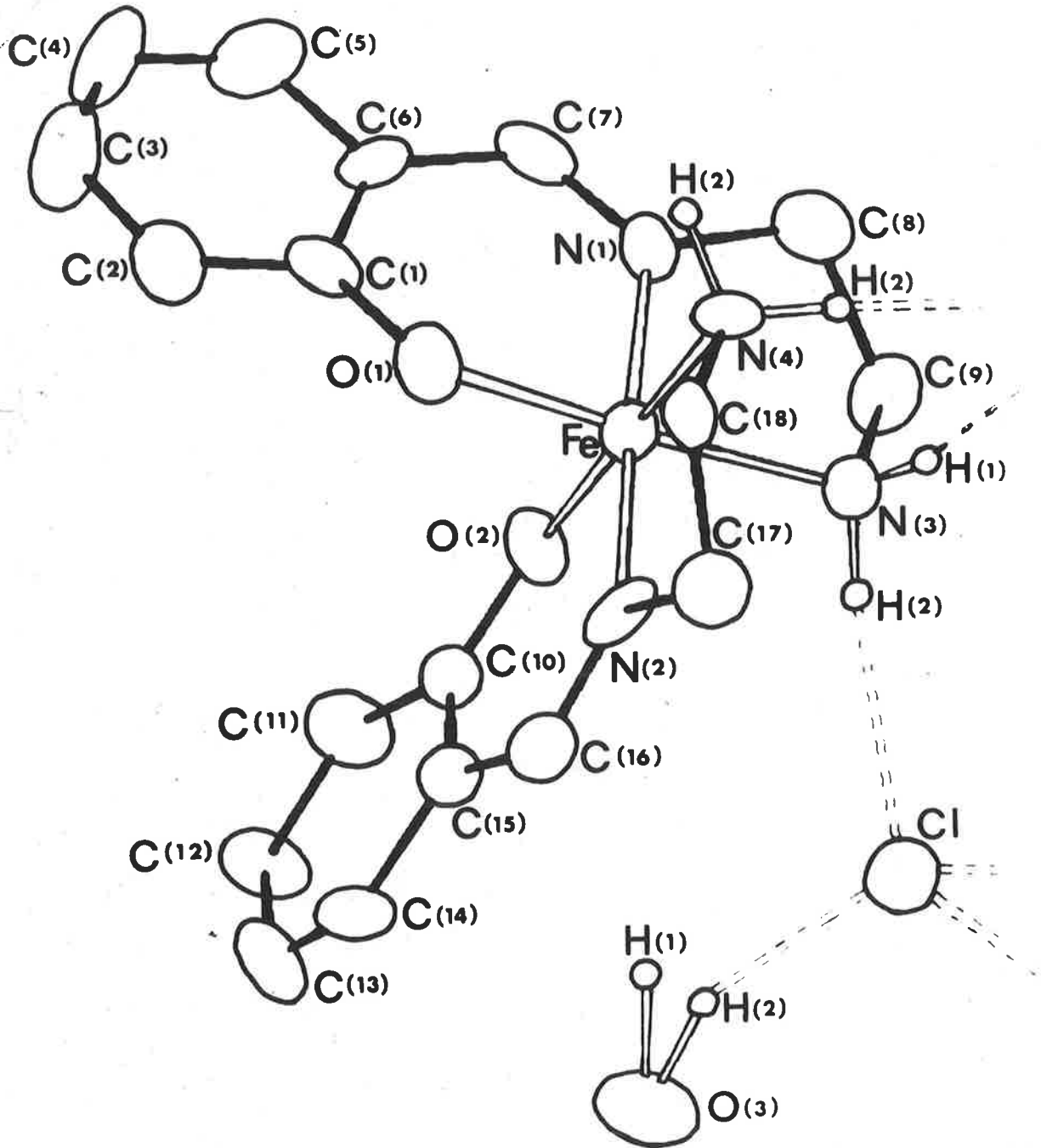
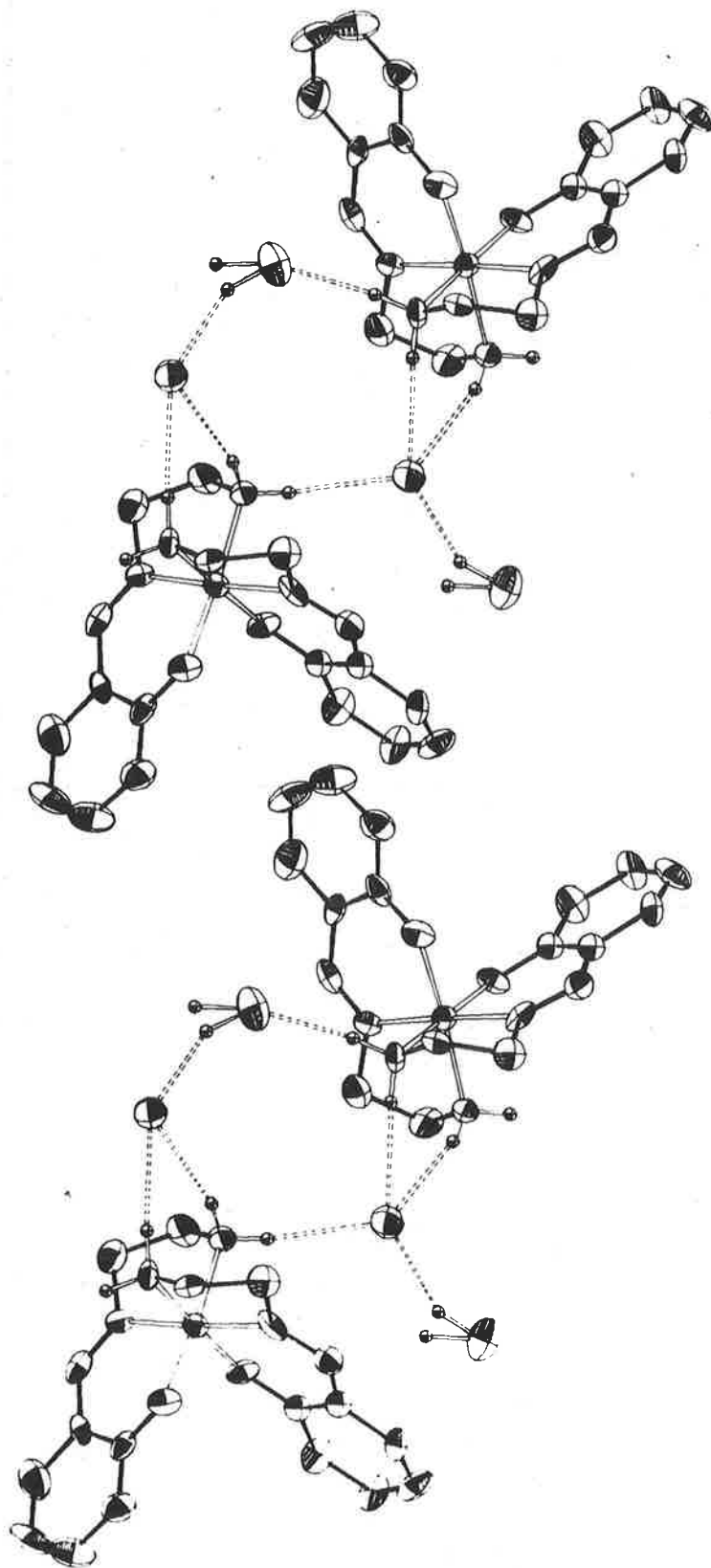


Figure 7.3

Stereoscopic view of the molecular structure with thermal ellipsoids of non-hydrogen atoms drawn at 50% probability



laboratory. For example, the data for the complex tris(biquanidine)cobalt(III)trichloride monohydrate, which has a similar orthorhombic space group, was obtained on the same equipment following a similar procedure. The structure was refined utilizing the same computer programs to a final R value of 0.021<sup>(148)</sup>.

It is believed that the comparatively high value of R for this study may be attributed to a number of cumulative sources of error.

(a) The morphology of the crystal fragment examined must be considered unfavourable in terms of size and shape. A major requirement, for satisfactory collection of data, is that the crystal be of approximately uniform dimensions and of such a shape that the whole crystal may be uniformly bathed in radiation of uniform intensity. An ideal crystal would have a spherical shape c.a. 0.3 mm in diameter<sup>(164)</sup>. The crystals utilized in this study could not be shaped readily and tended to cleave micaceously. The fragment selected was felt to represent an optimum compromise realising that considerable errors might be anticipated in the observed reflection intensities.

(b) Because of the flat, plate-like morphology of the fragment, it was mounted on a relatively thick, c.a. 0.5 mm diameter, glass fibre which would be expected to give rise to high background scatter - a further source of error.

(c) The bulk magnetic susceptibility of the sample of  $\text{Fe}(\text{saen})_2\text{Cl}\cdot\text{H}_2\text{O}$  was 2.11 B.M., which suggested slight contam-



ination with the high spin anhydrous species. The homogeneous appearance of crystal fragments under the microscope indicated that the high spin form of the complex was relatively evenly distributed throughout the crystalline mass. As some of the atomic parameters for the high spin moiety would be expected to differ from those of the low spin hydrate (Section 7.4), further errors in the reflection data may result.

An R value of 0.114 then, may be considered to be indicative of a structural determination in which the atomic parameters are essentially correct and represent a very close approximation to the 'true' molecular structure. It is worth noting that the ligand bond lengths lie within one standard deviation of the corresponding bonds in the Cr(III) and Co(III) complexes of the  $M(III)(saen)_2^+$  cation. In addition the R value compares favourably with those obtained for these similar structures viz.  $R = 0.114$  ( $M = Cr$ ) and  $R = 0.098$  ( $M = Co$ ) (105,108).

#### 7.4 DISCUSSION

##### (i) Configuration of the cation

Figure 7.2 clearly shows that the iron atom, in the cation  $Fe(saen)_2^+$ , is involved in octahedral coordination with the two tridentate saen ligands in the meridional configuration. In view of the fact that this configuration has also been established for  $Cr(saen)_2I$  (105) and  $Co(saen)_2I.H_2O$  (108), it would appear reasonable to propose that all of the salts of general formula  $M(III)(saen)_2X.nH_2O$  involved in this study, contain the cation  $mer-M(III)(saen)_2^+$ .

(ii) Spin state of Fe(III)

The low spin state for Fe(III) in  $\text{Fe}(\text{saen})_2\text{Cl}\cdot\text{H}_2\text{O}$ , which was initially proposed on the basis of the room temperature magnetic susceptibility and Moessbauer data, is further supported by this structural determination.

In a recent review article, the published structures of complexes with the related ligand salen have been discussed and compared<sup>(95)</sup>. Of particular interest to this study is the apparent influence of the nature of the metal on the metal-donor atom distances. When complexes of similar structure are compared, the following observations may be made<sup>(95)</sup>:

(a) The metal-phenolic oxygen distances appear to be relatively insensitive to the nature of the metal. The variation observed appears to be attributable to the type of structure in the complex, as would be expected, because bonding in the 'dimers' occurs via the phenolic oxygen. Thus no useful generalization may be deduced for these interatomic distances.

(b) On the other hand, the metal-imine nitrogen distances do show a clear trend. A clear correlation between these interatomic distances and the number of unpaired electrons on the central metal ion, as tabulated below, would seem to apply.

TABLE 7.5

Metal-imine nitrogen bond lengths

Metal	Co(III)	Cu(II)	Cr(III)	Fe(III)
Range of bond lengths (Å)	1.88-1.91	1.93-1.95	2.00-2.01	2.06-2.10
No. unpaired electrons	0	1	3	5

An alternative correlation may be observed with the effective ionic radii of the metal ions. Recently published data (e.g. Table 3.6 in Ref. 60 (1978), Second Edition) suggest that the order of the radii is  $\text{Co(III)} \approx \text{Fe(III) low spin} < \text{Cu(II)} < \text{Cr(III)} < \text{Fe(III) high spin}$ . Either, or indeed both, of these correlations with the M-N(imine) distances may be applied in the following consideration.

The M-N(imine) interatomic distances obtained in this study, 1.93 and 1.96 Å, are substantially less than the range for Fe(III) high spin, viz. 2.06-2.10 Å. This apparent contraction cannot be simply attributed to the difference in the ligand because the M-N(imine) distances for the Cr(III) and Co(III) salts correlate with those in the corresponding salen complexes<sup>(105,108)</sup>. Clearly then, the above evidence must be considered as confirming the low spin state for Fe(III) in the salt  $\text{Fe(saen)}_2\text{Cl}\cdot\text{H}_2\text{O}$ .

Similar Fe-N(imine) interatomic distances have been observed for the low spin ( $\mu_{\text{eff}} = 2.00$  B.M.) sulphur containing analogue, bis(2-aminoethyl thiosalicylideneiminato) iron(III) chloride,  $\text{Fe(mben)}_2\text{Cl}$ <sup>(165,166)</sup>. Presumably the low spin state of  $\text{Fe(mben)}_2\text{Cl}$ , which appears to resemble the complexes designated as Type B in this study, may be rationalized in terms of the presence of the sulphur atom in the tridentate ligand.

(iii) Water molecule - mode of bonding

The water is present in the crystal as a lattice water molecule which lies in a well defined position, as indicated by the relatively small thermal ellipsoid of  $\text{O}_3$  in Figs. 7.2

and 7.3. The thermal parameters for  $O_3$  appear to be approximately half those of a structure known to be a disordered hydrate<sup>(148)</sup>. Further, the water molecule appears to be bound into the lattice in a somewhat unusual manner in that one hydrogen atom is apparently not involved in hydrogen bonding. The proposed hydrogen bonding interactions have been illustrated in Fig. 7.4, with the 'hydrogen bonds' represented as dotted lines.

The reasoning behind this proposal has been based on criteria established, through wide experience, as indicative of hydrogen bonding<sup>(167,168)</sup>. All of the interatomic distances, (A-B), tabulated in Table 7.4 are within the expected range for such interactions but the 'potential' bond between  $O_3H_1$  and the chloride anion does not meet the additional criterion that the A-H-B angle be 'within about  $30^\circ$  of a straight angle'<sup>(167)</sup>.

In addition, the simple rationalization of the i.r. spectra of the Type A monohydrates discussed in Chapter 5, lends weight to the above proposal regarding the mode of bonding of the water molecule in such complexes.

Furthermore, the specific nature of these interactions involving the water molecule, clarify the observations discussed in Chapter 6. Clearly the aprotic nature of the solvent DMSO precludes the involvement of this molecule in a similar interaction.

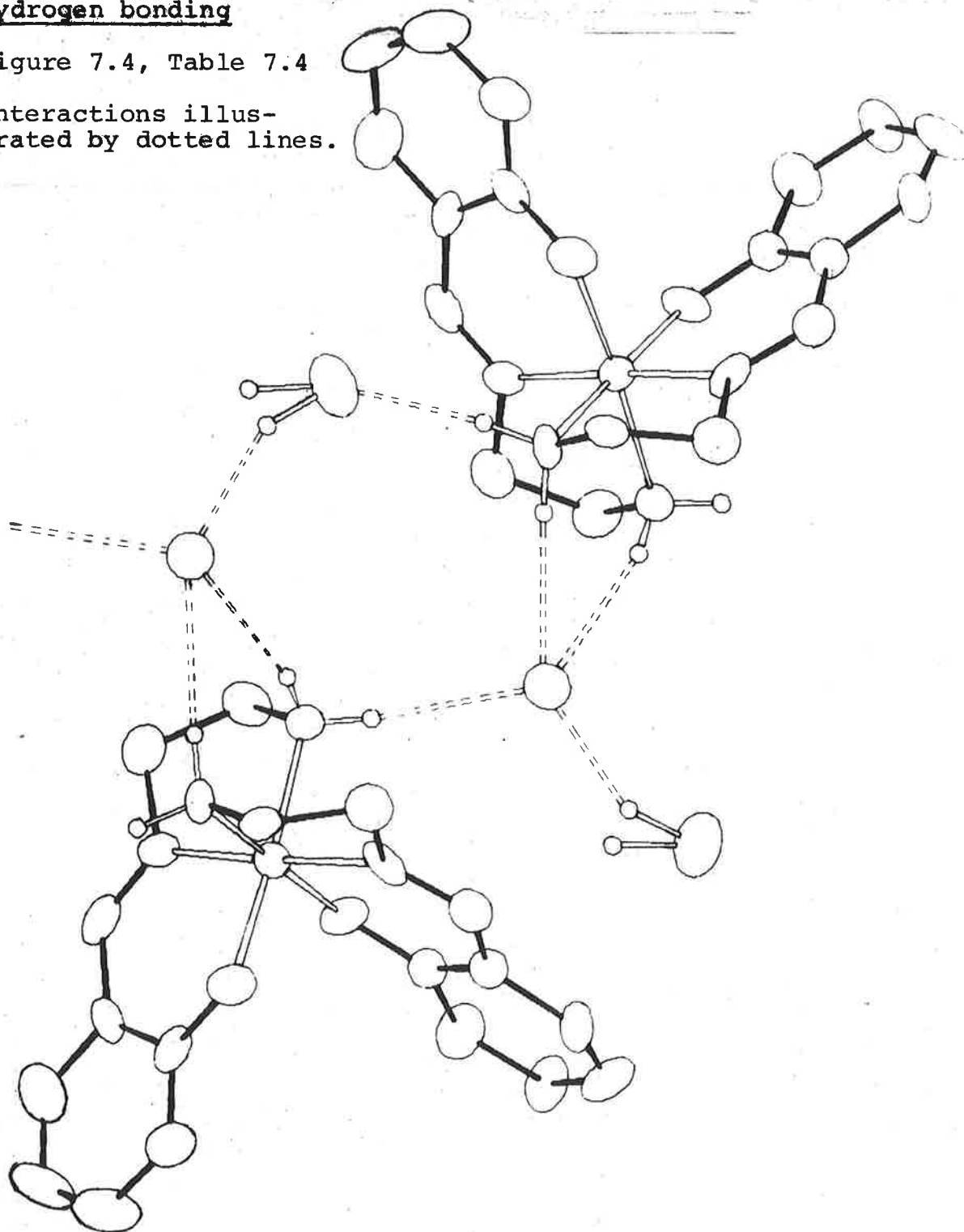
(iv) Role of the water molecule

The crystal structure does not immediately clarify the

## Hydrogen bonding

Figure 7.4, Table 7.4

Interactions illustrated by dotted lines.



A	H	B	A-B	A-H	H...B	Angle
O(3)	H(1)	C1	3.15 Å	1.19 Å	2.49 Å	113°
O(3)	H(2)	C1	3.15	1.12	2.10	153
N(3)	H(1)	C1	3.23	0.91	2.36	160
N(3)	H(2)	C1	3.28	0.91	2.39	166
N(4)	H(1)	C1	3.35	0.91	2.44	175
N(4)	H(2)	O(3)	2.97	0.91	2.07	167

role of the water molecule in the stabilization of the low spin state for Fe(III), however it is known that relative minor changes in the coordination sphere may result in spin crossover<sup>(168)</sup>. Consequently, it is proposed that variations in the environment of the ammine hydrogen atoms may be responsible for the necessary modification to the crystal field which leads to stabilization of the low spin state. The ammine protons are believed to be of significance because of the anion dependent hydrogen bonding effects evident from the proton n.m.r. spectra (Chapter 6).

The ideal situation for the following discussion would involve a comparison of the structural data for the hydrated and anhydrous chloride salts of the cation  $\text{Fe}(\text{saen})_2^+$ . As data for the anhydrous species have not been, and probably cannot be, obtained, it is necessary to consider the data available for complexes of Types A and B. Thus the iodide salts of the Cr(III) and Co(III) cations have been selected as a basis for comparison.

In both cases, the anion is involved in four close contact interactions which may be considered as hydrogen bonds<sup>†</sup>, thus for the Type B complex (Cr(III)) all four are N-H...I interactions, whereas for the Type A (Co(III)) complex only

---

†Footnote

In reference (20), the statement that the 'structure of the nonhydrated species  $\text{Cr}(\text{saen})_2\text{I}$  shows that only two of the ammine hydrogens on the cation are able to form hydrogen bonds' is incorrect. A cursory glance at the ORTEP diagrams for this structure<sup>(105)</sup> certainly suggested that this was the case. However, an atom search, based on the published atomic positions, revealed that symmetry transformed iodide ions have close contacts with the ammine nitrogen atoms indicative of all four ammine hydrogen atoms being involved in hydrogen bonds.

three are N-H....I, with the additional interactions O-H....I and N-H....O (water). The relevant interatomic distances have been tabulated below in Table 7.6. In addition, the corresponding interatomic distances for Fe(saen)<sub>2</sub>Cl.H<sub>2</sub>O and Fe(mben)<sub>2</sub>Cl (166) have been included, together with the Co(III) and Cr(III) ammine halides as listed below.

- (a) (±) Co(III)(en)<sub>3</sub>Cl<sub>3</sub>.2.8H<sub>2</sub>O and (±) Cr(III)(en)<sub>3</sub>Cl<sub>3</sub>.3H<sub>2</sub>O<sup>(170)</sup>  
- racemates with significant N-H....Cl interactions but no significant N-H....O or O-H....Cl interactions.
- (b) (+)<sub>D</sub> - Co(III)en<sub>3</sub>Cl<sub>3</sub>.H<sub>2</sub>O<sup>(171)</sup>  
- significant N-H....Cl, N-H....O, O-H....Cl interactions.
- (c) (±) Co(III)(en)<sub>2</sub>Ap.I.H<sub>2</sub>O<sup>(172)</sup> [Ap = acetylpyruvate]  
- significant N-H....I and N-H....O interactions.

TABLE 7.6  
Hydrogen bonding interactions for metal-ammine  
halide salts

	N-H....X N-X distances		O-H....X O-X distances		N-H....O N-O distances
	range Å	mean Å	range Å	mean Å	mean Å
Cr(saen) <sub>2</sub> I	3.68 - 3.89	3.74	-	-	-
Co(saen) <sub>2</sub> I.H <sub>2</sub> O	3.61 - 3.74	3.65		3.54	2.93
±Co(en) <sub>2</sub> Ap.I.H <sub>2</sub> O	3.62 - 3.66	3.64	>4		2.98
±Co(en) <sub>3</sub> Cl <sub>3</sub> .2.8H <sub>2</sub> O	3.26 - 3.46	3.35	>4		>4
±Co(en) <sub>3</sub> Cl <sub>3</sub> .H <sub>2</sub> O	3.12 - 3.43	3.31	3.21-3.30	3.25	2.98
±Cr(en) <sub>3</sub> Cl <sub>3</sub> .3H <sub>2</sub> O	3.27 - 3.43	3.35	>4		>4
Fe(saen) <sub>2</sub> Cl.H <sub>2</sub> O	3.23 - 3.35	3.27		3.15	2.97
Fe(mben) <sub>2</sub> Cl	3.29 - 3.62	3.38	-	-	-

From the data in Table 7.6:

- (1) For the hydrated ammine salts, the N-H....O (water) hydrogen bonds, as estimated from N-O interatomic

distances, appear to be of similar strength.

- (2) The O-H...Cl bond in  $\text{Fe}(\text{saen})_2\text{Cl}\cdot\text{H}_2\text{O}$  does not appear to be unusually strong.
- (3) For the Co(III) and Cr(III) tris-en salts, all N-H...Cl bonds are of similar strength to those in  $\text{Fe}(\text{saen})_2\text{Cl}\cdot\text{H}_2\text{O}$ .
- (4) The N-H...I interactions for the  $\text{Cr}(\text{saen})_2^+$  and  $\text{Co}(\text{saen})_2^+$  iodide salts do appear to be significantly different. This is also the case with the N-H...Cl interactions for the chloride salts of  $\text{Fe}(\text{saen})_2^+$  and  $\text{Fe}(\text{mben})_2^+$ .

In each case, the values for the N-X interatomic distances have been calculated from the published atomic positions to complete and to check the published data. The iodide salts are considered first. For  $\text{Cr}(\text{saen})_2\text{I}$ , the N-I distances are 3.68, 3.77, 3.80 and 3.91 Å whereas the three distances in  $\text{Co}(\text{saen})_2\text{I}\cdot\text{H}_2\text{O}$  are 3.61, 3.62 and 3.74 Å. According to the criteria relating to the 'strength' of hydrogen bonding, N-I distances between 3.6 and 3.8 Å may be considered as indicating a strong hydrogen bond<sup>(168)</sup>. Thus in  $\text{Cr}(\text{saen})_2\text{I}$  only three of the four N-H...I interactions are strong hydrogen bonds while one is substantially weaker. In  $\text{Co}(\text{saen})_2\text{I}\cdot\text{H}_2\text{O}$  all four of the ammine hydrogen atoms are involved in strong hydrogen bonds with three involved in N-H...I interactions and the other strongly bound to the water molecule via the N-H...O interaction.

In the case of  $\text{Fe}(\text{saen})_2\text{Cl}\cdot\text{H}_2\text{O}$ , applying the criterion for a strong bond that N-Cl distances be less than 3.4 Å<sup>(168)</sup>, it must be concluded that all four ammine hydrogens are involved in strong interactions, three N-H...Cl (3.23, 3.28 and



3.35 Å) and one N-H...O (2.97 Å). With the anhydrous complex Fe(mben)<sub>2</sub>Cl, three of the N-H...Cl interactions are strong (3.30, 3.30 and 3.29 Å), and one (3.62 Å) weak<sup>(166)</sup>. On dehydration of the Fe(saen)<sub>2</sub>Cl.H<sub>2</sub>O, a high spin species with a Type B i.r. spectrum was obtained. It would appear that the interactions for this species resemble those in Fe(mben)<sub>2</sub>Cl.

From the above discussion it is clear that the major differences between the Type B and Type A complexes may be related to the number of ammine protons involved in strong hydrogen bonds, viz. 4 in Type A, 3 in Type B. Clearly the water molecule in the Type A monohydrates plays an important role in that its incorporation into the molecular structure results in an additional strong hydrogen bonding interaction with an ammine proton when compared with the Type B case.

During recent years there has been much interest shown in spin-crossover systems as shown by the large number of publications and review articles in the literature for both Fe(II) and Fe(III) complexes. In both cases the data presented suggest that the spin state is extremely sensitive to apparently minor variations in the ligand<sup>(169)</sup>. The presence of an additional strong hydrogen bonding interaction would be expected to result in a slight increase in the electron density on the ammine nitrogen and thus enhance the crystal field experienced by the central metal ion to a slight extent.

That such a subtle interaction could 'tip the balance' in favour of the low spin state is somewhat surprising, but clearly this is the case.

Thus it is concluded that the water molecule must be considered responsible for the observation of the low spin state in  $\text{Fe(III)(saen)}_2\text{Cl}\cdot\text{H}_2\text{O}$  and in addition stabilizes that spin state. To the best of the author's knowledge, this represents the first case where not only spin-crossover but also spin state stabilization has been established as resulting from the incorporation of an apparently simple lattice water molecule into a molecular structure.

APPENDIX I

Computer programs utilized in the structural determination.

AUPTP - Program to read and process the paper tape output from a Stoe automatic diffractometer.

R.J. Hill, Adelaide University, 1973.

AULAC - Program for interlayer scaling, sorting and editing data.

M.R. Snow, Adelaide University, 1973.

ABSCOR - A crystallographic absorption correction program employing the Analytical method of H. Tompa, Acta Cryst. 19 (1965) 1014.

Modification by M.R. Taylor, Flinders University, 1971.

FUORFLS - Local modification of ORFLS.

W.R. Busing, K.O. Martin and H.A. Levy, Report ORNL-TM-35 Oak Ridge National Laboratory, (1962), Oak Ridge Tennessee.

FORDAPB - Local modification of FORDAP.

A. Zalkin, Lawrence Radiation Laboratory (1962), Livermore California.

ORTEPA - Local modification of ORTEP.

C.K. Johnson, Report ORNL-3794, Oak Ridge National Laboratory (1965).

PLANEH - Local modification of PLANET.

J.F. Blount, University of Sydney, (1966).

BLANDA - J. F. Blount, University of Sydney (1966).

APPENDIX II

Structure Factor Tables

	H	K	FOBS	FCAL		H	K	FOBS	FCAL		H	K	FOBS	FCAL
		**L =	0****			22	2	356	463		8	6	641	618
U	3	0	0	0		24	2	372	434		10	6	598	641
	4	0	3619	3538		26	2	639	685		12	6	264	251
U	5	0	0	0		28	2	171	109		14	6	151	84
	6	0	1753	1696		30	2	720	710		16	6	352	444
U	7	0	0	0		2	3	425	381		18	6	263	360
	8	0	761	738		4	3	755	817		20	6	543	621
U	9	0	100	0	E	6	3	2150	2160		22	6	174	269
	10	0	902	850		8	3	350	300		24	6	151	145
U	11	0	0	0		10	3	692	744		26	6	263	352
	12	0	290	272	E	12	3	2019	2071		28	6	199	307
	13	0	182	0		14	3	823	759	U	30	6	94	96
	14	0	2180	2217		16	3	645	674		2	7	1002	969
U	15	0	0	0		18	3	755	776	U	4	7	0	102
	16	0	2125	2095		20	3	898	923		6	7	667	712
U	17	0	0	0		22	3	181	80		8	7	1455	1528
	18	0	704	728		24	3	330	242		10	7	531	531
U	19	0	42	0		26	3	214	245		12	7	639	713
	20	0	777	819		28	3	756	767	U	14	7	64	214
U	21	0	0	0		30	3	345	346	U	16	7	132	171
	22	0	459	553		0	4	1483	1418	U	18	7	0	137
U	23	0	135	0		2	4	1239	1215	U	20	7	0	60
	24	0	425	459		4	4	439	442		22	7	381	351
U	25	0	0	0		6	4	357	293		24	7	619	579
	26	0	504	490		8	4	754	796	U	26	7	98	85
U	27	0	0	0		10	4	685	698		28	7	381	400
	28	0	0	132		12	4	222	183		30	7	205	199
U	29	0	150	0		14	4	347	327		0	8	211	280
	30	0	909	942	U	16	4	111	115	U	2	8	84	187
E	2	1	1132	1216		18	4	208	241		4	8	224	84
	4	1	964	993		20	4	1114	1113	U	6	8	0	53
	6	1	1078	1054		22	4	470	447	U	8	8	135	95
	8	1	1980	1937		24	4	837	904		10	8	157	108
	10	1	1176	1153	U	26	4	0	30	U	12	8	0	24
	12	1	915	943		28	4	200	232	U	14	8	112	32
	14	1	305	305		30	4	143	78		16	8	206	100
U	16	1	67	49		2	5	1161	1133		18	8	449	378
	18	1	571	553		4	5	493	453	U	20	8	116	186
	20	1	313	258	U	6	5	0	144	U	22	8	0	17
	22	1	350	284		8	5	772	829	U	24	8	0	120
U	24	1	0	9	U	10	5	123	163	U	26	8	0	32
	26	1	352	342	E	12	5	1291	1293	U	28	8	0	31
U	28	1	0	79		14	5	437	530		30	8	210	132
U	30	1	0	40		16	5	174	168		2	9	346	336
	0	2	2534	2481		18	5	741	756		4	9	270	236
	2	2	2341	2325		20	5	206	101		6	9	465	497
	4	2	601	553		22	5	252	258		8	9	1159	1205
	6	2	1089	1029	U	24	5	109	81		10	9	490	496
E	8	2	1832	1789		26	5	164	246		12	9	533	539
E	10	2	1527	1536		28	5	486	569		14	9	196	129
	12	2	676	677	U	30	5	0	206		16	9	220	195
	14	2	799	904		0	6	1143	1107		18	9	290	229
E	16	2	1712	1762		2	6	1054	996		20	9	248	114
	18	2	467	483		4	6	665	711		22	9	643	666
	20	2	1018	984	U	6	6	0	88		24	9	454	461

	H	K	FOBS	FCAL		H	K	FOBS	FCAL		H	K	FOBS	FCAL
U	26	9	0	79		27	1	363	392		12	3	338	349
	0	10	159	227		28	1	338	255		13	3	1186	1203
	2	10	164	64	U	29	1	0	95		14	3	490	519
	4	10	664	622		30	1	236	301		15	3	995	982
	6	10	441	398		31	1	285	243		16	3	199	145
	8	10	307	265	U	32	1	0	4		17	3	927	997
	10	10	456	464		33	1	598	601		18	3	507	495
	12	10	221	202	U	34	1	121	215		19	3	846	939
	14	10	260	102		35	1	425	422	U	20	3	128	28
	16	10	245	256		0	2	1093	1034		21	3	324	329
	18	10	143	237		1	2	605	642		22	3	241	234
	20	10	509	524		2	2	1035	1034		23	3	1060	1045
	22	10	212	176		3	2	976	997		24	3	512	423
U	2	11	0	85		4	2	458	500	U	25	3	117	56
	4	11	274	261		5	2	2895	2895		26	3	253	306
	6	11	285	181	U	6	2	0	11		27	3	661	739
	8	11	230	235		7	2	556	484		28	3	180	212
	10	11	254	142		8	2	290	225		29	3	307	269
	12	11	184	138		9	2	1729	1711	U	30	3	57	16
	14	11	245	339		10	2	440	364	U	31	3	0	105
U	16	11	0	116		11	2	811	742	U	32	3	0	32
	18	11	366	453		12	2	452	466	U	33	3	0	81
	0	12	202	261		13	2	785	781		0	4	506	460
U	2	12	127	77		14	2	254	232		1	4	286	335
	4	12	331	375		15	2	336	370		2	4	407	460
	6	12	403	376		16	2	202	140		3	4	139	120
U	8	12	0	63		17	2	263	169		4	4	324	360
	10	12	339	425		18	2	175	226		5	4	1125	1136
			**L = 1****			19	2	911	890		6	4	420	326
	1	1	1628	1642		20	2	232	183		7	4	432	445
	2	1	937	952		21	2	1172	1084	U	8	4	0	48
	3	1	2728	2748	U	22	2	0	16		9	4	689	709
U	4	1	0	80		23	2	340	401	U	10	4	119	68
	5	1	378	343		24	2	157	100		11	4	537	616
U	6	1	0	8		25	2	263	203		12	4	417	370
E	7	1	2681	2791		26	2	142	247		13	4	503	470
	8	1	1001	900		27	2	208	313		14	4	413	346
	9	1	1078	1117		28	2	363	246		15	4	526	633
	10	1	920	962		29	2	201	238		16	4	331	374
	11	1	594	620	U	30	2	0	89	U	17	4	133	80
	12	1	488	453		31	2	318	311		18	4	205	162
	13	1	489	559		32	2	170	49		19	4	692	671
	14	1	236	136		33	2	221	199	U	20	4	14	54
	15	1	388	413	U	34	2	0	48		21	4	1009	1061
	16	1	958	969	U	1	3	0	12		22	4	144	26
	17	1	1313	1301		2	3	250	265	U	23	4	0	139
	18	1	474	498		3	3	1798	1824	U	24	4	0	15
	19	1	600	651		4	3	819	795		25	4	533	543
U	20	1	58	127		5	3	765	729		26	4	186	173
	21	1	464	468	U	6	3	0	13		27	4	354	299
U	22	1	58	81		7	3	1000	1031		28	4	175	172
	23	1	1123	1093		8	3	332	343		29	4	195	242
	24	1	335	356		9	3	327	362	U	30	4	118	164
	25	1	722	709		10	3	673	637	U	31	4	0	56
	26	1	304	302	U	11	3	0	38	U	32	4	0	129

	H	K	FOBS	FCAL		H	K	FOBS	FCAL		H	K	FOBS	FCAL
U	1	5	0	51		24	6	138	136	U	23	8	0	64
	2	5	229	144		25	6	521	467		1	9	165	158
	3	5	353	363	U	26	6	0	154		2	9	226	59
U	4	5	83	90		27	6	392	396		3	9	357	399
	5	5	322	305	U	28	6	0	56		4	9	371	298
U	6	5	0	14		29	6	224	293		5	9	262	225
	7	5	720	640	U	1	7	0	85	U	6	9	0	172
	8	5	813	831	U	2	7	0	79		7	9	404	403
	9	5	476	456	U	3	7	0	28	U	8	9	43	81
	10	5	158	234		4	7	168	70	U	9	9	130	125
	11	5	750	796		5	7	154	61		10	9	228	33
U	12	5	31	145		6	7	144	256	U	11	9	80	109
	13	5	1075	1068		7	7	425	408	U	12	9	0	62
	14	5	250	64		8	7	159	55		13	9	309	315
	15	5	157	88		9	7	553	547		14	9	152	64
	16	5	253	406	U	10	7	0	78		15	9	180	234
	17	5	309	337		11	7	299	265		16	9	212	23
	18	5	291	256		12	7	245	290	U	17	9	0	142
	19	5	246	238		13	7	137	82		18	9	159	178
	20	5	188	124	U	14	7	94	126		19	9	374	277
U	21	5	0	9		15	7	216	229	U	0	10	132	166
	22	5	293	252		16	7	300	359		1	10	541	551
U	23	5	54	84	U	17	7	0	58	U	2	10	0	71
	24	5	151	204		18	7	292	265	U	3	10	0	128
U	25	5	0	40		19	7	232	120		4	10	162	100
U	26	5	0	41		20	7	292	174		5	10	485	466
	27	5	322	268	U	21	7	0	65	U	6	10	0	152
	28	5	143	25		22	7	200	270		7	10	285	231
	29	5	621	678		23	7	366	213		8	10	193	162
U	30	5	0	2		24	7	152	225		9	10	204	289
	31	5	230	194	U	25	7	101	97	U	10	10	0	86
	0	6	181	47		26	7	165	74		11	10	531	493
	1	6	329	397	U	0	8	70	22		12	10	160	103
U	2	6	126	61		1	8	1113	1107	U	13	10	114	158
U	3	6	47	112	U	2	8	0	131				**L =	2****
	4	6	659	596	U	3	8	0	67		3	0	1162	1121
	5	6	701	650	U	4	8	0	104		4	0	1343	1292
	6	6	191	108		5	8	795	777		5	0	969	923
	7	6	515	536		6	8	279	199	U	6	0	0	138
	8	6	409	415		7	8	239	207		7	0	176	80
	9	6	645	612		8	8	190	230		8	0	802	733
U	10	6	126	156		9	8	599	589		9	0	213	257
	11	6	859	861		10	8	397	238		10	0	1133	1042
U	12	6	102	136		11	8	607	574	U	11	0	39	240
U	13	6	0	147		12	8	185	91		12	0	289	260
U	14	6	0	121		13	8	195	127		13	0	864	852
	15	6	739	721	U	14	8	114	80		14	0	1017	1144
	16	6	214	283		15	8	861	868	E	15	0	1054	993
U	17	6	98	111	U	16	8	60	115		16	0	2449	2364
U	18	6	62	123		17	8	429	425	U	17	0	0	170
	19	6	287	327	U	18	8	0	77		18	0	917	883
U	20	6	125	123		19	8	193	82		19	0	187	227
	21	6	359	346	U	20	8	41	65		20	0	1143	1168
U	22	6	0	60	U	21	8	31	121		21	0	710	815
	23	6	243	206	U	22	8	0	49		22	0	290	404

	H	K	FOBS	FCAL		H	K	FOBS	FCAL		H	K	FOBS	FCAL
	23	0	402	434		8	2	283	130		29	3	175	191
	24	0	942	940		9	2	669	634		30	3	569	559
U	25	0	0	86		10	2	1632	1621		31	3	186	187
	26	0	897	909		11	2	635	647		32	3	256	210
	27	0	653	614	U	12	2	96	256	U	33	3	136	89
	28	0	482	555		13	2	852	855		0	4	163	88
U	29	0	93	20		14	2	1216	1207	U	1	4	123	87
	30	0	662	630		15	2	408	392	U	2	4	0	93
	31	0	294	277		16	2	1049	1108		3	4	323	324
	32	0	508	581		17	2	391	395		4	4	1450	1405
	33	0	237	164		18	2	196	235		5	4	459	495
U	34	0	51	111		19	2	532	576	U	6	4	42	205
U	35	0	84	192		20	2	624	718		7	4	752	741
	1	1	860	848		21	2	479	433		8	4	424	453
	2	1	1193	1228		22	2	246	339		9	4	393	333
	3	1	611	545	U	23	2	106	128		10	4	358	407
U	4	1	55	56		24	2	582	633		11	4	488	499
	5	1	269	72		25	2	337	324		12	4	446	395
U	6	1	0	77		26	2	409	393		13	4	572	571
	7	1	927	900	U	27	2	0	179	U	14	4	84	99
	8	1	868	839	U	28	2	0	125		15	4	158	112
U	9	1	42	46	U	29	2	0	28	U	16	4	0	32
	10	1	836	825		30	2	679	672		17	4	477	462
	11	1	177	103		31	2	267	256	U	18	4	0	37
	12	1	396	377		32	2	449	474	U	19	4	0	18
	13	1	789	787		33	2	180	61		20	4	833	814
U	14	1	85	73	U	34	2	0	149		21	4	427	386
	15	1	176	56	U	1	3	130	185		22	4	250	324
	16	1	224	39		2	3	493	579		23	4	441	363
	17	1	364	291	U	3	3	0	88		24	4	306	277
	18	1	327	246		4	3	1786	1799		25	4	435	451
U	19	1	59	26		5	3	970	954		26	4	182	137
	20	1	508	490	U	6	3	0	204	U	27	4	0	19
	21	1	189	241		7	3	284	294		28	4	187	179
	22	1	321	181	U	8	3	46	106		29	4	203	194
U	23	1	0	98	U	9	3	120	133	U	30	4	0	94
U	24	1	105	102		10	3	609	627		31	4	281	181
U	25	1	0	10		11	3	300	322	U	32	4	0	123
U	26	1	113	94		12	3	1757	1787		1	5	229	193
U	27	1	84	54		13	3	519	491		2	5	1269	1281
	28	1	297	132		14	3	384	426	U	3	5	110	91
	29	1	251	244		15	3	239	282		4	5	1002	967
	30	1	276	325		16	3	632	642		5	5	208	64
U	31	1	0	4		17	3	236	222		6	5	407	207
U	32	1	0	88		18	3	656	671	U	7	5	0	151
	33	1	278	94		19	3	204	205		8	5	1422	1462
U	34	1	0	78		20	3	275	317		9	5	286	285
	0	2	2356	2390		21	3	149	44		10	5	161	140
E	1	2	330	360	U	22	3	0	29	U	11	5	134	46
	2	2	378	335	U	23	3	114	67		12	5	1195	1244
	3	2	346	328	U	24	3	58	87		13	5	336	380
	4	2	487	449		25	3	251	322		14	5	769	743
	5	2	803	796		26	3	152	70		15	5	459	449
U	6	2	102	123		27	3	304	271		16	5	405	400
	7	2	229	290		28	3	686	681		17	5	161	250

	H	K	FORS	FCAL		H	K	FORS	FCAL		H	K	FORS	FCAL
	18	5	851	887		12	7	641	652		17	9	156	11
	19	5	685	680		13	7	447	459 U		18	9	129	181
	20	5	364	361		14	7	146	196 U		19	9	116	139
	21	5	191	320 U		15	7	0	169 U		0	10	0	38
	22	5	534	616		16	7	176	191		1	10	291	224
	23	5	261	297 U		17	7	0	147		2	10	276	141
	24	5	490	530		18	7	486	516		3	10	177	213
	25	5	249	135		19	7	206	238		4	10	436	373
	26	5	223	229 U		20	7	56	20		5	10	143	12
	27	5	262	230		21	7	180	104		6	10	378	324
	28	5	663	618		22	7	485	561 U		7	10	0	27
U	29	5	0	43 U		23	7	0	8 U		8	10	0	210
	30	5	304	275		24	7	644	595 U		9	10	0	160
	31	5	285	130		25	7	222	167		10	10	503	490
U	0	6	128	9 U		26	7	0	2 U		11	10	0	189
	1	6	262	301		0	8	175	49 U		12	10	0	99
	2	6	222	250		1	8	232	225 U		13	10	77	191
	3	6	273	309 U		2	8	0	88		**L = 3****			
	4	6	507	549 U		3	8	0	30 U		1	1	0	164
	5	6	182	247		4	8	238	148		2	1	577	581
	6	6	901	905		5	8	286	268		3	1	765	613
U	7	6	0	109		6	8	177	274		4	1	205	179
	8	6	221	120 U		7	8	125	256		5	1	1406	1440
U	9	6	0	22		8	8	396	500		6	1	356	316
	10	6	512	508		9	8	310	390		7	1	1257	1318
U	11	6	0	131		10	8	190	170		8	1	194	77
U	12	6	326	281		11	8	143	239		9	1	839	846
U	13	6	0	139 U		12	8	0	82 U		10	1	136	58
	14	6	259	202		13	8	344	343		11	1	439	360
U	15	6	0	123 U		14	8	0	140		12	1	619	634
	16	6	380	309 U		15	8	77	57		13	1	228	297
	17	6	465	419		16	8	145	113		14	1	819	820
	18	6	198	170 U		17	8	52	63		15	1	203	239
	19	6	289	259 U		18	8	0	21		16	1	437	465
	20	6	522	416 U		19	8	0	17		17	1	926	907
	21	6	594	637 U		20	8	0	21		18	1	293	307
	22	6	336	350 U		21	8	0	152		19	1	298	312
U	23	6	0	27		22	8	173	62 U		20	1	81	201
	24	6	179	103 U		23	8	0	97		21	1	684	702
	25	6	260	258 U		1	9	0	88 U		22	1	0	170
U	26	6	0	3		2	9	323	310		23	1	1086	1120
U	27	6	0	121		3	9	210	52		24	1	306	298
U	28	6	117	174		4	9	149	158		25	1	488	525
U	29	6	0	53		5	9	301	69 U		26	1	0	38
	1	7	493	467		6	9	386	415		27	1	464	453
	2	7	833	859 U		7	9	0	77		28	1	284	320
	3	7	288	268		8	9	716	692 U		29	1	0	20
	4	7	410	400 U		9	9	0	45 U		30	1	0	13
	5	7	544	507		10	9	334	385 U		31	1	100	164
	6	7	330	326		11	9	198	155		32	1	184	111
	7	7	341	330		12	9	267	244		33	1	183	250
	8	7	1310	1373 U		13	9	71	179 U		34	1	0	156
	9	7	267	232 U		14	9	56	151		0	2	1470	1453
	10	7	612	628		15	9	222	117		1	2	264	135
	11	7	401	463		16	9	211	287		2	2	1148	1145



	H	K	FORS	FCAL		H	K	FORS	FCAL		H	K	FORS	FCAL
	3	2	1103	1054	U	24	3	0	312		13	5	944	992
	4	2	776	774	U	25	3	68	49		14	5	164	104
	5	2	1578	1543		26	3	247	276		15	5	304	368
	6	2	378	347		27	3	339	298	U	16	5	26	109
	7	2	586	535		28	3	401	290		17	5	454	454
U	8	2	0	20		29	3	530	484	U	18	5	0	40
	9	2	366	437	U	30	3	0	142		19	5	375	450
	10	2	441	433	U	31	3	0	65	U	20	5	0	3
	11	2	1538	1549		32	3	278	318		21	5	194	191
	12	2	664	698		33	3	304	298		22	5	329	291
	13	2	349	380		0	4	742	695		23	5	172	69
U	14	2	114	204		1	4	258	303		24	5	197	25
	15	2	597	600		2	4	502	560	U	25	5	0	57
	16	2	152	140		3	4	500	443	U	26	5	0	21
	17	2	447	495	U	4	4	110	22		27	5	397	398
U	18	2	21	15		5	4	2005	2039		28	5	244	129
	19	2	701	722		6	4	736	723		29	5	386	403
	20	2	276	192	E	7	4	652	628		30	5	333	168
	21	2	691	749		8	4	145	73	U	31	5	0	67
U	22	2	0	41		9	4	1141	1154		0	6	411	399
	23	2	368	256		10	4	372	285		1	6	579	619
U	24	2	0	17		11	4	1106	1099	U	2	6	50	15
	25	2	217	150		12	4	634	642		3	6	209	225
	26	2	215	106	U	13	4	62	102		4	6	494	511
	27	2	617	643		14	4	320	332		5	6	598	692
	28	2	202	124		15	4	184	274	U	6	6	0	215
	29	2	147	164		16	4	503	502		7	6	1041	1013
	30	2	195	71	U	17	4	112	22		8	6	244	54
	31	2	229	187		18	4	337	262		9	6	859	855
	32	2	287	148		19	4	693	776		10	6	561	553
	33	2	355	294		20	4	354	338		11	6	867	826
U	34	2	88	105		21	4	844	856	U	12	6	64	305
	1	3	1022	1034		22	4	171	42	U	13	6	0	184
	2	3	482	500		23	4	299	302		14	6	194	239
	3	3	1681	1649		24	4	238	257		15	6	718	765
	4	3	416	423		25	4	553	564		16	6	452	442
	5	3	623	646		26	4	329	366		17	6	226	237
	6	3	258	254		27	4	561	510	U	18	6	0	135
	7	3	1447	1466		28	4	281	161		19	6	349	297
	8	3	1097	1082	U	29	4	134	108		20	6	498	446
U	9	3	22	113		30	4	310	169		21	6	470	510
	10	3	627	627		31	4	137	173		22	6	331	288
	11	3	456	387	U	32	4	0	58	U	23	6	98	103
	12	3	811	875		1	5	241	151		24	6	359	297
	13	3	827	873		2	5	238	246		25	6	611	592
	14	3	557	584		3	5	1415	1427		26	6	318	392
	15	3	474	405		4	5	506	559		27	6	323	410
U	16	3	0	93		5	5	661	654		28	6	204	43
	17	3	747	712		6	5	684	635		29	6	298	244
	18	3	416	451		7	5	207	224		1	7	192	103
	19	3	701	718		8	5	690	731		2	7	199	176
U	20	3	0	2		9	5	140	74		3	7	225	225
	21	3	352	392		10	5	220	246		4	7	168	220
	22	3	245	327		11	5	485	467		5	7	641	683
	23	3	638	637	U	12	5	89	115	U	6	7	134	290

	H	K	FOBS	FCAL		H	K	FOBS	FCAL		H	K	FOBS	FCAL
	7	7	260	287		11	9	194	143		33	0	160	67
	8	7	230	54		12	9	140	87	U	34	0	72	26
	9	7	214	231		13	9	218	277		1	1	514	569
	10	7	221	145		14	9	248	124		2	1	1211	1211
U	11	7	0	145	U	15	9	0	26		3	1	678	717
U	12	7	133	139		16	9	138	156		4	1	768	741
U	13	7	0	11		17	9	268	82	U	5	1	77	82
	14	7	382	421		18	9	154	78		6	1	720	655
	15	7	234	227		19	9	309	180		7	1	306	326
	16	7	288	147	U	0	10	115	95		8	1	585	583
	17	7	225	83		1	10	485	471		9	1	199	106
U	18	7	0	20	U	2	10	0	43	U	10	1	0	8
U	19	7	0	140	U	3	10	0	90	U	11	1	123	81
U	20	7	0	84	U	4	10	125	29	U	12	1	99	170
	21	7	251	327		5	10	344	305		13	1	530	587
U	22	7	100	187		6	10	227	215		14	1	879	844
	23	7	306	190	U	7	10	0	10	U	15	1	0	83
U	24	7	0	95	U	8	10	0	62		16	1	153	205
	25	7	248	216	U	9	10	0	184	U	17	1	0	64
	26	7	255	45		10	10	215	182		18	1	320	316
	0	8	205	39		11	10	170	117	U	19	1	0	41
	1	8	951	933	U	12	10	64	33		20	1	357	345
	2	8	157	24	U	13	10	0	154	U	21	1	0	75
	3	8	170	102				**L =	4****		22	1	361	200
	4	8	443	432		3	0	184	142	U	23	1	67	125
	5	8	429	418		4	0	242	265		24	1	289	219
	6	8	265	248		5	0	1335	1335		25	1	247	100
U	7	8	0	128		6	0	717	604		26	1	264	269
	8	8	367	369		7	0	581	629		27	1	357	312
	9	8	213	147		8	0	277	264		28	1	410	329
	10	8	304	268		9	0	746	793	U	29	1	0	141
	11	8	559	473		10	0	747	726	U	30	1	0	21
U	12	8	0	40		11	0	907	913	U	31	1	199	38
U	13	8	234	217		12	0	348	328	U	32	1	0	109
U	14	8	0	37		13	0	370	341		33	1	184	180
	15	8	881	863		14	0	205	259	U	34	1	105	7
	16	8	311	219		15	0	266	284		0	2	2214	2245
	17	8	424	417		16	0	1515	1583	E	1	2	264	204
U	18	8	47	19		17	0	147	140		2	2	763	745
	19	8	353	155		18	0	879	890		3	2	302	267
	20	8	253	293		19	0	305	319		4	2	1136	1076
	21	8	271	56		20	0	892	870		5	2	497	472
U	22	8	0	237		21	0	572	490		6	2	655	644
	23	8	184	43		22	0	296	322		7	2	787	773
	1	9	224	182		23	0	172	247		8	2	649	679
	2	9	237	244		24	0	977	902		9	2	503	501
U	3	9	109	93		25	0	153	95		10	2	483	449
U	4	9	27	242		26	0	421	402		11	2	921	892
U	5	9	0	170	U	27	0	108	129		12	2	170	54
	6	9	448	444		28	0	352	381		13	2	161	177
	7	9	162	151		29	0	196	226		14	2	755	811
	8	9	402	361		30	0	341	385		15	2	462	455
U	9	9	0	51	U	31	0	68	121		16	2	733	705
U	10	9	0	76		32	0	462	458	U	17	2	106	179

	H	K	FOBS	FCAL		H	K	FOBS	FCAL		H	K	FOBS	FCAL
U	18	2	138	26		4	4	866	875		26	5	246	170
	19	2	176	188		5	4	680	703		27	5	256	325
	20	2	392	417		6	4	177	173		28	5	696	694
	21	2	398	343		7	4	345	236		29	5	220	195
U	22	2	86	121		8	4	233	255	U	30	5	0	204
U	23	2	0	65		9	4	162	160		0	6	340	340
	24	2	373	312		10	4	382	370		1	6	218	180
	25	2	206	216		11	4	446	431		2	6	374	367
	26	2	370	309		12	4	815	769		3	6	315	347
U	27	2	112	184		13	4	193	112		4	6	422	427
	28	2	165	24		14	4	260	269		5	6	227	187
	29	2	230	185		15	4	323	274		6	6	399	375
	30	2	254	304		16	4	198	273		7	6	227	125
	31	2	316	281		17	4	270	265	U	8	6	56	65
	32	2	406	361		18	4	148	175		9	6	467	377
	33	2	200	261	U	19	4	0	208		10	6	485	504
U	34	2	0	68		20	4	735	766	U	11	6	141	59
	1	3	194	187	U	21	4	0	72		12	6	340	286
	2	3	484	474		22	4	499	433		13	6	261	184
	3	3	1012	1031	U	23	4	0	182	U	14	6	0	216
	4	3	1214	1191		24	4	305	276		15	6	385	392
	5	3	395	445		25	4	175	224	U	16	6	0	119
	6	3	267	160	U	26	4	61	334	U	17	6	136	76
	7	3	580	669	U	27	4	0	205		18	6	271	171
	8	3	308	209		28	4	188	156	U	19	6	0	17
	9	3	490	610	U	29	4	118	150		20	6	613	527
	10	3	494	509		30	4	409	345	U	21	6	106	17
	11	3	192	127		31	4	285	326		22	6	204	229
	12	3	1226	1254		32	4	250	40	U	23	6	0	47
	13	3	200	221		1	5	722	757		24	6	248	123
	14	3	593	487		2	5	1116	1133	U	25	6	0	114
U	15	3	130	74		3	5	550	559		26	6	170	56
U	16	3	188	122		4	5	991	1002	U	27	6	72	231
U	17	3	113	185	U	5	5	0	118	U	28	6	128	158
	18	3	285	298		6	5	357	359	U	29	6	0	29
	19	3	382	388		7	5	815	852		1	7	310	313
	20	3	277	301		8	5	1209	1243		2	7	556	619
	21	3	406	427		9	5	494	555		3	7	496	410
U	22	3	112	110	U	10	5	0	138		4	7	253	338
U	23	3	364	383	U	11	5	0	164	U	5	7	0	168
U	24	3	0	229		12	5	1231	1264		6	7	547	507
U	25	3	0	188		13	5	455	431		7	7	192	262
U	26	3	448	344		14	5	709	683		8	7	1104	1130
U	27	3	0	59		15	5	360	264		9	7	525	514
	28	3	378	417		16	5	298	383		10	7	283	248
	29	3	240	143		17	5	388	425		11	7	493	454
	30	3	203	371		18	5	591	683		12	7	536	537
	31	3	358	61		19	5	616	660		13	7	762	722
	32	3	321	239		20	5	380	359		14	7	384	404
	33	3	323	413		21	5	391	384	U	15	7	0	63
	0	4	573	558	U	22	5	99	133		16	7	428	324
	1	4	659	604		23	5	765	850		17	7	389	422
	2	4	267	312		24	5	443	551		18	7	579	565
	3	4	191	176	U	25	5	113	15		19	7	153	275

	H	K	FORB	FCAL		H	K	FORB	FCAL		H	K	FORB	FCAL
U	20	7	130	54	U	4	10	0	146		9	2	237	276
	21	7	177	70	U	5	10	0	175		10	2	171	152
	22	7	407	370		6	10	384	317		11	2	1038	1050
	23	7	357	324		7	10	272	100		12	2	451	491
	24	7	488	505	U	8	10	0	58		13	2	610	579
	25	7	367	288	U	9	10	0	190		14	2	352	417
	26	7	145	102		10	10	181	22	U	15	2	78	169
	0	8	272	204	U	11	10	0	176		16	2	903	918
U	1	8	81	40		12	10	152	171		17	2	268	310
	2	8	270	298		13	10	171	14	U	18	2	0	1
	3	8	175	103				##1 =	5****		19	2	328	298
U	4	8	0	95		1	1	1100	1127		20	2	398	409
	5	8	184	173		2	1	919	981		21	2	372	394
	6	8	156	36		3	1	824	833		22	2	274	171
	7	8	257	234		4	1	311	323	U	23	2	0	104
U	8	8	0	27		5	1	529	505	U	24	2	109	289
	9	8	307	178		6	1	252	213		25	2	337	217
U	10	8	119	233		7	1	633	645		26	2	235	234
	11	8	321	268		8	1	370	416	U	27	2	0	110
U	12	8	0	45		9	1	1003	1066	U	28	2	0	32
U	13	8	0	91	U	10	1	77	64		29	2	359	303
	14	8	191	104		11	1	477	428		30	2	339	351
U	15	8	0	95		12	1	1064	1096	U	31	2	93	19
U	16	8	0	240		13	1	197	246		32	2	220	134
U	17	8	93	211		14	1	310	273		33	2	249	285
U	18	8	120	39		15	1	439	407		34	2	238	152
U	19	8	0	136		16	1	558	597		1	3	741	749
U	20	8	70	135		17	1	591	548		2	3	438	393
	21	8	245	258		18	1	438	434		3	3	1627	1650
	22	8	172	42		19	1	396	348		4	3	637	695
U	23	8	134	77	U	20	1	0	257		5	3	272	170
	1	9	402	425		21	1	372	380		6	3	212	310
	2	9	248	104	U	22	1	0	235		7	3	1249	1252
	3	9	253	290		23	1	637	634		8	3	798	850
U	4	9	0	121		24	1	484	485	U	9	3	0	158
	5	9	275	247		25	1	314	328		10	3	315	280
	6	9	185	190		26	1	239	143		11	3	254	300
U	7	9	0	11		27	1	266	143		12	3	400	452
	8	9	411	454		28	1	451	422		13	3	749	709
	9	9	232	171	U	29	1	0	0		14	3	466	418
	10	9	416	463		30	1	149	67	U	15	3	0	40
U	11	9	0	33		31	1	196	162		16	3	222	223
U	12	9	0	160	U	32	1	0	153		17	3	525	475
	13	9	306	363	U	33	1	73	188	U	18	3	0	351
	14	9	219	79		34	1	189	162		19	3	570	574
	15	9	229	156		0	2	1002	1554	U	20	3	0	71
	16	9	250	121		1	2	600	588		21	3	299	239
	17	9	170	267		2	2	910	855		22	3	303	244
U	18	9	56	167	U	3	2	127	159		23	3	494	476
U	19	9	0	168		4	2	615	701		24	3	211	180
	0	10	320	120		5	2	198	256		25	3	276	110
U	1	10	122	230		6	2	394	386	U	26	3	136	10
U	2	10	0	52		7	2	506	518		27	3	271	297
	3	10	192	108		8	2	211	115		28	3	273	244

	H	K	FOBS	FCAL		H	K	FOBS	FCAL		H	K	FOBS	FCAL
U	29	3	36	296		17	5	316	370	U	12	7	121	20
	30	3	217	277		18	5	283	204	U	13	7	34	42
U	31	3	0	4		19	5	523	537	U	14	7	0	5
	32	3	269	294	U	20	5	0	82	U	15	7	0	7
	33	3	228	300		21	5	160	33	U	16	7	0	51
	0	4	926	867		22	5	495	400		17	7	178	66
	1	4	320	275		23	5	351	390	U	18	7	47	69
	2	4	414	416	U	24	5	135	109	U	19	7	0	185
	3	4	707	696		25	5	348	228		20	7	266	149
	4	4	368	354	U	26	5	0	88		21	7	260	166
	5	4	729	736		27	5	393	394	U	22	7	0	135
	6	4	739	781		28	5	229	113		23	7	331	243
	7	4	378	398		29	5	312	305	U	24	7	0	130
	8	4	218	237	U	30	5	0	93	U	25	7	0	20
	9	4	692	670		0	6	455	376		26	7	233	48
	10	4	768	693		1	6	492	464		0	8	504	537
	11	4	771	756	U	2	6	0	39		1	8	447	424
	12	4	276	191	U	3	6	0	75	U	2	8	0	153
	13	4	305	196		4	6	655	669		3	8	208	238
	14	4	332	410		5	6	480	492		4	8	654	645
U	15	4	128	104		6	6	440	490		5	8	165	218
	16	4	627	597		7	6	341	255		6	8	218	115
	17	4	298	246		8	6	445	467		7	8	229	284
	18	4	238	298		9	6	644	661	U	8	8	0	45
	19	4	259	327		10	6	643	637		9	8	413	443
	20	4	534	520		11	6	401	453		10	8	438	480
	21	4	181	192		12	6	294	185		11	8	324	375
	22	4	268	231		13	6	288	308		12	8	452	404
	23	4	263	127		14	6	268	246		13	8	378	313
	24	4	391	300		15	6	589	591		14	8	360	302
U	25	4	0	128		16	6	422	426		15	8	669	627
	26	4	263	271		17	6	363	327		16	8	369	386
	27	4	300	284	U	18	6	0	64		17	8	355	330
U	28	4	0	76		19	6	229	237	U	18	8	0	125
U	29	4	128	59		20	6	393	416	U	19	8	86	6
	30	4	386	266		21	6	311	285		20	8	362	423
	31	4	428	414		22	6	320	410		21	8	168	255
	32	4	293	378	U	23	6	136	131		22	8	252	275
	1	5	145	58		24	6	336	297	U	23	8	0	49
	2	5	334	361		25	6	355	328	U	1	9	70	149
	3	5	455	527		26	6	323	401	U	2	9	77	86
U	4	5	116	168		27	6	264	266		3	9	392	387
	5	5	404	440		28	6	150	24		4	9	165	204
	6	5	306	276		1	7	327	363		5	9	200	236
U	7	5	0	79		2	7	201	69	U	6	9	129	121
	8	5	609	717		3	7	217	288	U	7	9	0	113
U	9	5	0	69	U	4	7	0	33	U	8	9	130	193
	10	5	217	338	U	5	7	0	14		9	9	249	287
	11	5	274	307		6	7	191	66		10	9	180	156
	12	5	163	139	U	7	7	0	220		11	9	182	52
	13	5	578	599	U	8	7	0	275	U	12	9	0	125
U	14	5	0	117		9	7	547	506		13	9	173	229
	15	5	313	317		10	7	164	45		14	9	244	173
	16	5	291	137		11	7	152	189	U	15	9	70	109

	H	K	FORB	FCAL		H	K	FORB	FCAL		H	K	FORB	FCAL
U	16	9	95	3	U	5	1	106	183		24	2	342	356
U	17	9	0	91		6	1	576	547		25	2	514	452
U	18	9	59	42		7	1	430	396		26	2	348	254
	19	9	326	293	U	8	1	96	118		27	2	455	505
	0	10	208	246		9	1	238	253	U	28	2	0	151
	1	10	217	263	U	10	1	95	2		29	2	283	311
	2	10	210	95	U	11	1	0	66		30	2	201	221
	3	10	222	155		12	1	420	393		31	2	384	301
	4	10	235	162		13	1	168	243		32	2	382	346
	5	10	420	368	U	14	1	109	41		33	2	153	70
	6	10	297	287		15	1	228	203	U	34	2	0	32
U	7	10	140	7	U	16	1	0	3		1	3	252	277
U	8	10	0	8		17	1	436	440	U	2	3	0	18
	9	10	285	150		18	1	383	295		3	3	518	507
	10	10	179	210		19	1	378	382		4	3	715	768
	11	10	211	164	U	20	1	103	81		5	3	202	254
	12	10	244	175		21	1	195	250		6	3	225	232
	**L =		6****			22	1	213	57		7	3	719	714
	3	0	167	148	U	23	1	38	141	U	8	3	45	334
	4	0	372	397	U	24	1	0	279		9	3	472	452
	5	0	1177	1127	U	25	1	104	2		10	3	454	520
U	6	0	0	520	U	26	1	78	235	U	11	3	0	27
	7	0	632	656	U	27	1	130	30		12	3	161	246
	8	0	333	268		28	1	344	230		13	3	493	469
	9	0	1205	1155		29	1	169	69		14	3	309	237
	10	0	964	1000	U	30	1	0	32		15	3	342	365
	11	0	660	680	U	31	1	0	106	U	16	3	0	10
	12	0	349	350	U	32	1	138	12		17	3	586	616
	13	0	677	677		33	1	273	188		18	3	158	132
	14	0	642	641	U	34	1	0	43		19	3	669	715
	15	0	1318	1272		0	2	1588	1596		20	3	173	189
	16	0	1767	1778		1	2	478	490	U	21	3	134	91
U	17	0	147	79		2	2	432	442	U	22	3	0	83
	18	0	401	319	U	3	2	0	61		23	3	590	521
	19	0	1044	1028		4	2	771	723		24	3	340	239
	20	0	324	288		5	2	863	904	U	25	3	128	75
	21	0	960	947		6	2	454	463		26	3	360	512
U	22	0	0	85	U	7	2	0	172	U	27	3	71	100
	23	0	377	306		8	2	357	388		28	3	371	374
	24	0	414	429		9	2	339	372	U	29	3	0	124
	25	0	551	499		10	2	467	424	U	30	3	0	134
	26	0	257	304		11	2	588	588		31	3	297	293
	27	0	498	507	U	12	2	0	130		32	3	377	72
U	28	0	0	141		13	2	312	248		33	3	417	386
	29	0	280	232		14	2	333	315		0	4	323	379
	30	0	434	449		15	2	821	843		1	4	383	456
	31	0	478	443		16	2	723	762		2	4	261	100
	32	0	461	463		17	2	248	128	U	3	4	0	11
U	33	0	0	55		18	2	546	576		4	4	470	513
U	34	0	0	97		19	2	576	576		5	4	444	481
	1	1	339	385		20	2	614	555		6	4	517	614
	2	1	551	551		21	2	540	488	U	7	4	0	147
	3	1	597	591	U	22	2	142	207		8	4	234	22
	4	1	418	389		23	2	185	334		9	4	232	249

	H	K	FORS	FCAL		H	K	FORS	FCAL		H	K	FORS	FCAL
	10	4	314	270		1	6	264	27		0	8	180	111
	11	4	321	229		2	6	438	416		1	8	219	217
	12	4	357	210		3	6	359	471		2	8	316	474
	13	4	256	149		4	6	269	359		3	8	227	264
U	14	4	0	135	U	5	6	0	292	U	4	8	0	108
	15	4	309	280		6	6	170	159		5	8	215	225
	16	4	300	160		7	6	389	441		6	8	348	219
U	17	4	94	133		8	6	342	355		7	8	289	172
U	18	4	0	175	U	9	6	0	211	U	8	8	97	2
U	19	4	0	32	U	10	6	136	85		9	8	319	207
	20	4	256	317		11	6	198	390		10	8	279	62
	21	4	164	38		12	6	390	353	U	11	8	123	107
	22	4	220	299		13	6	266	231		12	8	229	106
	23	4	162	150		14	6	237	180	U	13	8	0	34
U	24	4	83	82	U	15	6	0	73	U	14	8	0	40
	25	4	153	146	U	16	6	128	132	U	15	8	0	132
	26	4	226	110		17	6	364	417		16	8	328	269
U	27	4	84	152		18	6	311	396	U	17	8	0	27
U	28	4	0	136	U	19	6	0	24		18	8	195	180
U	29	4	0	45		20	6	420	339		19	8	278	153
	30	4	192	164	U	21	6	0	31		20	8	198	33
	31	4	364	212	U	22	6	108	98	U	21	8	0	72
U	32	4	96	24		23	6	327	248	U	22	8	37	147
	1	5	716	727	U	24	6	0	13	U	23	8	0	21
	2	5	492	524	U	25	6	0	145		1	9	399	392
E	3	5	805	879		26	6	285	129	U	2	9	143	80
	4	5	515	582	U	27	6	0	75		3	9	535	481
	5	5	547	502	U	28	6	0	78	U	4	9	0	81
U	6	5	0	73	U	1	7	0	200		5	9	323	145
	7	5	764	811		2	7	233	231		6	9	215	353
	8	5	324	324		3	7	423	363		7	9	305	343
U	9	5	0	103	U	4	7	0	84		8	9	482	481
	10	5	247	219	U	5	7	0	88	U	9	9	0	140
	11	5	366	402	U	6	7	0	106		10	9	307	193
	12	5	568	702		7	7	447	490		11	9	281	199
	13	5	435	453		8	7	603	589	U	12	9	0	141
	14	5	199	198		9	7	354	344		13	9	373	385
	15	5	164	120		10	7	209	188	U	14	9	0	22
	16	5	393	418		11	7	233	308		15	9	240	167
	17	5	316	354		12	7	313	271		16	9	167	88
	18	5	425	397		13	7	708	684		17	9	192	245
	19	5	244	368	U	14	7	103	331	U	18	9	147	108
U	20	5	127	84		15	7	249	300		0	10	399	361
U	21	5	0	2		16	7	421	368		1	10	322	331
	22	5	153	105		17	7	526	447		2	10	160	16
	23	5	252	249		18	7	420	521	U	3	10	0	74
	24	5	264	193		19	7	279	291		4	10	401	362
U	25	5	111	216	U	20	7	0	75		5	10	409	423
U	26	5	0	51		21	7	166	109		6	10	256	147
	27	5	314	250		22	7	396	361	U	7	10	0	122
	28	5	374	332		23	7	369	371		8	10	244	21
	29	5	184	104		24	7	344	431	U	9	10	126	305
	30	5	215	211	U	25	7	140	103	U	10	10	148	26
	0	6	169	133	U	26	7	0	133		11	10	259	78

	H	K	F OBS	FCAL		H	K	F OBS	FCAL
	12	10	235	291	U	22	2	98	179
		**L =	7***		U	23	2	106	208
	1	1	181	138		24	2	516	497
	2	1	1065	1119		25	2	180	164
	3	1	242	139		26	2	222	139
	4	1	466	502		27	2	214	240
	5	1	1027	1021		28	2	257	154
	6	1	173	62	U	29	2	0	38
	7	1	1032	1059		30	2	319	247
	8	1	866	867		1	3	488	486
	9	1	493	573		2	3	605	631
U	10	1	0	32		3	3	474	478
U	11	1	0	45		4	3	470	511
	12	1	1549	1534		5	3	199	137
	13	1	451	350		6	3	343	360
	14	1	741	789		7	3	303	405
	15	1	566	528		8	3	878	931
	16	1	434	511	U	9	3	0	210
	17	1	499	512		10	3	185	71
	18	1	1048	958	U	11	3	0	124
	19	1	347	362		12	3	820	832
	20	1	423	396		13	3	466	504
	21	1	511	532	U	14	3	0	31
	22	1	549	553		15	3	352	124
	23	1	745	682		16	3	248	257
	24	1	510	540		17	3	250	86
	25	1	351	265		18	3	240	259
	26	1	292	292		19	3	281	255
U	27	1	0	174	U	20	3	106	240
	28	1	715	725	U	21	3	0	45
U	29	1	0	155		22	3	381	285
	30	1	485	375		23	3	270	225
	0	2	728	819	U	24	3	144	264
U	1	2	0	187		25	3	300	95
	2	2	559	547	U	26	3	0	119
	3	2	603	559		27	3	256	130
U	4	2	0	174		28	3	346	260
	5	2	749	772	U	29	3	47	176
	6	2	498	477		0	4	985	1047
	7	2	245	225		1	4	178	227
U	8	2	0	51		2	4	434	436
	9	2	487	420		3	4	297	270
	10	2	506	532		4	4	423	437
	11	2	494	484		5	4	241	297
U	12	2	121	174		6	4	424	435
	13	2	176	261		7	4	321	288
	14	2	407	387		8	4	204	294
	15	2	232	389	U	9	4	0	14
	16	2	689	715		10	4	378	466
	17	2	381	482		11	4	634	616
	18	2	529	515	U	12	4	0	145
	19	2	194	90	U	13	4	132	86
	20	2	488	528		14	4	345	372
	21	2	280	237	U	15	4	148	27



	H	K	FORS	FCAL		H	K	FORS	FCAL
	16	4	404	443		16	6	361	315
	17	4	459	503	U	17	6	0	151
	18	4	317	212	U	18	6	0	63
	19	4	351	362	U	19	6	0	298
	20	4	288	234		20	6	549	481
U	21	4	0	93		21	6	349	283
U	22	4	0	65	U	22	6	0	204
	23	4	254	208	U	23	6	0	7
	24	4	274	175	U	1	7	9	20
	25	4	264	192	U	2	7	0	106
U	26	4	151	56		3	7	227	73
	27	4	247	353	U	4	7	0	103
	1	5	166	209		5	7	490	466
U	2	5	0	154	U	6	7	109	62
	3	5	953	1017		7	7	234	295
U	4	5	126	135		8	7	309	118
	5	5	259	350		9	7	182	46
	6	5	186	284		10	7	435	368
	7	5	220	146	U	11	7	0	64
	8	5	521	451		12	7	227	97
	9	5	285	309		13	7	180	73
	10	5	311	391	U	14	7	60	50
	11	5	285	103	U	15	7	0	9
U	12	5	46	88	U	16	7	0	3
	13	5	241	136	U	17	7	111	90
U	14	5	0	180	U	18	7	117	66
U	15	5	0	103		19	7	221	76
U	16	5	0	19		20	7	194	164
	17	5	186	104		0	8	495	519
U	18	5	88	134		1	8	446	283
U	19	5	0	195	U	2	8	0	77
U	20	5	0	50		3	8	512	482
	21	5	292	232		4	8	460	514
	22	5	276	303		5	8	268	240
U	23	5	142	67		6	8	455	389
U	24	5	0	207		7	8	170	219
	25	5	332	240	U	8	8	70	21
U	26	5	124	38		9	8	292	354
	0	6	837	827		10	8	469	511
	1	6	271	266	U	11	8	0	33
	2	6	154	60		12	8	473	450
	3	6	179	102		13	8	373	414
	4	6	480	509		14	8	351	311
U	5	6	0	143		15	8	397	393
U	6	6	0	109		16	8	396	331
	7	6	192	176	U	1	9	62	151
U	8	6	120	87	U	2	9	0	117
U	9	6	146	82		3	9	352	240
	10	6	387	369	U	4	9	59	65
U	11	6	103	47	U	5	9	0	70
	12	6	336	207		6	9	273	73
	13	6	261	136		7	9	298	33
U	14	6	104	202	U	8	9	151	136
	15	6	299	335	U	9	9	0	147

## The Crystal Structure of Bis[N-(2-aminoethyl)salicylaldiminato] iron(III) Chloride Monohydrate, a Low Spin Iron(III) Complex Stabilized by Lattice Water [1]

A. P. SUMMERTON

*School of Chemical Technology, S. A. Institute of Technology, Levels Campus, Pooraka, South Australia, 5098*

A. A. DIAMANTIS and M. R. SNOW

*Department of Physical and Inorganic Chemistry, University of Adelaide, Adelaide, South Australia, 5001*

Received July 15, 1977

The crystal structure and molecular configuration of bis[N-(2-aminoethyl)salicylaldiminato] iron(III) chloride monohydrate,  $Fe(III)(Saen)_2Cl \cdot H_2O$ , has been determined by X-ray diffraction techniques. The crystals are orthorhombic with space group  $Pbca$  and cell dimensions  $a = 32.694(22)$ ,  $b = 10.083(7)$  and  $c = 12.274(8) \text{ \AA}$ . The structure was solved by the heavy atom technique and refined by the full-matrix least-squares method with 1587 reflections to an R factor of 0.114 (on F).

The iron atom is octahedrally coordinated by the two tridentate ligands in the meridional configuration. Strong hydrogen bonding occurs between the ammine hydrogens, water molecule and chloride ion, accounting for the stabilization of the low spin state in the hydrated solid over the high spin state found when dehydrated.

### Introduction

A series of compounds of general formula  $M(III)-(Saen)_2X \cdot nH_2O$  has been prepared for  $M = Cr, Fe$  and  $Co$ . The value of  $n$  can be 1 or 0 depending on the anion  $X$ . The chlorides of all three metals are monohydrates, and powder diffraction data indicated that all three compounds are isostructural. These complexes, as well as other hydrates in the series, show unusual features arising from the presence of the water molecule.

A brief summary follows:

(1) The water molecule gives rise to two intense bands in the O–H stretch region of the i.r. spectrum. The first band occurs at  $3620 \text{ cm}^{-1}$  and is extremely narrow with a peak width at half-height ( $\nu_{1/2}$ ) of  $20 \text{ cm}^{-1}$ . The second is slightly broader ( $\nu_{1/2} = 50 \text{ cm}^{-1}$ ) and occurs between  $3,350$  and  $3,450 \text{ cm}^{-1}$ . The position of this latter band is different for each metal and also varies with the nature of  $X$ .

(2) Experiments conducted on the isostructural chloride salts showed that the iron and chromium

compounds can be dehydrated by heating at  $100^\circ \text{C}$  in a vacuum for several hours. It is not possible to dehydrate the cobalt complex.

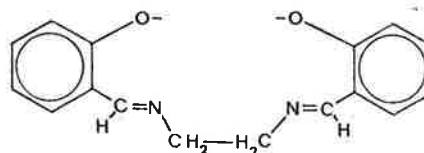
(3) Evidence from n.m.r. and conductance studies suggests the water remains bound in solution.

(4) The iron complex is low spin ( $\mu_{\text{eff.}} = 2.11 \text{ B.M.}$ ) but high spin when dehydrated and in solution ( $\mu_{\text{eff.}} = 5.96 \text{ B.M.}$ ). Iron complexes with  $n = 0$  are high spin (e.g.  $Fe(Saen)_2I$ ,  $\mu_{\text{eff.}} = 6.06 \text{ B.M.}$  [2]).

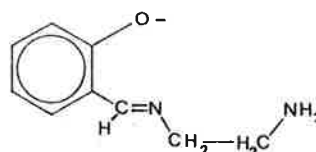
This structure determination was undertaken in order to ascertain the mode of bonding of the water molecule, which stabilizes the low spin state of iron(III).

Details of the preparation, spectra and chemical properties of the series of compounds will be the subject of a later publication.

Salen



Saen



### Experimental

Crystals suitable for structure determination were prepared by reaction of Iron(III)Salen Chloride and 1,2 diaminoethane in ethanol. Subsequent recrystallization from ethanol–diisopropyl ether gave deep blue plates.

TABLE I. Positional and Thermal Parameters ( $\times 10^4$ ). The form of the anisotropic thermal ellipsoid is  $\text{Exp} [-(\beta_{11}h^2 + \beta_{22}k^2 + \beta_{33}l^2 + 2\beta_{12}hk + 2\beta_{13}hl + 2\beta_{23}kl)]$ 

Atom	x/a	y/b	z/c	$\beta_{11}$	$\beta_{22}$	$\beta_{33}$	$\beta_{12}$	$\beta_{13}$	$\beta_{23}$
Fe	1522 (1)	357 (3)	251 (3)	4.6 (0.3)	55.9 (2.7)	27.9 (3.9)	-0.6 (0.8)	0.5 (0.8)	3.4 (2.6)
Cl	2204 (2)	871 (6)	4890 (7)	7.7 (0.6)	86.5 (6.1)	80.6 (9.8)	3.8 (1.5)	-6.2 (1.7)	-9.6 (6.1)
O(1)	1026 (4)	-428 (14)	-173 (13)	6 (1)	90 (16)	26 (19)	2 (4)	-2 (4)	-11 (14)
O(2)	1264 (4)	1721 (13)	1056 (14)	5 (1)	86 (17)	29 (19)	7 (4)	2 (3)	-11 (13)
O(3)	3473 (6)	1328 (16)	162 (19)	15 (2)	78 (18)	137 (28)	10 (6)	1 (7)	7 (18)
N(1)	1553 (5)	-636 (16)	1592 (16)	4 (2)	68 (19)	38 (24)	2 (5)	0 (5)	0 (15)
N(2)	1518 (5)	1347 (14)	-1119 (16)	7 (2)	45 (17)	29 (23)	-10 (5)	5 (5)	-30 (14)
N(3)	2072 (5)	1064 (18)	713 (20)	5 (2)	67 (19)	55 (26)	-1 (5)	-4 (5)	15 (16)
N(4)	1796(5)	-1058 (17)	-681 (20)	7 (2)	35 (16)	68 (27)	-1 (5)	-4 (5)	16 (16)
C(1)	757 (6)	-972 (20)	518 (22)	7 (3)	67 (24)	36 (35)	11 (6)	6 (6)	16 (21)
C(2)	367 (7)	-1223 (23)	100 (26)	7 (2)	98 (27)	57 (37)	7 (6)	4 (7)	-4 (24)
C(3)	87 (7)	-1852 (30)	822 (30)	7 (3)	167 (40)	51 (43)	-4 (8)	5 (8)	-21 (30)
C(4)	179 (8)	-2265 (28)	1872 (32)	7 (3)	142 (37)	80 (47)	-12 (8)	13 (8)	-12 (29)
C(5)	559 (9)	-2044 (26)	2266 (29)	13 (3)	80 (26)	92 (42)	-6 (7)	2 (9)	-1 (26)
C(6)	866 (6)	-1402 (17)	1582 (22)	8 (2)	29 (19)	43 (33)	-4 (5)	1 (6)	-7 (18)
C(7)	1265 (7)	-1220 (21)	2149 (25)	9 (2)	63 (21)	49 (35)	9 (6)	-3 (7)	13 (20)
C(8)	1959 (8)	-568 (23)	2163 (31)	9 (2)	67 (25)	77 (38)	4 (6)	-1 (7)	2 (23)
C(9)	2134 (7)	793 (25)	1923 (26)	-8 (2)	95 (26)	43 (35)	-8 (7)	-9 (7)	-2 (22)
C(10)	1044 (6)	2690 (19)	633 (23)	<sup>a</sup> 2.35 (0.43)					
C(11)	768 (8)	3435 (26)	1313 (24)	11 (3)	99 (26)	24 (33)	8 (7)	3 (7)	3 (23)
C(12)	548 (7)	4459 (21)	911 (26)	11 (3)	57 (23)	40 (34)	13 (7)	9 (7)	-20 (20)
C(13)	580 (7)	4827 (24)	-202 (29)	7 (2)	92 (28)	71 (37)	9 (7)	-13 (7)	-19 (25)
C(14)	816 (7)	4103 (21)	-888 (26)	9 (2)	37 (20)	88 (37)	2 (6)	1 (7)	9 (20)
C(15)	1060 (6)	3056 (20)	-484 (23)	<sup>a</sup> 2.40 (0.42)					
C(16)	1316 (6)	2446 (23)	-1332 (26)	7 (2)	72 (22)	55 (36)	-3 (6)	-2 (7)	5 (20)
C(17)	1768 (8)	757 (24)	-1988 (26)	<sup>a</sup> 3.52 (0.51)					
C(18)	1717 (6)	-734 (23)	-1882 (27)	4 (2)	88 (26)	101 (38)	4 (6)	2 (7)	28 (23)

<sup>a</sup>Isotropic thermal parameter refinement only for C(10), C(15), and C(17).

TABLE II. Hydrogen Atoms. Positional ( $\times 10^4$ ) and Isotropic Thermal Parameters.<sup>a</sup>

	x/a	y/b	z/c	B (Å <sup>2</sup> )
C(2) H	295	-994	-600	3.50
C(3) H	175	-1997	574	3.50
C(4) H	15	-2683	2293	3.50
C(5) H	624	-2297	2966	3.50
C(7) H	1306	-1504	2853	3.50
C(8) H(1)	2194	-1288	1876	4.50
C(8) H(2)	1920	-688	2982	4.50
C(9)H(1)	2438	810	2106	4.50
C(9) H(2)	1986	1493	2373	4.50
C(11) H	741	3208	2036	3.50
C(12) H	375	4923	1364	3.50
C(13) H	441	5556	-457	3.50
C(14) H	817	4295	-1621	3.50
C(16) H	1335	2832	-2009	3.50
C(17) H(1)	1669	1070	-2732	4.50
C(17) H(2)	2068	1013	-1891	4.50
C(18) H(1)	1922	-1215	-2366	4.50
C(18) H(2)	1427	-1006	-2095	4.50
N(3) H(1)	2273	654	324	3.50
N(3) H(2)	2083	1953	590	3.50
N(4) H(1)	2070	-1062	-550	3.50
N(4) H(2)	1690	-1868	-518	3.50
O(3) H(1)	3468	145	216	3.50
O(3) H(2)	3318	332	78	3.50

<sup>a</sup>All parameters calculated except the positional parameters for O(3) H(1) and O(3) H(2).

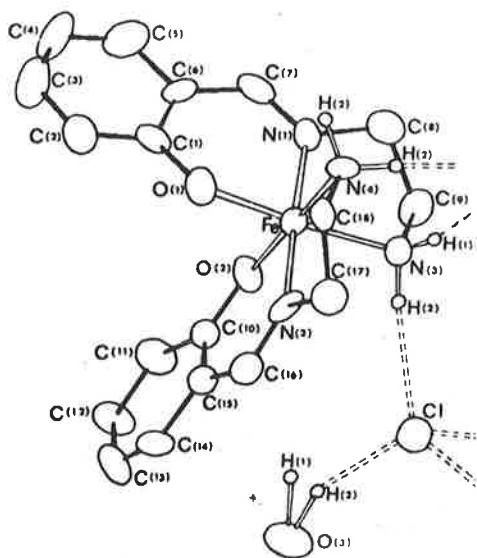


Figure 1. Perspective view showing the atom labelling scheme.

Preliminary Weissenberg photographs (CuK $\alpha$  radiation Ni filter) established the space group, and the cell parameters were estimated from the  $\omega$  scans of h00, 0k0 and 00l reflections on a Stoe Weissenberg automatic diffractometer.

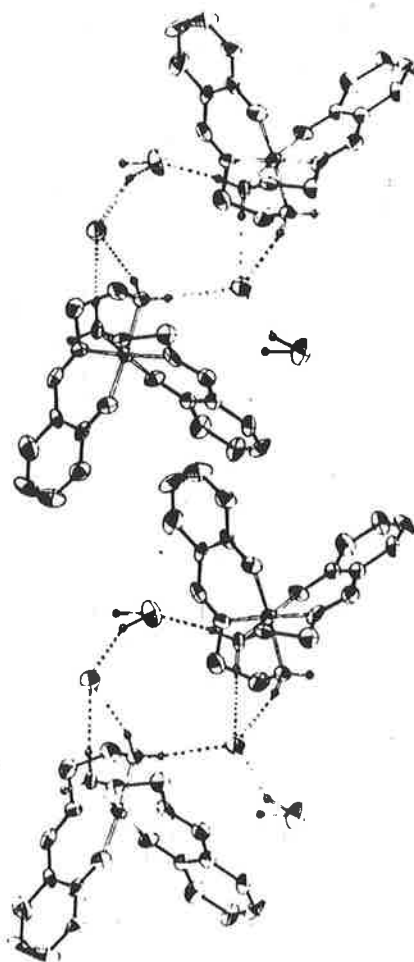


Figure 2. Stereoscopic view of the molecular structure with thermal ellipsoids drawn at 50% probability. (except for H atoms, where the scale is arbitrary).

The crystal data are:

Space Group, Pbc<sub>a</sub>;  $M = 435.7$ ;  $a = 32.694(22)$ ;  $b = 10.083(7)$ ;  $c = 12.274(8)$  Å;  $U = 4046.2$  Å<sup>3</sup>;  $D_c = 1.430$ ;  $D_m = 1.43(1)$  gcm<sup>-3</sup> (by flotation);  $Z = 8$ ;  $\mu(\text{MoK}\alpha) = 8.4$  cm<sup>-1</sup>;  $\lambda(\text{MoK}\alpha) = 0.7107$  Å.

Intensities were measured on the diffractometer with MoK $\alpha$  radiation, utilizing the  $\omega$  scan technique controlled by variable scan and scan time routines as previously described [3]. A single crystal, mounted along  $c$ , ( $0.15 \times 1.0 \times 1.5$  mm<sup>3</sup>) was used and data for hk0-7 collected, yielding a total of 2718 reflections, including 1587 non-zero reflections [ $I \geq 3\sigma(I)$ ] used to solve the structure. Absorption, Lorentz and polarization corrections were applied.

#### Structure Determination

The three dimensional Patterson function enabled location of the iron position. The chloride ion, carbon, nitrogen and oxygen atom positions were

TABLE III. Interatomic Distances and Angles with Their Standard Deviations.

Distances			
Fe-Cl	4.37 (.01) A	C(3)-C(4)	1.39 (0.4) A
Fe-O (3)	4.06 (.02)	C(4)-C(5)	1.35
Fe-O (1)	1.88	C(5)-C(6)	1.46
Fe-O (2)	1.89	C(6)-C(1)	1.42
Fe-N(1)	1.93	C(6)-C(7)	1.49
Fe-N(2)	1.96	C(7)-N(1)	1.31 (.03)
Fe-N(3)	2.02	N(1)-C(8)	1.50
Fe-N(4)	2.04	C(8)-C(9)	1.52 (.04)
O(1)-C(1)	1.34 (.03)	C(9)-N(3)	1.52 (.03)
C(1)-C(2)	1.40 (.04)	O(2)-C(10)	1.32
C(2)-C(3)	1.42	C(10)-C(11)	1.44 (.04)
		C(11)-C(12)	1.35 (.04) A
		C(12)-C(13)	1.42
		C(13)-C(14)	1.36
		C(14)-C(15)	1.41
		C(15)-C(10)	1.42
		C(15)-C(16)	1.47
		C(16)-N(2)	1.32 (.03)
		N(2)-C(17)	1.47
		C(17)-C(18)	1.52 (.04)
		C(18)-N(3)	1.53 (.03)
Angles			
O(1)-Fe-O(2)	93.7 (2.0)°	C(5)-C(6)-C(1)	119.5 (2.5)°
O(1)-Fe-N(1)	93.6	C(1)-C(6)-C(7)	127.6
O(1)-Fe-N(2)	88.3	C(6)-C(7)-N(1)	116.3 (2.0)
O(1)-Fe-N(3)	175.8	C(7)-N(1)-C(8)	114.5
O(1)-Fe-N(4)	86.0	N(1)-C(8)-C(9)	106.5
O(2)-Fe-N(1)	87.4	C(8)-C(9)-N(3)	107.6
O(2)-Fe-N(2)	94.3	C(9)-N(3)-Fe	109.2
O(2)-Fe-N(3)	89.7	Fe-O(2)-C(10)	125.2
O(2)-Fe-N(4)	177.2	O(2)-C(10)-C(15)	123.5
N(1)-Fe-N(2)	177.3	C(15)-C(10)-C(11)	116.5 (2.5)
N(1)-Fe-N(3)	84.1	C(10)-C(11)-C(12)	121.3
N(1)-Fe-N(4)	95.3	C(11)-C(12)-C(13)	120.7
N(2)-Fe-N(3)	93.9	C(12)-C(13)-C(14)	120.0
N(2)-Fe-N(4)	83.0	C(13)-C(14)-C(15)	120.3
N(3)-Fe-N(4)	90.8	C(14)-C(15)-C(10)	120.9
Fe-O(1)-C(1)	124.3	C(10)-C(15)-C(16)	126.5
O(1)-C(1)-C(2)	123.0	C(15)-C(16)-N(2)	119.8 (2.0)
C(6)-C(1)-C(2)	120.7 (2.5)	C(16)-N(2)-C(17)	118.2
C(1)-C(2)-C(3)	116.0	N(2)-C(17)-C(18)	106.0
C(2)-C(3)-C(4)	124.9	C(17)-C(18)-N(4)	106.0
C(3)-C(4)-C(5)	118.9	C(18)-N(4)-Fe	108.4
C(4)-C(5)-C(6)	119.9	N <sub>3</sub> -Cl-N <sub>4</sub>	52.0

TABLE IV. Interatomic Distances and Angles for Potential Hydrogen Bonds, A-H·····B.

A	H	B	A-B	A-H	H···B	Angles
O(3)	H(1)	Cl	3.15 A	1.19 A	2.49 A	113°
O(3)	H(2)	Cl	3.15	1.12	2.10	153
N(3)	H(1)	Cl	3.23	0.91	2.36	160
N(3)	H(2)	Cl	3.28	0.91	2.39	166
N(4)	H(1)	Cl	3.35	0.91	2.44	175
N(4)	H(2)	O(3)	2.97	0.91	2.07	167

obtained from three dimensional difference syntheses. Full-matrix least-squares refinement employing anisotropic temperature factors for all atoms (except C(10), C(15) and C(17)) converged to a conventional *R* value of 0.12. A difference Fourier Synthesis showed no peaks of height greater than  $1.03 \text{ e } \text{Å}^{-3}$ . Two of the more intense peaks were in the region of atom O(3). At this stage, the

positions of all ligand hydrogen atoms were calculated and included in further cycles of refinement. After convergence to a final *R* value of 0.114 [4], a further difference synthesis revealed the two peaks near atom O(3) were still present. These peaks were assigned to hydrogen atoms O(3) H(1) and O(3) H(2). Scattering factors were taken from ref. 5, those for iron and chlorine being corrected for the effects of anomalous scattering ( $\Delta f'$ ,  $\Delta f''$ ) [6]. All data processing was carried out on a CDC 6400 computer at Adelaide University with programs described previously [3].

Tables I to IV show the final parameters and molecular geometry, with estimated standard deviation in parentheses. The atom labelling scheme is shown in Figure 1. Final observed and calculated structure factor tables are available.\*

\*Copies are available on application to the Editor-in-Chief.

## Discussion

The cation clearly has a bis-tridentate ligand arrangement in common with the recently determined structures of Cr(III)(Saen)<sub>2</sub>I [7] and Co(III)(Saen)<sub>2</sub>I·H<sub>2</sub>O [8], in the meridional configuration.

The possible hydrogen bonding interactions between the complex cation, water molecule and chloride ion are listed in Table IV. According to accepted criteria, regarding interatomic distances and angles for such interactions [9], all may be considered as hydrogen bonds, with the exception of the O(3)—H(1)·····Cl interaction where the angle of 113° is far too low. Figure 2 shows the hydrogen bonding interactions as broken lines. The water molecule has specific interactions with both the complex and the anion and lies in a well defined position in the lattice. One hydrogen atom of the water molecule interacts with the anion whereas the other may be considered as effectively 'free' of significant interactions.

In hydrates where both hydrogen atoms are known to be involved in hydrogen bonds, the O—H stretching band is observed as a single broad envelope with a band width typically of the order of 200 cm<sup>-1</sup> [10].

However, it is well known that O—H stretching bands can be extremely sharp. In discussions of the O—H stretching region of the infra-red, many authors assign a very sharp band between 3650 and 3590 cm<sup>-1</sup> to 'free' O—H [10, 11]. Examination of published i.r. spectra of alcohols reveals the band width is often as low as  $\nu_{1/2} = 20$  cm<sup>-1</sup> [12]. The sharpness of the bands observed in this complex must be related to the mode of bonding of the water molecule, in particular the presence of only one hydrogen-bonded arm. A simple qualitative description of the observed spectrum is to assign the band at 3620 cm<sup>-1</sup> as a free O—H stretch and the other as a hydrogen bonded O—H stretch.

The low spin state of this iron(III) complex, which is further supported by the large quadrupole splitting of 2.75 mm sec<sup>-1</sup> obtained from the Mössbauer spectrum [13], is of interest because of its effect on the Fe to donor-atom distances. As recently discussed in a review article on the related Salen series, the metal to imine-nitrogen bond distance is sensitive to the nature of the metal [14]. It appears that such distances are dependent on the number of unpaired electrons on the metal. In the case of high-spin iron(III) Salen complexes, the metal to imine-nitrogen distances are in the range 2.06–2.10 Å, whereas in this study the range is 1.93–1.96 Å. This apparent contraction is not due to the difference in ligand as the corresponding distances for Co(III) and Cr(III) Saen complexes agree with those in the Salen series [7, 8]. It must then be considered as consistent with the presence of a low spin central metal ion.

Although the crystal structure does not clarify the role played by the water molecule in stabilization of the low spin state, it is known that small changes in the crystal field can bring about crossover [15]. As a possible explanation, it is suggested that the environment of the ammine hydrogens may be responsible for such a variation in crystal field.

The crystal structure of the non-hydrated species Cr(Saen)<sub>2</sub>I shows that only two of the ammine hydrogens on the cation are able to form hydrogen bonds [7]. The high spin complex Fe(Saen)<sub>2</sub>I has been assumed to have a similar molecular geometry on the basis of the similarity of the respective i.r. spectra [2]. Figure 2 clearly shows that in this study all four ammine hydrogens are involved in interactions, three with chloride ions, one with the water molecule. This would be expected to result in a slight increase in electron density on the ammine nitrogen, and enhance the crystal field experienced by the central metal ion.

Much interest has been shown of late in spin-cross-over systems and consequently a number of review articles have appeared in the literature for both iron(II) and (III) complexes. In both cases, the data presented suggest that the spin state is extremely sensitive to apparently minor variations in the ligand [15]. In the complex described above then, it is perhaps not surprising that such a subtle interaction as that between a ligand and a lattice water molecule may be sufficient to 'tip the balance' in favour of the stabilization of the low spin state.

## Acknowledgements

The authors are grateful to Mr. J. Westphalen, School of Applied Physics, S.A.I.T., for assistance in obtaining the initial Weissenberg photographs.

## References

- 1 Presented, in part, at the R.A.C.I. Division of Coordination and Metal-Organic Chemistry, *Seventh Conference (COMO 7)*, La Trobe University, Victoria, February (1977).
- 2 A. Van den Bergen, K. S. Murray, B. O. West and A. N. Buckley, *J. Chem. Soc. A*, 2051 (1969).
- 3 M. R. Snow, *Acta Crystallogr.*, **30**, 1850 (1974).
- 4 The unusually high *R* value is in part due to the unfavourably thin crystal plate chosen and high background scatter from the thick glass fibre to which it was attached. However the value compares favourably with those for similar structures, e.g. *R* = 0.114 [ref. (7)] and *R* = 0.098 [ref. (8)].
- 5 D. T. Cromer and J. B. Mann, *Acta Crystallogr., Sect. A*, **24**, 321 (1968).
- 6 D. T. Cromer, *Acta Crystallogr.*, **18**, 17 (1965).
- 7 A. P. Gardner, B. M. Gatehouse and J. C. B. White, *Acta Crystallogr., Sect. B*, **27**, 1505 (1971).
- 8 T. H. Benson, M. S. Bilton and N. S. Gill, *Aust. J. Chem.*, **30**, 261 (1977).
- 9 G. H. Stout and L. H. Jensen, "X-ray Structure Determination", Mc Millan, London (1968), p. 303 and references cited therein.

- 10 G. C. Pimentel and A. L. Mc Clellan, "The Hydrogen Bond", Freeman, San Francisco (1960), chapter 3, pp. 67-141.  
W. C. Hamilton and J. A. Ibers, "Hydrogen Bonding in Solids", Benjamin, New York (1968), p. 86.
- 11 L. J. Bellamy, "The Infra-Red Spectra of Molecules", Methuen, London (1964), chapter 6.  
C. N. R. Rao, "Chemical Applications of Infra-Red Spectroscopy", Academic Press, London (1963), pp. 175-188.  
H. A. Szymanski, "Interpreted Infra-Red Spectra", Plenum Press Data Division, New York (1966), Vol. 2, pp. 25-29.
- 12 "Documentation of Molecular Spectroscopy", Butterworths Scientific Publications, London (1967), Spectral cards 1966 to 1972.
- 13 A. P. Summerton, *paper presented at COMO 6*, Adelaide (1975).
- 14 M. Calligaris, G. Nardin and L. Randaccio, *Coord. Chem. Rev.*, **7**, 385-403 (1972).  
N. J. Hair and J. K. Beattie, *Inorg. Chem.*, **16**, 2, 245-250 (1977).
- 15 S. A. Cotton, *Coord. Chem. Rev.*, **8**, 185-223 (1972).  
H. A. Goodwin, *Coord. Chem. Rev.*, **18**, 293-325 (1976).

## REFERENCES

- (1) R.J. Forbes and E.J. Dijksterhus, "A History of Science and Technology", Vol. 2, Pelican Paperback, London (1963) p.489.
- (2) J.H. Richards, D.J. Cram, G.S. Hammond, "Elements of Organic Chemistry", McGraw-Hill, Tokyo (1967) p.1-4.
- (3) Ref. (1), p.473.
- (4) S.J. Lippard, "Progr. Inorg. Chem.", 18 (1973) p.(vi) to (viii) - introduction.
- (5) R.H. Bailes and M. Calvin, "J.Amer.Chem.Soc.", 69 (1947) p.1886.
- (6) F. Calderazzo and C. Floriani, "J.Chem.Soc.D.", (1967) p.139.
- (7) G. Costa, G. Mestroni and E. de Savorgnan, "Inorg.Chim. Acta", 3 (1969) p.323.
- (8) D. Crowfoot-Hodgkin, "Proc.Roy.Soc., Ser.A", 288 (1965) 294.
- (9) R.H. Holm, G.W. Everett, Jr. and A. Chakravorty, "Progr. Inorg.Chem.", 7 (1966) p.83.
- (10) M.D. Hobday and T.D. Smith, "Coord.Chem.Rev.", 9 (1972-73) 311.
- (11) M. Gerloch and F.E. Mabbs, "J.Chem.Soc.A", (1967) 1900.
- (12) P. Pfeiffer and T. Tsumaki, "Annalen", 503 (1933) 84.
- (13) M. Gerloch, J. Lewis, F.E. Mabbs and A. Richards, "J. Chem.Soc.A.", (1968) p.112.
- (14) J. Lewis, F.E. Mabbs, A. Richards and A.S. Thornley, "J.Chem.Soc.A" (1969) p.1993.
- (15) E. Fluck, "Chemical Applications of Moessbauer Spectroscopy", Academic Press, New York, (1968) p.284 (editors V.I. Goldenskii and R.H. Herber).
- (16) G.M. Bancroft, A.G. Maddock and R.P. Randl, "J.Chem. Soc.A" (1968) p.2939.
- (17) A. van den Bergen, K.S. Murray, B.O. West and A.N. Buckley "J.Chem.Soc.A" (1969) p.2051.
- (18) S.A. Cotton, "Coord.Chem.Rev.", 8 (1972) p.187.
- (19) M. Gerloch and F.E. Mabbs, "J.Chem.Soc.A" (1971) p.2041. M. Gerloch, J. Lewis, F.E. Mabbs and A. Richards, "Nature", 212 (1966) p.809.
- (20) A.P. Summerton, A.A. Diamantis and M.R. Snow, "Inorg. Chim.Acta", 21 (1978) p.121.



- (21) F. Basolo and R.G. Pearson, "Mechanisms of inorganic reactions", Wiley and Sons, New York (1963) p.368-375.
- (22) K. Nakamoto, "Infrared spectra of Inorganic and Coordination Compounds", Wiley and Sons, New York, p.161-176.
- (23) A.H. Norbury, "Advances in Inorganic and Radiochemistry", Vol. 17 (1975) p.254.
- (24) P. Rigo and M. Bressnan, "J.Inorg.Nucl.Chem.", 37 (1975) p.1813.
- (25) P.G. David, "J.Inorg.Nucl.Chem.", 35 (1973), p.1463.
- (26) S. Yamada and K. Iwasaki, "Bull.Chem.Soc.Jap.", 42 (1969) 1463; "Inorg.Chim.Acta" 5 (1971) p.3.
- (27) S. Yamada, H. Nishiwaka and E. Yoshida, "Proc.Japan.Acad." 40 (1964) p.211.
- (28) G. Costa, G. Mestroni and L. Stefani, "J.Organometal.Chem." 7 (1967) p.493.
- (29) M. Calligaris, G. Nardin and L. Randaccio, "J.Chem.Soc.D" (1969) 1248.
- (30) K. Yamanouchi and S. Nawoda, "Inorg.Chim.Acta", 9 (1974) p.161.
- (31) R.J. Cozens and K.S. Murray, "Aust.J.Chem.", 25 (1972) p.911.
- (32) Ref. (16), p.2939; Ref. (13) p.112-113.
- (33) K.S. Murray, "Coord.Chem.Rev.", 12 (1974) p.1-35.
- (34) W.M. Reiff, G.J. Long and W.A. Baker, Jr. "J.Amer.Chem.Soc." 90 (1968) 6347.
- (35) E.J. Olszewski and D.F. Martin, "J.Inorg.Nucl.Chem." 26 (1964) p.1577.
- (36) R.C. Weast, Editor, CRC "Handbook of Chemistry and Physics" 56 (1975-76) p.B 66-160.
- (37) G. Marr and B.W. Rockett, "Practical Inorganic Chemistry" van Nostrand-Reinhold, London (1972) p.365-370.
- (38) W.J. Geary, "Coord.Chem.Rev.", 7 (1971) p.81-122.
- (39) Ref. (36), p.D 153.
- (40) G.J. Janz and R.P.T. Tomkins, "Non-aqueous Electrolyte Handbook", Academic Press, London (1972) Vol. I, Chapter 3.
- (41) D.J. Pietrzyk and C.W. Frank, "Analytical Chemistry", Academic Press, New York (1974) p.130.
- (42) H.C. Clark and A.L. Odell, "J.Chem.Soc., London" (1956) p.520.

- (43) J. Hires, "Acta Physica et Chemica", 4 (1958) p.120.
- (44) J. Hires and L. Hackl, "Acta Physica et Chemica", 5 (1959) p.19.
- (45) S.M. Crawford, "Spectrochim.Acta", 19 (1963) p.255.
- (46) H.H. Jaffe and M. Orchin, "Theory and Applications of Ultraviolet spectroscopy", Wiley, New York (1962) p.257.
- (47) E.D. Olsen, "Modern Optical Methods of Analysis", McGraw-Hill, New York (1975) p.83-108.
- (48) B. Bosnich, "J.Amer.Chem.Soc.", 90 (1968) p.627.
- (49) R.S. Downing and F.L. Urbach, "J.Amer.Chem.Soc." 92 (1970) p.5861.
- (50) C.K. Jorgensen, "Progr.Inorg.Chem.", 12 (1970) p.101.
- (51) J.A. Bertrand and P.G. Eller, "Inorg.Chem.", 13 (1974) p.927.
- (52) Ref. (47), p.68.
- (53) A.I. Vogel, "Practical Organic Chemistry", 3rd Edition, Longmans, London, (1966) p.169-170.
- (54) Analytical data provided by suppliers of spectral grade methanol, viz. Merck  $\leq$  0.03%, Fluka  $\leq$  0.05%.
- (55) T.M. Dunn "Modern Coordination Chemistry", Interscience, New York, (1960) Chapter 4, p.230-295.
- (56) R.J. Philips and J.P. Williams, "Inorganic Chemistry", Clarendon Press, Oxford, (1966) Vol. II, p.395-406.
- (57) F. Basolo and R.G. Pearson, "Mechanism of Inorganic Reactions", John Wiley and Sons, London, (1963) p.371.
- (58) C.K. Jorgensen  
(a) "Progr.Inorg.Chem.", 4 (1962) p.111-119.  
(b) "Absorption Spectra and Chemical Bonding in Complexes" Pergamon (1962) p.107-134.  
(c) "Adv.Chem.Phys.", 5 (1963) p.61-69.  
(d) "Oxidation Numbers and Oxidation States", Springer-Verlag, New York (1969) p.84-106.
- (59) D. Sutton, "Electronic Spectra of Transition Metal Complexes", McGraw-Hill, London (1968).
- (60) J.A. Huheey, "Inorganic Chemistry", Harper and Row (1972) Chapter 8, p.294-365.
- (61) Ref. (60), Chapter 6, p.225-235.
- (62) R.G. Pearson, "J.Chem.Educ.", 45 (1968) p.581, 643.
- (63) G.H. Aylward and T.J.V. Findlay, "S.I. Chemical Data", Wiley and Sons, Sydney (1971) p.70-71.
- (64) C.C. Addison and D. Sutton, "Progr.Inorg.Chem.", 8 (1967) p.195-286.

- (65) H.H. Schmidtke, "Physical Methods in Advanced Inorganic Chemistry", Interscience, London (1968) p.116.
- (66) G.K. Wertheim, "Mössbauer Effect; Principles and Applications", Academic Press, New York (1964), p.1-19.
- (67) R.H. Herber, "Progr.Inorg.Chem.", 8 (1967) p.1-41.
- (68) E. Fluck, "Advances in Inorganic and Radiochemistry", 6 (1964) p.433-489.
- (69) G.M. Bancroft and R.H. Platt, "Advances in Inorganic and Radiochemistry", 15 (1972) p.59-241.
- (70) Ref. (66) p.20; Ref. (67) p.3; Ref. (68) p.442-443; Ref. (15) p.127.
- (71) C.R.C. Handbook, Ref. (36) p.B 261.
- (72) Ref. (66) p.14; Ref. (67) p.23; Ref. (68) p.445.
- (73)  $\gamma_M = 14.36$  keV ((66) p.52); 14.41 keV ((36)p.B 341); 14.38 ((15) p.121).
- (74) Ref. (15) p.444.
- (75) Ref. (66) p.15; Ref. (67) p.16.
- (76) Calculated according to Ref. (66) p.5-6.
- (77) Ref. (66) p.8-17.
- (78) Ref. (15) p.235.
- (79) Ref. (67) p.17.
- (80) Ref. (69) p.61.
- (81) Ref. (66) p.62; Ref. (69) p.64.
- (82) R.H. Herber, "Mössbauer Effect Methodology", 1, Plenum Press, New York (1965) p.3.
- (83) Ref. (69) p.63.
- (84) Ref. (69) p.62; R.E. Watson and A.J. Freeman, "Phys.Rev." 120 (1960) p.1125.
- (85) Ref. (15) p.269; Ref. (67) p.18; Ref. (68) p.454, 483.
- (86) Ref. (68) p.487.
- (87) Ref. (69) p.63.
- (88) Ref. (15) p.60-65; Ref. (66) Chapter 6; Ref. (67) p.10; Ref. (69) p.64-66.
- (89) Ref. (69) p.67-71.
- (90) Ref. (69) p.210-214.

- (91) Ref. (69) p.128, 173, 182.
- (92) Ref. (69) p.175-179.
- (93) D.A. Skoog and D.M. West, "Fundamentals of Analytical Chemistry", Holt, Rinehart and Winston, London (1973) p.41-58.
- (94) M. Gerloch and F.E. Mabbs, "J.Chem.Soc.A" (1967) 1598.
- (95) M. Calligaris, G. Nardin and L. Randaccio, "Coord.Chem. Rev.", 7 (1973) p.385.
- (96) Ref. (60), Chapter 3.
- (97) Ref. (15), Chapter 2.
- (98) J.L. Culhane, J. Herring, P.W. Sanford, G. O'Shea and R.D. Phillips, "J.Sci.Instrum.", 43 (1966) p.908.
- (99) R.L. Cohen, "Rev.Sci.Inst." 37 (1966) p.260-261, 977.  
R.L. Cohen, P.G. McMullin and G.K. Wertheim, "Rev.Sci. Inst." 34 (1963) p.671.
- (100) R. Zane, "Nucl.Inst. and Methods", 43 (1966) p.333.
- (101) R.L. Cohen, "Rev.Sci.Inst.", 37 (1966) p.957.
- (102) Y. Hazoni, "Rev.Sci.Inst.", 38 (1967) p.1760.
- (103) Ref. (21) p.105.
- (104) M.J. O'Connor and B.O. West, "Aust.J.Chem.", 21 (1968) p.369.
- (105) A.P. Gardner, B.M. Gatehouse and J.C.B. White, "Acta Cryst.", B27 (1971) p.1505.
- (106) K. Dey and R.L. De, "Z.Anorg.Allg.Chem.", 402 (1973) p.120.
- (107) T.H. Benson, M.S. Bilton, N.S. Gill and M. Sterns, "J.C.S.Chem.Comm.", (1976) p.936.
- (108) T.H. Benson, M.S. Bilton and N.S. Gill, "Aust.J.Chem.", 30 (1977) p.261.
- (109) K. Dey and K.C. Ray, "J.Inorg.Nucl.Chem.", 37 (1975) p.695.
- (110) L.J. Boucher, "J.Inorg.Nucl.Chem.", 36 (1974) p.531-536.
- (111) F.A. Cotton, "Modern Coordination Chemistry", Interscience, New York, (1960), Chapter 5, p.363.
- (112) Ref. (22) p.143.
- (113) Ref. (22) p.155-156.
- (114) C.M. Harris and E.D. McKenzie, "J.Chem.Soc.A." (1969) p.746.
- (115) Ref. (22) p.73, 84.

- (116) Ref. (20) p.126 and references cited therein.
- (117) B.N. Figgis and J. Lewis, "Modern Coordination Chemistry" Interscience, New York (1960), Chapter 6, p.406.
- (118) Ref. (22) p.83, 84.
- (119) D.F. Evans, "J.Chem.Soc." (1959) p.2003.
- (120) P. Coggin, A.T. McPhail, F.E. Mabbs, A. Richards and A.S. Thornley, "J.Chem.Soc.A.", (1970) 3296.
- (121) Inorganic Syntheses, Vol. II (1946) p.217-220.
- (122) A. van den Bergen, K.S. Murray, M.J. O'Connor, Nadja Rehak and B.O. West, "Aust.J.Chem.", 21 (1968) p.1505-15.
- (123) E.D. Becker, "High resolution N.M.R.", Academic Press, New York (1970), Chapter 4, p.59-84.
- (124) Ref. (123) p.233-234.
- (125) N.S. Baccha, D.P. Hollis, L.F. Johnson and E.A. Pier, "High resolution N.M.R. spectra catalog", Varian Associates (1963), Vols. I and II.
- (126) Ref. (123) p.53-54, 113-115.
- (127) C.H. De Puy and K.L. Rinehart, Jr., "Introduction to Organic Chemistry", Wiley International, New York (1975) p.110.
- (128) Ref. (123) p.215-220.
- (129) G.H. Searle, S.F. Lincoln, F.R. Keene, S.G. Teague and D.G. Rowe, "Aust.J.Chem.", 30 (1977) p.1221-28.
- (130) Ref. (123) p.189.
- (131) M.H. Chisolm and S. Godleski, "Progr.Inorg.Chem.", 20 (1976) p.299.
- (132) J.V. Dubrawski, Ph.D. thesis, Department of Physical and Inorganic Chemistry, Adelaide University (1977) p.109-122.
- (133) M.F. Tweedle and L.J. Wilson, "J.Amer.Chem.Soc.", 98 (1976) p.4824.
- (134) B.D. Sarma and J.C. Bailar, Jr., "J.Amer.Chem.Soc.", 77 (1955) p.5476.
- (135) W.L. Reynolds, "Progr.Inorg.Chem.", 12 (1970) p.1-99.
- (136) G.H. Stout and L.H. Jensen, "X-ray Structure Determination", McMillan, London (1968) p.73-76.
- (137) Ref. (136) p.85-87.
- (138) Ref. (136) p.90-93.
- (139) Ref. (136) p.94-97.

- (140) Ref. (136) p.97-98.
- (141) Ref. (136) p.98-106.
- (142) Ref. (136) p.107-115.
- (143) Ref. (136) p.114.
- (144) Chart PC32, Weissenberg coordinate system showing overlapping festoons generated by an orthogonal lattice.
- (145) Ref. (136) p.136.
- (146) "International tables for X-ray Crystallography", Vol. I - "Symmetry groups", Kynoch Press, Birmingham (1969) p.150.
- (147) C.K. Prout, "Physical Methods of Advanced Inorganic Chemistry", Interscience, London, p.8-11.
- (148) M.R. Snow, "Acta.Cryst.", B, 30 (1974) p.1850.
- (149) Ref. (136) p.79-80.
- (150) Ref. (147) p.11-14.
- (151) Ref. (146), Vol. III.
- (152) A.D. Rae, "Acta.Cryst.", 19 (1965) p.683-684.
- (153) Ref. (147) p.14-17.
- (154) Ref. (136) p.278-288.
- (155) Ref. (147) p.22-24.
- (156) Ref. (136) p.372-375.
- (157) Ref. (147) p.25-26.
- (158) Ref. (136) p.376-393.
- (159) D.T. Cromer and J.B. Mann, "Acta.Cryst.", A, 24 (1968) p.321.
- (160) D.T. Cromer, "Acta.Cryst.", 18 (1965) p.17; 19 (1965) p.224.
- (161) Ref. (136) p.246.
- (162) Ref. (136) p.242-243.
- (163) Ref. (136) p.416-419.
- (164) Ref. (136) p.67-69.
- (165) G.D. Fallon and B.M. Gatehouse, "J.Chem.Soc.", (Dalton) 13 (1975) p.1344.
- (166) M. Corrigan, Ph.D. Thesis, Monash University (1977) p.67.
- (167) Ref. (136) p.303.

- (168) W.C. Hamilton and J.A. Ibers "Hydrogen Bonding in Solids", Benjamin, New York (1968) p.86.
- (169) (a) S.A. Cotton, "Coord.Chem.Rev.", 8 (1972) p.185-223.  
(b) H.A. Goodwin, "Coord.Chem.Rev.", 18 (1976) p.293-325.
- (170) A. Whuler, C. Brouty, P. Spinet and P. Herpin, "Acta. Cryst.", B, 31 (1975) p.2069.
- (171) M. Iwata, K. Nakatzu and Y. Saito, "Acta.Cryst.", B, 25 (1969) p.2562.
- (172) B.M. Gatehouse and M.J. O'Connor, "Acta.Cryst.", B, 32 (1976) p.3145.
- (173) F. Calderazo and C. Floriani, "J.Chem.Soc.A." (1971) p.3665.
- (174) S. Sarasukutty and C.P. Prabhakaran, "J.Inorg.Nucl.Chem." 39 (1977) p.374-376.